

https://dspace.org/

Settlement analysis of deep foundations

Maupah, Denford S

2021
https://hdl.handle.net/10539/32993

Downloaded from a DSpace repository. https://dspace.org/



Settlement Analysis of Deep Foundations

A research project submitted in partial fulfilment of the requirements of the degree of MSc (Eng) [Civil and Environmental Engineering]

Student Name: **DENFORD S MAUPAH**
Student No: **2063874**

Supervisor: **DR THUSHAN C EKNELIGODA**

Date of Initial Submission: 30/04/2021
Date of Submission of Corrected Report: 25/10/2021

DECLARATION

I, **Denford Smart MAUPAH,** (Student No: **2063874**), am a student registered for the **Research Project – Settlement Analysis of Deep Foundations** in the year **2021.**

I hereby declare as follows:

- I am aware that plagiarism (the use of someone else's work without their permission and/or without acknowledging the original source) is wrong.
- I confirm that the work submitted for assessment for the above course is my own unaided work except where I have explicitly indicated otherwise.
- I have followed the required convention in referencing the thoughts and ideas of others.
- I understand that The University of the Witwatersrand may take disciplinary action against me if there is a belief that this is not my own unaided work or that I have failed to acknowledge the source of the ideas or words in my writing.

Signed



Denford Smart MAUPAH

Date: 22/10/2021

ABSTRACT

This paper reviews the various methods of settlement prediction of single piles and pile groups founded in cohesive, cohesionless and layered soils. The methods of settlement analysis can be grouped into three classes which are: (i) purely empirical such as that by Mayerhof (1959) for both single and pile groups, Focht (1967) for single pile and Skempton (1953) applicable to pile groups, (ii) simplified analytical or theoretical, which use elastic theory to come up with design charts and (iii) numerical methods which are computer based solutions. These range from the complex finite element and boundary element methods to fairly straightforward 'Pile' computer suite found in Prokon.

The settlement of single piles is dependent on the applied load, pile length, pile diameter and the type of soil along the pile shaft and at the base of the pile. The load-carrying capacity of a pile is influenced by the same factors which affect settlement, except the applied load which does not influence the pile capacity in any way. Single piles can be straight-shafted, sometimes referred to as conventional piles in this report, or have an enlarged base. Pile base enlargement has the effect of increasing the pile base, and hence, total pile load capacity, while at the same time leads to a reduction in settlement of a pile. Piles in sand tend to settle less but develop more shaft resistance than those founded in clay, for a pile of same geometry and supporting same load. However, piles founded in cohesive soil mobilise higher tip resistance than those founded in sand for the same applied load.

The settlement of piles predicted using various empirical, theoretical and/or analytical methods has displayed a fair measure of agreement with the computer program-determined settlement. Very close matching has also been exhibited with results of manual calculations, computer analysis results and those settlements measured from test piles in case histories. In some few cases, the level of agreement was not very close and this can be attributed mainly to the soil modelling in order to derive input soil parameters compatible with 'Pile' computer method that has been adopted for computer analysis.

The analysis of a single pile is extended to the consideration of the settlement interaction between two identical piles, a system which represents the simplest form of a pile group. Such an analysis is then extended to the case of a general floating pile group. Due to the large number of variables involved, it is not possible to present parametric solutions for all the possible situations. Consequently, in this paper, the settlement analysis of 2x1, 2x2, 3x3 and 4x4 pile groups have been considered. Pile group settlement is dictated by pile length, pile spacing, pile diameter, founding soil type pile group size and the applied load.

The load-carrying capacity of a pile group can be notably less than the sum of capacities of the single piles making up the group. In any situation, both the immediate and consolidation settlements of the group are greater than those of a single carrying the same working load as that supported by each pile in the group. This is so because the zone of soil which is stressed by the entire group extends to a much greater width and depth than the zone beneath a single pile. Therefore, the group action failure mode needs to be checked during the design of pile group foundation and similarly, the single pile failure mode should also be evaluated especially where an individual pile in the group leads to the whole pile group failure. Therefore explicit settlement checks must be made an integral part of any pile foundation design.

DEDICATION

This one is in memory of my parents, **Venganayi Smart** (1938-2012) and **Anna** (1939-2013) **Maupa**, who would have cherished my accomplishment. May their souls rest in eternal peace.

ACKNOWLEDGEMENTS

I wish to express my sincere gratitude to my supervisor, Dr Thushan C Ekneligoda, whose encouragement, understanding and invaluable guidance have made it possible for me to complete my study. His unlimited availability greatly helped me and lessened the burden of limited access to library facilities imposed on mankind by the ravaging Covid-19 pandemic. I deeply appreciate.

Special thanks go to Dr Luis Alberto Torres Cruz for his comments to my project proposal. His comments, without doubt, added more value to my research. Special thanks also go to Professor John Ndiritu, the Postgraduate Coordinator at Wits, for guiding me on the University requirements on thesis format and his speedy responses to quires pertaining my studies for the entire duration.

Allow me to also take this opportunity to thank the Directors of Desma Consulting Engineers who agreed to meet all my tuition fees during my studies at Wits. Without this funding, my aspiration to attain this postgraduate qualification would have remained a pipe dream. Financial support was also received from my brother and sister-in-law, Mr Bruce and Mrs Victoria Mawere, my nephews, Andrew Bwanya, Munyaradzi and Tawanda Mushimbo and my cousin, Charles Nyika. They provided the 'balance of payment support' because my almost fulltime engagement with this project and the demand of the other courses over a period of more than two years meant that my earnings got affected at work. I will forever be grateful to all of them.

I have also received a lot of support from family members – brothers, sisters and their children, in-laws and workmates. I will single out our Office Administrator, Ms Patience Majoni and IT consultant, Mr Munyaradzi Goora for being there when needed. I am very clear in my mind that this support spurred me on when the going got tough during my studies. I nearly threw in the towel! I want to specifically acknowledge the inspirational support and encouragement from Johnson Tendai Chademana, who studied the same programme and graduated at Wits in 2015. He played a very pivotal role for which I am very grateful.

My acknowledgements would be totally incomplete without mentioning my wife Rudo, sons, Tinashe and Takunda, who constitute the greater part of my world and whose support and encouragement I have never lacked. Thank you so much.

Table of Contents

ABSTRACT iii
ACKNOWLEDGEMENTS v
LIST OF FIGURES x
LIST OF TABLES xiv
LIST OF SYMBOLS xv
CHAPTER ONE 1
1 INTRODUCTION 1
1.1 Problem Statement 3
1.2 Aim and objectives 3
1.3 Organisation of the thesis 4
CHAPTER TWO 5
2 LITERATURE REVIEW 5
2.1 Deep foundations 5
2.2 Types of piles 5
2.2.1 Concrete piles 6
2.2.2 Steel piles 8
2.2.3 Timber piles 8
2.2.4 Plastic piles 9
2.2.5 Composite piles 9
2.3 Installation of piles 9
2.3.1 Effects of pile installation 9
2.4 Load capacity of piles 12
2.4.1 Load capacity of a single pile 12
2.4.2 Load capacity of a pile group 12
2.5 Pile load and integrity testing 15
2.5.1 Working piles 15
2.5.2 Trial piles 15
2.6 Pile foundation action 15
2.7 Settlement of a single pile 16
2.7.1 Meyerhof (1959) method 18
2.7.2 Coyle and Reese (1966) method 18
2.7.3 The T-z method 19
2.7.4 Focht (1967) method 21
2.7.5 Poulos and Davis (1968) method 22

2.7.6 Mattes and Poulos (1969) method 27
2.7.7 Butterfield and Banerjee (1971) method 30
2.7.8 Vesic (1977) method 31
2.7.9 Randolph and Wroth (1978) method 33
2.7.10 Poulos and Davis (1980) method 38
2.7.11 Poulos (1989) method 41
2.7.12 Fleming (1992) method 44
2.8 Pile Group Settlement 49
2.8.1 Skempton (1953) method 50
2.8.2 Meyerhof (1959) method 50
2.8.3 Vesic (1977) method 50
2.8.4 Poulos (1968b) method 51
2.8.5 Butterfield and Banerjee (1971) method 56
2.8.6 Poulos and Mattes (1971b) method 58
2.8.7 Randolph and Wroth (1979 60
2.8.8 Poulos and Davis (1980) method 63
2.8.9 Randolph (1985) method 67
2.8.10 Equivalent raft method 69
2.8.11 Poulos (1989) method 72
2.8.12 Mylonakis and Gazetas (1998) method 77
2.9 Numerical Methods 78
2.9.1 Calculation of ultimate bearing capacity 80
2.9.2 Deformation of single pile foundation 82
CHAPTER THREE 88
3 METHODOLOGY 88
3.1 Data used 88
3.1.1 Applied load, Q_u 88
3.1.2 Pile length, L (=L_P) 88
3.1.3 Pile cross-section dimensions 88
3.2 Soil properties 88
3.2.1 Clayey soil site 89
3.2.2 Sandy soil site 89
3.2.3 General case of a pile founded in layered soil 90
3.3 Methods of analysis 90
3.3.1 Validation of Prokon's 'Pile' programme for 'numerical' method 90

3.3.1.1 Solution for pile capacity in cohesive soil 91
3.3.1.2 Solution for pile capacity in cohesionless soil 95
3.4 Comparison between calculated and measured settlement of test piles (case histories) 98
3.4.1 Wembley, England 98
3.4.2 Iskenderun, Turkey 101
3.4.3 Baku, Azerbaijan 103
3.5 Basis of selection of empirical methods to apply 104
CHAPTER FOUR 105
4 SETTLEMENT CALCULATIONS AND COMPARISON OF RESULTS 105
In this chapter, settlement calculations were carried out using the various empirical, analytical and/or theoretical methods and computer method covered in Chapter 2 105
4.1 Single Pile Settlement Calculations by empirical, analytical and/or theoretical methods 105
4.1.1 Pile founded in cohesive soil 105
4.1.2 Pile founded in non-cohesive soils 115
4.1.2.3 Randolph and Wroth (1978) method 116
4.1.3 Pile founded in layered soil 119
4.2 Pile settlement computation using 'Pile' computer package 121
4.2.1 Pile settlement calculation using computer method for cohesive soil 122
4.2.2 Pile settlement calculation using computer method for non-cohesive soil 122
4.2.3 Pile settlement calculation using computer method for layered soil 123
4.3 Single pile settlement comparison 123
4.3.1 Comparison for piles founded in uniform cohesive soil 124
4.3.2 Settlement comparison for same load on varying pile length and vice versa 126
4.3.3 Comparison for piles founded in uniform cohesionless soil 128
4.3.4 Comparison for piles founded in layered soil 130
4.4 Pile Group Settlement Calculations 132
4.4.1 Pile groups founded in cohesionless soil 132
4.4.2 Pile groups founded in cohesive soil 135
4.5 Comparison of pile group settlement 140
4.5.1 Pile group settlement in non-cohesive soil 140
4.5.2 Pile group settlement in cohesive soil 141
4.6 Computer method for pile group analysis 146
CHAPTER FIVE 147
5 DISCUSSION AND CONCLUSIONS 147

5.1 Discussion.....147
5.2 Conclusions 147
REFERENCES 149
APPENDIX A 151
GEOLOGICAL MAP OF HARARE AND ITS ENVIRONS 151
APPENDIX B - TABLES 153

LIST OF FIGURES

Figure 2.1: Schematic diagram showing a shallow and deep (pile) foundation 6
Figure 2.2: Sectional elevation and cross-sectional detail of pile types. 8
Figure 2.3: Stresses and strains near the shaft and base of a pile. 10
Figure 2.4: Pile group and pile cap arrangements..... 13
Figure 2.5: Relationship between no. of piles and ultimate load capacity of a pile group….. 14
Figure 2.6: Schematic depiction of settlement of piles.. 17
Figure 2.7: Loaded column and loaded pile..... 17
Figure 2.8: Load-transfer analysis, after Coyle and Reese (1966) 19
Figure 2.9: Schematic representation of the T-z method.. 20
Figure 2.10: Movement ratio for end bearing pile on rigid base, after Focht (1967) 22
Figure 2.11: Stresses acting on a single pile and on adjacent soil, after Poulos and Davis (1968)..... 23
Figure 2.12: Distribution of side shear for various approximations to pile action, after Poulos and Davis (1968) 24
Figure 2.13: Displacement of a pile in a finite layer for *v=0.5*), after Poulos and Davis (1968) 25
Figure 2.14: Effect of enlarged base on base load 26
Figure 2.15: Shear stress distribution along a pile, after Mattes and Poulos (1969) 28
Figure 2.16: Settlement of the top of a compressible pile, after Mattes and Poulos (1969).... 29
Figure 2.17(a): Compressible pile displacement pattern, after Butterfield and Banerjee (1971) 31
Figure 2.17(b): Load-displacement curves to determine settlement factor, f for compressiblepiles, after Butterfield and Banerjee (1971)..... 31
Figure 2.18: Plan view of the shear zone around a pile 33
Figure 2.19: Uncoupling effects due to the pile shaft and pile base (a): upper and lower soil layers, (b): deformation patterns of lower and upper layers (after Randolph and Wroth, 1978)..... 34
Figure 2.20: Equilibrium of soil around a settling pile 34
Figure 2.21: Comparison of actual and approximate surface settlement profiles for a rigid punch, after Randolph and Wroth (1978)..... 37
Figure 2.22: Comparison of Equation 2.34 results and corresponding results obtained by Banerjee (1970) integral equation analysis, after Randolph and Wroth (1978)..... 38
Figure 2.23: Determination of settlement influence factor I_0, after Poulos and Davis (1980) 39
Figure 2.24: Correction factor for pile compressibility, R_k 40
Figure 2.25: Depth correction factor for settlement, R_h..... 40
Figure 2.26: Poisson's ratio correction factor for settlement, R_v..... 40
Figure 2.27: Pile base modulus correction factor for settlement, R_b, after Poulos and Davis (1980) 41
Figure 2.28: Influence factor for settlement of a single floating pile, after Poulos (1989) 43
Figure 2.29: Variation of settlement, Δ and settlement/load, Δ/P, after Fleming (1992) 44
Figure 2.30: Individual base and shaft performance, after Fleming (1992) 45
Figure 2.31: Elastic shortening for a non-rigid (compressible) pile 48
Figure 2.32: Simplified method of calculation of elastic shortening, after Fleming (1992) ... 48
Figure 2.33: Group of two floating piles, after Poulos (1968b)..... 51

Figure 2.34: Settlement interaction for 2-pile group and 3 and 4-pile symmetrical group, afterPoulos (1968b)....53
Figure 2.35: Effect of L/D on the interaction between piles in a group, after Butterfield and Banerjee (1971)....57
Figure 2.36: Effect of compressibility on the interaction between piles in a group, after Butterfield and Banerjee (1971)....58
Figure 2.37: Comparison of load-ettlement ratios for symmetric pile groups containing up to 4 rigid piles, after Randolph and Wroth (1979)....62
Figure 2.38(a): Interaction factors for pairs of rigid piles in homogeneous soil with *v*=0.4, after Randolph and Wroth (1979)....63
Figure 2.38(b): Interaction factors for pairs of rigid piles in non-homogeneous soil with v=0.4, after Randolph and Wroth (1979)....63
Figure 2.39: Pile group in plan depicting superposition via the interaction factor method afterPoulos and Davis (1980)....64
Figure 2.40: Section through a 3x3 pile group....65
Figure 2.41: Influence of soil modulus on interaction factor (after Poulos and Davis, 1980).65
Figure 2.42: Influence of bearing stratum stiffness on interaction factors (after Poulos and Davis, 1980)....66
Figure 2.43: Efficiency of square pile groups at different spacing (after Randolph, 1985) 68
Figure 2.44: Efficiency of square pile groups for piles of different stiffness ratios, after Randolph (1985)....68
Figure 2.45: Distribution of vertical stress by the 2:1 method....69
Figure 2.46: Schematic diagram of (a) a 3x3 pile group and (b) the equivalent raft method for a floating pile group (after Tomlinson, 1986)....70
Figure 2.47: Influence of geometric parameters on group settlement ratio (after Poulos, 1989)....74
Figure 2.48: Variation of group reduction factor with group breadth (after Poulos, 1989).....74
Figure 2.49: Settlement ratio exponent for driven piles, *S=3D*, (after Poulos, 1989)....76
Figure 2.50: Settlement ratio exponent for bored piles, *S=3D*, (after Poulos, 1989)....76
Figure 2.51: Diffraction coefficient (after Mylonakis and Gazetas, 1998)....78
Figure 2.53: Everett's side shear transfer function compared with Tavenas' (1971) result.....84
Figure 2.54: Everett's (1991) side shear transfer function compared with Vijayvergiya (1969) and Kraft and et al (1981) functions....85
Figure 2.55: Everett's (1991) end bearing transfer function for a Franki pile in clay compared with the Kontich result.....86
Figure 2.56: Proposed end bearing function for a bored pile base in soft rock compared to Wilson (1976) (after Everett, 1991)....87
Figure 3.1(a): 'Pile' Output summary and graphs showing variation settlement with load and load with pile length for a pile founded in cohesive soil, D_s=D_b=1.0m.....92
Figure 3.1(b): 'Pile' Output summary and graphs showing variation settlement with load and load with pile length for a pile founded in cohesive soil, D_s=1.0m and D_b=1.5m.....93
Figure 3.2(b): Load distribution along pile length, D_s=1.0m and D_b=1.5m....95
Figure 3.3 Comparison of results from Fleming (1992) study with those of Whitaker and Cooke (1966): pile H at Wembley....99
Figure 3.4 Comparison of results from Fleming (1992) study with those of Whitaker and

Cooke (1966): pile N at Wembley. 99
Figure 4.1 Variation of pile settlement with pile diameter and length using the T-z method 105
Figure 4.2 Variation of pile settlement with pile diameter and length after Focht (1967)..... 106
Figure 4.4 Variation of pile settlement with D_0 and length after Mattes and Poulos (1969) . 108
Figure 4.5 Variation of pile settlement with pile diameter and length after Butterfield and Banerjee (1971) 109
Figure 4.8 Variation of pile settlement with pile diameter and length after Randolph and Wroth (1978) 110
Figure 4.7 Variation of pile settlement with pile diameter and length after Poulos and Davis (1980) 111
Figure 4.8 Variation of pile settlement with pile diameter and length after Poulos (1989)... 111
Figure 4.9 Load/settlement curves (typical form) for D0=1.5m and pile length, L=30 after Fleming (1992) 112
Figure 4.10 Variation of pile settlement with pile diameter and length after Fleming (1992) 113
Figure 4.11 Variation of pile settlement with pile diameter and length, founded in sand using the T-z method 115
Figure 4.12 Variation of pile settlement with pile diameter and length after Randolph and Wroth (1978) 116
Figure 4.13 Variation of pile settlement with pile diameter and length founded in sandy soil after Poulos (1989) 117
Figure 4.14 Load/settlement curves (typical form) for D_0=1.5m and pile length, L=30 after Fleming (1992)..... 118
Figure 4.15 Variation of pile settlement with pile diameter and length founded in non-cohesive soil after Fleming (1992)..... 118
Figure 4.16 Variation of pile settlement with pile diameter and length, founded in layered soil using the T-z method – layered soil..... 119
Figure 4.17 Variation of pile settlement with pile diameter and length for layered soil after Randolph and Wroth (1978)..... 120
Figure 4.18 Variation of pile settlement with pile diameter and length for layered soil after Poulos (1989) 121
Figure 4.19 Variation of pile settlement with pile diameter and length calculated using ‘Pile’ computer method for cohesive soil 122
Figure 4.20 Variation of pile settlement with pile diameter and length calculated using ‘Pile’ computer method for noncohesive soil 122
Figure 4.21 Variation of pile settlement with pile diameter and length calculated using ‘Pile’ computer method for layered soil..... 123
Figure 4.22(a) Comparison of settlement computed by different methods for a single pile founded in uniform cohesive soil for L=10m..... 124
Figure 4.22(b) Comparison of settlement computed by different methods for a single pile founded in uniform cohesive soil for L=20m..... 124
Figure 4.22(c) Comparison of settlement computed by different methods for a single pile founded in uniform cohesive soil for L=30m..... 125
Figure 4.22(d) Comparison of settlement computed by different methods for a single pile founded in uniform cohesive soil for L=40m..... 125
Figure 4.22(e) Comparison of settlement computed by different methods for a single pile fou

nded in uniform cohesive soil for L=50m 126
Figure 4.23(a) Comparison of settlement computed by different methods for a single pile founded in uniform non-cohesive soil for L=10m 128
Figure 4.23(b) Comparison of settlement computed by different methods for a single pile founded in uniform non-cohesive soil for L=20m 129
Figure 4.23(c) Comparison of settlement computed by different methods for a single pile founded in uniform non-cohesive soil for L=30m 129
Figure 4.23(d) Comparison of settlement computed by different methods for a single pile founded in uniform non-cohesive soil for *L*=40m 130
Figure 4.23(e) Comparison of settlement computed by different methods for..... 130
a single pile founded in uniform non-cohesive soil for L=50m 130
Figure 4.24(a) Comparison of settlement computed by different methods for a single pile founded in layered soil for L=10m..... 131
Figure 4.24(b) Comparison of settlement computed by different methods for a single pile founded in layered soil for L=20m..... 131
Figure 4.24(c) Comparison of settlement computed by different methods for a single pile founded in layered soil for L=30m..... 131
Figure 4.24(d) Comparison of settlement computed by different methods for a single pile founded in layered soil for L=40m..... 132
Figure 4.24(e) Comparison of settlement computed by different methods for a single pile founded in layered soil for L=50m..... 132
Figure 4.25 Pile group settlement variation with pile diameter, length and pile group size for S/D0=3 and v=0.5 after Poulos (1968b) 135
Figure 4.26 Pile group settlement variation with pile diameter, length and pile group size for S/D0=3 and v=0.5 after Poulos and Mattes (1971b)..... 137
Figure 4.27 Pile group settlement variation with pile diameter, length and pile group size for *Ep*=30GPa and *Es*=30MPa after Poulos (1989)..... 138
Figure 4.28 Pile group settlement variation with pile diameter, length and pile group size using the equivalent raft method after Tomlinson (1986) 140
Figure 4.29 Variation pile group settlement with pile diameter for L=10m for (a) 2x2, (b) 3x3 and (c) 4x4 pile groups..... 142
Figure 4.30 Variation pile group settlement with pile diameter for L=20m for (a) 2x2, (b) 3x3 and (c) 4x4 pile groups..... 143
Figure 4.31 Variation pile group settlement with pile diameter for L=30m for (a) 2x2, (b) 3x3 and (c) 4x4 pile groups..... 143
Figure 4.32 Variation pile group settlement with pile diameter for L=40m for (a) 2x2, (b) 3x3 and (c) 4x4 pile groups..... 144
Figure 4.33 Variation pile group settlement with pile diameter for L=50m for (a) 2x2, (b) 3x3 and (c) 4x4 pile groups..... 145

LIST OF TABLES

Table 2.1 Typical values of C_p 32
Table 2.2 Influence factors, I_s for vertical displacement under flexible and rigid areas carrying uniform pressure. 36
Table 2.3 Soil settlement parameters (Janbu, 1963) 71
Table 2.4 Typical SPT and UCS values for saturated clays 81
Table 2.5 Limiting values of *f* and *q* 81
Table 2.6 Typical SPT results, descriptors and dry densities 82
Table 2.7 Common values of K3 (after Everett, 1991) 86
Table 3.1(a) Allowable pile capacity for a pile in cohesive soil with L=20m, Ds=1.0m; Db=1.0m (conventional pile) 92
Table 3.1(b) Allowable pile capacity for a pile in cohesive soil with L=20m, Ds=1.0m, Db=1.5m (enlarged base pile) 93
Table 3.2(a) Comparison of load-carrying capacity and settlement for L=20m, Ds=Db=1.0m 94
Figure 3.2(a): Load distribution along pile length, Ds=Db=1.0m 94
Table 3.2(b) Comparison of load-carrying capacity and settlement for L=20, Ds=1.0m, Db=1.5m 95
Table 3.4(a) 'Pile' computer output summary for pile H at Wembley, England after Whitaker and Cooke (1966) 100
Table 3.4(b) 'Pile' computer output sammary for pile N at Wembley, England after Whitaker and Cooke (1966) 100
Table 3.4(c) Wembley, England - Summary of actual and calculated results 100
Table 3.5 Idealised soil profile and parameters at IPPP site 101
Table 3.6 Pile settlement values obtained by different methods compared with pile tests results (Mert and Ozkan, 2019) and 'Pile' computer method results at IPPP site 102
Table 3.7 – Idealised soil profile and parameters at Baku Hotel site 103
Table 3.8 Pile settlement values obtained by different methods compared with pile tests results and 'Pile' computer results at Baku Hotel site 103
Table 4.1 Settlement calculation results (after Meyerhof, 1959) 115
Table 4.2(a) Comparison of single pile settlement computed by various methods for same loading with varying D_0, and L founded in cohesive uniform soil, P=250kN 127
Table 4.2(b) Comparison of single pile settlement computed by various methods for same pile length L, with varying D_0 and P founded in cohesive uniform soil, L=30m 128
Table 4.3–2^2, 3^2 and 4^2 – Pile group settlement after Skempton (1953) 133
Table 4.4 –2^2, 3^2 and 4^2 – Pile group settlement in sand 140

LIST OF SYMBOLS

A_p, A_{pi}	Cross-sectional area of pile
B, B_p	Width of shallow foundation, Square pile cross-sectional dimension
c	Undrained cohesive strength of soil
c_a	Adhesive strength between the pile shaft and the soil
D, D_0, D_s, d	Shaft diameter for a circular pile
D_b, D_B, d_b	Pile base diameter for pile with enlarged base
Δ_b, Δ_s	Pile base and pile shaft settlement respectively
E_p, E_s	Young's modulus of the pile material and soil around pile shaft respectively
E_B, E_b	Young's modulus of the soil below pile base
E_u	Undrained Young's modulus of the soil
f	Unit skin friction
F, P, Q/Q_0	Single pile applied load
G, G_s, G_{si}	Shear modulus of soil
H, T_{CL}	Thickness of soil layer, thickness of compressible layer
I_s, I_ρ	Pile settlement influence factor
I_0	Settlement influence factor for an incompressible pile
j	Stress exponent in Janbu's method
K	Pile stiffness factor
K_s, K_{si}	Pile shaft stiffness
K_b, K_{bi}	Pile base stiffness
L, L_p, L_{pi}	Pile length
L_0	Upper length of a pile carrying no load or low loads by friction
L_F	Length of a pile transferring load to soil by friction
m	Modulus number in Janbu's method
M_R	Pile movement ratio
M_s	Flexibility factor representing movement of a pile relative to the soil when transferring load by friction
ŋ	Pile group efficiency factor
ρ, ρ_1, ρ_p	Single pile settlement
q	Stress due to applied load at pile base
Q_b, P_b	Load applied at pile base/pile base capacity or resistance
Q_s, P_s	Load applied to pile and carried by shaft friction/pile shaft capacity
Q_g, Q_G, P_G	Applied pile group load
R_G, R_s	Pile group reduction factor, pile group settlement ratio
r_m	Radius at which settlement or stress in soil becomes insignificantly small
S, S_1, S_ρ	Single pile settlement
S_G, ρ_G	Pile group settlement
$R_{b, h, k, v}$	Correction factor bearing stratum, depth, compressibility of pile and Poisson's ratio of soil
U_b, U_B, Us	Ultimate pile base load, ultimate pile shaft friction load
ζ	$\ln(r_m/r_0)$
v, v_s, v'	Poisson's ratio of the soil, Poisson's ratio of soil skeleton
Z, z	Embedment depth, depth of point of interest below ground.

CHAPTER ONE

1 INTRODUCTION

Limit state is a condition of a structure beyond which it does not fulfill the relevant design criteria. The European Code of practice EN1997-1, Eurocode 7: Geotechnical Design - Design Rules, Section 2.7.1.1 requires that where relevant, it shall be verified that specified limit states are not exceeded by structural elements. SANS 10160 is not a geotechnical design code but a basis of design and makes reference to relevant sections of Eurocode 7 for design. SANS 10160 is specific that STR (and STR-P) and GEO limit states must be assessed and combined with the requirements of Eurocode 7, which specifies that the following limit states be checked:

- EQU which is loss of equilibrium of the structure or ground, considered as a rigid body in which the strengths of structural materials and ground are not significant in providing resistance.
- STR which is concerned with internal failure or excessive deformation of the structure or structural elements, including piles, in which the strength of the structural materials is significant in providing resistance. STR-P is a variation of STR limit state and is used for self-weight dominated structures.
- GEO which deals with failure or excessive deformation of the ground in which the strength of the soil or rock is important in providing resistance.
- ACC aims to ensure that the structure is able to tolerate specific accidental events and, when accidents occur, subsequently maintains structural integrity for a sufficient period under usually reduced environmental conditions, to enable implementation of the necessary interventions to mitigate the risk.
- SLS, serviceability limit state, which represents the criteria governing normal function or operational use for a structure in service.
- ULS, ultimate limit state, which represents the failure of the structure and its components when subjected to extreme actions.

The ultimate load which a piled foundation is capable to carry represents the limit state for the load-carrying capacity of that pile. However, pile deformations at this ultimate state are of insignificant consequence if the integrity of the structure supported on the piles is compromised as a result of excessive deformations. Therefore the deformation characteristics of the pile under an applied load below ultimate, are of more significance. This is SLS, and usually represents the working load conditions imposed on the pile. Thus settlement could be one of the most important features in single pile and pile group design, implying that accurate settlement prediction is key to the performance-based design of piles as it is critical to the SLS of the whole structure concerned.

Foundations are divided into two categories, vis-à-vis shallow and deep foundations. The settlement of piles, a type of deep foundations, is much more difficult to estimate than that of shallow foundations because of many reasons, some of which are:

a) The mechanism of stress transfer at the pile base and along the pile shaft is very different, a phenomenon known as the constitutive behaviour of piles.
b) Layering because piles pass through layers of soil which have different stiffness.
c) Pile slenderness as piles have high slenderness (pile length L, to diameter D_0, ratio, L/D_0), because they are long relative to their cross-sectional dimension, D_0 or width B_p for square piles. Consequently, pile compression (called elastic shortening), can be fairly significant.

d) The elasto-plastic condition of soil which arises from the fact that piles carry the highest load at their top where the soil is weakest. Therefore soil may be approaching failure at the top of the pile but elastic at the bottom and hence, still below ULS. Thus, the top soil mass may reach ULS but still far from failure at the pile tip.

It is therefore important to load-test sample piles in order to ascertain the limiting states of the pile. (Knappett and Craig, 2012)

Several procedures exist for the estimation of single pile settlement, ranging from traditional methods which rely on either an arbitrary assumption of shear distribution along the pile shaft and the use of conventional one-dimensional theory by Terzaghi (1948, as cited in Poulos and Davis, 1980)), empirical relationships to complicated nonlinear finite element and finite difference analyses.

Similarly, there are also a number of methods for the computation of settlement behavior of pile groups varying from closed form solutions to sophisticated computer-based methods. The load transfer mechanism in pile groups involves a fairly complex interaction of piles, surrounding soil and the pile cap. This complex reaction is in turn influenced by factors such as soil properties, pile group arrangement or geometry, pile-soil interaction, pile cap setting - is pile cap off the ground or part-supported on the ground, among other factors. Quantifying the above factors accurately is difficult, hence no single method is capable of fully accounting for the above factors' effects on pile group settlement. (Poulos and Davis, 1980)

In the design of pile foundations, settlement rather than bearing capacity, is often the controlling factor and therefore, pile foundation settlement must be assessed as accurately as possible. Because of this, a thorough understanding of the empirical methods which are generally used to determine the settlement of deep foundations, need not be overemphasised. Settlement, defined as the total vertical displacement that occurs at the foundation level, is categorized into immediate and consolidation settlement. The overall immediate settlement of a pile foundation is a combination of the settlement of the soil mass as a whole (reduction of volume/air void ratio in the soil), axial compression of the pile (pile elastic shortening) and slip between soil-pile interfaces due to loss of shaft resistance.

The stress distribution within a soil mass from an applied load or stress is determined by assuming that the soil is an elastic, homogeneous, linear, isotropic and a semi-infinite material. A semi-infinite mass is bounded on one side and extends infinitely in all other directions, which is also called an elastic half space**.** As each soil particle is loaded, it can either move into an unoccupied space (void) or deform when it comes in contact with another soil particle. If it deforms, it does so in the half space which is defined by the contact area that increases with deformation until the stress stabilises. This part of soil movement is recoverable and is called elastic settlement. If the soil moves into unoccupied space, this part is called re-orientation of the soil grains (compaction or decrease in void ratio), which is generally irrecoverable and thus results in permanent deformation of the soil mass, but not the individual particles.

Immediate settlement takes place as the load is applied up to a time period of within seven days from date of load application while consolidation, also called long-term settlement, takes months to years to develop. Elastic settlement analysis is done for all fine-grained soils including silts and clays with a degree of saturation, $S_{sat} \leq 90\%$ and for all coarse-grained soils with a large coefficient of permeability $>10^{-3}$m/s. Consolidation settlement analysis is used for saturated or nearly saturated, fine-grained soils where the Terzaghi theory of one-

dimensional consolidation applies. (Bowles, 1982). The theory states that any quantifiable change in the stress to a soil is a direct result of a change in the effective stress of the soil.

The methods of settlement analysis in deep foundations can be widely classified into three categories which are:

(a) Empirical for which examples include such methods as those derived by Meyerhof (1959) and Focht (1967) applied for single piles and those by Skempton (1953) and Meyerhof (1959) for pile groups. Empirical methods are based on observation and/or experience as opposed to theory or logic.

(b) Simplified analytical (also called theoretical), which use elastic theory to provide design charts from where settlement can be read-off or derived. Simplified analytical methods are semi-empirical as they are partly based on field data collected from instrumented piles, simplistic approximations and some parameters obtained from empirical data.

(c) Numerical methods such as finite element and finite difference analyses, which are the most common numerical methods. Numerical analysis involves the study of algorithms [sets of (computer) instructions designed to carry out specific tasks] that use numerical approximation to solve mathematical analytical problems.

1.1 Problem Statement

Pile foundations were not common in Zimbabwe until about a decade ago because shallow foundations were mainly adequate for the 3 to 4 storey structures which have characterised construction in Zimbabwe over the last two or so decades due to economic decline. The harsh economic environment which has prevailed in the country since the turn of the millennium, has restricted the size of buildings constructed and thus prevented the adoption of pile foundations out of need occasioned by large loads generated by structures to be supported.

Most urban areas in Zimbabwe, particularly in the capital Harare, had fairly accurate geotechnical maps with 'problem soils' areas generally left as green areas during early planning years. However, the harsh economic conditions afore mentioned have led to significant rural-urban migration thus putting pressure on housing demand. As a result, previously avoided areas are now being developed into mainly housing and commercial areas. The soils common in such areas are not capable of carrying loads, some for even single storey structures, at shallow depths, thus requiring pile foundations to transfer loads to more competent but deep levels.

This increased use of pile foundations to transmit structural loads to deeper, more competent strata, even for single storey buildings at times, has motivated this research into the settlement analysis of deep foundations.

1.2 Aim and objectives

The aim of the research is to analyse the settlement of deep (pile) foundations and apply the techniques learnt to the analysis and design of pile foundations in Zimbabwe, particularly in Harare. This final goal will be achieved through the following objectives:

i) The study of the available empirical methods of pile foundations settlement and critically review such empirical methods of settlement analysis of deep foundations.

ii) a) Developing deep foundations numerical models and validating them with existing case studies from Harare, Zimbabwe and other parts of the world.

b) Simulating some deep foundations numerical models to determine the accuracy of the empirical and semi-empirical methods.

1.3 Organisation of the thesis

The research will be divided into 5 chapters as follows:

Chapter 1 – Introduction

Chapter 2 – Literature review and critique - Deep foundations: The different types of pile foundations and their method of installation are reviewed, including the single pile and pile group's load-carrying capacity in different soil types. Piles carry load by shaft friction and pile base resistance. If 80% or more of the load is carried by shaft resistance, then a pile is called a friction or floating pile and if the reverse, an end bearing pile. Pile load integrity testing for both working and test piles is also briefly discussed in this chapter. A detailed narration of methods of deep foundations settlement analysis and a critical review of the methods covered will be done in this chapter. The other method of pile settlement prediction is by numerical means, the finite element and finite difference methods being among the most commonly used. Financial constraints meant that the software for use in the project could not be procured. 'Pile', a suite in Prokon software was thus used for computer method-determined settlement. The program was validated first before the results could be used for comparisons carried out in Chapter 4 of this report. Details of how 'Pile' program works are covered in section 2.9 of this chapter.

Chapter 3 – Methodology: A detailed explanation of the methodological approach will be given here including the methods of data collection and the use of the data in settlement analysis of piles and pile groups. The methodical choices are also evaluated here.

Chapter 4 – Settlement calculations and comparison of results. Deep foundations settlement calculations would be done using the empirical methods and compared to results obtained through validated numerical models developed. In 'Pile', the soil is modelled. The pile is not divided into small segments.

Chapter 5 – Discussion and Conclusions. The conclusions drawn from this study are numerated and discussed.

CHAPTER TWO

2 LITERATURE REVIEW

A foundation is a structural component which transfers loads from the superstructure to the soil. Foundations are divided into two categories called shallow and deep foundations. A shallow foundation is one where the ratio of the embedment depth Z, to the minimum plan dimension B (the width), is given by: $Z \leq 2B$.

2.1 Deep foundations

In foundation design, there arises situations where the use of shallow foundations is uneconomic or impractical. Such situations include the following:

- when large concentrated loads are applied to the foundations,
- when the estimated settlement of shallow foundations exceeds the tolerable limit,
- when the differential settlement for shallow foundations, due to variable soils or non-uniform structural loads, is excessive,
- when near surface soils have low resistance, i.e., have low strength and/or stiffness,
- where large structures are situated on very heterogeneous (not uniform in composition) soils or where the soil layers are inclined,
- where displacements must be kept small for structures which are sensitive to settlement,
- in marine environments where tidal, flow or wave action, in a process called scouring, may erode material from around shallow foundations and
- when the structural loads consist of lateral loads, moments and uplift forces whether singly acting or in combination.

(Knappett and Craig, 2012; Budhu, 2011)

The effects of the above would be to increase the plan dimensions and/or the embedment depth of a shallow foundation, thus requiring larger areas of land which come at prime costs, particularly in urban areas where high rise buildings are common. Foundations must not encroach onto adjacent properties or servitudes, hence shallow foundations under such circumstances would be too expensive and difficult to construct thereby making deep foundations the ideal alternative. Basements, buoyancy rafts, caissons, cylinders, shafts and pile foundations are some of the types of deep foundations in general use. The most common type of deep foundation is the pile. This paper reviews the settlement of pile foundations only.

A pile is a slender structural member that is installed in the ground to transfer structural loads, which may be axial or lateral loads or moments, to soils at some significant depth below the base of the superstructure. Superstructures which cannot be economically and structurally supported on shallow foundations are normally carried by pile foundations, which are synonymous with deep foundations in this report, and are mainly circular or square in cross-section with an outside diameter, D_0 or a width, B_p that is very much smaller compared to their length, L_p, i.e.: $L_p >> D_0$. Figure 2.1 shows schematic diagrams of a shallow and deep foundation.

2.2 Types of piles

Piles may be divided into two main categories according to their method of installation. Driven piles are formed by driving shells or tubes fitted with a driving shoe, into the ground. The tubes or shells are then filled with concrete after driving. Also included in this category are piles formed by placing concrete as the driven shells or tubes are withdrawn. The installation of any type of driven pile causes displacement and disturbance of the soil around the pile, except in

the case of steel H piles and tubes where the displacement is small.

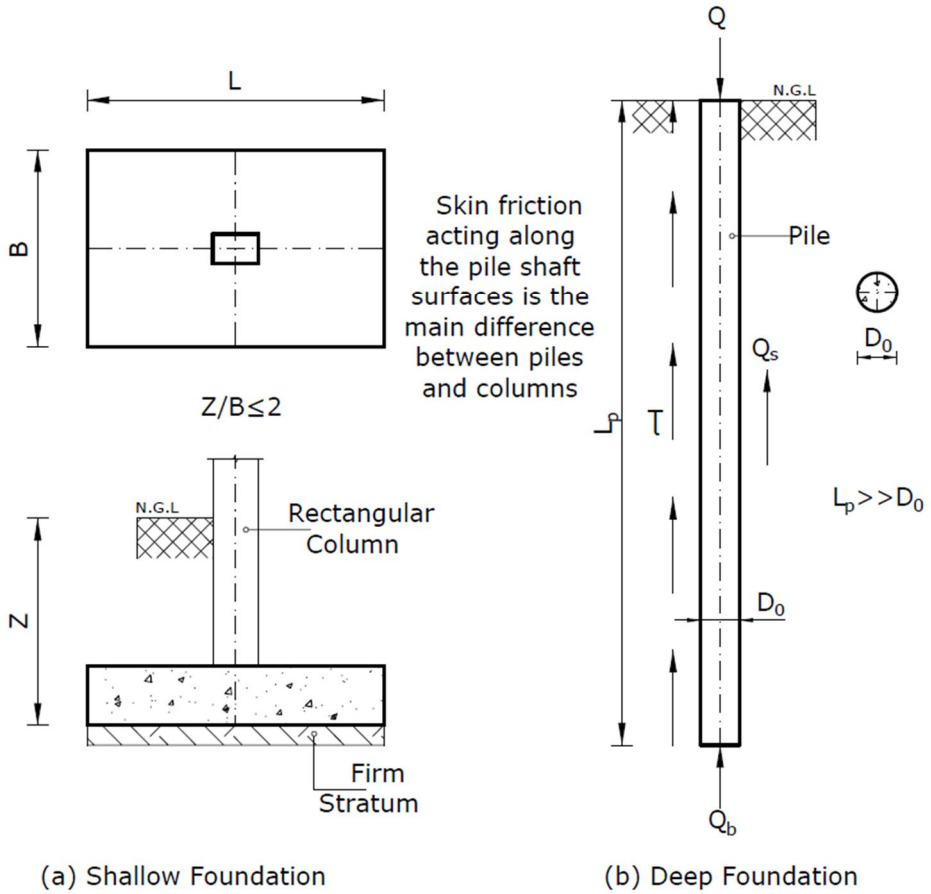


Figure 2.1: Schematic diagram showing a shallow and deep (pile) foundation

The other category consists of piles which are installed without soil displacement. The soil is removed by boring or drilling to form a shaft. Concrete is then cast in the shaft to form the piles called bored or drilled piles. The shaft may be cased or uncased, that being dictated by the type of soil and the environment. In clays, the shaft maybe enlarged by underreaming which results in a pile that has a larger base area in contact with the soil as depicted in Figure 2.2(g). Apart from concrete, piles may also be made from steel, timber, plastic or composites. The following basic information would be required as a minimum, before considering what type of pile is best suited to a particular project:

- Detailed geotechnical information
- Structural details including loading
- Allowable total and differential settlement
- Knowledge of the site and its surroundings

The choice of appropriate pile type is thus influenced mainly by sub-surface conditions, location and topography of the site, structural characteristics of the proposed superstructure and the geotechnical properties of the soil. Sub-surface soil and water conditions usually represent the most significant factors. Figure 2.2 shows the schematic representation of various types of piles which are summarized as follows:

2.2.1 Concrete piles

There are several types of concrete piles that are in common use, which include, but are not limited to:

- Cast-in-place concrete piles which fall under the driven pile category. They are formed by driving cylindrical steel shells into the ground to desired depths and then filling the cavity of the shell with fresh concrete. The steel shell is used for construction convenience and does not contribute to the load transfer capacity of the pile. Its purpose is to open a hole in the ground and to keep it open until a concrete pile has been constructed. The concrete may be plain or reinforced. Plain concrete is used when the structural loads are purely compressive. A designed steel reinforcement cage would be required if the pile has to carry lateral loads and thus transfer moments.
- Pre-cast concrete piles, usually square, circular or octagonal in cross-section, are fabricated in a factory or construction yard from reinforced pre-stressed concrete. Precast concrete piles are the preferred type in cases where the length of the pile is known in advance. They present transportation challenges as they are usually very long and are difficult to cut to size or lengthen as the site situation dictates.
- Micro piles are also known as mini piles, pin piles or needle piles. They are small-diameter pipe piles usually 50-340mm diameter. They are pushed or driven into the ground and are ideal for sites with low headroom, congested areas, sites with restricted access and for foundation repair and/or strengthening.

- Franki Pile – The Franki driven cast-in-situ piles have been used extensively throughout Southern Africa for more than half a century and remain the most popular pile type at present. The Franki pile is suited to structures that vary from single storey residential or industrial buildings to multi-storey office blocks because of the large range of sizes available and the incorporation of an enlarged base. The enlarged base formed at the bottom of the Franki pile is its main feature because its formation leads to an increased end-bearing area. Additionally, when the enlarged base is formed, the displacement of the soil results in the compaction and preloading of the soil surrounding the enlarged base. There are variations in installation techniques in order to adapt to special construction applications.

- Continuous Flight Auger (CFA) piles
  This piling system is fast and generally very economical but has its limiting considerations which have prevented its widespread use.
  The advantages of CFA are:
  (i) High production levels achievable in good appropriate soils
  (ii) System economical in suitable soils
  (iii) Low noise level which is limited to engine noise of piling rigs
  (iv) There is no vibration associated with CFA piles

The limitations of CFA piles are:

a) Adequate monitoring of the rig operator to ensure correct flow of concrete/grout and pressure and rate of extraction of the flight, etc.
b) The drilling operation reduces the strength of the soil around the pile which leads to inferior load/deflection curves relative to driven piles.
c) Soil from the operation, including that which falls off the flight, can contaminate the concrete/grout.
d) There is very limited indication of soil strength during the drilling and the maximum depth of CFA is about 25m.

e) CFA have to be cast to ground level which results in wastage of concrete and additional labour costs for trimming the piles to level.

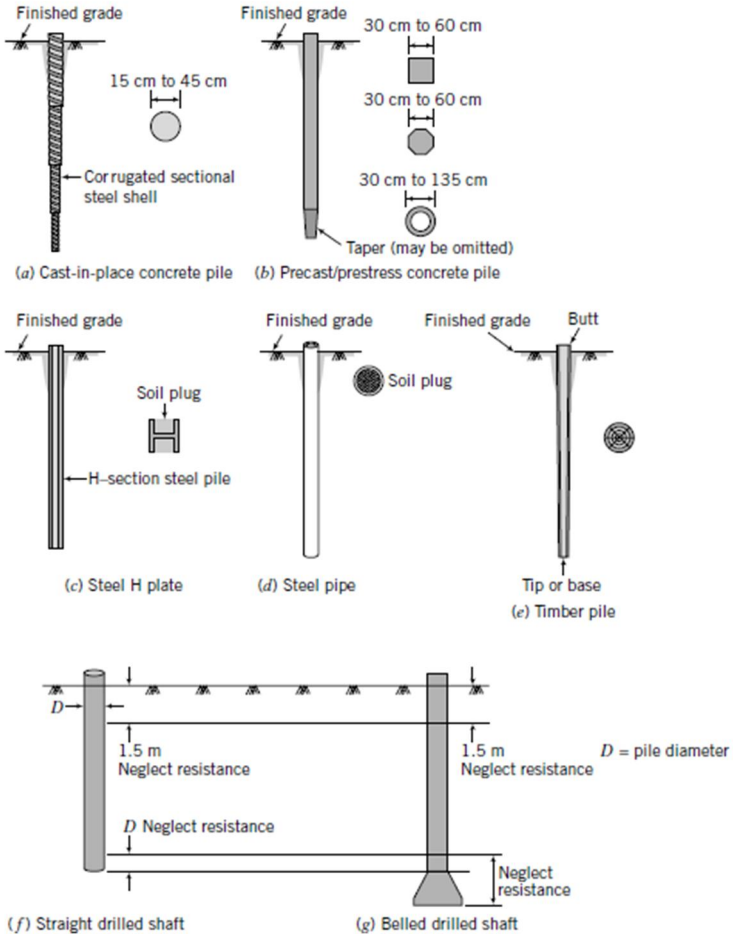


Figure 2.2: Sectional elevation and cross-sectional detail of pile types. Adapted from **Soil Mechanics and Foundations** (p. 511), M. Budhu, 2011, John Wiley and Sons Inc.

2.2.2 Steel piles

Steel piles include cylindrical, tapered and H type piles. H piles are non-displacement piles which are made from rolled steel sections. They can be welded to lengths of up to 70m. Steel piles are usually driven into the ground with open ends. When the piles are expected to penetrate through rocks and boulders, the ends are made into conical tips. In order to increase the load-carrying capacity of the steel pipe piles, the soil plug, shown in Figure 2.2(c), is removed and replaced with concrete to form concrete-filled steel piles.

2.2.3 Timber piles

Timber piles are displacement piles and have been used from long back. The famous Taj Mahal Mausoleum, a UNESCO World Heritage Site located in India's Agra City in Uttah Pradesh and built from 1632-53, is supported on ebony (a type of timber) pile foundations. The length of timber piles is dependent on the type of tree from which the timber was harvested but are commonly 12m long with longer piles achieved by splicing a number of piles. The major disadvantages of timber piles are susceptibility to:

1) Termite attack
2) Marine organisms attack

3) Rotting within zones exposed to seasonal moisture variations.

2.2.4 Plastic piles

These consist of a variety of composite materials like polymer composites, PVC and recycled plastics. They are used in special applications as corrosive and/or marine environments and in soil zones exposed to seasonal moisture variations.

2.2.5 Composite piles

Concrete, steel and timber can be combined to form composite piles. A part of a steel pile in a corrosive environment can be covered in concrete while a timber pile part susceptible to termite attack, can be replaced by concrete or steel, etc.

2.3 Installation of piles

Piles can be placed into the ground by driving them in, in the case of driven piles or by installing them in a pre-drilled hole in the case of bored piles. A variety of equipment is available for use in pile installations. The method of installation of piles needs to be carefully considered or selected because it causes irreversible changes to the soil stress and strain states and also creates intolerable noise and vibration during construction/installation. Caution must be exercised during pile installation because the compressive or tensile strength of the pile material must never be exceeded by the maximum installation stress for piles installed by driving from the top. Information on the compressive or tensile strength of pile material is normally available to pile installers.

2.3.1 Effects of pile installation

Pile driving imposes impact loading onto the soil. When the hammer strikes a pile, it sets up a stress wave which propagates through the pile shaft which, in turn, transfers the stress to the surrounding soil. When a pile is pushed into the soil, this imposes a continuous static load on the soil. Whether a pile is installed by driving or pushing, the installation load is applied quickly such that undrained conditions can be presumed to prevail. Under undrained conditions, zero volume change is assumed. Piles generate some of their resistance at their base in bearing, called base resistance, Q_b. Due to their significant length, and hence, surface area, piles can also generate resistance along the shaft due to interfacial friction between the pile material and the soil. This is called the shaft resistance or skin friction, Q_s. Q_b and Q_s are depicted in Figure 2.1 and depicted in Figure 2.3.

The shear stress, τ, imposed on the soil and the radial compression to the soil mass around the pile may lead to soil failure. The stresses on a soil element, A, at a radius, r, near the pile shaft, are as depicted in Figure 2.3 (b). There would be different stresses for each of the layers if the soil along the pile shaft is layered. It is evident from Figure 2.3(b) that the stresses on the soil element are not simple. Although it is possible to apply mechanics to solve for these stresses, replicating them and the mode of deformation would be very complicated for practical applications. Consequently, the mode of deformation near the shaft is taken to be similar to simple shear. Thus the soil element A near the shaft-soil interface is dragged down, as shown in Figure 2.3(a)

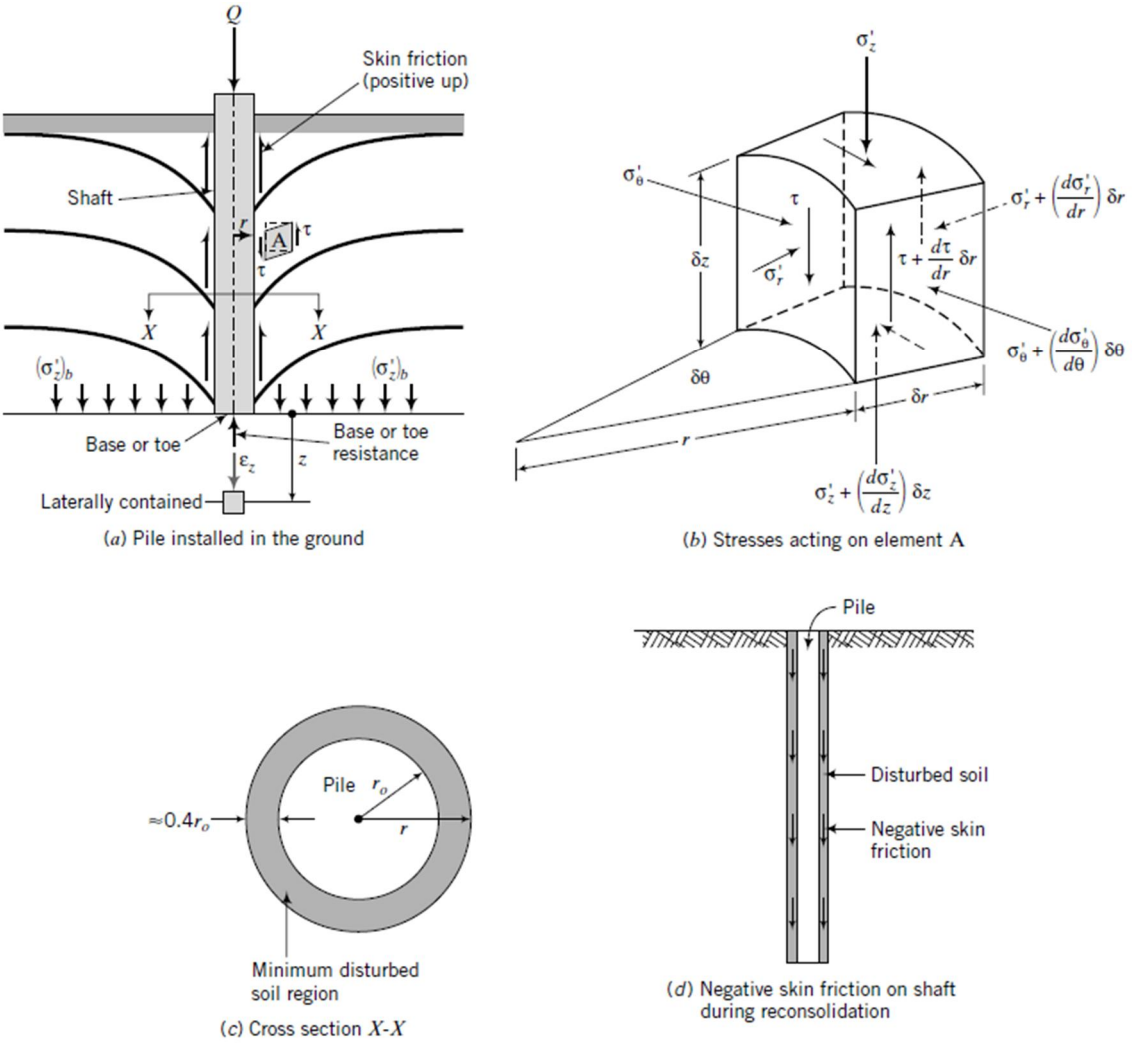


Figure 2.3: Stresses and strains near the shaft and base of a pile. Adapted from **Soil Mechanics and Foundations** (p. 516), M. Budhu, 2011, John Wiley and Sons Inc.

During installation of displacement piles, the volume of the soil displaced will be equal to the volume of the pile. This displaced volume of soil mass is called disturbed or remoulded soil mass. Consider a pile of length L, and radius r_0, and assuming a right cylinder of soil is compressed over an annular area of thickness r-r_0, where r is the external radius of the displaced soil, as shown in Figure 2.3(c) above. If the remolded soil heaves by say ΔL, the outside radius, $r \approx 1.4r_0$. This means that a cylinder of soil of annular thickness greater than 40% of the pile radius, is disturbed. Thus the thickness of the soil in the softening zone is about $0.4r_0$. It is called the softening zone because the stiffness of this disturbed soil is lower than that of the undisturbed soil. The soil in this zone is likely to be at critical state, a state when there is a unique relationship between shear stress, effective normal shear stress and water content (or specific volume or void ratio), being unique and independent of the initial stress or stress path. Interfacial shear stress will lead to a further increase in the thickness of the disturbed zone which results from dilatant response of the soil. At high shear rates, soil, being a dilatant material, reacts by an increase in volume due to formation of holes within its mass.

During pile installation, excess pore-water pressure develops and will only dissipate after installation, resulting in reconsolidation of the disturbed cylindrical soil mass indicated in

Figure 2.3(c). During reconsolidation, negative skin friction is imposed on the pile shaft, negative because it acts in the same direction as the applied compressive force, thereby reducing the load-carrying capacity of the pile. Negative skin friction phenomena is depicted in Figure 2.3(d). However, the dissipation of excess pore-water pressure leads to an increase in the soil strength because the effective stress increases. This is so because contacts between soil grains are effective in resisting applied stresses in a soil mass. Under an applied load, the total stress in a saturated soil sample is composed of intergranular stress and the pore water pressure. When pore water drains out from a soil, the contact between the soil grains increases, which increases the level of intergranular stress. This intergranular contact stress is called the effective stress σ', defined as the difference between the total stress σ, and the pore water pressure u, i.e. $\sigma' = \sigma - u$.

During pile installation, a soil element directly under the pile base will be under axial compression, tending to compress as well as shear. The difference between the vertical and lateral stresses causes the shearing. However, this soil element is more severely constrained than the one near the pile shaft-soil interface, confined laterally and vertically. The overburden pressure, σ_z', further restricts its movement. The level of compression imposed on this soil element is dependent on the:

a) soil's compressibility, which is the ease with which soil decreases in volume (soil densification) under an applied compressive load.
b) soil's hydraulic conductivity which is the ease with which pores of a saturated soil permit water movement.
c) soil's crushability, which is the ease with which particles of granular soils can be broken into smaller pieces due to an applied external force and
d) The magnitude of the applied load.

Fine-grained soils have a low hydraulic conductivity and the excess pore-water pressure would thus not dissipate quickly. Therefore the soil mass just below the pile base would be practically incompressible because of the incompressible nature of both water and soil solids. This may lead to extraordinary, but temporary resistance to pile driving or pushing, which should not be confused with long-term pile-load capacity.

The deformation of a saturated soil is more complicated than that of a dry soil since water, which fills the voids, must be squeezed out of the soil grains before readjustment of the soil grains can happen. However, when the load on a saturated soil is quickly increased, the increase is initially carried by the pore water which results in the buildup of an excess pore water pressure, $\triangle u$, being water pressure greater than the hydrostatic pressure. Hydrostatic pressure is pressure exerted by a fluid at equilibrium at a given point within the fluid due to gravity. As the drainage of the water continues, more and more load is transferred from the pore water to the soil grains until the excess pore water pressure has dissipated completely and the soil grains readjust to a denser configuration under the applied load. This time dependent process is called consolidation and results in a decreased void ratio and an increased unit weight, compared to conditions before the load was applied. Therefore when pile installation is complete, excess pore water pressure will dissipate, leading to settlement. For an overconsolidated soil, i.e., a soil that has experienced a vertical effective stress that was greater than its present vertical stress, negative excess pore water pressure develops within the soil below the base. The pore water pressure of a soil is negative when the soil's voids are partially filled with water. Surface-tension forces operate to achieve a suction effect and the shear strength of the soil increases, albeit temporarily.
(Budhu, 2011)

2.4 Load capacity of piles

The ultimate bearing capacity of a pile or pile group is the maximum load which it can carry without failure or excessive settlement of the ground.

2.4.1 Load capacity of a single pile

As already discussed in section 2.3.1, it has been indicated that it is difficult to account for:

i) change in stress and strain states of soil from installation effects
ii) the variability of the soil type
iii) the differences in construction quality practice.

Consequently, the computation of pile load capacity is an approximation which relies on empirical and semi-empirical relationships. Thus the ultimate load capacity, Q, of a pile loaded in compression equals the sum of the skin friction, Q_s, acting on the sides of the pile shaft and the end-bearing, Q_b, at the base or tip or toe of the pile as shown in Figure 2.1:
i.e.: $Q = Q_b + Q_s$. The self-weight of the pile is normally included with the dead load or neglected altogether for piles of cross-sectional areas < $0.07m^2$.

(a) In sand Soils:

The Terzaghi bearing capacity equation: $q_{ult} = c'N_c + \gamma z N_q + 0.5\gamma B N_y$,
$c'N_c$ is the cohesion term, $\gamma z N_q$ is the surcharge term and $\gamma B N_y$ is the self-weight (density) term. The density term in the above equation is negligible in piles and thus usually ignored. Sandy soils are cohesionless, hence the cohesion term is in the above Terzaghi bearing capacity equation becomes zero. $\therefore q_{ult} = \gamma z N_q$.

(b) In clay Soils:

The capacity of single piles founded in clay soil is given by: $Q = Q_b + Q_s$, where Q is ultimate pile capacity, Q_b is ultimate pile end bearing capacity and Q_s is ultimate pile skin friction

For any pile installed in clayey or sandy soils, if the skin friction is greater than 80% of the pile load capacity, the pile is deemed a friction pile, and the reverse, an end bearing pile.

Several other methods exist for the computation of the load-carrying capacity of single piles. The variations mainly arise from the method of computation of factors of Q_b and Q_s. Piles are also sometimes subjected to horizontal loads and hence, moments, apart from the vertical loads already covered. The capacity of such piles is computed differently. This paper covers piles which are loaded with vertical compressive axial loads only. .

2.4.2 Load capacity of a pile group

Piles are usually grouped in most situations due to the limitations of the load-carrying capacity of single piles of practical diameter, *D*. They are arranged in geometric shapes as rectangles, circles, squares, octagons, etc., at a spacing *S*, centre to centre C/C, where $S \geq 2D$. Single piles are connected at their top by a reinforced concrete pile cap, which may or may not be in contact with the ground. When off the ground, it is referred to as a free-standing pile group. The structural load is applied to the pile cap which then distributes the load to the individual piles in the group. If the pile cap is in contact with the ground, some of the load would be directly transferred to the soil. Figure 2.4 shows some pile group arrangement and sectional details.

The load-carrying capacity of a pile group is not necessarily equal to the sum of the load capacities of single piles forming the group. If the piles are spaced at a sufficient distance apart,

the group capacity may approach the sum of the individual pile capacities. In fine-grained soils as clay, the outer piles tend to carry more load than the inside piles while in coarse-grained soils as sands, Vesic (1969), found that centre piles carry 20-50% more load than the perimeter piles. The ultimate load capacity of a pile group is related to the load-carrying capacity of a single pile through an efficiency factor **(ŋ)**, defined as:

$$\eta = \frac{\text{ultimate load capacity of the group}}{\text{sum of ultimate load capacities of individual piles}} \tag{2.1}$$

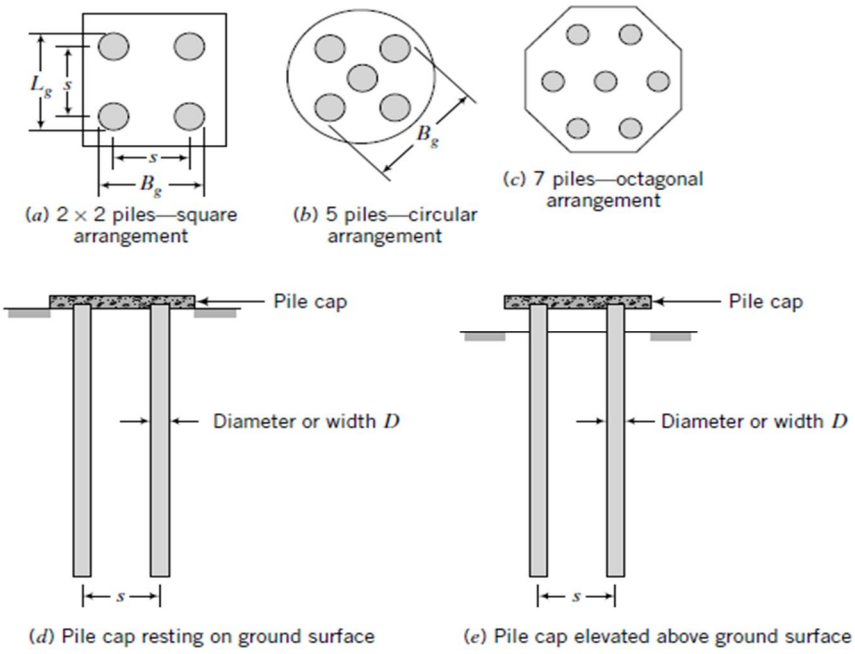


Figure 2.4: Pile group and pile cap arrangements. Adapted from **Soil Mechanics and Foundations** (p. 547), M. Budhu, 2011, John Wiley and Sons, Inc.

(a) Pile group in clay soil

The efficiency ŋ, of a free-standing pile group with friction (also called floating) piles is about 1.0 at relatively large spacing, decreasing with decreasing spacing. However, that of end bearing piles in a group is always considered to be equal to 1, implying that grouping has no effect on the load capacity of end bearing piles in clays. Several empirical relationships exist which try to relate pile group efficiency to pile spacing. The Converse-Labarre formula (Bolin 1941) is one such relationship represented as:

$$\eta = 1 - \frac{\arctan(D_0/S)}{\left[\frac{m(n-1)+n(m-1)}{mn}\right]}/90 \tag{2.2}$$

Where

m = number of rows, n = number of piles in a row, D_0 = pile diameter, S = C/C spacing of piles

$$\therefore\ Q_{g=}\ \eta\left(\sum_1^n Q\right) \tag{2.3}$$

Where:

Q_g is the ultimate load capacity of the group, Q is ultimate load capacity of individual pile.

The soil failure mode to be investigated to determine load capacity of pile group for above is called single pile failure mode. The key assumption in single pile failure mode is that each pile will mobilise its full capacity. However, the wide variation of the efficiency values obtained

using different empirical formulae led to reliability concerns over the calculation of ŋ using empirical relationships.

One of the most widely used methods to estimate pile group load capacity is given by Terzaghi and Peck (1948) where the pile group load capacity is the lesser of:

a) The sum of the ultimate capacities of the individual piles in the group and
b) The bearing capacity for the block failure of the group, i.e.: the rectangular block B_gxL_g $\Rightarrow$ $Q_g = B_g L_g c N_c + 2(B_g+L_g)Lc_{av}$, where Q_g = ultimate pile group load capacity, c = undrained cohesion at base of pile group, L = length of piles, N_c = bearing capacity factor corresponding to depth, L, c_{av} = average cohesion between surface and depth, L, L_g = pile group length and B_g is pile group width – see Figure 2.4(a).

Here, the mode of failure to be investigated to determine pile group load capacity is called block failure which may occur when the spacing of the piles is small enough to cause the pile group to fail as one unit. Figure 2.5 illustrates the relationship between the ultimate load capacity of a pile group of specified dimensions, and the number of piles in the group. The graph also shows the translation between single pile failure and block failure as the number of piles increases. It can be deduced from the graph that there is no advantage gained if more piles are used after a certain number as the pile group capacity reaches a peak with a specific number of piles in the group.

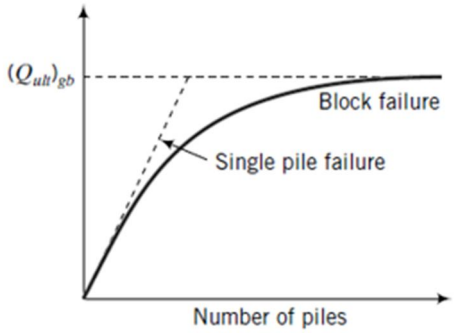


Figure 2.5: Relationship between no. of piles and ultimate load capacity of a pile group. Adapted from **Soil Mechanics and Foundations** (p. 547), M. Budhu, 2011, John Wiley and Sons, Inc.

For a pile group with a pile cap cast on the surface of the soil (see Figure 2.4(d)), the ultimate load capacity of the group is taken as the lesser of the following values:

i) the ultimate load capacity of a block containing the piles plus the ultimate load capacity of that portion of the pile cap outside the perimeter of the block
ii) the sum of the ultimate load capacity of pile cap and piles acting individually, i.e.: for a group of n piles of diameter D_0, and length L, supported by a rectangular pile cap of width, $\boldsymbol{B_c}$ and length, $\boldsymbol{L_c}$:

$$Q_g = n(c_{av}A_g + A_b c_b N_c) + N_{cc} c_c (B_c L_c - \frac{\pi D_0^2}{4}) \qquad (2.4)$$

Where c_{av}=average adhesion along pile, c_b=undrained cohesion at pile tip level, c=undrained cohesion beneath pile cap, N_c is bearing capacity factor for pile, N_{cc} is bearing capacity factor for rectangular pile cap, B_cxL_c, $L_c \geq B_c$, A_g = area of pile group, A_b is area of pile base.

(b) Pile group in sand

There is relatively limited information on pile groups in sand relative to those in clay but laboratory tests have established that generally, in sand, the efficiency, $\eta > 1$. Vesic (1969), carried out tests on large pile models and the results showed that a pile cap significantly contributes to the load capacity of the pile group, particularly in the case of smaller groups of 4 piles or less. For practical purposes, the contribution of the pile cap can be taken as the bearing capacity of a strip footing of a width equal to the distance from the edge of the pile cap to the outside of the pile. Vesic measured the pile base point load separately from the pile shaft load and concluded that when the efficiency of closely packed piles is greater than 1, the increased efficiency comes from the shaft resistance not the pile base resistance. The broad conclusion drawn from Vesic's tests results is that the overall efficiency of piles in sand is likely to be greater than 1 unless the sand is very dense or the piles are too widely spaced.

Various other empirical methods exist for estimating pile groups load-carrying capacities in both clays and sands.

2.5 Pile load and integrity testing

Pile load testing is done in order to ascertain that the pile constructed is capable of supporting the loads for which it was designed and is normally done for most large piling projects. By conducting full scale tests on piles, more economic piled foundation design can be achieved. Pile testing is also crucial for the determination of the load-settlement behavior of single piles, which, in turn, enable pile group settlement to be predicted. Integrity tests help in the detection of any structural defects in the pile shaft. Tests can be carried out on working piles or trial piles.

2.5.1 Working piles

The maximum test load is normally limited to 1.5 times the design working load. This is done in order to limit chances of damaging the pile. Test loads which are double the design working load are possible but should be done when necessary. Load tests are carried out on working piles as a quality control measure to check the pile's performance against specifications, check on the pile's structural integrity and verification of its design parameters.

2.5.2 Trial piles

Trial piles are specifically constructed for load testing and therefore, can be loaded to failure, which provides more accurate design information that can result in design adjustments to more economical levels. On large piling contracts, the extra costs of contrasting trial piles can often be recovered several times over from savings achieved through the resulting economies in design. For settlement-sensitive structures, ultimate load test results guide in the specification of working load for settlement acceptance criteria.

In pile design, verification of the serviceability limit state involves ensuring that the settlement of a pile under applied loads will not adversely affect the supported structure.
(Budhu, 2011; Byrne and Berry, 2008)

2.6 Pile foundation action

The action of deep foundations depends on the construction method adopted. A pile foundation may consist of a single pile or a number of piles installed fairly close to each other, at a spacing of say, S, (normally, $2D_0 < S \leq 5D_0$), and joined by a slab, which is known as a pile cap, cast on top of the piles. If a rigid pile cap is used to combine single piles, the action of the resulting group will be different from the behavior of single piles. Consequently, the settlement of a

single pile is estimated differently from that of a pile group, implying that the settlement of a single pile and that of a pile group should be analysed separately. The total settlement of a single pile or a pile group is the sum of the elastic settlement and the consolidation settlement. The determination of consolidation settlement is relatively straightforward compared to the elastic settlement. This paper reviews the evolution of the methods of mainly immediate settlement analysis of both single piles and pile groups and apply the concepts to the analysis and design of pile foundations in buildings built in Harare, Zimbabwe where the use of pile foundations even for single storey structures, is now common.

2.7 Settlement of a single pile

A single pile is one which does not have any interaction effects with adjacent piles when loaded. The spacing between the piles will depend on the solution modelled and the ground conditions but must always be large enough to avoid any interaction effects with adjacent piles. A pile under axial load will impose a complex system of stresses in the supporting soil and a corresponding system of deformation. Assuming no slip at the interface of the soil and the pile, integration of the deformation of the affected elements in the vertical direction will yield movement at the pile head but if axisymmetric behavior is assumed, mapping the distribution of the stress in the soil by considering the dimensions of the pile, the method of installation, the magnitude of the axial load and the types of soil, remains elusive.

The measurement of pile settlement is arduous because when load from a structure is applied to a pile foundation system, piles are immediately axially compressed, a type of settlement, and somewhat pushed into the ground, (another type of settlement) as the load is transferred from the pile head down the pile shaft and out into the soil. The transfer of the load from the pile occurs by shear stress along the pile shaft associated with relative movements between the pile shaft and the soil. The load that is not resisted by the shaft reaches the pile toe and cause the pile toe to move a small distance into the ground, called pile tip settlement. The whole process establishes a balance, an equilibrium between the applied load and the shaft and toe resistances mobilized. The associated movements are called load-transfer movements. So, in summary, when a load is applied to a pile, the pile settles into the soil and the pile material compresses due to the load.

As already highlighted in section 1.0 of this report, the settlement of a pile is thus much more difficult to estimate due to several reasons such as:

a) constitutive behaviour which arises from the very different mechanism of stress transfer at the pile base and along the pile shaft.
b) layering of soil as piles normally pass through layers of soil with different stiffness.
c) pile slenderness L_p/D_0. Piles are long compared to the diameter, hence shortening of the pile due to compression may be significant in magnitude.
d) elasto-plastic conditions which exist because loads carried by piles are highest at the top where the soil is weakest.

Figure 2.6 shows a pile which is loaded with a compressive load, P and the settlement at the top, y, which can be measured. Assuming the compression of the pile due to the load is (**c**). Now, because of the compression of the pile and referring to Figure 2.6, $y \neq s$, but $y = s+c$. Pile compression (**c**), cannot be physically measured.

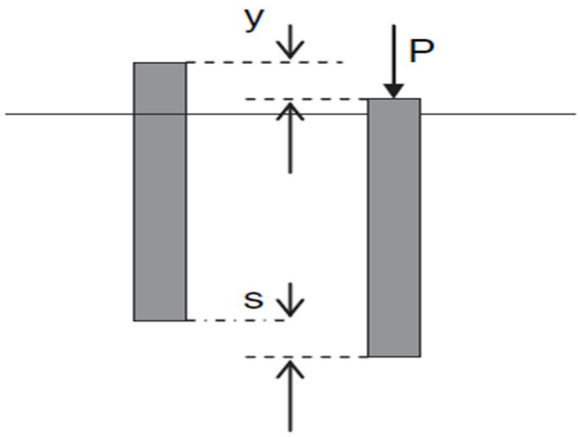


Figure 2.6: Schematic depiction of settlement of piles. Adapted from **Pile Design for Structural and Geotechnical Engineers** (p. 195), R. Rajapaske, 2007, Butterworth-Heinemann.

Figure 2.7 shows a column and a pile subjected to a compressive axial load, *F*. Hooke's Law, ($F = Kx$, where K is a material constant and x is the magnitude of compression or elongation), cannot be applied to compute the compression of the pile because of skin friction acting on the pile shaft. If a strain gauge is attached at the mid-point of both the column and the pile as shown in Figure 2.7, strain at these points can be measured and corresponding stress can thus be calculated.

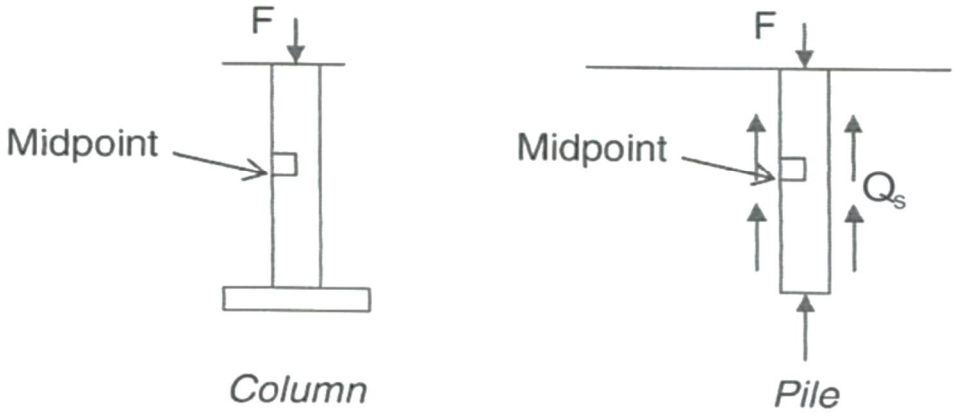


Figure 2.7: Loaded column and loaded pile. Adapted from **Pile Design for Structural and Geotechnical Engineers** (p. 196), R. Rajapaske, 2007, Butterworth-Heinemann.

Stress at midpoint of column = F/A_c, while Stress at midpoint of pile = $(F-Q_s)/A_p$, where A_c, A_p is the cross-sectional area of the column and pile respectively, Qs = unit skin friction, (f) x pile diameter (D_0) x depth to midpoint. From the above, it can be deduced that:

1) the stress along the column is constant while that along the pile varies with depth since total skin friction at a given point depends on the depth to that point, measured from the top of the pile.
2) because of skin friction, Hooke's equation, $F = Kx$, cannot be used directly for piles.

Many methods exist for the estimation of the settlement of single pile foundations, ranging from fairly simple empirical methods, to load-transfer methods, elasticity theory-based approaches to sophisticated numerical methods such as finite element and finite difference analyses. The significant difference between the various methods is in the assumptions that are made with regards to the shear stress distribution along the pile shaft but in most these methods, the pile is divided into several uniformly loaded elements. For elasticity theory-based approaches, a solution is obtained by imposing compatibility constraints between the displacements of the pile and the adjacent soil for each element of the pile. Pile displacements are obtained from pile compressibility considerations when the pile is axially loaded while soil displacements are obtained from Mindlin (1936, as cited by Poulos and Davis, 1980) equation, used to find the deformation as a function of a force at any position in the interior of a semi-infinite, elastic, homogeneous and isotropic mass. Detailed description of the various empirical methods are outlined below.

2.7.1 Meyerhof (1959) method

From an analysis of many load tests for piles in sand, Meyerhof suggested that at loads less than approximately one-third of the ultimate loads, and provided that no softer layers exist beneath the pile, settlement, ρ_p, of a pile could be estimated from:

$$\rho_p = \frac{D_0}{30FoS} \tag{2.5}$$

Where; D_0 is the base diameter of the pile, FoS is factor of safety and $2.0 \leq FoS$ at working load.

2.7.2 Coyle and Reese (1966) method

The settlement prediction of axially loaded single pile foundations is often analysed using the load-transfer, also called the t-z method (see section 2.7.3), which was developed by Coyle and Reese (1966). Curves which show the relationship between the ratio of the adhesion or load-transfer to the soil shear strength versus pile movement are required. Such curves are generated from data measured from field tests on instrumented piles and from laboratory tests carried out on model piles. The curves were originally developed by Seed and Reese (1957).

In practice, a number of such curves would be required to describe the load transfer along the entire length of the pile. The following steps summarise Coyle and Reese's load-transfer method.

1) The pile is divided into several segments, as shown in Figure 2.8 where only 3 segments are shown for clarity.
2) A small pile tip settlement, ρ_t, is assumed. $\rho_t = 0$ may be assumed but in reality, $\rho_t > 0$ since the pile tip undergoes some movement, no matter how small, unless the pile is end bearing and on rock.
3) Calculation of the point resistance, P_t, caused by the pile tip movement, ρ_t. Assuming the pile tip to be rigid and circular, P_t may be approximated from Boussinesq theory which gives:

$$P_t = \frac{2D_0E_b\rho_t}{(1-v^2)} \tag{2.6}$$

Where; E_b and v are the modulus and Poison's ratio of the soil below the tip of the pile. E_b and v are obtained from triaxial tests or from the back-analysis of pile load test results.

4) A vertical displacement, ρ_3, in the bottom segment at its mid height, is assumed. Further, assume $\rho_3 = \rho_t$ for the initial trial. With this assumed value of $\rho_3 (= \rho_t)$, the suitable curve of load-transfer/soil shear strength versus pile movement is used to find the appropriate ratio.
5) From shear strength versus depth graphs, the strength of the soil at the depth of the segment is obtained. The load-transfer (or adhesion) is then calculated from: τ_a = ratio (found in 4) above) x shear strength. The load, Q_3 on the top of segment 3, can be calculated from:

$$Q_3 = P_t + \tau_a L_3 P_3 \qquad (2.7)$$

Where L_3 is the length of segment 3 and P_3 is the average perimeter of segment 3
6) Assuming a linear variation of the load in the segment, the elastic deformation at the midpoint of the pile segment is calculated from:

$$\Delta^1\rho_3 = \left(\frac{Q_m + P_t}{2}\right)\left(\frac{L_3}{2A_3E_p}\right) \qquad (2.8)$$

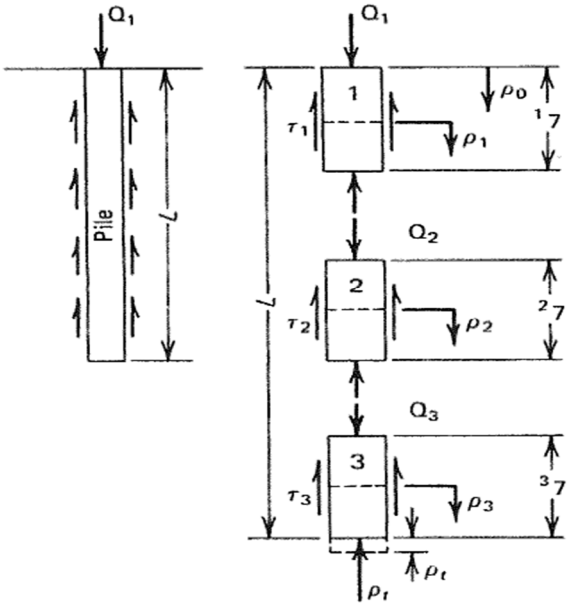


Figure 2.8: Load-transfer analysis. Adapted from **Pile Foundation Analysis and Design** (p. 72), H.G. Poulos and E.H. Davis, 1980, John Wiley and Sons.

Where $$Q_m = (Q_3 + P_{t)}/2 \qquad (2.9)$$

A_3 = cross-sectional area of segment 3 and E_p is the pile material Young's modulus.
7) The new mid height movement is given by: $\rho_3' = \rho_t + \Delta_{\rho 3}'$. This value of ρ_3' is compared with the estimated value of ρ_3(=ρ_t from step 4). If the calculated value of movement, ρ_3', does not agree with ρ_3 within specified limits, steps 2 to 7 are repeated and a new midpoint movement value obtained.
8) When convergence is achieved, the next segment up, i.e.: segment 2 in this case, is considered. The process is done for all the segments until a value of the load, Q_0, and displacement, ρ_0, for the top of the pile are obtained. The procedure is repeated using different assumed tip movement values until a series of Q_0 and ρ_0 values are obtained. These are then used to plot a load-settlement curve from the computed data.

2.7.3 The T-z method

The T-z method, initially proposed by Seed and Reese (1957), is an expedient means of predicting the settlement of a single pile under axial load. In this method, the pile elements are broken into multiple segments which are supported by discrete linear elastic springs, representing the soil-pile interaction by capturing the contribution of both the skin friction (t-z springs) and end bearing (q-z springs), as shown in Figure 2.9. Therefore the t-z and q-z relationships dictate the predicted load-settlement response. The spring properties may be determined analytically by use of Randolph and Wroth (1978) elastic mode, defining the reaction of the pile, *T*, for a given relative pile-soil displacement, z.

With reference to Figure 2.9, the i^{th} pile element is loaded by the force coming from the sections above it, F_i. Assuming a linear and elastic pile element with a Young's modulus, E_{pi}, cross-sectional area, A_{ip} and length, L_{si}, the pile element may compress by an amount of $\Delta_{zi} - \Delta_{zi+1}$ under the load, F_i. The average vertical movement of pile element relative to surrounding soil $= (\Delta_{zi} + \Delta_{zi+1})/2$. This vertical movement generates a resistive force, T_{si}, in the T-z spring. For equilibrium, which should prevail if the pile is below the ULS;

$$F_i = F_{i+1} + K_{si}\left(\frac{\Delta_{zi}+\Delta_{zi+1}}{2}\right) \qquad (2.10)$$

Where K_{si} $(=2\pi L_{si}G_{si}/ln(2r_m/D_0))$ is the T-z spring stiffness, and for an elastic soil, determined from Equation 2.30, Randolph and Wroth (1978) covered in section 2.7.9 of this paper..

From Hooke's Law, compression (or stretch), *x* is given by: $x = F/K$, where *K* is the stiffness of the material to which a compressive (or tensile) force, *F* is applied. In Figure 2.9, the displacements, $\Delta_{zi} and\ \Delta_{zi+1}$ are related to each other through the elastic compression of the pile under the average force in the pile element. Average force in pile element $= (F_i + F_{i+1})/2$, and stiffness, $K = \frac{A_{pi}E_{pi}}{L_{si}}$, Compression $= \Delta_{zi} - \Delta_{zi+1} = \frac{F_i+F_{i+1}}{2} / \frac{A_{pi}E_{pi}}{L_{si}}$

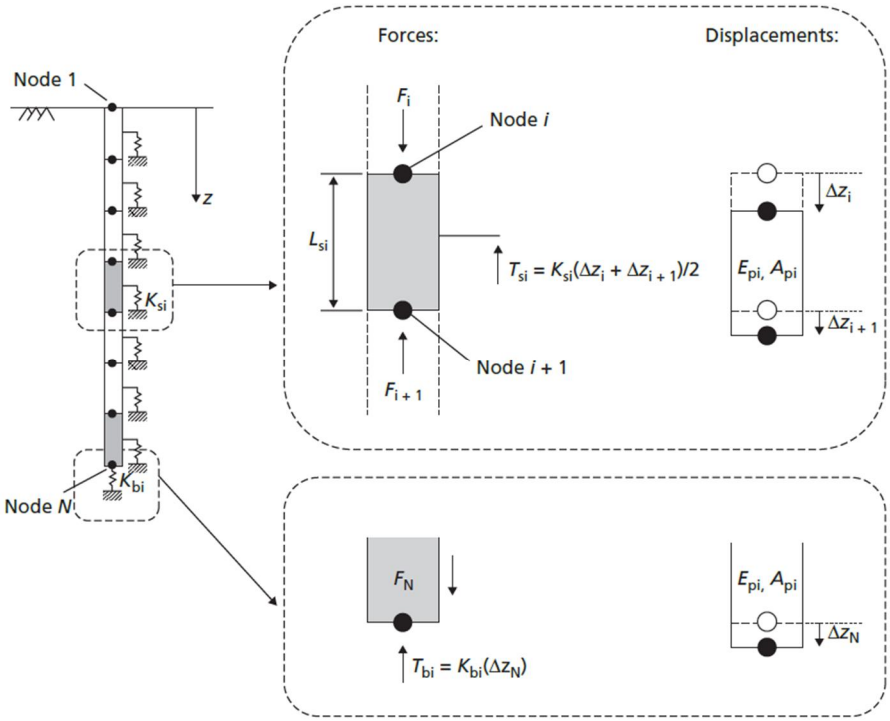


Figure 2.9: Schematic representation of the T-z method. Adapted from **Craig's Soil Mechanics** (p.345), J.A. Knappett and R.F. Craig, 2012, Spon Press.

$$\Rightarrow \quad \Delta_{zi} - \Delta_{zi+1} = \frac{L_{si}}{A_{pi}E_{pi}}\left(\frac{F_i + F_{i+1}}{2}\right) \tag{2.11}$$

The objective of the analysis is to determine the unknown distribution of forces, F_i and displacements, Δ_{zi} along the pile. Just as is the case with Coyle and Reese (1966), an initial estimate of the pile head settlement (total settlement) at node 1 is made. The displacements of the nodes for the rest of the pile can be determined from Equation 2.11. The displacement, Δ_{zN} at the node *N*, at the base of the pile corresponds to the compression of the elastic spring representing the pile base response. The force at node *N* is given by the following equation:

$$F_N = K_{bi}\Delta_{zN} \tag{2.12}$$

Where:

K_{bi} is the stiffness at the pile base. K_{bi} can be calculated from Equation 2.31 and 2.32 as covered in section 2.7.9 of this paper, $K_{bi}=2D_0G_{si}/(1-\nu)$. Different soil springs can be defined at base, K_{bi}, and along the pile shaft, K_{si}, which implies that the T-z method takes into account the constitutive behaviour of piles as highlighted in section 2.7 a). With a known force at node *N*, (pile base and from Equation 2.12, the force at each of the nodes above can be determined, in turn, using Equation 2.10. The pile load recovered at node 1 (top of the pile) will not equal the applied working load, unless a reasonably accurate estimate of the pile head displacement was initially guessed. An iterative process is thus required to estimate the pile head settlement which results in the recovery of the applied working load at the pile head. Since the values of F_i and $\triangle_{zi}$ are interdependent at each node, the solution procedure can therefore be automated using a spreadsheet.

Different pile properties as E_{pi}, A_{pi} and L_{si} can be defined for each pile element, thus making the T-z method account for soil layering and piles with changing cross-section, as the case with tapered piles.

2.7.4 Focht (1967) method

Focht proposes an empirical solution after observing data from a number of load tests for piles in clay soils and has related the observed settlement, ρ, of a pile bearing on a stiffer stratum, at the working load, to a movement ratio, M_R, defined as:

$$M_R = \frac{\text{Settlemenr of pile}}{\text{Elastic shortening of pile}} \tag{2.13}$$

Theoretical values of M_R are shown in Figure 2.10 for a pile on rigid bearing stratum. Similar graphs for end bearing pile on non-rigid stratum, though not included in this report, are also available.

$$\text{Pile head settlement,} \quad \rho = M_R\left(\frac{P.L}{E_pA_p}\right) \tag{2.14}$$

Where *P* is the load applied to a pile of length, *L* with a pile material Young's modulus of E_p and a pile cross-sectional area of A_p. Focht has observed from actual tests that for most practical pile dimensions, $0.5 < M_R < 2.0$. This is in reasonably close agreement with the theoretical results shown in Figures 2.10.

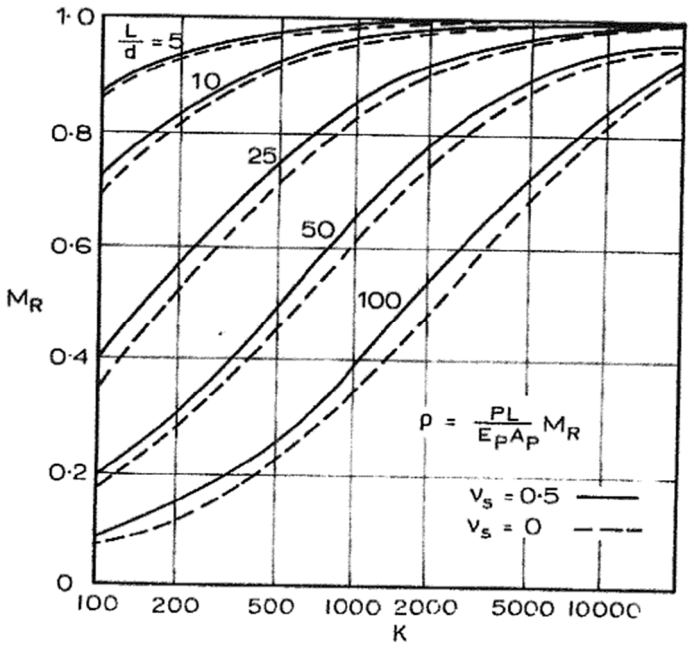


Figure 2.10: Movement ratio for end bearing pile on rigid base (after Focht, 1967)

2.7.5 Poulos and Davis (1968) method

Most existing methods of settlement prediction of a single pile foundation are elastic-based and rely on arbitrary assumptions of how the piles transfer their load to the soil, and generally compute settlement by means of one-dimensional theory. Terzaghi's one-dimensional (vertical axis being the one of interest) consolidation theory states that all quantifiable changes in stress to a soil (compression, deformation, shear resistance) are a direct result of a change in effective stress. Apart from Poulos and Davis (1968), several investigators such as D'Appolonia and Romualdi (1963), Thurman and D'Appolonia (1965), Salas and Belzunce (1965), Nair (1967), Mattes and Poulos (1969), Butterfield and Banerjee (1971), Banerjee and Davis (1977), Randolph and Wroth (1978), among others, have employed elastic-based analyses. In almost all the methods, the pile is divided into several uniformly loaded elements and a solution is obtained by imposing compatibility between displacements of the pile and the adjacent soil for each element. (Poulos and Davis, 1980)

Poulos and Davis (1968) noted that while several problems which have to do with a single pile such as the behavior of a floating and end bearing pile and the influence of negative friction or down-drag have been considered, solutions published then did not address the influence of such variables as the length to diameter ratio of the pile, the depth of the soil layer and the soil parameters on settlement behavior of a pile. The following assumptions were made by Poulos and Davis (1968):

a) The shear stress is distributed uniformly around the circumference of the pile. Earlier investigators as Salas and Belzunce (1965) and Thurman and D'Appolonia (1965), assumed a vertical point load acting on the axis of the element. The other loading which may be conveniently considered to represent the shear stress on the pile element is a uniform vertical line load acting down the axis of the pile element.
b) The sides of the pile are rough, the base is perfectly smooth, i.e.: no shear stresses are developed on the base.

c) The soil is initially considered to be ideal homogeneous, isotropic, elastic half-space, with elastic parameters of Young's modulus and Poisson's ratio which are not influenced by the presence of the pile
d) The pile and the soil are initially stress-free and that no residual stress exist in the pile resulting from its installation.

Poulos and Davis used linear elastic theory to analyse the behavior of a single axially loaded incompressible cylindrical pile where a wide range of length to diameter ratios is considered and influence factors for the settlement of a pile in a semi-infinite mass and a finite layer are given for different values of Poisson's ratio. They also investigated the effects of slip between the pile and the soil including that of an enlarged pile base then provided approximate solutions for the rate of settlement of a single pile. They presented results which apply to the case of a single pile in soft clay where the pile is practically incompressible relative to the surrounding soil.

2.7.5.1 Method of analysis

The pile is assumed to be made up of *n* number of cylindrical elements each being acted on by a uniform shear loading, p and a uniform radial stress, σ, and a circular base with a uniform vertical stress, p_b. The correct distribution of p, σ and p_b will be that which satisfies the conditions of displacement compatibility listed below, i.e.: if the pile is incompressible, each element must suffer:

i) equal vertical displacement, ρ_z and
ii) zero radial displacement, ρ_r

However Mattes (1967), found that consideration of compatibility of vertical and radial displacements yields almost the same results as those obtained by considering the compatibility of vertical displacements alone. The radial stresses are of the order of 0.005 times the shear stress on the pile and are thus ignored by Poulos and Davis. Only the compatibility of vertical displacements are considered.

A typical element, *i*, in Figure 2.11 was considered. The vertical displacement of the soil adjacent to the pile at *i* due to stress on an element *j* can be determined, from where the displacement of the soil at *i* due to all the *n* elements can be evaluated.

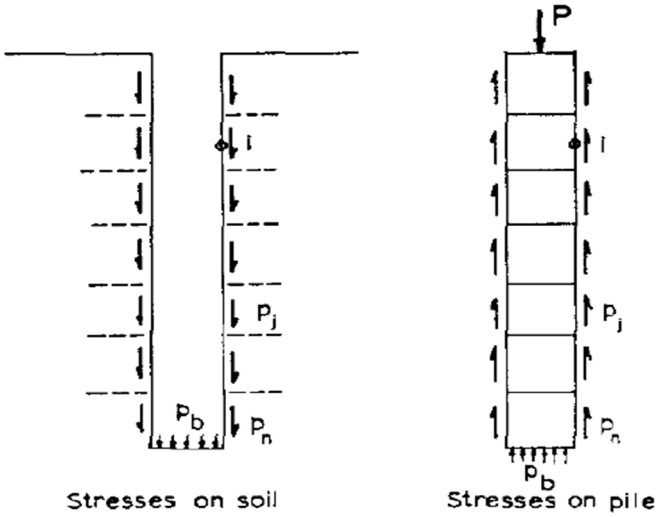


Figure 2.11: Stresses acting on a single pile and on adjacent soil (after Poulos & Davis, 1968)

The base displacement may also be determined in terms of the vertical displacement factor for the base due to shear stress on element *j* and the vertical displacement factor for the base due to uniform vertical stress on the base itself.

For the pile, the displacement of all the points is uniform and equating this displacement to unity and equating the displacement of the pile and that of the soil adjacent to the pile yields solutions which give the distribution of p and the value of p_b for unit displacement. The equilibrium condition, $P = \sum_{j=1}^{j=n}(p_j \pi d^2 L/n) + p_b \pi d^2/4$ is applied and the vertical displacement for unit applied load can thus be obtained. *P* is the applied load on a pile of diameter, *d* and length, *L*.

2.7.5.2 Representations of the forces applied to the pile by the soil

With regards to assumption 2.7.5 a) above, Figure 2.12 shows a comparison that Poulos and Davis made between the distributions of the shear stress along the pile, using the three possible types of loading which may conveniently be assumed to represent the shear stress on a pile element, for a length to diameter ratio, *L/d=100* and Poisson's ratio of the soil, *v=0.5*. The base has been assumed to carry no load in all the three possible load cases. It is evident from Figure 2.12 that for this particular case, distribution of stresses from line and ring representations closely agree while that obtained from the point load representation is considerably different. It tends to be more uniform along the pile than the other solutions. It was found, through experimental work, that piles having *L/d* ratio significantly less than 100, with the approximation of shear stresses as ring loads, most closely represent the action of the pile. The other two representations were found to become increasingly inaccurate. Further, it can be deduced from Figure 2.12 that even for a slender pile, the base has a small but significant modifying effect on the distribution of the shear stress on the shaft. Thus in their analysis, Poulos and Davis make allowance for the load taken by the base but assuming the pressure on the base to be uniform, thus ignoring non-uniformity of pressure caused by rigidity. They note that a more refined analysis is possible by considering the base as a series of uniformly loaded rings and including their displacements in the analysis. However, because the base exerts a relatively small modifying influence on the whole pile behavior, the more rigorous analysis is deemed unnecessary. Base influence is significant for very short piles.

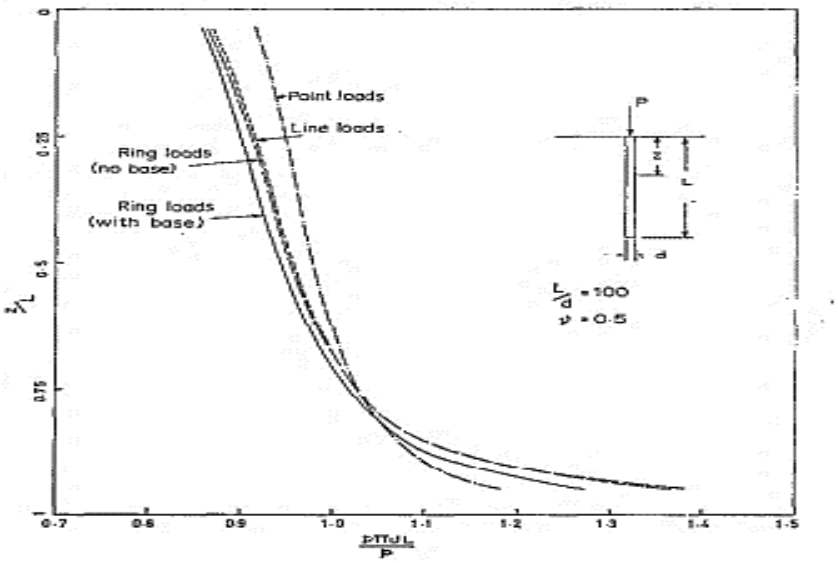


Figure 2.12: Distribution of side shear for various approximations to pile action (after Poulos and Davis, 1968)

2.7.5.3 Solutions for a pile in an elastic half-space

Poulos and Davis solved base displacement equations for a wide range of *L/d* ratios and four different values of the Poisson's ratio, *v*, to obtain shear stress and displacement distribution of a friction pile in a semi-infinite mass. The shape of the distributions obtained is similar to that in Figure 2.12 but with slight distortions, probably arising from the small number of pile segments used. However, the general change in shear stress distribution with decreasing *L/d* was evident.

The displacement factors obtained from an analysis of the displacement equations equated to unity, are plotted for the Poisson's ratio *v*=0.5 which is more applicable for undrained conditions which prevail during pile installation. These displacement factors for long piles can be worked out from the right-hand side of Figures 2.13. Poulos and Davis (1968) also investigated the effect of pile texture, comparing perfectly smooth piles when soil does not stick, hence no shear stress is developed on the pile shaft, and rough piles. Comparison of the smooth and rough piles showed that the presence of side adhesion has a dominant effect in the reduction of pile settlement, more so for long piles. At the other extreme end of an infinitely long pile, the rough pile undergoes zero settlement while the smooth pile's settlement is finite. However, the perfectly smooth condition is very unlikely to be achieved in practice, thus the analysis of a rough pile is more applicable to field conditions, particularly under working loads. The load-settlement behavior of rough piles changes as the load is increased towards ultimate and local shear failure occurs on the interface between the shaft and the soil at higher stress locations.

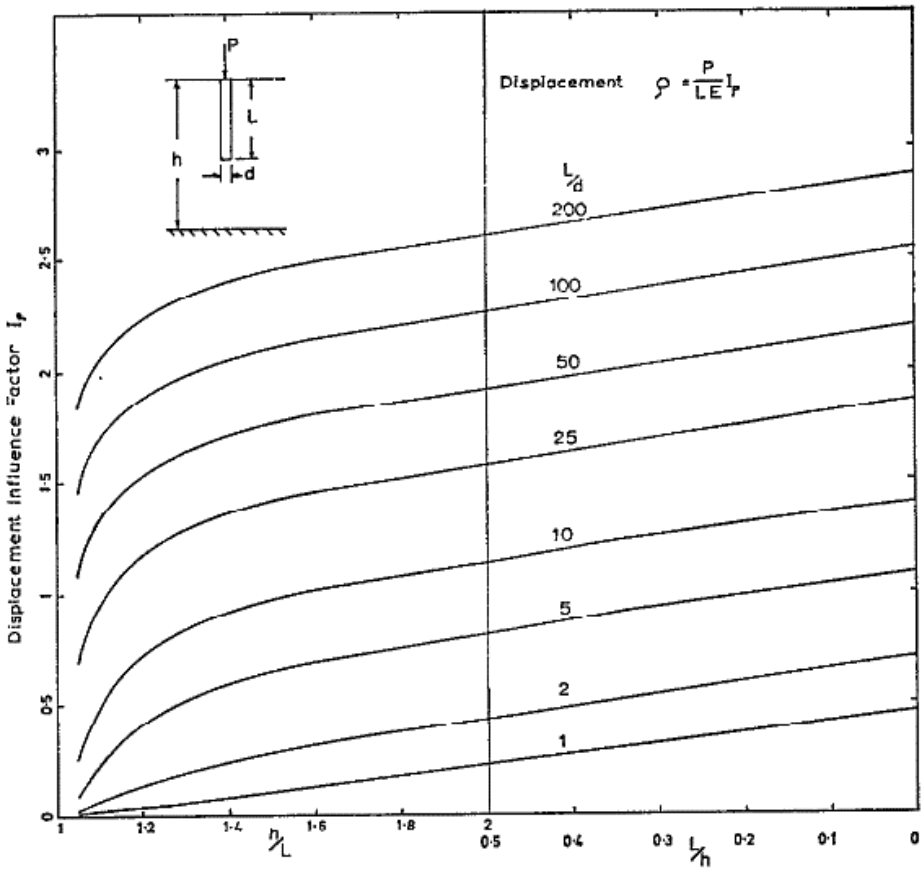


Figure 2.13: Displacement of a pile in a finite layer for *v=0.5* (after Poulos and Davis, 1968)

2.7.5.4 Immediate settlement contribution to total final settlement

Poulos and Davis (1968) also found that the immediate settlement of a single rough pile is more dominant than consolidation settlement. For a practical range of values of L/d, the immediate settlement contributes the bigger portion of final total settlement, even for $0 \leq v \leq 0.5$. Whitaker and Cooke (1966), carried out full-scale sustained load tests and the results confirmed that for increments of loads well below ultimate, the amount of consolidation settlement of a single pile is very small compared to the immediate settlement. It is only when the load approaches ultimate when significant time-dependent settlements occur, which may be due to shear creep and/or pore pressure dissipation. This, therefore, implies that the predominant part of the total final settlement of a single pile occurs immediately on load application. For that reason, consideration of the rate of settlement of a single pile is not of significant importance. The above solutions by Poulos and Davis are valid only when conditions in the soil remain elastic and the shear stresses along the pile shaft are less than the adhesive strength.

2.7.5.5 Solutions for a pile with an enlarged base

Their analysis of a single pile behavior with an enlarged base assumes a pile base diameter, d_b,, which is, in most cases, greater than the pile shaft diameter, d. Figure 2.14 shows the variation of the load taken by the base with the ratio, d_b/d, for a pile in a semi-infinite mass. The following can be deduced from Figure 2.14:

a) As d_b increases, the load taken by the base also increase, which would be expected because pile base capacity then increases.
b) The smaller the value of L/d, the more rapid the rate of increase of the base loading with increasing base diameter.
c) For values of $L/d<5$, even a relatively small enlargement of the base results in almost all the load being taken by the base.
d) The base has little influence on the small amount of load that is transferred to the base for slender piles.

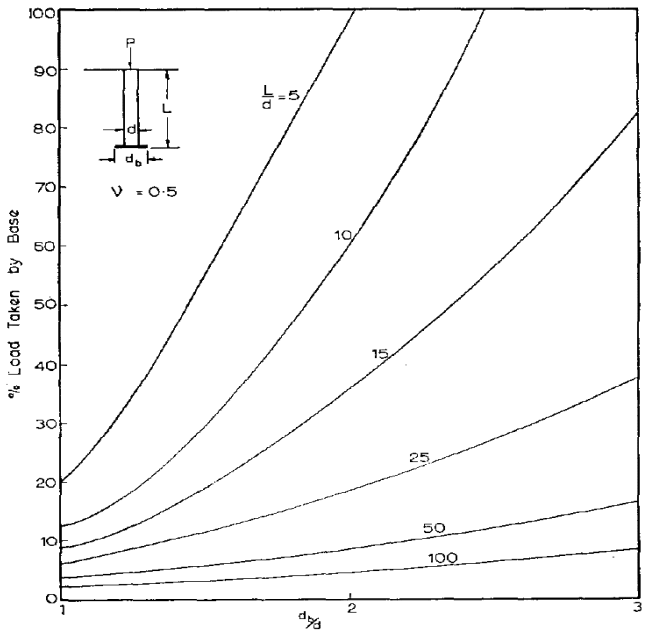


Figure 2.14: Effect of enlarged base on base load

Whitaker and Cooke (1961, as cited in Poulos and Davis, 1968) carried out tests on model piles with enlarged bases in soft, remoulded clay and also carried out tests on full-scale piles with enlarged bases in London Clay. The results obtained showed that there is a fairly close

agreement between the theoretical and the observed results. Whitaker and Cooke (1966) also confirmed, with their full-scale tests, that an enlarged pile base tends to increase the settlement at any given fraction of applied load to the ultimate load, noting that the ultimate load for a pile with an enlarged pile base will be greater than that for a pile without an enlarged. (Poulos and Davis, 1980)

2.7.6 Mattes and Poulos (1969) method

Mattes and Poulos (1969) employed linear elastic theory to analyse the settlement behavior of a circular compressible floating (friction) pile of length L, and outer diameter d, in an elastic half-space. A_p is the area of the pile shaft which is not necessarily equal to $\pi d^2/4$. This enables a tubular pile section, with a cap on its toe, to be considered, apart from solid piles. The pile is divided into n equal cylindrical elements. Any element, j, is acted upon by a uniformly distributed vertical shear stress, p_j, around the circumference. The base is considered as a rigid circular disc of diameter d_b, and d_b is assumed to be greater than d, thus the behavior of a pile with an enlarged base may also be analysed. The elastic parameters, E_s and v_s, being the Young's modulus and Poisson's ratio of the soil respectively, are assumed constant for the surrounding soil layer and that these parameters remain unchanged due to the presence of the pile.

It is a necessary condition for Mattes and Poulos (1969) solution that at any point along the pile, the displacements of the soil adjacent to the pile must be compatible with those of the pile itself. According to Mattes (1969), consideration of both vertical and radial displacements leads to solutions which are insignificantly different from those obtained by considering the vertical displacements only. Therefore, only the compatibility of vertical displacements is considered in this method, the displacements being calculated at midpoint of the outer surface of each element and at the centre of the base. The vertical displacement of the soil due to the shear stress along the pile may be obtained by double integration of the Mindlin (1936) equation for vertical displacement around the surface of each pile element.

Derivations for a floating compressible pile yield a vertical shear stress, p, expressed in terms of the pile stiffness factor, $K = (E_p/E_s)\,.R_A$, where E_p and E_s is the Young's modulus of the pile material and the surrounding soil respectively and $R_A = 4\,A_p/\pi d^2$, which is the area ratio, being the ratio of the area of the pile shaft to the area bounded by the outer circumference of the pile. For the case of a solid pile, R_A=1. The pile stiffness factor K, is a measure of the relative compressibility of the pile. Less compressible piles have higher K values. $K = \infty$ is the limiting case of an incompressible pile. Piles may be considered very compressible for $K \leq 100$, while K=1 means that the compressibility of the pile is the same as that of the surrounding soil.

In obtaining their solutions described below, Mattes and Poulos divided the pile into ten elements, similar to the number of elements adopted by Poulos and Davis (1968), who found that the 10 elements yield satisfactory results. It has also been established that for a given value of pile stiffness K, the behavior of a pile is not dependent on the value of the area ratio, R_A. Therefore, the solutions proposed by Mattes and Poulos are relevant for solid and tubular piles and for other piles of any cross-sectional shape but having a cylindrical outer surface with a cap at the toe of the pile. Further, most of the solutions are for purely elastic behavior of a conventional pile, i.e. pile without an enlarged base. Solutions for a pile with an enlarged base are also proposed, together with those for a conventional pile in which local yield along the

pile shaft (but not the base) occurs.

2.7.6.1 Load transfer along the pile

Figure 2.15 below shows typical elastic distribution of shear stress p, along a pile in an elastic half-space for *L/d=25* and two widely different values of pile stiffness factor, *K*. The value of p is expressed in the dimensionless form $p\pi dL/P$, and, for each value of *K*, distributions are as shown for $v_s = 0$ and $v_s = 0.5$. From Figure 2.15, it may be noted that:

a) For high values of K (say K=5000), the distribution of p along the pile shaft is approximately uniform, with the maximum value occurring near the pile tip.
b) This distribution is similar to that of an incompressible pile. Therefore, for *L/d*=25 and with a high value of *K* (*K=5000* in this case), the pile is in fact, incompressible.
c) For smaller values of *K*, say *K<50*, the shape of the stress distribution is significantly different from that for *K>5000*. Very high shear stresses occur near the pile head with smaller values at the toe.
d) For both cases of *K<50* and *K>5000*, the value of v_s has little influence on the shear stress distribution except near the pile top where p is small for v_s=0 than for v_s=0.5.

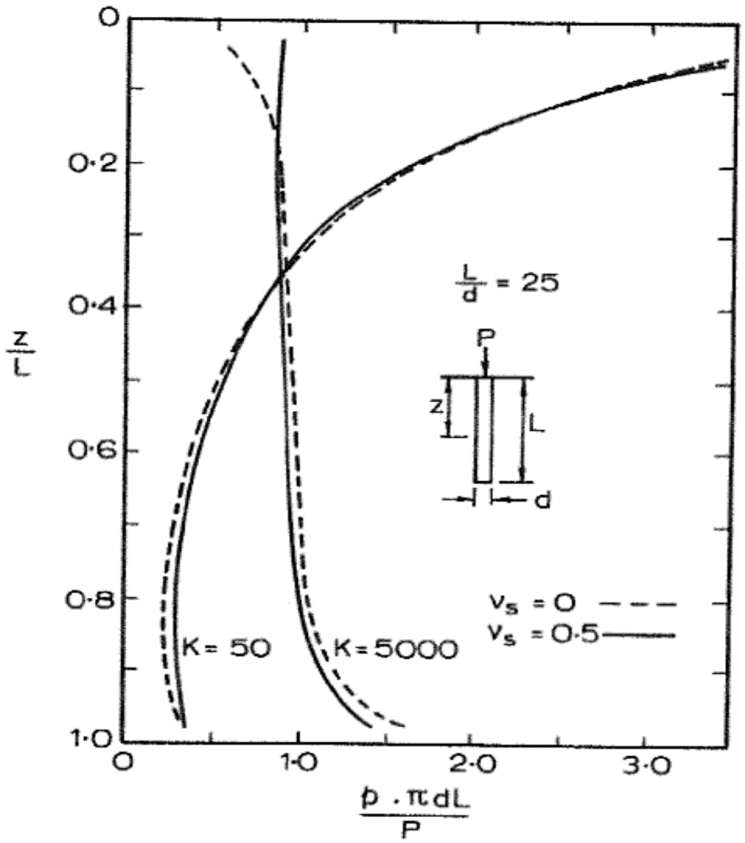


Figure 2.15: Shear stress distribution along a pile (after Mattes and Poulos, 1969)

2.7.6.2 Pile settlement

Mattes and Poulos conveniently expressed pile displacement in terms of dimensionless influence factors. Figure 2.16 below shows the displacement influence factor, I_ρ of the top of a compressible pile in an elastic half-space, for v_s=0.5, plotted against pile stiffness factor *K*, for various values of *L/d*. The actual pile settlement *S*, is given by:

$$S = \frac{P}{E_s L} I_\rho \qquad (3.15)$$

Where P is the applied vertical axial load, E_s is the Young's modulus of the soil and L is the pile length. From Figure 2.16, the influence of K on pile settlement is apparent and can be summarized as follows:

- For small values of L/d, $\boldsymbol{I_\rho}$ is almost independent of K over the range of K values under consideration.
- As L/d increases, the value of K has a greater influence on the pile settlement. The value of $\boldsymbol{I_\rho}$ increases significantly as K decreases. As an example, and referring to Figure 3.11, for a pile with $L/d=100$, a decrease in K value from $K=10000$ to $K=100$ results in an increase in settlement of about 278%. Thus, as L/d increases, the value of K at which the pile may be considered as incompressible increases.

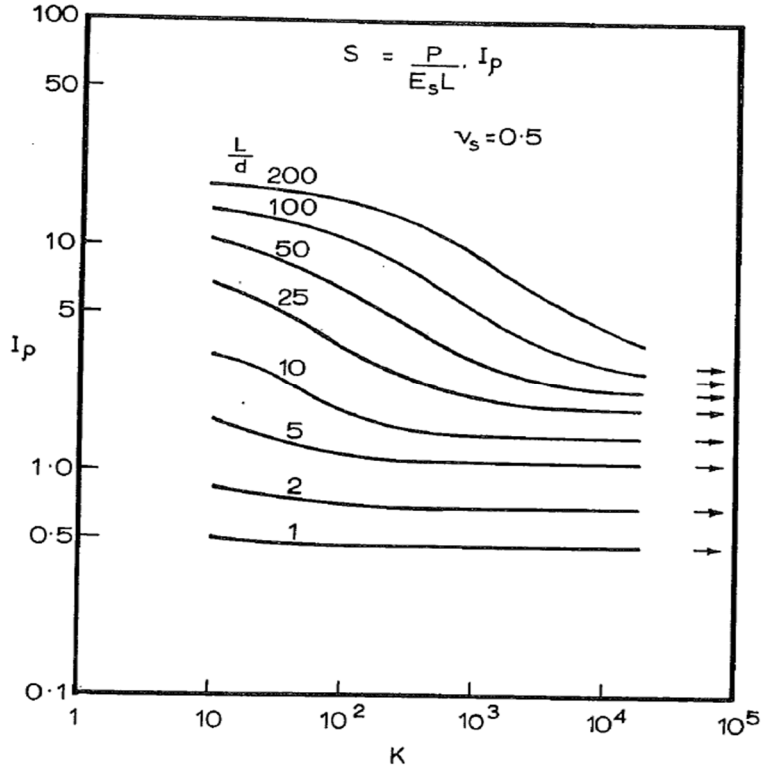


Figure 2.16: Settlement of the top of a compressible pile (after Mattes and Poulos, 1969)

The influence factors deduced from Figure 2.16 are for v_s=0.5 only. v_s=0.5 applies to the case of immediate pile settlement in a saturated clay. However, it has been established that the value of v_s has relatively little influence on the value of I_ρ. Although the influence factors for $v_s = 0$ are slightly less than for $v_s = 0.5$, the maximum difference has been established to be less than about 25%. For compressible piles, it is thus sufficiently accurate and also conservative, to use I_ρ values for $v_s = 0.5$ for all values of v_s. Mattes and Poulos also note that there is a decrease in top displacement and corresponding increase tip displacement of a pile with increasing pile stiffness coefficient K, and that for very compressible piles, the top displaces much more than the tip, but as K increases, the settlement of the head decreases while that of the toe increases.

2.7.6.3 Immediate settlement contribution to total final settlement

As is the case with an incompressible pile, the major portion of the total final settlement occurs

as immediate settlement for a compressible pile.

Mattes and Poulos also found that:

- Although there is a slight tendency for ρ_i/ρ_{TF} to decrease as K decreases, this ratio is nearly independent of K for high values of v_s, ρ_i and ρ_{TF} are the single pile settlement and total final settlement respectively.
- Even for the extreme case of a very compressible pile ($K=1$), in a soil with $v_s'=0$, ρ_i/ρ_{TF} is approximately 10% less than that for an incompressible pile.
- Immediate settlement is the most significant component of the total final settlement of a pile, even if the pile is very compressible.

2.7.6.4 Piles with enlarged base

Poulos and Davis (1968), found that an enlarged base only has significant influence on the settlement behavior of relatively short piles (piles with $\sim L/d<15$). Consequently, due to the effect of finite compressibility of a pile in reducing the load transmitted to the base of a conventional pile, it is inferred that the load transferred to the base of a pile with an enlarged base will similarly be reduced by the compressibility of the pile.

2.7.7 Butterfield and Banerjee (1971) method

Methods of settlement prediction suggested by Poulos and Davis (1968) and Mattes and Poulos (1969) analysed the effects of the pile length to diameter ratios, pile base enlargement, thickness of the elastic layer, pile compressibility, among other factors. Their analyses were based, in part, on the following assumptions, apart from that of ideal elasticity.

a) The pile shaft load was replaced by a uniform vertical shear stress on the surface of each of the n number of small cylindrical pile elements.
b) The pile base was assumed to be a smooth disc whose diameter is greater than the pile shaft diameter across which the base load was uniformly distributed.
c) The disturbance of the continuity of the elastic half space due to the presence of the piles was not taken into consideration.

Butterfield and Banerjee (1971) proposed a method which eliminated assumptions b) and c) above and show that assumption b) has a significant effect on the response of under reamed piles and very short plain piles. They further showed that significant errors occur in the calculated values of radial stress components in the vicinity of a loaded pile due to assumption c).

Pile displacements are obtained from pile compressibility considerations when the pile is axially loaded while soil displacements are obtained from Mindlin's equations for the displacement within a soil mass by loading within the mass. Figure 2.17(a) shows compressible pile displacement pattern where W is the vertical displacement of a pile of diameter, D, and length, L, under a vertical load, P. They produced a series of load-settlement curves for different values of $L/$D as shown in Figure 2.17(b). The graphs also show the effect of the compressibility ratio, $\boldsymbol{\lambda}$, on the load-displacement behavior of plain piles over a range of L/D ratios. The following significant features of the curve are notable:

1) The effects of $\boldsymbol{\lambda}$ are negligible for shorter piles (piles where L/D is smaller than 20)
2) The results converge to the rigid surface disc solution as L/D approaches zero.

[$\lambda = E_p/G$, where E_p is the Young's modulus of the pile material and G is the shear modulus of the half space material whose Poisson's ratio is equal to μ $(=v)$]

This report analyses the effect of pile base enlargement on settlement. Settlement behavior of under reamed piles with more than one bulb formed along the pile shaft, is not covered in this study.

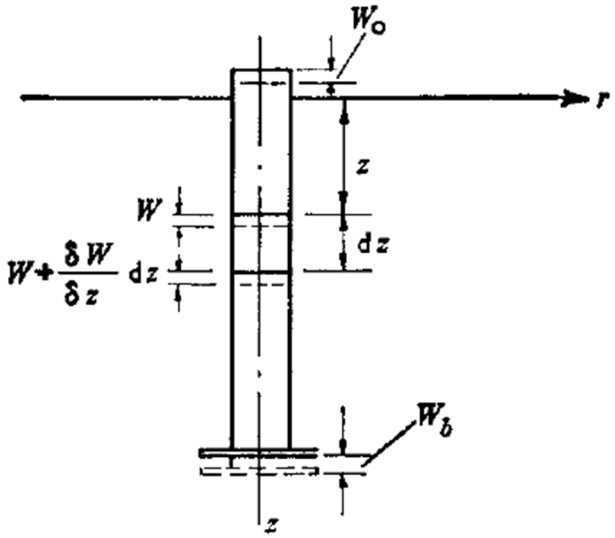


Figure 2.17(a): Compressible pile displacement pattern after Butterfield and Banerjee, (1971)

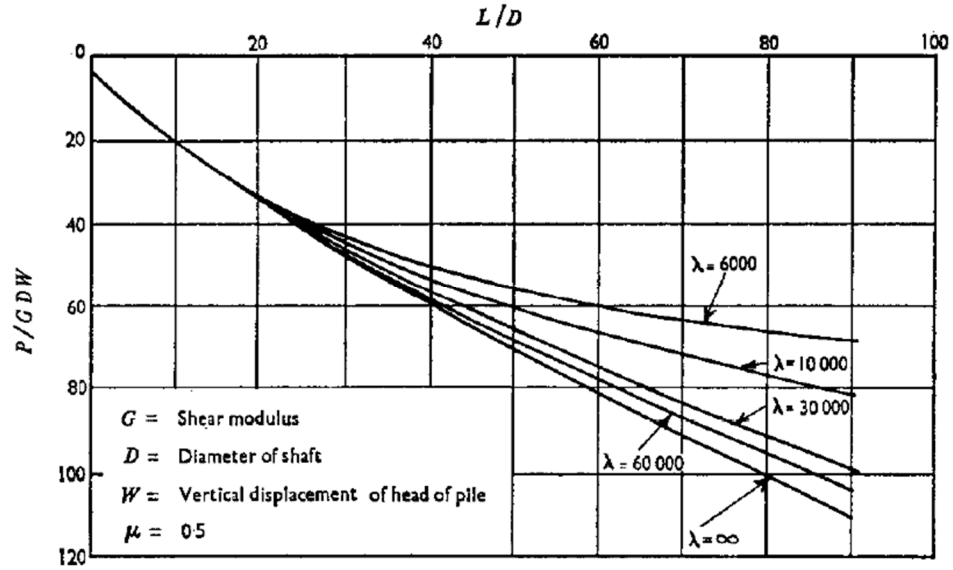


Figure 2.17(b): Load-displacement curves to determine settlement factor, f, for compressible piles (after Butterfield and Banerjee, 1971)

2.7.8 Vesic (1977) method

Vesic (1977) method is a semi-empirical procedure to predict the settlement of single piles and divides the settlement of single piles into three distinct parts, vis-à-vis:

- Settlement due to axial deformation/pile compression
- Settlement at pile base
- Settlement due to skin friction

2.7.8.1 Settlement due to axial deformation

It is not easy to accurately estimate the load distribution along the length of a pile as skin friction, acting along the pile shaft carries part of the load. In some cases, skin friction is so dominant such that very little load develops at the base of the pile. Axial compression of the pile is directly associated with the pile shaft load distribution.

The axial compression is calculated from the following semi-empirical expression:

$$S_a = \frac{(Q_b + aQ_s)L}{A_p E_p} \quad (2.16)$$

Where S_a = settlement due to axial compression of the pile, Q_b = load transferred to the pile at the base, a = 0.5 for clay soil (an empirical value), a = 0.67 for sandy soil (an empirical value), Q_s = total skin friction load, L is the length of pile, A = cross-sectional area of the pile and E_p = Young's modulus of the pile material

2.7.8.2 Settlement due to skin friction

The load transmitted to the base of the pile will cause the soil just under the pile base to settle.

Settlement at pile base, $$S_b = \frac{(C_p \mathrm{x} Q_b)}{D_0 q_0} \quad (2.17)$$

Where C_p = empirical coefficient, D_0 = pile diameter, q_0 = ultimate end bearing capacity, Q_b = point load transmitted to the soil at the pile base. Table 2.1 shows some typical values of the empirical coefficient, C_p.

Table 2.1: Typical values of C_p (Rajapakse, 2008, p.202)

Soil Type	Driven Piles	Bored Piles
Dense sand	0.02	0.09
Loose sand	0.04	0.18
Stiff clay	0.02	0.03
Soft clay	0.03	0.06
Dense silt	0.03	0.09
Loose silt	0.05	0.12

Note: Bored piles have higher C_P values compared to driven piles. Higher C_P values would result in higher settlement at the pile point.

2.7.8.3 Settlement due to skin friction

Skin friction, which acts in an upward direction along a pile shaft, will stress the surrounding soil when loaded. An equal and opposite force acts on the surrounding soil, meaning that the force due to the pile load on the surrounding soil would be in a downward direction.

When the pile is loaded, it moves down slightly, dragging the surrounding soil with it, thus causing pile settlement due to skin friction.

Settlement due to skin friction, $$S_s = \frac{(Cs \mathrm{x} Q_s)}{L q_0} \quad (2.18)$$

Where $C_s = (0.93+0.16 \mathrm{x} L/D_0)C_p$. C_s is an empirical coefficient, C_p = empirical coefficient from Table 3.1 above, Q_s = total skin friction load, L = length of pile of diameter, D_0.

Pile head settlement, $$S_h = S_a + S_s + S_b \quad (2.19)$$

2.7.9 Randolph and Wroth (1978) method

Randolph and Wroth described the analysis of a single vertically loaded rigid pile in detail. The analysis is based on an elastic soil characterised by a shear modulus *G*, which may or may not, vary with depth, and a Poisson's ratio, *v*. Consider a pile of radius, r_0 and a soil layer at radius r_m as depicted in plan in Figure 2.18. The soil which surrounds the pile is divided into two layers by an imaginary line AB, drawn at the base of the pile as shown in Figure 2.19.

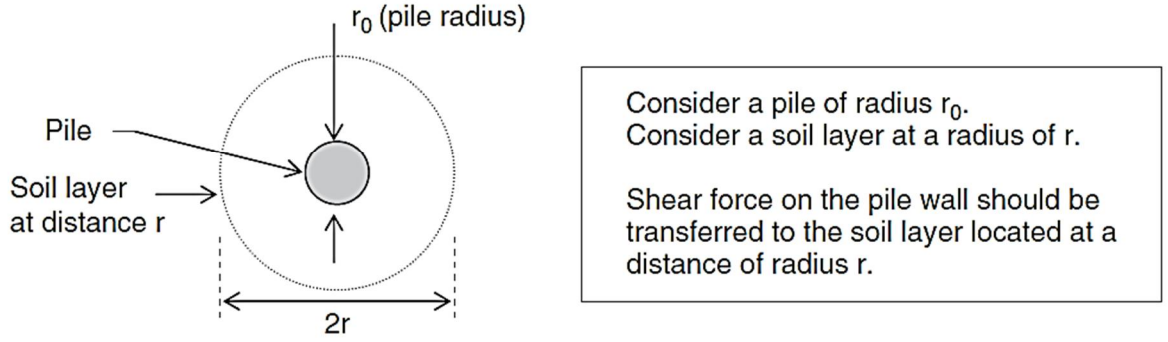


Figure 2.18: Plan view of the shear zone around a pile, r=r_m. Adapted from **Pile Design for Structural and Geotechnical Engineers** (p. 199) R. Rajapaske, 2007, Butterworth-Heinemann.

Initially, the soil above the line AB is assumed to be deformed by stresses transferred from the pile shaft while the soil below the line AB is assumed to be deformed by the stresses at the pile base only. However, there is an interaction between the upper and the lower layers. This interaction has the effect of limiting the deformation of the upper layer of the soil, reducing such deformation to negligible levels at some radius, r_m.

When the pile of radius r_0 is loaded by a vertical compressive load *Q*, the pile stresses the soil immediately next to the pile shaft leading to settlement of the soil in contact with the pile shaft. Soil particles further away from the pile experience less stress, implying that these soil particles settle less. This is in accordance with Saint-Venant's principle of diminishing stress with increasing distance from source of stress. Experimental work has shown that soil particles lying at some radius, $r_m \geq L$, the length of the pile, can be considered to be unstressed. In all the calculations involving it, r_m=L throughout this report.

Along the pile shaft, if the adhesive strength has not been exceeded at the pile-soil interface, the pile will impose a shear mode of deformation on the surrounding annuli of soil as shown in Figure 2.20. For the soil annulus to be in vertical equilibrium and assuming the shear stress between the soil particles and the pile shaft to be τ_0 (τ_0 is the average skin friction and the skin friction is dependent on the depth in sandy soil.), Shear force acting on a unit length of the pile = $\tau_0$xpile perimeter= $\tau_0 2\pi r_0$, where r_0 *(=D0/2)* is the radius of the pile. If τ_s is the shear stress of the soil at a distance r_m from the centre of the pile, then:$\tau_0 2\pi r_0 = \tau_s 2\pi r_m$

$$\Rightarrow \tau_s = \tau_0 r_0 / r_m \qquad (2.20)$$

In the case of piles, the stiffness is usually defined in terms of the shear modulus, *G*, instead of the Young's modulus. Shear modulus, G is defined as: *G* = shear stress/shear strain, and G is related to E by: $G = E/[2(1+v)]$, where *E* = Young's modulus and *v* = Poisson's ratio.

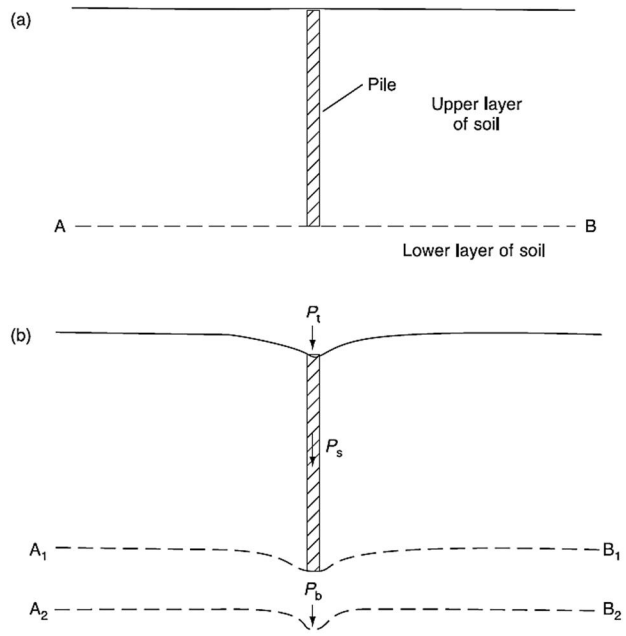


Figure 2.19: Uncoupling effects due to the pile shaft and pile base (a): Upper and lower soil layers, (b): Deformation patterns of lower and upper layers (after Randolph and Wroth, 1978). Adapted from **Settlement Analysis of Piles and Pile Groups,** Short Course in Soil-Structure Engineering, Part 1: Deep Foundations – Piles and Barrettes (p. 117), C.W.W. Ng, et al, 2004, ICE Publications.

Assume shear strain at radius, $r = \gamma, \Rightarrow \mathrm{G} = \frac{shear\ stress}{\text{shear strain}} = \frac{\tau_s}{\gamma} = \frac{\tau_0 r_0}{\mathrm{r}.\gamma}, \ \therefore \ \gamma = \frac{\tau_0 r_0}{\mathrm{r.G}}$

Assume the settlement at a radius r to be equal to *S*,

$\Rightarrow$ shear strain, $\gamma = \frac{dS}{dr}, \ \therefore dS = \gamma dr$, Hence, $S_s = \int_r^{r_1} \gamma dr = \int_r^{r_1} \frac{\tau_0 r_0}{\mathrm{r.G}} dr,$

$$\therefore \ S_s = \frac{\tau_0 r_0}{G} \ln\left(\frac{r_m}{r_0}\right), \text{ for } r_0 \leq r \leq r_m \qquad (2.21)$$

and $S_s = 0$ for $r_m > r$

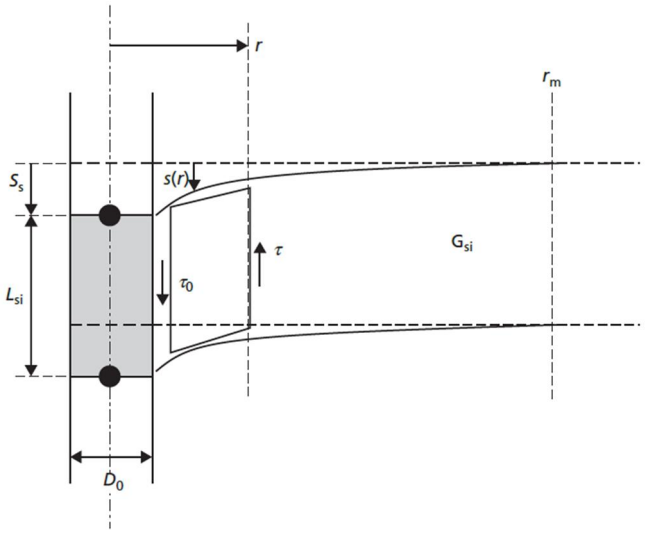


Figure 2.20: Equilibrium of soil around a settling pile. Adapted from **Craig's Soil Mechanics** (p.343), J.A. Knappett and R.F. Craig, 2012, Spon Press.

Where r_m is the influence zone radius which varies with type of soil and pile diameter. In this report, r_m is taken as equal to the pile length, L_p and is the value of r_m adopted in all calculations. Shear stress beyond the distance r_m (=L_p) is vanishingly small. Therefore the settlement of the pile shaft may be written as:

$$S_s = \zeta \frac{\tau_0 r_0}{G}, \text{ where } \zeta = \ln(r_m/r_0) \qquad (2.22)$$

The above approximate derivation of the pile shaft settlement in terms of τ_0 shows the following important features of pile response to axial loading:

1) Stress changes induced in the soil are mainly in shear, decreasing inversely with distance from the pile axis. Therefore, only soil very close to the pile shaft is going to be highly stressed.
2) The resulting deflections decrease with the logarithm of distance from the pile axis, thus significant deflections extend for some distance away from the pile, up to approximately one pile length.
3) The deflection (settlement) of the pile shaft, S_s, normalised by the pile radius, r_0, is ζ times the local shear strain, τ_0/G, in the soil. The parameter ζ, is found to vary between 3 and 5, with an average value of 4 (Baguelin and Frank, 1979 as cited in Ng, Simons, and Menzies (2004)).

Equation 2.22 is particularly important to deduce the magnitude of settlement necessary to mobilise full shaft friction. It can been proven that full shaft friction will be mobilized for local displacements in the range of 1-4% of r_0, by substituting limiting values of τ_0 into Equation 2.22.

From Figure 2.20 the force along the pile shaft which results in settlement,
$S_s = \frac{\tau_0 r_0}{G} \ln(\frac{r_m}{r_0})$, is given by:

$$Q_s = 2\pi r_0 L_{si} \tau_0 \qquad (2.23)$$

If a compressive load P (kN) is applied to a pile resulting in a pile settlement of say y (m), Stiffness of pile-soil system = P/y. From elastic theory settlement analysis and with the definition of soil-pile stiffness defined above, soil-pile shaft stiffness, $K_s = \frac{Q_s}{S_s}$, $\Rightarrow K_s = \frac{Q_s}{S_s} = 2\pi r_0 L_{si} \tau_0 G/[\tau_0 r_0 ln(r_m/r_0)]$

$$K_s = \frac{2\pi L_{si} G}{\ln(\frac{r_m}{r_0})} \qquad (2.24)$$

Similarly, $K_b = Q_b/S_b$, where Q_b is the load carried at the pile base and s_b is the settlement of the pile base. For a circular pile assumed to be rigid at its base, as L_p/D_0 is very large, the pressure, q, at the base of the pile is given by:

$q = Q_b/A_p = 4Q_b/\pi D_0^2$,

$s_b = qD_0(1-v^2)I_s/E_s$, $E_s = G/[2(1+v)]$.

From Table 2.2, the influence factor, $I_s = 0.79$, for circular and rigid.

$\Rightarrow s_b = 4Q_b D_0(1-v^2)I_s/2\pi D_0^2 G(1+v) = 2Q_b(1-v)I_s/\pi D_0 G$, since $(1-v^2)=(1-v)(1+v)$

$K_b = Q_b/s_b = Q_b/2Q_b(1-v)I_s x\pi D_0 G = \pi D_0 G/2x0.79(1-v) = 2D_0 G/(1-v)$

$\therefore$ for a circular pile $K_b = \frac{4r_0 G}{(1-v)} = \frac{2D_0 G}{(1-v)}$ (2.25)

For a square pile assumed to be rigid at its base, the pressure, q, at the base of the pile is given

by: $q = Q_b/B_p^2$, where B_p is the square pile dimension. From Table 2.2, the influence factor, $I_s = 0.82. \Rightarrow K_b = Q_b/s_b = 2B_pG/[I_s(1-v)]$

$\therefore$ for a square pile $$K_b = \frac{2.44B_pG}{(1-v)} \quad (2.26)$$

Table 2.2: Influence factors, I_s' for vertical displacement under flexible and rigid areas carrying uniform pressure. (Knappett and Craig, 2012, p.301)

Shape of area		***I_s(flexible)***			***I_s (rigid)***
		Centre	***Corner***	***Average***	***Average***
Square	(L/B=1)	1.12	0.56	0.95	0.82
Rectangle	L/B=2	1.52	0.76	1.30	1.20
Rectangle	L/B=5	2.10	1.05	1.83	1.70
Rectangle	L/B=10	2.54	1.27	2.25	2.10
Rectangle	L/B=100	4.01	2.01	3.69	3.47
Circle		1.00	0.64	0.85	0.79

Randolph and Wroth (1978) analytical method of determining pile head settlement is applicable to rigid piles, where the settlements are the same all the way along the pile, i.e.: $S_s = S_b = S_r$ where S_r is the overall settlement at the top of the rigid pile. The applied load at the top of the rigid pile, $Q = Q_b+Q_s = K_bS_r+K_sS_r = S_r(K_b+K_s)$

$$\therefore S_r = \frac{Q}{(K_b+K_s)} \quad (2.27)$$

Where K_s and K_b are the stiffness of the soil along the pile shaft and at the pile base, defined by Equations 2.24 and 2.25/2.26 respectively.
In Figure 2.19, the pile base acts as a rigid punch on the surface of the lower layer of the soil. According to Timoshenko and Goodier (1970, as cited in Ng et al. (2004)), the settlement of the pile base is given by Boussinesq (1885) solution, i.e.:

$$s_b = \frac{Q_b(1-v)}{4r_oG} \quad (2.28)$$

According to Saint-Venant principle, the difference between the effects of two different statically equivalent loads becomes very small, hence, negligible, at sufficiently large distances from the load. Therefore, at some distance from the base of the pile, the loading can be assumed to be a point load. The settlement around a point load decreases inversely with radius and is given by:

$$s_r = \frac{Q_b(1-v)}{2\pi rG} \quad (2.29)$$

The ratio of the settlement, S_r (Equation 2.29) to the settlement of the pile base S_b, (Equation 2.28) for a given load is:

$$\frac{s_r}{s_b} = \frac{\frac{Q_b(1-v)}{2\pi rG}x4r_0G}{Q_b(1-v)} = \left(\frac{2}{\pi}\right)\frac{r_0}{r} \quad (2.30)$$

Again, from Saint-Vanant principle the settlement caused by the pile base at a large radius should be equal to that due to a point load. Therefore the settlement profile at the top of the lower layer of the soil in Figure 2.19 may be approximated as follows:

$$s_r = s_b \frac{2}{\pi}\frac{r_0}{r} = c.s_b \frac{r_0}{r}, \text{ where } c = \pi/2 \qquad (2.31)$$

The profile of Equation 2.31 is found to be in close agreement with the true settlement profile around a rigid punch which is shown in Figure 2.21, from where it is evident that the agreement is excellent, particularly for $r>2r_0$. It can also be seen from Figure 2.21 that the effect of the base loading falls off more rapidly than that of the shaft loading as given by Equation 2.21.

For a rigid pile, shaft settlement is the same along the pile and equal to the pile base settlement. According to Franki (1974, as cited in Ng et al. (2004)), the shear strain in the soil next to the pile shaft can be assumed to be constant with depth. This implies that the average shear stress τ_0, is proportional to the shear modulus at that depth. For soils whose shear modulus varies proportionally with depth, a factor, ρ, which defines the degree of homogeneity, is defined by:

$$\rho = \frac{G_{1/2}}{G_1} \qquad (2.32)$$

Where $G_{1/2}$ is the shear modulus at the pile mid-point and G_1 is the soil shear modulus at the pile base. In layered soil, the equivalent shear modulus, G_{eq}, is the weighted harmonic mean of the individual layers' shear moduli.

The total load transferred to the soil from the pile shaft may, after manipulation of Equations 2.21 and 2.32, be written in the following form: $Q_s = 2\pi r_0 L_p \tau_0 = 2\pi L_p \frac{s_s}{\zeta} G_{1/2}$, But $G_{1/2} = \rho G_1$ and $\zeta = \ell n(r_m/r_0)$. $\therefore\ Q_s = 2\pi L_p \frac{s_s}{\zeta} \rho G_1 \qquad (2.33)$

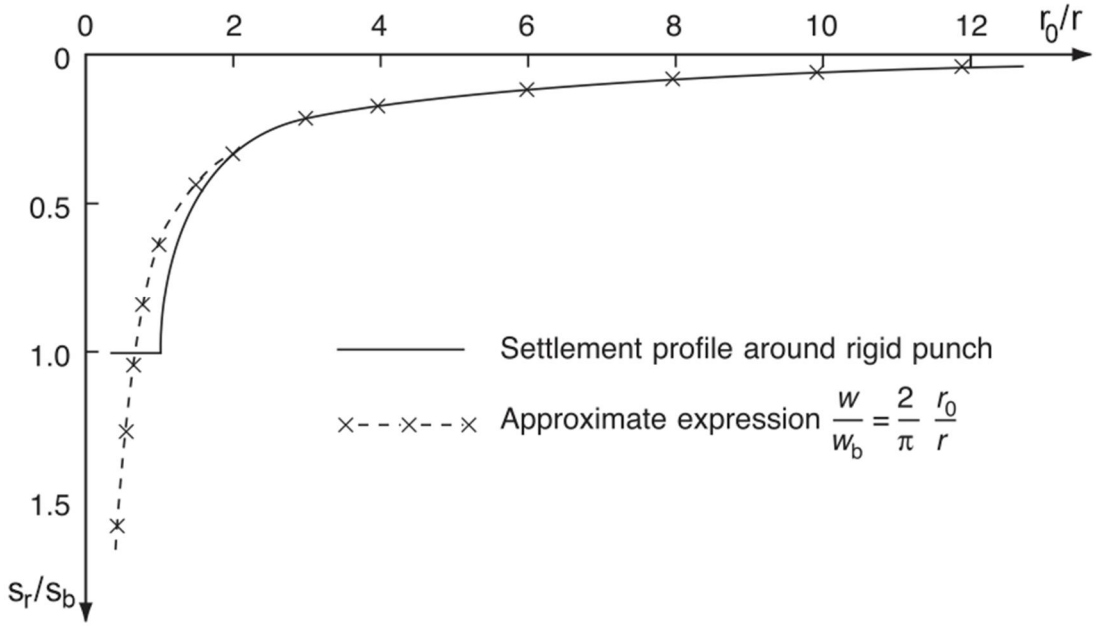


Figure 2.21: Comparison of actual and approximate surface settlement profiles for a rigid punch (after Randolph and Wroth, 1978)

The overall load-settlement ratio for a rigid pile can thus be written as follows:

$$\frac{Q}{G_1 r_0 s_r} = \frac{Q_b}{G_1 r_0 s_b} + \frac{Q_s}{G_1 r_0 s_s} = \frac{4}{(1-\nu)} + \frac{2\pi\rho L_p}{\zeta r_0} \qquad (2.34)$$

Equation 2.34 has been found to be in close agreement with results from finite element and

integral-equation analyses. Randolph (1977) and Randolph and Wroth (1978) determined that the suitable value of the maximum radius, r_m, beyond which settlement is negligible, is defined by:

$$r_m = 2.5\rho L_p(1-v) \quad (2.35)$$

However, for all calculations in this report, r_m=L(=L_p), where L is the pile length..
Figure 2.22 shows a comparison of results obtained from Equation 2.34 and corresponding integral-equation analysis results (Banerjee, 1970, as cited in Ng et al. (2004)) for a rigid pile in an incompressible and homogeneous soil. There is a very good agreement of results over a significant range of L_p/r. L_p/r defines the pile's slenderness ratio.

The solution given by Equation 2.34 may be extended to compressible piles and with minor modifications, to under-reamed piles and end bearing piles. According to Randolph and Wroth, the maximum radius of influence r_m, would need to be reduced for end bearing piles.
If the pile is compressible, i.e., not rigid, $S_s \neq S_b \neq S_r$ and the equation 2.28, no longer holds. Randolph and Wroth (1978), present a rather sophisticated solution for settlement computation of compressible piles. The T-z method is therefore generally used to estimate settlement of compressible piles as it is considered easier to apply. The T-z method has been covered under section 2.7.3 of this paper.

The Randolph and Wroth (1978) approach is expressed in a closed form (a mathematical expression stated using a finite number of standard operations) and is therefore, in that closed form, very convenient for spreadsheet and mathematical programming. However, the approach has a number of limitations, in particular, the assumptions that the soil is elastic, the soil stiffness increases linearly with depth along the pile shaft and that the pile shaft is of uniform diameter

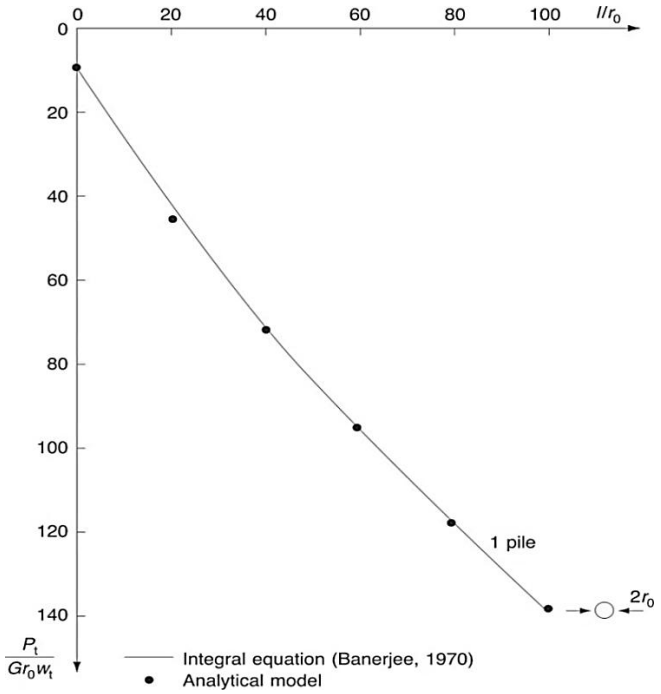


Figure 2.22: Comparison of Equation 3.30 results and corresponding results obtained by Banerjee (1970) integral equation analysis (after Randolph and Wroth, 1978)

2.7.10 Poulos and Davis (1980) method

Poulos and Davis (1980) suggested an elastic-based solution applicable to both floating and

end bearing piles. They expressed the settlement of the top and the tip of the pile in terms of the settlement of an incompressible pile in a half-space with correction factors for:

a) Pile compressibility
b) Finite depth of layer on rigid base
c) Soil's Poisson ratio, v_s
d) Total depth of soil layer

A homogeneous soil mass with a constant Young's modulus, E_s and Poisson's ratio, was assumed.

2.7.10.1 Floating pile:

The settlement of a pile head, ρ, is given by:

$$\rho = \frac{PI}{dEs} \tag{2.36}$$

Where $I = I_0 R_k R_h R_v$

I_0 is the settlement-influence factor for an incompressible pile in semi-infinite mass for v_s=0.5, R_k is the correction factor for the compressibility of a pile, R_h=correction factor for layer for finite depth layer on a rigid base, R_v = correction factor for Poisson's ratio and
d (=D_0) is the diameter of the pile.

The values of I_0, R_K, R_h and R_v are obtained from graphs shown in Figures 2.23 – 2.26. In Figure 2.23, d_b is the diameter of an enlarged base where applicable and it can be observed that there is a decrease in the settlement of a pile of constant diameter as the length of the pile increases. Poulos and Davis (1968) also observed that settlement decreases in the presence of an enlarged pile base, although the effect is only significant for relatively short piles. Figure 2.24 demonstrates that pile compressibility leads to an increase in pile settlement, particularly for slender piles, while the effect of a finite layer is to decrease the settlement as depicted in Figure 2.25. Figure 2.26 shows that a decrease in Poisson's ratio, v_s with Young's modulus, E_s being constant, leads to a decrease in settlement. However, the influence of v_s is relatively mild.

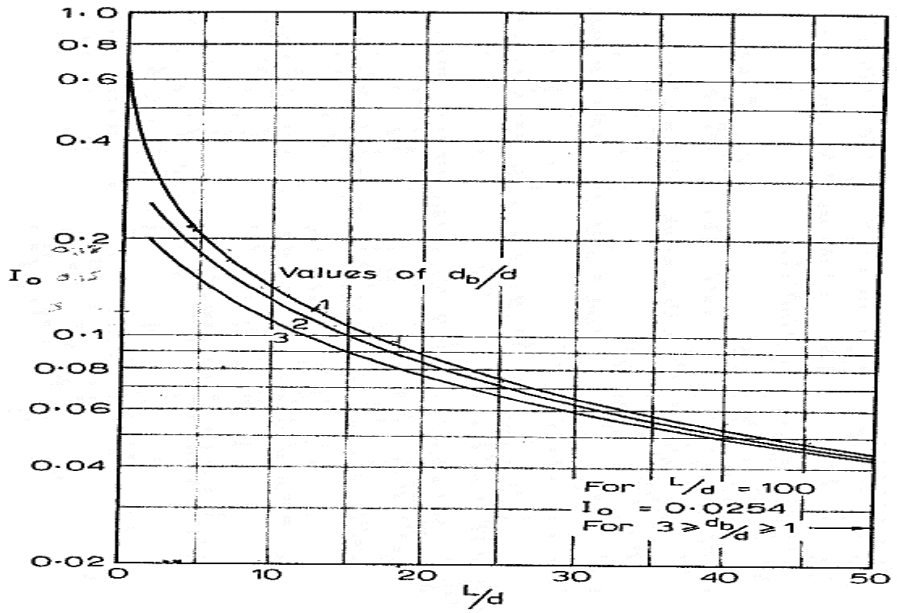


Figure 2.23: Determination of settlement influence factor I_0 (after Poulos and Davis, 1980)

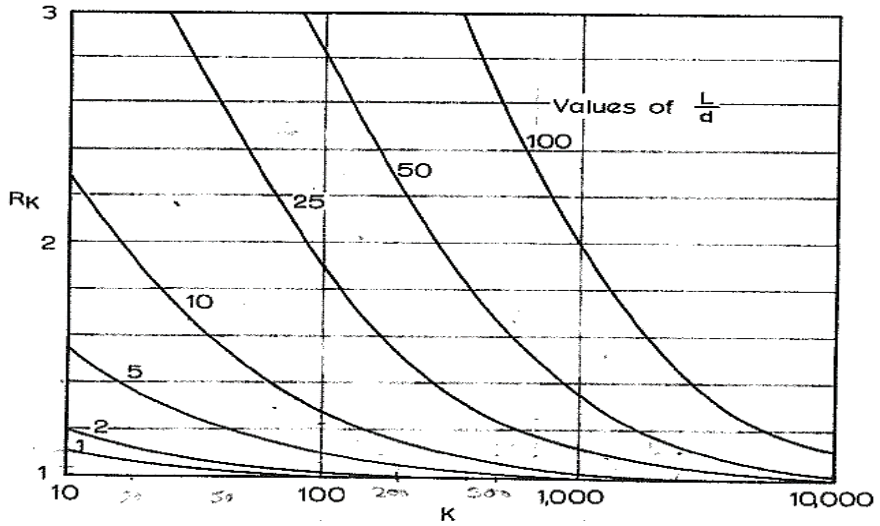


Figure 2.24: Correction factor for pile compressibility, R_k

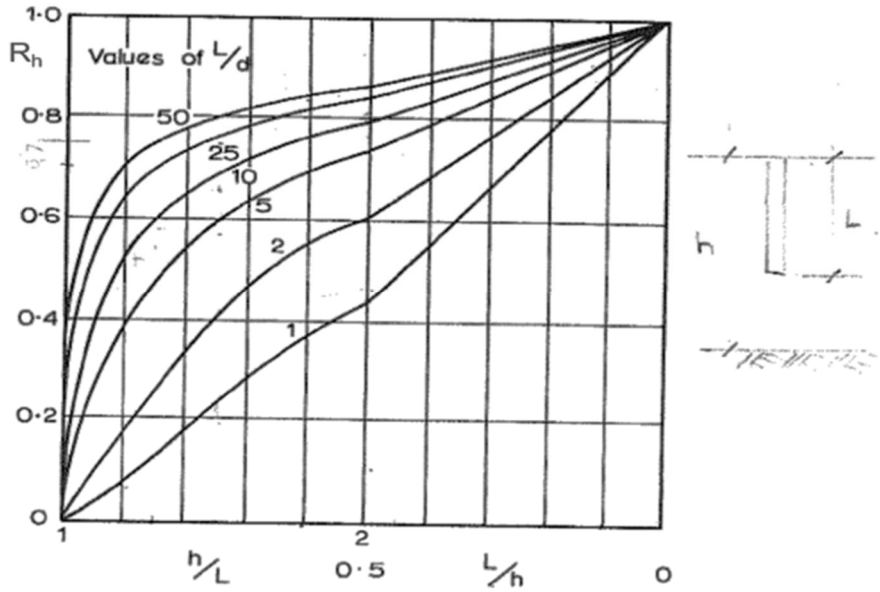


Figure 2.25: Depth correction factor for settlement, R_h

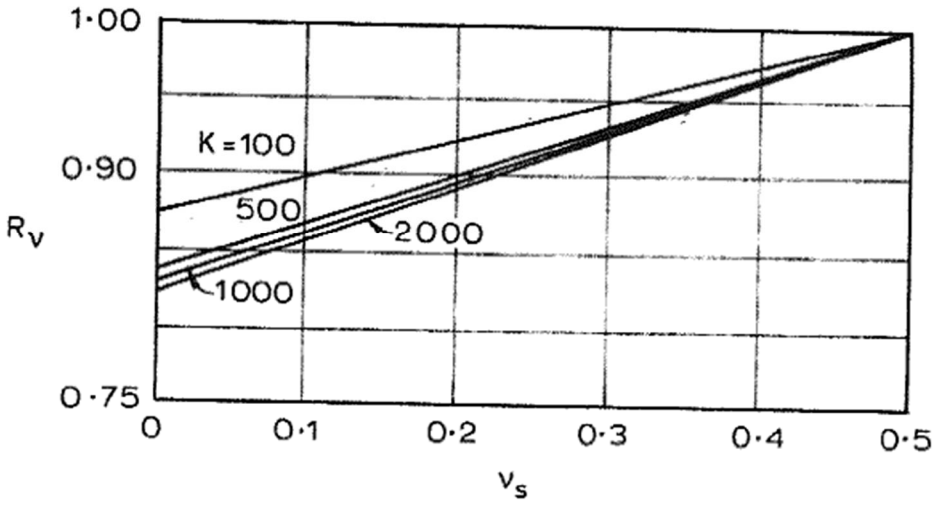


Figure 2.26: Poisson's ratio correction factor for settlement, R_v

2.7.10.2 End bearing pile

The pile is assumed to be on stiffer stratum and $L=h$ – refer to sketch in Figure 2.25. The settlement, ρ, of the pile is given by:

$$\rho = \frac{PI}{dEs} \tag{2.37}$$

Where $I = I_0 R_k R_b R_v$

I_0, R_k, and R_v have the same definition as that for floating piles given above and obtained from Figures 2.23, 2.24, and 2.26 respectively, R_b = correction factor for stiffness of bearing stratum. Values of R_b are obtained from Figure 2.27. The bearing stratum has the effect of reducing pile settlement, such effect being more pronounced for relatively short piles on a stiff bearing stratum. For notably slender piles (piles for which $L/d \geq 100$), the bearing stratum has insignificant influence on settlement of a pile because $R_b \approx 1$ for most practical values of pile stiffness factor, K.

The expressions of settlement in both Equations 2.36 and 2.37 give approximate values of settlement because some of the effects are assumed to be mutually independent. As an example, the effect of finite layer depth is assumed to be independent of pile stiffness factor, K, though this is not necessarily, strictly, correct. However, the use of correction factors is deemed to render results accurate enough for practical purposes.

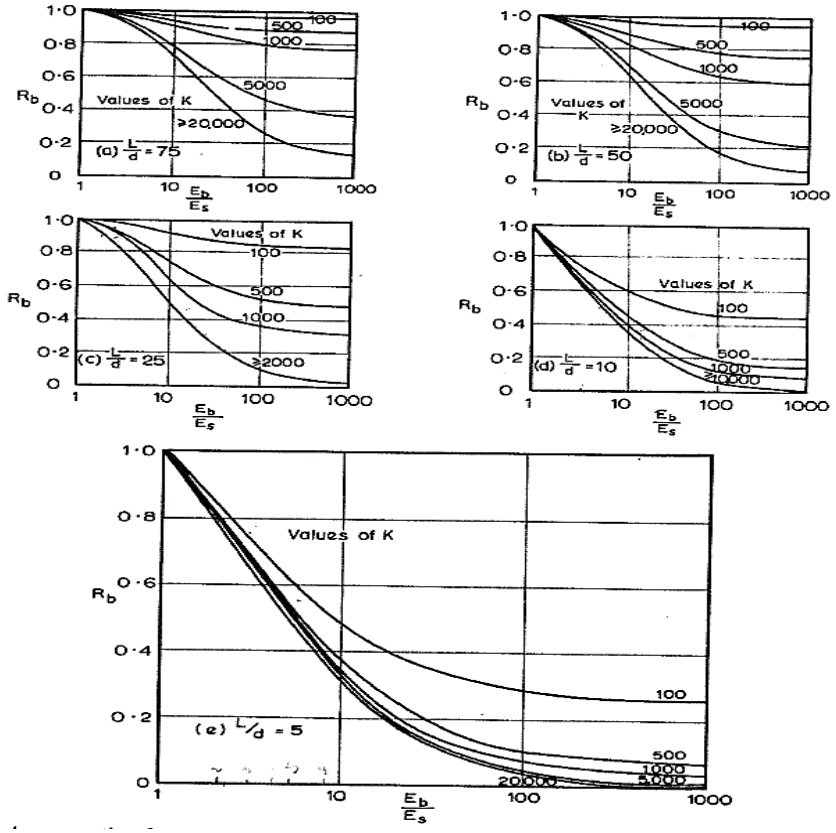


Figure 2.27: Pile base modulus correction factor for settlement, R_b (after Poulos and Davis, 1980)

2.7.11 Poulos (1989) method

Poulos develops a solution for the elastic settlement for a single pile using continuum analysis. With this approach, it is only possible to derive proper results for much idealized problems that

involve linear soil behavior and one- or two-layer elastic soil masses. An implicit assumption in the elastic continuum analysis is that: if incremental tensile stresses are developed in the soil mass from loading of the pile, the soil continues to respond elastically. This is a reasonable assumption if the overall stress conditions remain compressive due to the compressive overburden stresses.

2.7.11.1 Pile settlement behaviour

Sometimes, the finite element method is used to evaluate the soil displacement factors in order to extend the range of problem for which proper results can be derived, but the sophisticated nature of the data required in finite element analysis solution is not normally available from conventional site investigation. The finite element method is complicated, costly and time-consuming. Poulos' solutions have been obtained from boundary element analysis based on elastic continuum theory, with an elastic or elastic-plastic interface model using simplified distributions of the soil's Young's modulus and shaft resistance with depth, which may be constant or increasing linearly. The boundary element analysis was chosen as a reasonable compromise between excessive complexity of the finite element method and unacceptable simplicity of the empirical methods. The settlement of a single pile is mainly governed by the following parameters which are dimensionless:

a) The length to diameter ratio, L/d.
b) The pile stiffness factor, K, being the ratio of the Young's modulus of the equivalent solid pile section, E_p, to the Young's modulus of the soil, E_s, i.e.: $K=E_p/E_s$.
c) The ratio of the Young's modulus of the bearing stratum, E_b, at the pile base to the Young's modulus of the soil, i.e.: E_b/E_s.

The immediate settlement, S_e, of a floating pile is given by:

$$S_e = \frac{PI_\rho}{dE_s} \tag{2.38}$$

Where I_ρ is an influence factor dependent on L/D ratio and pile stiffness factor, K. $K=E_p/E_s$. P is the applied axial load.

Figure 2.28 shows the influence of parameters L/d and K on single floating pile from where it can be deduced that the settlement decreases as L/d and K increase. This was confirmed by experimental evidence presented by Butterfield and Ghosh (1977, as cited in Poulos, 1989). The soil mass under a pile is subjected to compression from end bearing. However, for friction piles, the settlement due to end bearing is small compared to that due to skin friction and is often ignored.

The elastic shortening of the pile, S_p, is determined from column theory, which, for a pile embedded in a homogeneous soil, is given by:

$$S_p = \frac{PLC}{E_p A_p} \tag{2.39}$$

Where C is the reduction factor to account for the fact that the vertical strain decreases with the embedded length of the pile. For most soils, $C\approx0.5$, but for soft clay soils, $C\approx0.7$. Elastic shortening is only significant for slender piles (piles for which $E_p/E_s<500$). Therefore total immediate settlement, S_{et}, for a floating pile, is given by: $S_{et}=S_e+S_p$

$$\Rightarrow \quad S_{et} = \frac{PI_\rho}{dE_s} + \frac{PLC}{E_p A_p} \tag{2.40}$$

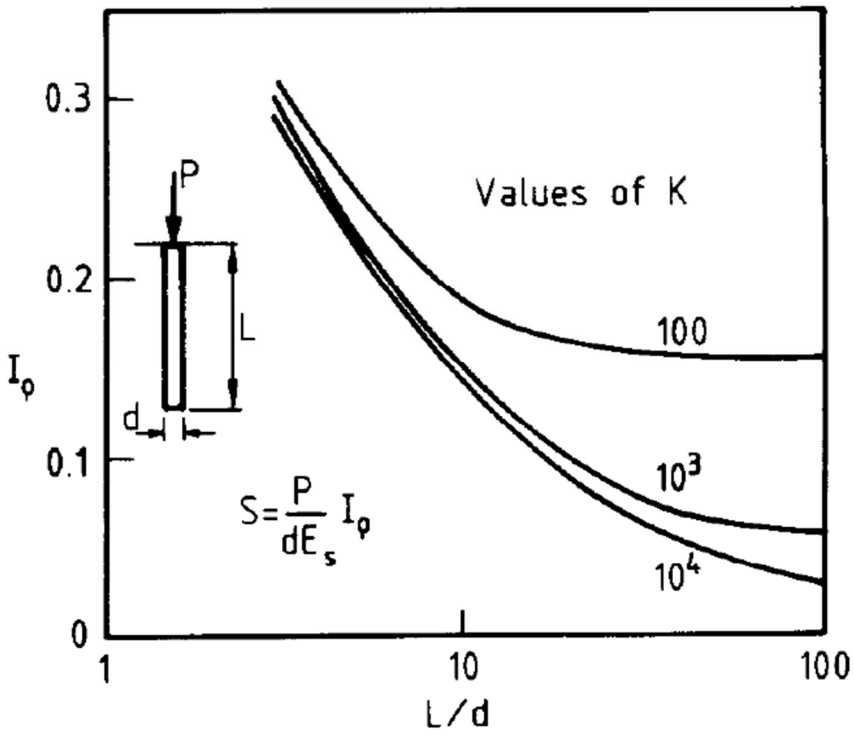


Figure 2.28: Influence factor for settlement of a single floating pile (after Poulos, 1989)

Poulos also found that a slender and/or compressible pile settlement is not substantially influenced by the nature of the bearing stratum by comparison of the settlement of an end bearing pile and a friction pile for the same value of pile stiffness factor, *K=1000*. It was found that that for *L/d>~50*, the reduction in settlement due to the bearing stratum is less than 40%, even for a bearing stratum which is much stiffer than the overlaying soil. This implies that there would be little to be gained by founding a pile base on a stiffer stratum if reduced settlement is desirable for long piles. It was thus concluded that increasing the pile diameter and/or pile stiffness is likely to produce desirable effects. It follows, therefore that there is a critical length for a friction pile in a homogeneous soil, beyond which any further increase in pile length does not result in any more reduction in settlement. This critical length L_c, normalised to the pile diameter d, (or width), is given by Hull (1987) as in Equation 3.43 below, noting that $K = E_p/E_s$, A_p is the cross-sectional area of the pile of diameter, *d*.

$$\mathrm{L_c/d} = \sqrt{(\pi E_p A_p / E_s d^2)} = \sqrt{(\pi K A_p / d^2)} \tag{2.41}$$

Poulos also noted that pile settlement and load transfer are also influenced by the distribution of the soil's Young's modulus along the pile shaft and that for a typical floating pile in two different soils, the influence of distribution of the soil's Young's modulus:

- For the homogeneous soil, the shear stress distribution is comparatively uniform with depth.
- For the Gibson soil, shear stress increases with depth, a Gibson soil being an elastic soil in which the soil modulus increases linearly with depth from zero at surface.

2.7.11.2 Settlement proportions

Poulos (1989) found that the bigger portion of total final settlement of a single pile is immediate settlement which occurs on application of the load because the load is transferred to the soil by shear, essentially, with relatively little change in mean stress, i.e.: the majority of settlement of a single pile is from shear deformation rather than volumetric deformations. For values of Poisson's ratio, $v_{s'}$, of an effective soil skeleton of the order of 0.3-0.4, and practical values of L/d, theory suggests that the ratio, S_i/S_{TF} of immediate to total final settlement of a pile in a homogeneous soil, is more than 0.90 and almost independent of L/d. Mattes and Poulos (1971) proved this theoretical conclusion through their model tests on brass piles in kaolin and Whitaker and Cooke (1966) through their sustained loading field tests. Theory also has it that at normal working loads (of the order of 0.4-0.5P_u, where P_u is the ultimate load), non-linear behavior of soil does not, generally, have significant effect on single pile settlement. Model tests by Butterfield and Abdrabbo (1983, as cited in Poulos (1989)) supported this theoretical conclusion.

2.7.12 Fleming (1992) method

The finite element method's complexity makes it not possible for regular practical applications. Therefore there remained the need for a simpler approach that could be easily correlated with site experience and common parameters that Geotechnical Engineers are familiar with, hence Fleming (1992) uses the hyperbolic model to analyse and predict the settlement at the top of a single pile under sustained loading. Chin (1970) popularised the method of plotting the behaviour of both footings and piles according to the hyperbolic method, such that most Geotechnical Engineers are aware of the use of the hyperbolic function for the back-analysis of the pile load-settlement curve. This method was widely adopted though it was not linked with soil parameters but was rather used for defining ultimate loads. Fellenius (1980) has drawn attention to the fact that Chin's method tends to overpredict but acknowledges that there is little doubt that in most cases, depending on the plotting method, linear functions represent pile performance very well.

Initially suggested by Chin (1970, 1972) and Vail (1973, as cited in Fleming, 1992), it is generally accepted that plot A represents shaft friction while plot B represents total load in Figure 2.29. Though not precise due to the nature of hyperbolic functions, it is easily accepted that individually, shaft and base performance are of hyperbolic form.

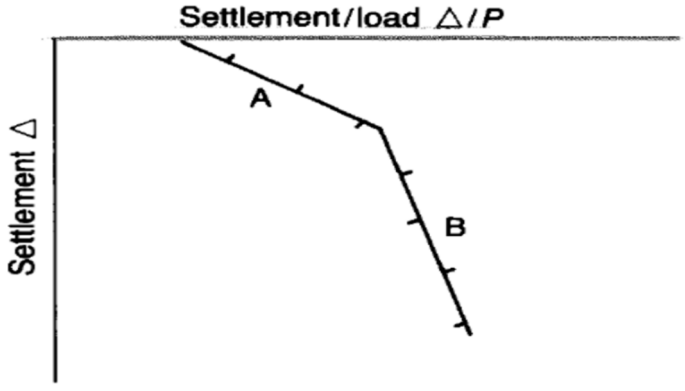


Figure 2.29: Variation of settlement, Δ and settlement/load, Δ/P (after Fleming, 1992)

Fleming once remarked that settlement forecasting is perhaps the most important aspect of pile design and is complicated by structural stiffness, pile load redistribution, construction techniques, group effects, among other factors. Settlement control normally governs in pile

design because if the performance of a single pile cannot be adequately predicted, it presents some challenges as many specifications would be difficult to comply with in the absence of some understanding of the mechanisms involved.
Figure 2.30 below represents a typical plot as used by Chin when considering a rigid pile. The gradient of plot A represents ultimate shaft friction, U_s, while that of plot B represents the ultimate end bearing, U_b. Gradient of line A=U_s=Change in verticals/Change in horizontals

$$\therefore\ U_s = \frac{\Delta_s}{\frac{\Delta_s}{P_s} - K_s} \tag{2.42}$$

Rearranging Equation 2.42 to make Δ_s the subject of the formula gives: $U_s\left(\frac{\Delta_s}{P_s} - K_s\right) = U_s$; $\Rightarrow \frac{U_s\Delta_s}{P_s} - U_sK_s = \Delta_s;\ \Rightarrow \frac{\Delta_s(U_s}{P_s} - 1) = U_sK_s$; which yields

$$\Delta_s = \frac{K_sU_sP_s}{U_s - P_s} \tag{2.43}$$

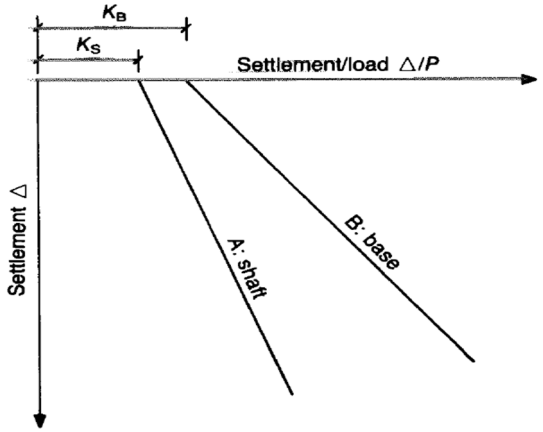


Figure 2.30: Individual base and shaft performance (after Fleming, 1992)

Similarly, the base performance is expressed as follows:

$$\Delta_b = \frac{K_bU_bP_b}{U_b - P_b} \tag{2.44}$$

Where Δ_s is the settlement of the pile shaft head at any load P_s, Δ_b is the base settlement at load P_b. Δ_b for rigid piles also equals the settlement at the pile head, K_s and K_b are intercepts of plot A and plot B on the horizontal axis respectively. K_b and K_s are also related to the base resistance Q_b and shaft resistance, Q_s through the following: $P_b = \frac{\Delta_b}{K_b + \frac{\Delta_b}{P_b}}$; $P_s = \frac{\Delta_s}{K_s + \frac{\Delta_s}{P_s}}$ or $q_s = \frac{\Delta_s}{K_s + \frac{\Delta_s}{q_s}}$, where Q_{bu} or q_{bu} = ultimate pile base resistance, total or unit value, Q_{su} or q_{su} = ultimate pile shaft resistance, total or unit value

2.7.12.1 Shaft friction and settlement

According to Fleming (1992), experimental evidence has shown that the settlement of a pile shaft is a direct function of the pile diameter, D_s. Further, a considerable number of studies also indicate that K_s is an inverse function of U_s, which means that the settlement for a given load

decreases with increasing ultimate shaft load, i.e.:

$$K_s = \frac{M_s D_s}{U_s} \tag{2.45}$$

Where M_s is a dimensionless flexibility factor in the form of an angular rotation. Substituting this value of K_s into Equation 2.43 gives the following: $\Delta_s = \frac{K_s U_s P_s}{U_s - P_s} = \frac{M_s D_s U_s P_s}{U_s(U_s - P_s)}$

$$\Rightarrow \Delta_s = \frac{M_s D_s P_s}{U_s - P_s} \tag{2.46}$$

Where M_s is, in fact, the tangent slope at the origin of the hyperbolic function representing shaft friction.

Randolph (1991) indicated that M_s is the equivalent of $\zeta \frac{\tau_0 r_0}{G}$, where $\zeta = \ln(r_m/r_0)$ in a slight variation of the Randolph and Wroth (1978) notation, where r_m is the radius at which soil settlement is negligible, r_0 is the radius of the pile, τ_0 is the shear stress at the pile surface and G is the shear modulus of the soil. According to Randolph and Wroth, $500 \leq G \leq 2000$, hence M_s would be expected to have a value in the range of 0.001 to 0.004.

2.7.12.2 Pile base load and settlement

The settlement of a circular footing is usually expressed as:

$$\Delta_b = \frac{\pi q D_b}{4E_b}(1 - v^2) f_1 \tag{2.47}$$

Which reduces to:

$$\Delta_b = \frac{0.6075 q D_b}{E_b} \tag{2.48}$$

When v=0.3 and f_1=0.85 which are the average values. E_b is the deformation secant modulus of the soil beneath the pile base, q is the stress due to the applied load at the base, Δ_b.is the base settlement, D_b is the pile base diameter, v is the Poisson's ratio and f_1 is a standard settlement reduction factor related to the foundation depth, being directly proportional to increasing load for a specific foundation.

The secant modulus (used to describe the stiffness of soil in the inelastic region of the stress-strain curve) from a load-settlement relationship is usually evaluated at 25% of the ultimate stress in a non-linear relationship. Therefore, if, at a load $P_b = U_b/4$, and equating Equations 2.44 and 2.48, K_b can be determined at the point where the hyperbolic and the linear functions intersect, i.e.: $\Delta_b = \frac{K_b U_b P_b}{U_b - P_b}$ Equation 2.44 and $\Delta_b = \frac{0.6075 q D_b}{E_b}$ Equation 2.48 $\therefore \Delta_b = \frac{K_b U_b P_b}{U_b - P_b} = \frac{0.6075 q D_b}{E_b}$; $\Rightarrow K_b = \frac{0.6075 D_b (U_b - P_b)}{E_b U_b P_b} = \frac{0.6075 x 4 P_b D_b (U_b P_b)}{\pi U_b P_b D_b^2} = \frac{2.43(U_b - U_b/4)}{U_b - P_b} = \frac{0.58}{D_b E_b}$

$$K_b \approx \frac{0.6}{D_b E_b} \tag{2.49}$$

Substituting this value of K_b into Equation 2.44 and manipulating, yields:

$$\Delta_b = \frac{0.6}{D_b E_b (\boldsymbol{U_b - P_b})} \tag{2.50}$$

Equation 2.50 enables an expression of the total load/settlement function to be derived.

2.7.12.3 Total settlement

For a purely rigid pile, the sum of the shaft load and pile base load gives the total load at any given settlement, Δ_T, i.e. :

$$P_T = P_s + P_b, \quad (2.51) \text{ and}$$
$$\Delta_T = \Delta_s = \Delta_b, \quad (2.52)$$

After manipulation of Equation 2.46, the shaft load can be written as:

$$P_s = \frac{U_s \Delta_s}{(M_s D_s + \Delta_s)} \quad (2.53)$$

The base load, P_b, can similarly be expressed as follows, after some manipulation of Equation 2.50:

$$P_b = \frac{D_b E_b U_b \Delta_b}{(0.6U_b + D_b E_B \Delta_b)} \quad (2.54)$$

From Equation 2.51, $P_T = P_s + P_b = \frac{U_s \Delta_s}{(M_s D_s + \Delta_s)} + \frac{D_b E_b U_b \Delta_b}{(0.6U_b + D_b E_B \Delta_b)}$.

But $\Delta_T = \Delta_s = \Delta_b$ from Equation 2.52 $\Rightarrow$ $P_T = \frac{U_s \Delta_T}{(M_s D_s + \Delta_T)} + \frac{D_b E_b U_b \Delta_T}{(0.6U_b + D_b E_B \Delta_T)}$

$$P_T = \frac{a\Delta_T}{(c + \Delta_T)} + \frac{b\Delta_T}{(d + e\Delta_T)} \quad (2.55)$$

Where: $a = U_s$; $b = D_b E_b U_b$, $c = M_s D_b$; $d = 0.6U_b$ *and* $e = D_b E_b$.

To solve for Δ_T for any specific value of P_T, the above equation is arranged in the form:

$$(eP_T - ae - b)\Delta_T^2 + (dP_T + ecP_T - ad - bc)\Delta_T + cdP_T = 0, \quad (2.56)$$

For simplification and handling convenience, let $(eP_T - ae - b) = f$, $(dP_T + ecP_T - ad - bc) = g$ *and* $cdP_T = h$, $\Rightarrow \boldsymbol{f\Delta_T^2 + g\Delta_T + h = 0}$, which is in the general quadratic formula form. The total settlement Δ_T, can thus be obtained by solving the quadratic equation using the quadratic formula:

$$\Delta_T = \frac{-g \pm \sqrt{g^2 - 4fh}}{2f} \quad (2.57) \text{ and}$$

adopting only the positive value of Δ_T.

2.7.12.4 Elastic shortening of piles

Elastic shortening of a pile shaft under a compressive load leads to an increase in settlement calculated from Equation 2.57. This settlement depends on:

i) relative development of load transfer between the soil and the pile along the pile shaft
ii) any free length or near friction-free length at the pile head
iii) load being transferred at the pile base

Figure 2.31 depicts the concept of pile elastic shortening which occurs in non-rigid piles.

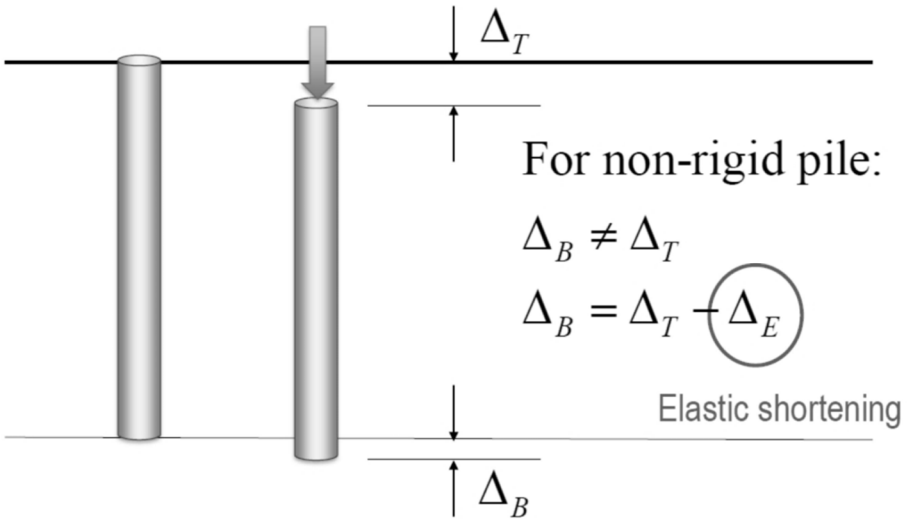


Figure 2.31: Elastic shortening for a non-rigid (compressible) pile (after Fleming, 1992)

Fleming (1992) noted that to work out elastic shortening would involve some fairly accurate evaluation of the load transfer flexibility factor M_s, and that any such procedure would involve dividing the pile into several segments and compatibility strains studied at various levels. The procedure would thus be iterative, hence cumbersome and involving complications associated with varying soil strata and thickness. Consequently, Fleming suggested a simplified method which consists of three stages of elastic shortening of loaded piles. The stages are listed below, with reference to Figure 2.32.

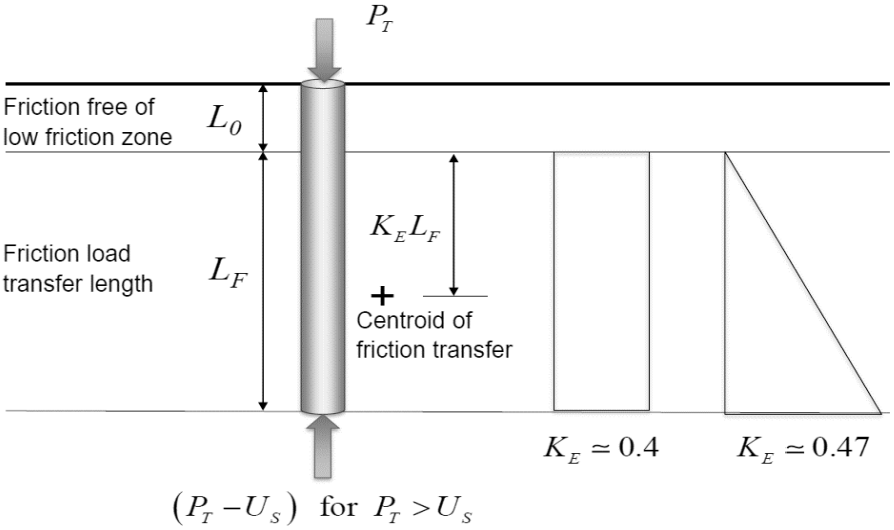


Figure 2.32: Simplified method of calculation of elastic shortening (after Fleming, 1992)

a) a free or low friction length extending to a distance, L_0, from the pile head
b) a length, L_F, over which friction is transferred
c) the whole pile shortening as a column after the ultimate shaft friction has been reached.

For case a) above, the settlement, Δ_1, is derived as follows:

$E_c = \frac{\sigma}{\varepsilon} = \frac{\frac{P_T}{A_p}}{\varepsilon} = \frac{P_T}{A_p \Delta_1 / L_0}$, strain, $\varepsilon = \Delta_1 / L_0$, $\Rightarrow E_c A_p \Delta_1 = P_T L_0 \Rightarrow \Delta_1 = \frac{P_T L_0}{E_c A_p}$, $But\ A_p = \pi D_S^2 / 4$

$$\Delta_1 = \frac{4 L_0 P_T}{\pi D_S^2 E_c} \qquad (2.58)$$

Where E_c is the Young's modulus for the pile material in compression, with all other parameters having already been defined.

For the second stage, (case b) above), elastic shortening takes place during load increase to the stage when ultimate skin friction has been fully mobilised. For uniform friction, elastic shortening will be equivalent to that of a column of effective length, $K_E L_F$, where K_E is the coefficient applied to the friction length L_F, to give the effective columnar length, $K_E L_F$. Both K_E and M_s are important parameters in the determination of the early slope of the load/settlement relationship. Friction development takes place faster at the top of this section than at its base. This effective length is about 70-80% of the distance from the top of the friction transfer length to the centroid of the friction load transfer diagram in Figure 2.32.
The stage 2 elastic shortening is derived in a similar manner to that of the first stage as follows:
$\sigma = \frac{P_T}{A_p};\ \varepsilon = \frac{\Delta_1}{K_E L_F};\ E_c = \frac{\sigma}{\varepsilon} = \frac{P_T}{A_p} x \frac{K_E L_F}{\Delta_2}.\ \therefore \Delta_2 = \frac{K_E L_F P_T}{A_p E_c}$

$$\Rightarrow \Delta_2 = \frac{4 K_E L_F P_T}{\pi D_S^2 E_c} \qquad (2.59)$$

In the third stage, the applied load, $P_T \geq U_s$, the shaft ultimate load. $K_E = 1.0$. Therefore the additional load causing extra elastic shortening over the full length, L_F, is equal to $(P_T - U_s)$. Following similar steps to those for the derivation of Δ_1 and Δ_2, with P_T replaced by $(P_T - U_s)$ yields:

$$\Delta_3 = \frac{4(P_T - U_S) L_F}{\pi D_S E_c} \qquad (2.60)$$

Therefore total settlement for $P_T \leq U_s$ is given by: $\Delta_{E1} = \Delta_1 + \Delta_2 = \frac{4 L_0 P_T}{\pi D_S^2 E_c} + \frac{4 K_E L_F P_T}{\pi D_S E_c}$

$$\Delta_{E1} = \frac{4 P_T}{\pi D_S^2} \frac{(L_0 + K_E L_E)}{E_c} \qquad (2.61)$$

For $P_T > U_s$, the total elastic shortening, Δ_E is derived as follows: $\Delta_E = \frac{4}{\pi D_S^2 E_c}(P_T - U_s) + \frac{4}{\pi D_S^2 E_c} P_T (L_0 + K_E L_F) = \frac{4}{\pi D_S^2 E_c}[P_T L_F - U_s L_F + P_T L_0 + P_T K_E L_F]$

$$= \frac{4}{\pi D_S^2 E_c}[P_T (L_0 + L_F) - U_s L_F + K_E P_T L_F]$$

and recognising that in the last term in brackets, P_T may be taken as equal to U_s.

$$\Delta_E = \frac{4}{\pi D_S^2 E_c}[P_T (L_0 + L_F) - U_s L_F (1 - K_E] \qquad (2.62)$$

Therefore, by combining Equation 2.57 and 2.60 or 2.61, the total settlement, including a fairly accurate estimate of elastic shortening, of a single pile for a given vertical compressive load up to the ultimate load, can be determined. The solution procedure for the hyperbolic method can be automated using a spreadsheet as demonstrated in calculations.

2.8 Pile Group Settlement

When piles are installed fairly close together, at a spacing, S, which is typically $2D_0 < S \leq 5D_0$, they are joined by a slab called a pile cap, cast on top of the piles to form a pile group. The pile cap may be in contact with the soil, in which case part of the structural load is directly carried onto the soil below the cap. A free-standing pile group is when the pile cap is clear of

the ground surface. However, the effect on group settlement of the pile cap being in contact with the soil is relatively small unless the pile spacing is large and the group is relatively small. Even at unusually large spacing of say $10D_0$, the reduction in settlement due to the pile cap contact with the ground hardly exceeds 5%, hence for most practical purposes, the influence of the pile cap contact with the ground surface on settlement at working loads, can be ignored.

Various methods also exist for estimating the settlement behavior of a pile group. The load transfer mechanism in a pile group involves a complex interaction of piles, pile cap and the surrounding soil. Consequently, the settlement of a pile group can differ substantially from that of a single pile at the same loading level. Piles in a group interact with each other and the degree of interaction depends on the spacing between them. The smaller the spacing, the greater the interaction and the larger the settlement. Pile group settlement is influenced by:

i) The pile spacing, *S,* to pile diameter, *D*, ratio
ii) The number, *n*, of piles in the group
iii) The pile length *L,* to its diameter *D,* ratio, *L/D.*
iv) The pile geometry and
v) Pile-soil interaction, among other factors.

This paper reviews some the various methods used for pile group settlement analysis as outlined below.

2.8.1 Skempton (1953) method

Traditionally, estimates of pile group settlement were based on either empirical data or on simplified approaches based on Terzaghi's one-dimensional consolidation theory. Skempton devised an empirical approach for a pile group settlement in sand on the basis of a limited number of field observations and suggests that the pile group settlement, ρ_g, is related to a single pile settlement, ρ_1 as follows:

$$\rho_g/\rho_1 = [(4B + 2.7)/(B + 3.6)]^2 \qquad (2.63)$$

Where B is the width of the pile group in metres. Skempton's method is not applicable to cohesive soils.

2.8.2 Meyerhof (1959) method

For driven piles (and displacement caissons) in sand, Meyerhof suggests the following normalised relationship for a square pile group:

$$\rho_g/\rho_1 = S(5 - \tfrac{S}{3})/(1 + \tfrac{1}{r})^2 \qquad (2.64)$$

Where S the ratio of pile spacing to pile diameter and $\boldsymbol{r}$ is is the no of rows in the square group, ρ_g and ρ_1 are the pile group and single pile settlement respectively. Meyerhof's method also has limitations of being applicable to non-cohesive soils only.

(Poulos and Davis, 1980)

2.8.3 Vesic (1977) method

Vesic proposed an empirical relationship to determine the settlement of a pile group in sandy soil defined as follows:

$$S_g/S_1 = [B/D_0]^{1/2} \qquad (2.65)$$

Where: S_g is the settlement of the pile group, S_1 is the settlement of a single pile at same average loading, B is the width (smaller dimension) of the pile group and D_0 is the diameter of the single

pile.

2.8.4 Poulos (1968b) method

Having successfully used the elastic theory to analyse the settlement behaviour of a single pile, Poulos (1968b) uses the same theory to examine the settlement behaviour of incompressible floating pile groups at working loads, by extending single pile analysis to a consideration of the settlement interaction between two identical floating piles, a system which represents the simplest form of a pile group. The analysis of a 2-pile group is then extended to the case of a general floating pile group, where two limiting cases are considered, which are:

a) The case of a perfectly rigid pile cap, when all piles in the group settle equally, and
b) That of a perfectly flexible pile cap where all piles carry an equal load.

Since is not possible to present solutions for all possible practical situations, Poulos presents solutions which are confined mainly to square pile groups with a maximum of 25 piles. The following assumptions are made:

1) The piles are assumed to be incompressible to make the solutions relevant for the case of a pile group in a soft clay.
2) No slip is assumed between the pile and the adjacent soil, hence the solutions are valid only while purely elastic conditions prevail.
3) It is assumed that the pile groups are free-standing, i.e.: the underside of the pile cap is not in contact with the surface of the soil. Consequently, raft-action of the pile cap need not be considered.

2.8.4.1 Analysis of a group of two piles

A group of identical, equally loaded piles as shown in Figure 2.33 is considered.

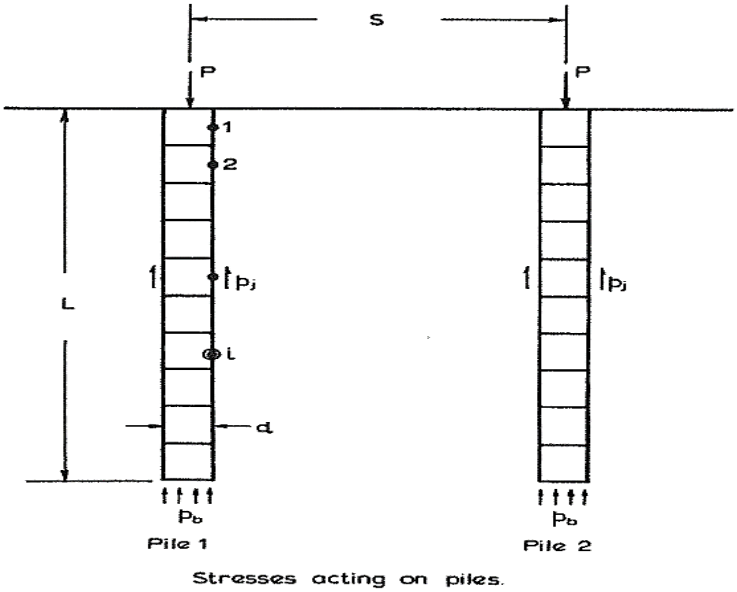


Figure 2.33: Group of two floating piles (after Poulos, 1968b)

Each pile is divided into *n* cylindrical elements with a uniformly loaded base. Taking assumptions 1) and 2) above into consideration, the pile and the soil displacements at the centre of each element may be equated. The equations for the pile displacement are derived in the same way as described for a single pile already discussed in section 2.7.5 of this report. The resulting system of equations is solved to get the unknown shear stresses and displacements along the piles. The analysis of a two-pile group is thus similar to that of a single pile except

that the soil-displacement influence matrix for a 2-pile group includes contribution from the second pile.
Results of the above said analysis were conveniently expressed in terms of an interaction factor, $\boldsymbol{\alpha}$, which is defined as the fractional increase in deformation (which may be deflection or rotation at the pile head but this report is restricted to vertical displacement only) of a pile due to the presence of a similarly loaded neighbouring pile.

$$\Rightarrow \alpha = \frac{\text{Additional settlement caused by an adjacent pile}}{\text{Settlement of the pile under its own load}} \quad (2.66)$$

The pile under consideration and the adjacent pile carry the same load. For a group of two piles, $0 \leq \alpha \leq 1$, where $\alpha = 1$ corresponds to zero spacing between the piles, ie: one pile superimposed on the other while $\alpha = 0$ is for an infinity spacing between the piles.

Poulos (1968b) plotted values α against the centre-to-centre spacing, S, between the piles for various values of the ratio, L/*d* for the case of Poisson's ratio, $v = 0.5$ and made the following observations for two piles in an elastic half space:

- The interaction factor decreases with increasing pile spacing
- Values of the interaction factor remained fairly high at large spacings of about 40*d*
- *L/d* has a marked influence on value of interaction factor, increasing as L/d increases, the effect becoming more pronounced as the pile spacing increases
- The effects of the Poisson's ratio on the interaction factor was found to be insignificant as that for v=0.5 is marginally less than that for v=0.

Poulos (1968b) also investigated the effect of the presence of an underlying rigid base on the interaction between two piles for the case of *L/d=25* and $v = 0.5$ and plotted values of α against pile spacing, S/d for values of the dimensionless layer depth, *h/L* for the range: $1.2 \leq h/L \leq \infty$. The following observations were made from the resulting plots:

- It was noted that the rigid base tends to 'damp' the interaction, particularly at large spacings where the value of the interaction factor in a finite layer is significantly less than that for a semi-infinite mass.
- When the ratio *h/L*>~2.5, the interaction factor is not significantly affected by the layer depth for close spacings, h being the depth of underlying rigid base.
- For shallow layers, the interaction factor is markedly reduced by the rigid base, even for close spacings.

2.8.4.2 Analysis of symmetrical pile groups

A symmetrical pile group is one where the arrangement of the piles is such that all the piles in the group behave identically. Poulos (1968b) extends the analysis of a two-pile group to any number of piles in a symmetrical group where the piles are spaced equally around the circumference of a circle, each pile displacing equally and carrying an equal load. Displacement equations are formed by equating pile displacements to soil displacements as already covered for a single pile. The resulting simultaneous equations are solved to obtain the shear stress distribution and displacement of each pile.
In Figure 2.34, the interaction factor, $\boldsymbol{\alpha}$ is plotted against the spacing S/d between the piles for symmetrical groups of three and four piles, along with the 2-pile group, for the case of *L/d=25* and $v = 0.5$.

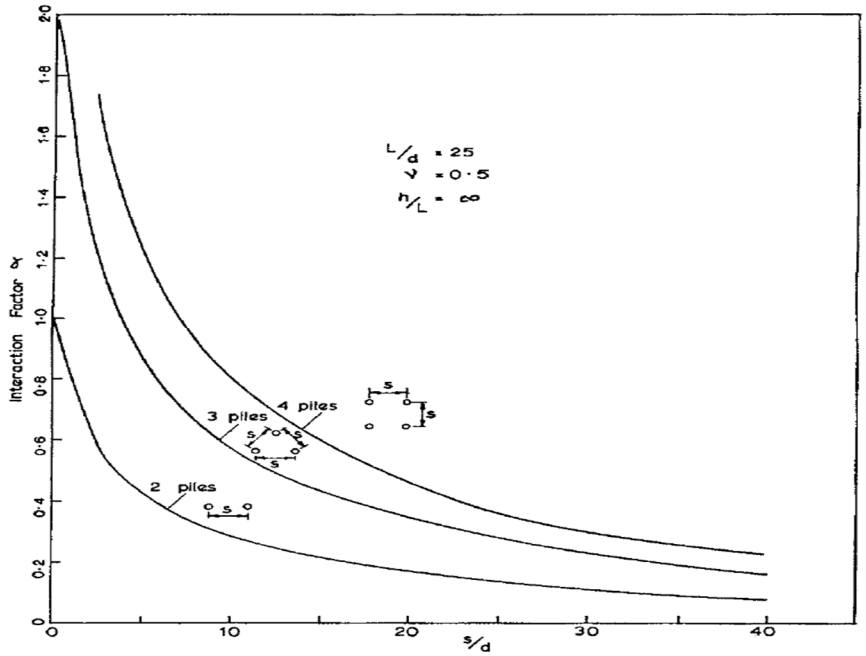


Figure 2.34: Settlement interaction for 2-pile group and 3 and 4-pile symmetrical group (after Poulos, 1968b)

It is obvious from the plots that the additional settlement of each pile in the group due to the adjacent piles is almost equal to the sum of the displacement increases due to each of the adjacent piles in turn. Thus for a 3-pile group, the value of $\boldsymbol{\alpha}$ is almost twice the value for the 2-pile group at the same spacing, while that for a 4-pile group at a spacing of *S*, the value of $\boldsymbol{\alpha}$ is given by:

$$\alpha = 2\alpha_1 + \alpha_2 \tag{2.67}$$

Where α_1 is the value of α at a spacing of *S* diameters, α_2 is the value of α for two piles at a spacing of $\sqrt{2}.S$ diameters. Therefore the corresponding displacement of each pile in the group due to equal loads P_1 in each pile is given by:

$$\rho = P_1\rho_1(2\alpha_1 + \alpha_2) \tag{2.68}$$

Where ρ_1 is the displacement of a single pile under a unit load.

2.8.4.3 Proportion of load taken by base

Poulos also investigated the magnitude of load taken by the base for each pile group for various pile spacings and observed that:

- At close spacings, increased interaction leads to an increase in the load transmitted to the base of each pile in the group compared with the single pile case.
- The base load increase becomes more visible as the number of piles in the group increase.
- The base load decreases with increasing pile spacing until at about *S=25d* when it becomes identical to that of a single pile.

2.8.4.4 Analysis of general pile groups

The principal of superposition allows stress increase at a given point in a soil mass in a certain

direction, from different loads, to be added together, for a linear, elastic soil mass. Poulos (1968b) reckons that the applicability of the principle of superposition to symmetrical three and four-pile groups suggests that the displacement of any symmetrical pile group may be determined from the relationship between the interaction factor, α and pile spacing to diameter, *S/d* ratio, for a two-pile group. Hence it appears logical to extend the use of the principle of superposition to the analysis of pile groups which are not symmetrical. For the general pile group, two limiting conditions similar to those of symmetrical pile groups are considered, vis-à-vis:

a) Equal loads in all piles which corresponds to a perfectly flexible pile cap
b) Equal settlement of all piles corresponding to a perfectly rigid pile cap.

A group consisting of *m* piles was considered. The displacement of any pile *k* in the group is, by superposition, given by:

$$\rho_k = \rho_1 \sum_{j=1}^{j=m} P_j \alpha_{kj} \qquad (2.69)$$

Where α_{kj} is the value of α for piles corresponding to the spacing between pile *k* and pile *j*, P_j is the load on pile *j*, ρ_1 is the displacement of a single pile under a unit load. If P_G is the total load on the pile group, then:

$$P_G = \sum_{j=1}^{j=m} P_j \qquad (2.70)$$

For the case of equal loads in all piles, $P_j = P_G/m$, thus Equation 2.69 can be used directly to calculate the displacement of each pile in the group and hence, the maximum settlement and differential settlement between the piles. For the case of equal settlement, the displacements are equated to give *m* simultaneous equations which may be solved for the unknown loads, P_j, in the group, thus the settlement of the group may be determined. Therefore, the analysis of any general pile group requires a knowledge of the relationship between the interaction factor α and pile spacing for a two-pile group, relying on the assumption that the principle of superposition holds for a general pile group as it does for symmetrical groups.

The following are some of the variables considered in obtaining solutions for the settlement of general pile groups:

a) The type of the group, b) The *L/d* ratio of the piles in the group, c) The relative depth, *h/L* of the soil layer, d) Poisson's ratio of the soil layer, e)The centre to centre spacing, *S/d* of the piles.

Poulos confines the analysis primarily to square groups of 4, 9, 16 and 25 piles which are also denoted as 2^2, 3^2, 4^2 and 5^2 groups respectively, because an exhaustive consideration of every practical arrangement is not feasible.

2.8.4.5 Settlement of pile groups with a perfectly rigid pile cap

Settlement ratio is one of the common parameters used in the consideration of pile group settlement. The settlement ratio, R_s, is defined by:

$$R_s = \frac{\text{Average settlement of the pile group}}{\text{Settlement of a single pile carrying the same average load as a pile in the group}} \qquad (2.71a)$$

Values of *Rs* can be worked out from Tables B1 and B2 for for friction pile groups with rigid pile cap on deep soil mass and for end-bearing pile groups with rigid pile cap bearing on rigid

stratum respectively. Group reduction factor, R_G, is another parameter that is used to conveniently express group settlement, and is defined by:

$$R_G = \frac{\text{Average settlement of the pile group}}{\text{Settlement of a single pile carrying the same total load as the group}} \quad (2.71b)$$

R_G is a meaningful parameter in an elastic soil where the variation between load and settlement is linear and failure mode where a single pile failure under the group load must not develop. For a group of *m* piles, the settlement ratio is related to the group reduction factor by the following:

$$R_s = mR_G, \ \Rightarrow \ R_G = R_s/m \quad (2.72)$$

Equation 2.72 implies that R_G represents the reduction in settlement which results from using a pile group as opposed to a single pile to carry a given load. The actual group settlement S_G, is given by:

$$S_G = R_s S_1 = mR_G S_1 \quad (2.73)$$

Where S_1 is the settlement of a single pile carrying the same average load as a pile in the group, which, from Poulos and Davis (1968):

$$S_1 = \frac{P}{E_S L} I_1 \quad (2.74)$$

Where *P* is the single pile load, *L* is the pile length, E_S is the Young's modulus of the soil surrounding the pile and I_1 is the displacement influence factor for a single pile. Therefore the total load on the group, P_G=*m*P. This implies that the pile group settlement S_G, is given by:

$$S_G = \frac{P_G}{EL} R_G I_1 \quad (2.75)$$

Values of I_1 are contained in Table B3 for a range of values of *h*/L and *L/d*, while values of R_G are contained in Table B4. The appropriate values of I_1 and R_G are applied to Equation 2.75 in order to calculate the settlement of a pile group with a rigid pile cap in terms of a single pile. It is clear from Table B4 that as *h/L* decreases, the value of R_G decreases for a given spacing due to the 'damping effect' of the rigid base, i.e.: the rigid base has the effect of restricting the settlement of the pile group. The value of R_G, and hence settlement, for any given spacing, increases as *L/d* increases for symmetric pile groups.

Poulos also investigated the variation of R_G with spacing for 2, 3, 5 and 6-pile groups and found that there is reduction in settlement as the number of piles in the group increases, for a given spacing between the individual piles. It was also concluded that at a relatively close spacing of say *S*<*5d*, the use of more piles to reduce settlement becomes ineffective at the same spacing. The variation of R_G with pile group breadth was also investigated, pile group breadth being equal to the pile diameter, *d* + centre to centre pile spacing, *S*, between the outermost piles. It was found that except for the four pile group, the value of R_G is more or less the same value up to a group breadth of about *16d* thus implying that over a significant range of breadth, the settlement of a pile group is basically dependent on the breadth of the group rather than the number of piles in the group. Full-scale field test results by Berezantzev, Khristoforov and Golubkov (196, as cited in Poulos, 1968b) confirmed this theoretical conclusion. Consequently, in pile group design, the use of fewer piles at a relatively large spacing would generally be more preferable to many piles at close spacing for economic reasons. However, there are

limitations to pile spacing beyond which economic construction of a pile cap of adequate rigidity may not be practical.

2.8.4.6 Proportion of settlement

In pile group design, just like in single piles, consolidation settlement is generally of secondary importance. It therefore implies that in pile foundation, accurate predictions of rates of settlement are not critical.

2.8.4.7 Settlement of pile groups with perfectly flexible pile cap

For the case of a perfectly flexible pile cap, all piles take equal load.

2.8.4.8 Maximum settlement

For a square pile group, maximum settlement occurs at the centre pile/piles while minimum settlement occurs at the corner piles. For the limiting cases of $S=0$ and $S=\infty$, the maximum settlement, S_{max}, for a pile group with a flexible pile cap is given by: $S_{max}=S_R$, where S_R is the settlement of a pile group with a rigid pile cap. For spacing in between the limits, $S_{max}>S_R$ but comparisons have revealed that S_{max}/S_R is almost independent of pile spacing for a practical range of spacings up to approximately $20d$. Therefore, the estimation of the maximum settlement of a pile group with a flexible pile cap can be done in steps as follows:

a) Determination of S_R, the settlement of a group with a rigid pile cap from values of R_G in Table B4.
b) Multiplication of S_R by an appropriate value of S_{max}/S_R, S_{max}/S_R values being obtained from Table B5.

The values of S_{max}/S_R tabulated in Table B5 are for the case of $L/d=25$ and $\nu=0.5$, for different values of h/L for 3^2, 4^2 and 5^2 groups. It can be deduced from Table B5 that S_{max}/S_R increases as the number of piles in the group increases and that h/L does not have a significant effect on S_{max}/S_R at close spacings. However, for $S\geq10d$, the ratio S_{max}/S_R decreases rapidly as h/L decreases. S_{max}/S_R slightly decreases as L/d increases.

2.8.5 Butterfield and Banerjee (1971) method

Poulos (1968) presented an approximate general study of axially loaded groups of incompressible piles based on the following assumptions, in addition to those of ideal elasticity:

a) The pile shaft load was replaced by a uniform vertical shear stress on the surface of each of a suitable number of small cylindrical elements.
b) The pile base was assumed to be a smooth disc, not necessarily of the same diameter as the pile shaft, across which the base load was uniformly distributed.
c) The disturbance of the continuity of the elastic half-space due to the presence of the piles was ignored.

Butterfield and Banerjee (1971) obtained the response of rigid and compressible single piles embedded in a homogeneous, isotropic, linear and elastic medium by means of a rigorous analysis based on Mindlin's solutions for a point load in the interior of an ideal elastic medium and extended it to the analysis of axially loaded rigid and compressible pile groups with floating pile caps and piles spaced in an arbitrary manner.
(Poulos and Davis, 1980)

The results are presented as a series of graphs showing the effect of length to diameter ratio, pile spacing, the ratio of the modulus of elasticity of the pile material, E_p, to the shear modulus, G, of the soil, E_p/G, on the response to a range of typical pile groups. Figures 2.35 and 2.36 show the effect of L/d and compressibility λ, on the interaction between piles. In both cases, a

range of $600 \leq \lambda \leq \infty$ is considered. This about covers the range of material properties of major practical interest. $\lambda = E_p/G$.

The settlement ratio, R_s, for the groups of 2, 3 and 4 compressible plain piles under a rigid pile cap is plotted against the normalized spacing, *S/D* for the case of *L/D=20* and *40* and $\lambda = 6000$ and ∞, as depicted in Figures 2.35 and 2.36. R_s is defined as the ratio of the vertical displacement of the pile cap under a load of *nP* to that of a single pile under a load, *P*, where *n* is the number of piles in the group, *n=1, 2, 3, 4* in this case. It is evident from the graphs that *Rs* is strongly influenced by *L/D* and that the effect of λ is negligible for all the short piles (piles for which *L/D<40*), where *L* is the pile length, of diameter, *D=d*. It can also be noted that:

a) *Rs* remains at approximately 1.5 for the longer piles even when *S>32D*, *S* being the pile spacing.
b) The principle of superposition (Poulos, 1968), does not hold that well for compressible piles than it does for incompressible piles as evidenced by the curves which are not as nearly uniformly spaced as those in Figure 2.35.

Butterfield and Banerjee (1971) method of analysis of compressible pile groups takes into account radial deformation compatibility conditions. Effects of radial stresses are small and negligible for most practical situations.

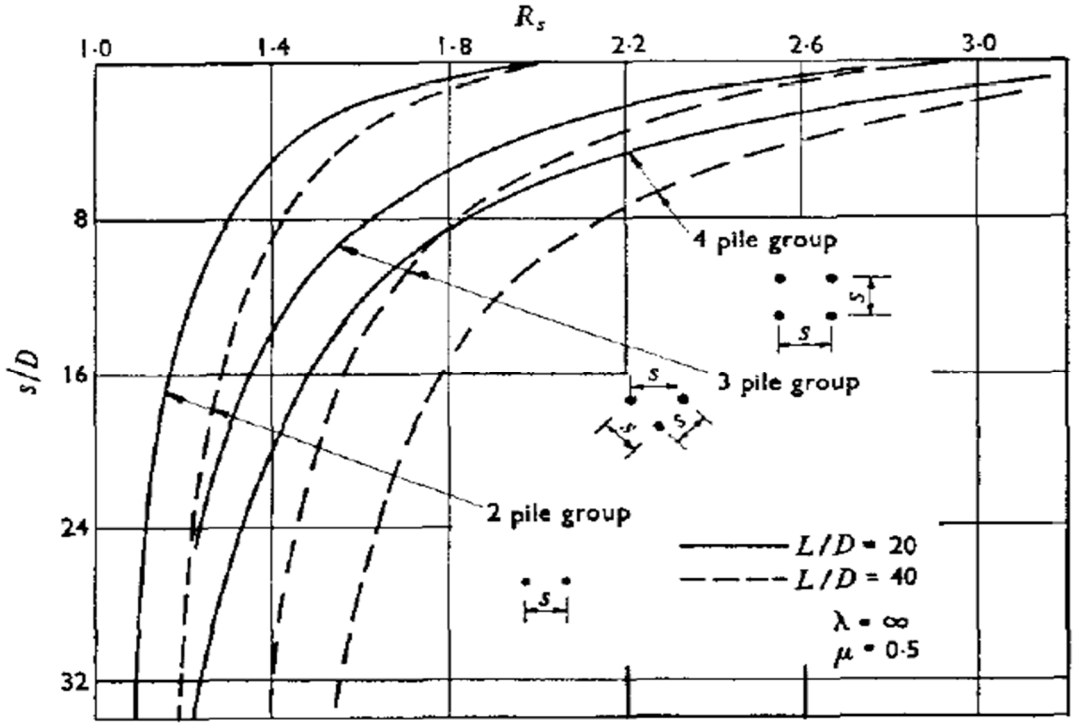


Figure 2.35: Effect of L/D on the interaction between piles in a group (after Butterfield and Banerjee, 1971)

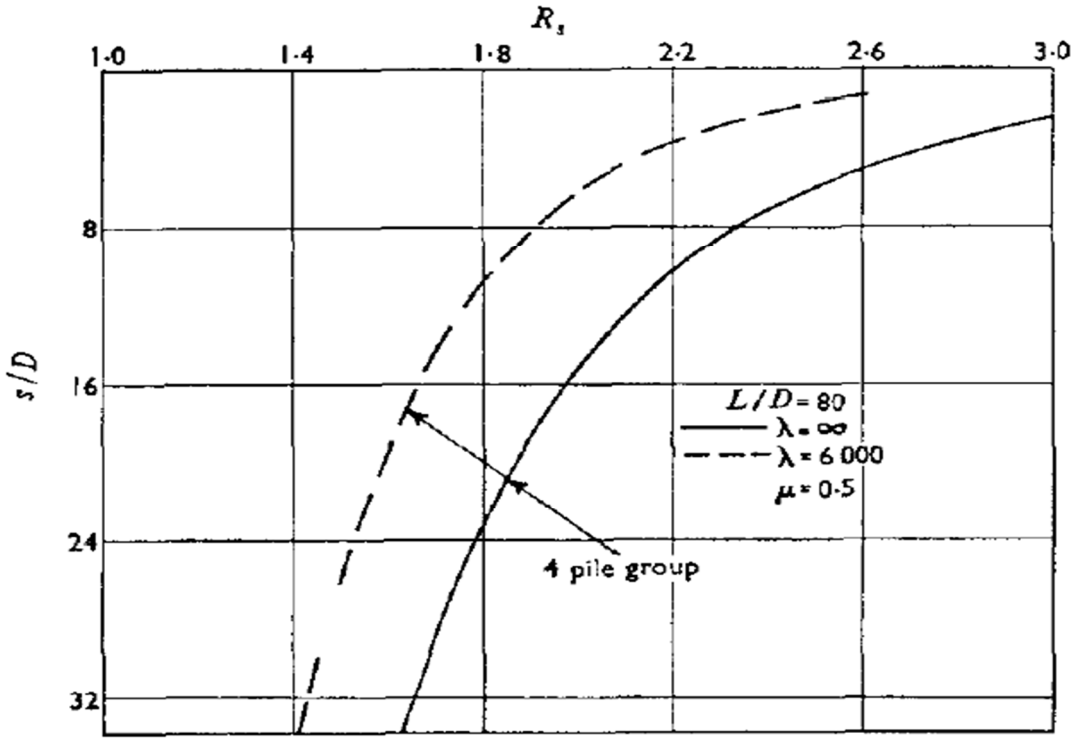


Figure 2.36: Effect of compressibility on the interaction between piles in a group (after Butterfield and Banerjee, 1971)

2.8.6 Poulos and Mattes (1971b) method

Poulos and Mattes (1971) presented a method for the analysis of the behaviour of groups of compressible floating and end-bearing piles, amenable to hand calculations. The shear stresses acting on the pile surface are approximated by a series of uniformly distributed loads acting around the pile shaft surface. Theoretical solutions for the settlement and load distribution in compressible pile groups were presented with emphasis on examining the influence of relative compressibility of the piles on the pile groups. The following are some of the assumptions made:

1) The floating piles are in a semi-infinite elastic mass and end-bearing piles rest on a rigid bearing stratum.
2) All pile groups are free-standing, i.e.: it is assumed that there is no contact between the bottom of the pile cap and the top surface of the soil.
3) The effects of yield within the soil were ignored.

2.8.6.1 Analysis of a group of two piles

Two cases were considered which are:

a) Floating piles of two equally loaded, identical, cylindrical piles in an elastic half-space with constant elastic parameters, Young's modulus of the soil, E_s and Poisson's ratio, v_s. The piles are of length, L, diameter, d, cross-sectional area, A_p and spaced at centre to centre distance S. The elastic modulus of the pile material is E_p.
b) End-bearing piles – two equally loaded identical piles of diameter, d, length, L, cross-sectional area, A_p and material elastic modulus, E_p, resting on a perfectly rigid base.

The pile stiffness factor, K, is an important parameter because it is a measure of the compressibility of the pile relative to the soil. The smaller the value of K, the more compressible

is the pile. K is defined by: $K = (E_p/E_s)R_A$, where $R_A = A_p/(\pi d^2/4)$, R_A being the area ratio and for solid piles, R_A=1.

It is convenient to define additional displacement at the top of the pile due to an equally loaded identical pile in terms of an interaction factor, α, as already defined in section 2.7.4 of this report, where the pile of interest and the adjacent pile carry an equal load. Typical interaction curves showing the relationship between α and the dimensionless centre to centre spacing, *S/d* for various values of *L/d* and *K* were plotted for floating piles and end-bearing piles. In all cases, Poisson's ratio of *v=0.5* was used with the piles divided into 10 equal elements. The following observations were made from the plotted variations of α, S/d, L/d and K:

- Interaction decreases as spacing increases for both floating and end-bearing piles.
- For relatively floating compressible floating piles, interaction remains significant at relatively large spacings.
- Floating piles generally tend to have increased interaction as pile stiffness increase. However, this trend is reversed for slender and very compressible piles, e.g.: piles for which *K≤10*.
- Interaction increases as *L/d* decreases for end-bearing piles because more load is then transferred to the bearing stratum, but for floating piles, interaction generally decreases as stiffness increases. The interaction between end-bearing piles is mostly much less than for corresponding floating piles.

Solutions presented by Poulos and Mattes (1971b) are for the case of piles in an elastic half-space, but the solutions for a single pile obtained by the same investigators suggest that the finite layer will only significantly influence group behavior for relatively incompressible piles. In such cases, the interaction factors obtained by Poulos (1968) for incompressible piles in finite layer, may be used. The influence of a bearing stratum of finite compressibility for end bearing pile groups may be inferred from the solutions for a single end bearing pile from Poulos (1971). The bearing stratum may be considered rigid if the ratio of the modulus of bearing stratum, E_b to the soil modulus, E_s, is greater than 100, i.e.: $E_b/E_s>100$. Relatively, compressible short piles are markedly influenced by the base compressibility for small values of E_b/E_s. When E_b/E_s is small, an approximate but conservative estimate of the interaction factor may be obtained by considering the value of α for the corresponding floating pile. For all other cases involving relatively slender and relatively compressible piles, values of α for an end-bearing pile on a rigid base may be used with sufficient accuracy.

2.8.6.2 Typical solutions for square pile groups

Investigations were carried out for 4, 9, 16 and 25 pile-groups, also denoted as 2^2, 3^2, 4^2 and 5^2 groups respectively, for both floating and end-bearing piles. The case of piles being equally loaded, i.e.: piles with a flexible pile cap and the load distribution and settlement of a group with a rigid pile cap, were considered.

2.8.6.2(a) Floating pile group

Table B6 shows the group reduction factor, R_G, for typical floating pile groups with rigid pile caps, for different groups. It can be deduced that for all groups, R_G decreases as the pile spacing increases and, for almost all cases, R_G also decreases as pile stiffness factor K, decreases, except for slender and very compressible piles at very close spacings. R_G also decreases as the number of piles in the group increases. Poulos and Mattes (1971b) also investigated the variation of R_G with group breadth and found that the influence of the number of piles in the group is not that

significant and that R_G does not vary considerably with the number of piles in the group, for larger pile groups but on group breadth. Poulos (1968b) also noted the dependence of pile group on group breadth as opposed to the actual number of piles in the group for large pile groups.

For compressible pile groups, the major portion of total final settlement also occurs as immediate settlement. Pile compressibility is also found to have insignificant influence on the value of S_u/S_{TF}, immediate settlement to total final settlement.

2.8.6.2(b) End-bearing pile groups

Group reduction factors for end-bearing pile groups with rigid pile caps are contained in Table B7 for a wide range of *L/d, S/d,* group size and *K*. From Table B7 it is evident that R_G decreases as pile stiffness increases and reaches its maximum value of *1/m*, ie: no interaction between the piles, the smaller the value of *L/d* and at closer spacings. R_G also decreases with increasing number of piles in the group. However, when R_G was plotted against group breadth it was observed that there also appears to be a limiting curve as the number of piles in the group increases, as is the case for floating pile groups.

The ratio S_u/S_{TF} for end-bearing piles is found to be closer to 1. Generally, for most practical cases, consolidation settlement is less than 10% of the total final settlement. For the case of end-bearing piles with a flexible pile cap, the maximum settlement occurs at the centre piles with the minimum at the corners.

2.8.7 Randolph and Wroth (1979) method

Practically, the use of interaction factors is one of the most useful and significant concept to emerge from the linear elastic theory analytical work, an interaction factor having already been defined as the fractional increase in pile deformation due to the presence of a similarly loaded nearby pile. Therefore, if the stiffness of a single pile under a given form of load is *K*, then a load, *P*, will give rise to a deformation, *w*, given by:

$$w = P/K \tag{2.76}$$

If two identical piles are subjected to a load, *P*, then each pile will deform by an amount, *w*, given by:

$$w = (1 + \alpha)\, P/K \tag{2.77}$$

The value of α depends on the geometry and spacing of the two piles and the relative soil-pile stiffness. The use of interaction factors may be seen as being equivalent to superposing the separate deformation fields that each pile would give rise to by itself, in order to arrive at the overall deformation. This approach has been confirmed experimentally from tests on instrumented piles at field scale (Cooke, 1974; Ghosh, 1976; Abdrabbo, 1976, as cited in Randolph and Wroth,1979). Due consideration should be taken of the different amounts of interaction along the pile shaft and the pile base – the constitutive behaviour of piles.

From Randolph and Wroth (1978), see section 2.7.9 of this report, the settlement at the pile mid-depth is given by:

$$w(r) = \zeta \frac{\tau_0 r_0}{G}, \text{ where } \zeta = \ln(r_m/r_0) \tag{2.78}$$

The settlement profile at the pile base is given by:

$$w(r) = w_b . c . \frac{r_0}{r}, \text{ where } c=2/\pi \tag{2.79}$$

While the overall load-settlement ratio of a rigid pile was computed and written in the dimensionless form:

$$\frac{P_t}{G_L r_0 w_t} = \frac{P_b}{G_L r_0 w_b} + \frac{P_s}{G_L r_0 w_s} = \frac{4}{(1-v)} + \frac{2\pi\rho}{\zeta}\frac{L}{r_0} \tag{2.80}$$

The resulting analytical solutions consider that shear strength around the pile shaft would decay inversely with radius, leading to logarithmic decay in vertical displacements, all limited to a maximum radius of influence r_m, beyond which deflections in the soil are assumed to become vanishingly small. Considering two piles, the overall settlement of the pile may be written as the sum of the settlement due to its own loading, w_1, plus that due to the neighbouring pile's displacement field, w_2. Therefore:

$$w = \mathrm{w}_1 + w_2 \tag{2.81}$$

At the pile mid-depth:

$$w = \mathrm{w}_1 + \mathrm{w}_2 = \frac{\tau_0 r_0}{G}\left[\ln\left(\frac{r_m}{r_0}\right) + \ln\left(\frac{r_m}{S}\right)\right] \tag{2.82}$$

Where S is the spacing of the piles, being the distance between the centre-lines of the piles. S is therefore the average radius of one pile as seen from the other pile. The load-settlement ratio for each pile shaft is now given by:

$$\frac{P_s}{G_L r_0 w_s} = \frac{2\pi\rho}{\left[\zeta + \ell n\left(\frac{r_m}{S}\right)\right]}\frac{L}{r_0} \tag{2.83}$$

Similarly, the settlement of the pile base is given by:

$$w = w_1 + w_2 = \frac{P_b(1-v)}{4 r_0 G}\left(1 + \frac{c r_0}{S}\right) \tag{2.84}$$

Hence

$$\frac{P_s}{G_L r_0 w_b} = \frac{4}{(1-\mathrm{v})} \cdot \frac{S}{\left(1+\frac{c r_0}{S}\right)} \tag{2.85}$$

Therefore the load-settlement ratio for each of the two similarly loaded piles is given by

$$P_t = P_b + P_s = w_t\left(\frac{P_b}{w_b} + \frac{P_s}{w_s}\right) \tag{2.86}$$

and

$$\left(\frac{P_t}{G_L r_0 w_t}\right)_2 = \frac{4}{(1-v)} \cdot \frac{S}{(r_0 c + S)} + \frac{2\pi\rho}{\left[\zeta + \ell n\left(\frac{r_m}{S}\right)\right]}\frac{L}{r_0} \tag{2.87}$$

Equation 2.87 above can be extended to a case of equally loaded symmetrical pile groups which, for a 3-pile group, with the piles positioned at the corner of an equilateral triangle of sides of length, S, the expression becomes:

$$\left(\frac{P_t}{G_L r_0 w_t}\right)_3 = \frac{4}{(1-v)} \cdot \frac{S}{(2 r_0 c + S)} + \frac{2\pi\rho}{\left[\zeta + 2\ell n\left(\frac{r_m}{S}\right)\right]}\frac{L}{r_0} \tag{2.88}$$

For a square group with piles at the corner of a square of side, S, the expression becomes:

$$\left(\frac{P_t}{G_L r_0 w_t}\right)_4 = \frac{4}{(1-v)} \cdot \frac{S}{(2.707 r_0 c + S)} + \frac{2\pi\rho}{\left[\zeta + \ell n\left(\frac{r_m^3}{S}\right)\right]} \frac{L}{r_0} \qquad (2.89)$$

The results obtained from Equations 2.87, 2.88 and 2.89 were compared with the results of the integral equation analysis (Banerjee, 1970) for rigid piles in homogeneous and incompressible soil, at a spacing of $S=5r_0$, and shown in Figure 2.37 where it is apparent that there is good agreement between the two methods, for pile groups, just as is the case for a single pile.

Equation 2.87 increased settlement for a given load can be written as follows:

$$\left(\frac{G_L r_0 w_t}{P_t}\right)_2 = (1+\alpha)\left(\frac{G_L r_0 w_t}{P_t}\right)_1 \qquad (2.90)$$

Where α is the interaction factor. This factor may be calculated from Equation 2.80 and 2.89 for various pile slenderness ratios and different pile spacings. Figure 2.38(a) shows typical plots for piles in homogeneous soil with a Poisson's ratio, $v=0.4$.

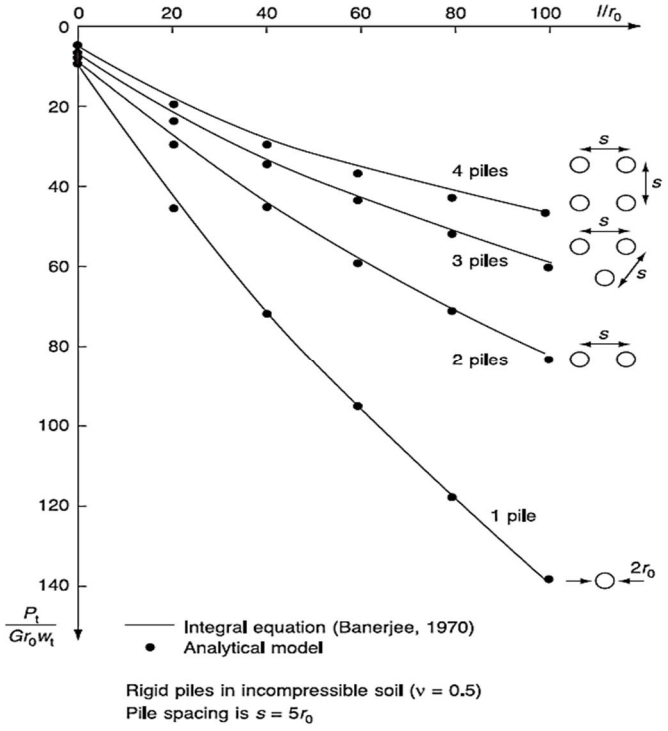


Figure 2.37: Comparison of load-settlement ratios for symmetric pile groups containing up to 4 rigid piles (after Randolph and Wroth, 1979)

The results are compared with those from integral equation solutions and exhibit good agreement. Figure 2.38(b) shows interaction factors for a pair of rigid piles in non-homogeneous soil for the case of $v=0.4$ and varying degree of homogeneity, $\rho = G_{L/2}/G_L$, where $G_{L/2}$ and G_L are the values of the shear modulus of the soil at pile mid-depth and at the pile base respectively. $L/r_0=l/r_0=40$.

In real soil, the non-linear nature of the soil deformation leads to less interaction than predicted by a linear elastic analysis, since deformation will be confined more to the vicinity of the pile. Therefore, the Randolph and Wroth (1979) method may provide realistic predictions of pile interaction of comparable accuracy to that of the more rigorous integral equation analysis.

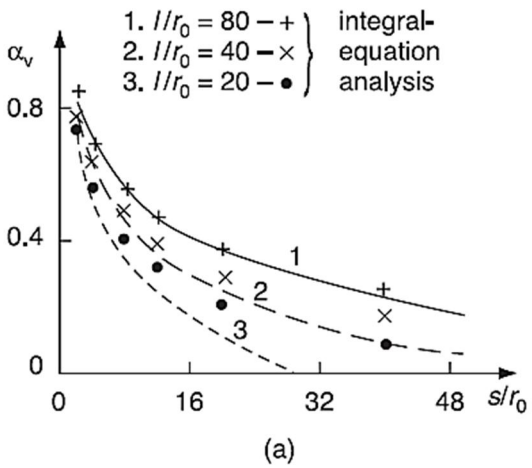


Figure 2.38(a): Interaction factors for pairs of rigid piles in homogeneous soil with *v=0.4* (after Randolph and Wroth, 1979)

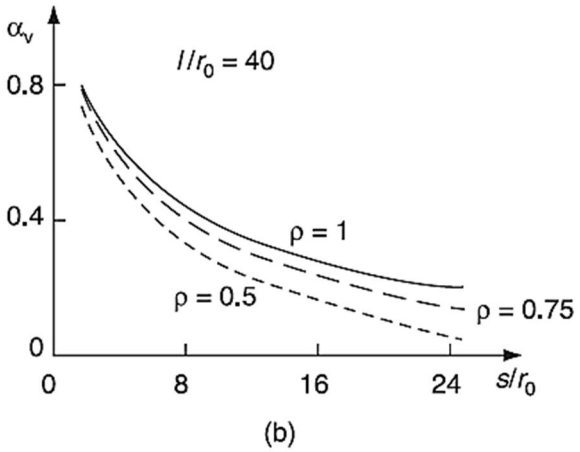


Figure 2.38(b): Interaction factors for pairs of rigid piles in non-homogeneous soil, *v=0.4* (after Randolph and Wroth, 1979)

(Ng, et al. 2004)

2.8.8 Poulos and Davis (1980) method

The interaction factor method by Poulos and Davis (1980) is one of the common ways by which pile group behavior is analysed. Referring to Figure 2.39 the settlement, w_i, of a pile i, within a group of n piles is given by:

$$w_i = \sum_{j=l}^{n} \left(P_{av} S_1 \alpha_{ij}\right) \qquad (2.91)$$

Where P_{av} is average load on a pile within the group, S_1 is the settlement of a single pile under unit load, also called the pile flexibility, α_{ij} is the interaction factor for pile i due to any other pile j within the group, corresponding to the spacing S_{ij} between piles i and j.

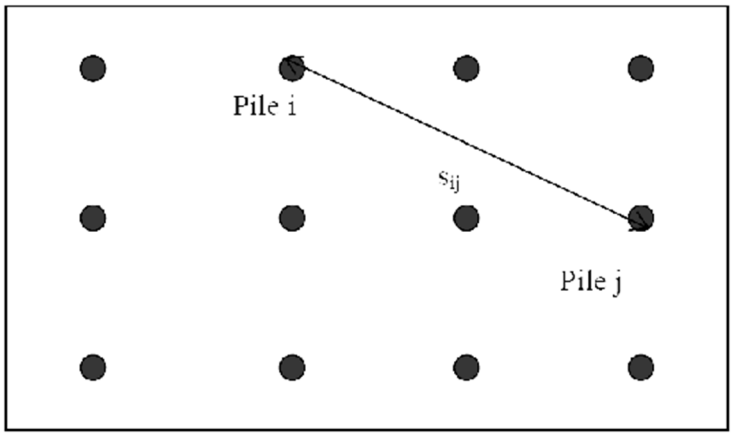


Figure 2.39: Pile group in plan depicting superposition via the interaction factor method (after Poulos and Davis, 1980)

Equation 2.91 can be written for each pile to produce a total of *n* simultaneous equations. These, together with the equilibrium equation, can be solved for two simple conditions which are:

a) Condition of known load on each pile, in which case the settlement of each pile can be directly computed from the above equation. The pile cap would be assumed to be flexible and there will usually be differential settlement among the piles in the group.
b) The condition of a rigid (non-rotating) pile cap, in which case all piles settle equally. There will be a uniform settlement but a non-uniform distribution of load in the piles.

Originally, interaction factors were calculated from boundary element analysis and plotted in graphical form of interaction factor versus the ratio of the pile spacing to diameter, *S/d*. Further, the interaction factors were applied to the total flexibility, S_I, of the pile, inclusive of both elastic and non-elastic components of single pile settlements, being based on the assumption that the soil was a homogeneous elastic medium of constant modulus with depth. This assumption is an oversimplification of reality. Consequently, some substantial improvements and extensions have been made to the original interaction factor method by Poulos (1968). Some of the important changes and/or improvements are:

- Consideration of changing soil modulus with depth.
- The consideration of bearing stratum on which the piles are founded.
- The consideration of different stiffness of the soil between the piles and that at the pile-soil interface, the soil between piles being stiffer due to small strain levels existing between the piles.
- Consideration of the effect of compressible underlying layers below the founding layer.

(Poulos and Davis, 1980)

The significance of the above developments in the interaction factor method is reviewed by Poulos and Davis (1980) and summarized below, with reference to the general case of a simple pile group section shown in Figure 2.40.

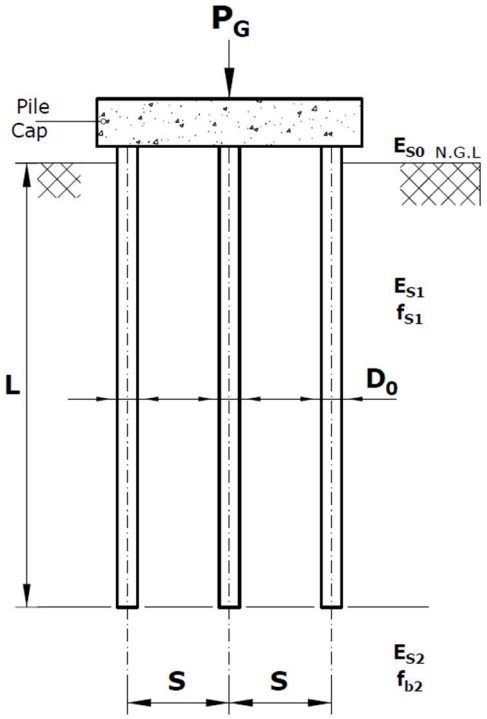


Figure 2.40: Section through a 3x3 pile group

Note: E_{S0}, E_{S1} and *E_{S2} (=E_{SL})* refer to the modulus of the soil at the surface, along the pile shaft and at the base of the pile, respectively.

2.8.8.1 Influence of non-homogeneity of the soil layer

Figure 2.41 compares the relationship between the interaction factor and *S/d* ratio for the following cases:

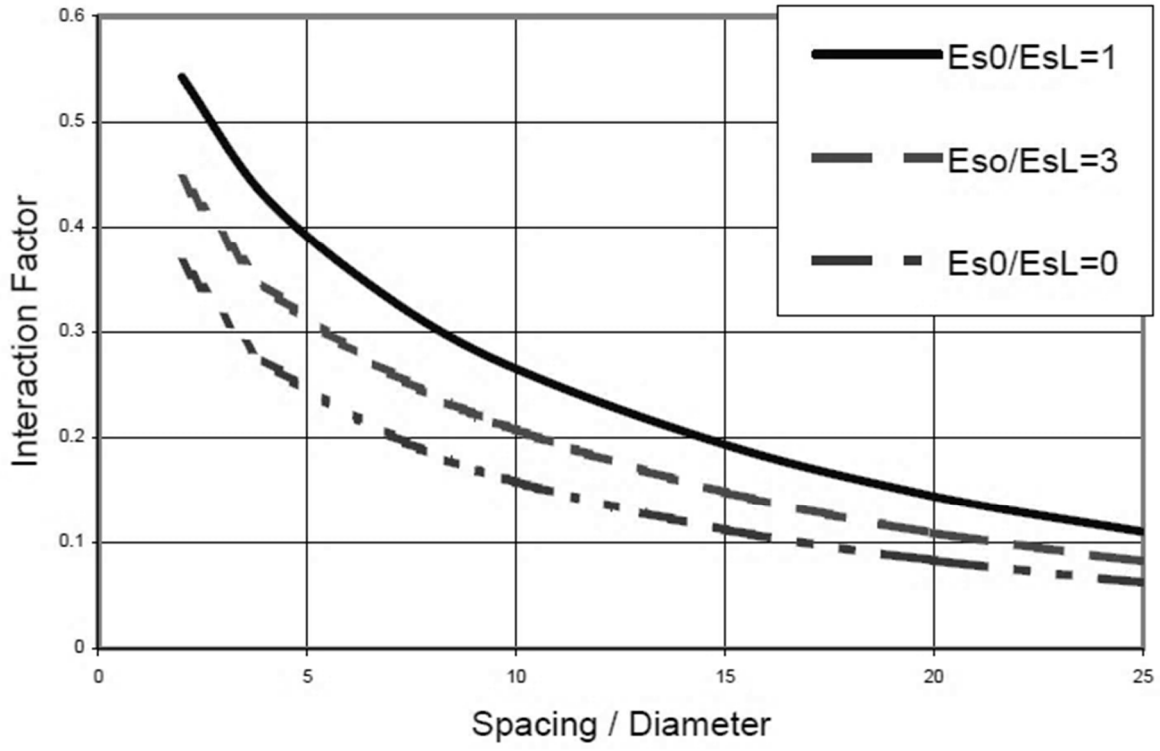


Figure 2.41: Influence of soil modulus on interaction factor (after Poulos and Davis, 1980)

a) A homogeneous soil layer with a soil modulus that is constant with depth of soil, $E_{S0}=E_{SL}$.
b) A case of a soil where the surface modulus is equal to 3 times that of the base, $E_{S0}=3E_{S2}$.
c) A case of a non-homogeneous soil layer whose modulus varies linearly with depth, from zero at the surface, also commonly referred to as a Gibson soil, which has the same average modulus as the uniform layer.

It is deduced from Figure 2.41 that the interaction factor of the non-homogeneous soil is less than that for the uniform layer. This, therefore, implies that use of the interaction factor for the uniform layer in estimating the group settlement of a non-uniform layer will lead to an overestimate, hence conservative, group settlement prediction.

2.8.8.2 Influence of the stiffness of the bearing stratum

The effect of the stiffness of the bearing stratum, E_{S2}, as a multiple of the stiffness of the overlying soil, E_{S1}, is shown in Figure 2.42. The interaction factor, α, decreases as the stiffness of the bearing stratum, relative to the soil, increases. Therefore the presence of a hard layer at the bottom of the soil layer substantially reduces the interaction factor and hence, the settlement of pile groups at relatively small pile spacings. It follows that the use of solutions for a deep layer may thus lead to substantial overestimation of pile interactions and hence, pile group settlements.

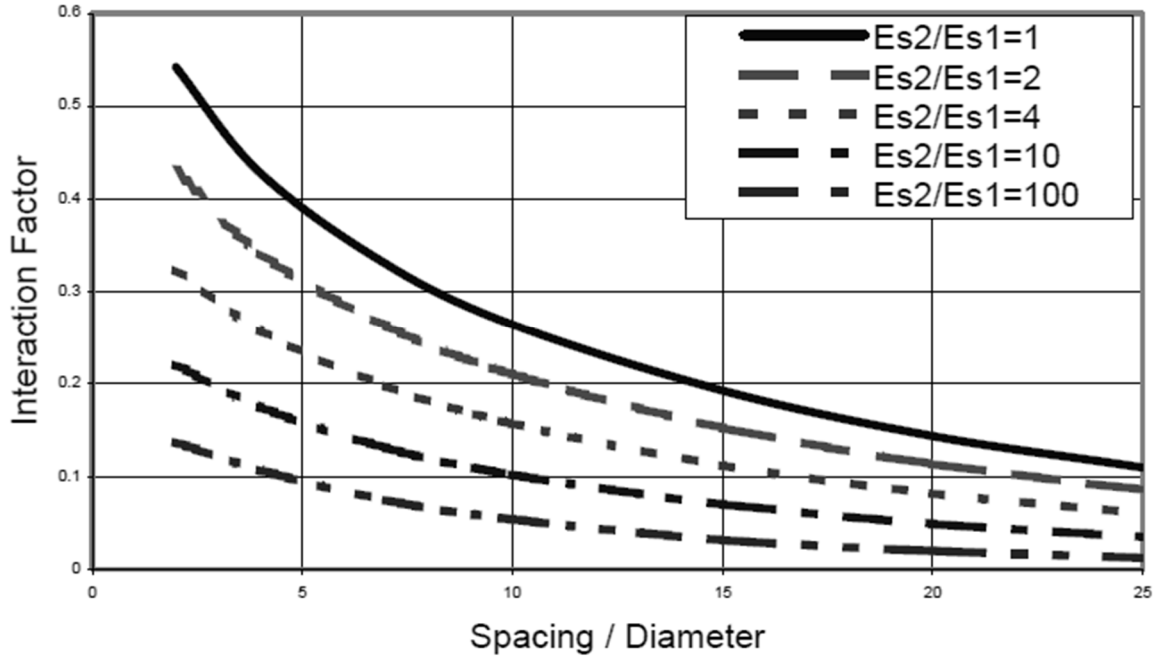


Figure 2.42: Influence of bearing stratum stiffness on interaction factors (after Poulos and Davis, 1980)

2.8.8.3 Influence of stiffer soil between the piles

It is now recognized that the stiffness (or modulus) of a soil mass decreases with increasing strain level, thus it would be expected that for a pile group, the strain level will increase as the pile-soil interface is approached. Therefore the stiffness of the soil at the pile-soil interface is smaller than that between the piles at some distance from the pile shafts. Poulos (1988) demonstrated that the presence of the stiffer soil between the piles can lead to a substantial reduction in interaction factor between two piles, by assuming very simplified distributions of soil modulus with distance from pile shafts. Poulos (1989) demonstrated that such an approach

gave satisfactory agreement with the field test results on a pile group in clay (O'Neill et al, 1982, as cited in Poulos and Davis, 1980).

2.8.8.4 The effects of compressible underlying layers

Poulos and Davis (1980) also investigated and concluded that the presence of soft compressible layers below the pile tips can result in significant increases in settlement of pile groups, although settlement of a single pile is largely unaffected by the presence of compressible layers, (Golder and Osler, 1968). The larger the group, the greater the effect of the underlying compressible layer on settlement. It follows that ignoring the presence of compressible layers leads to an under prediction of the pile group settlement. Conversely, if proper account of stiffer layers below the pile tips is not taken into consideration, an overestimation of group settlement may result because of the increasing soil/rock stiffness with decreasing strain level.

2.8.9 Randolph (1985) method

It has already been demonstrated in earlier sections that the superposition principle is used to extend the solution for single piles to cover the axial response of large pile groups, but the computational effort involved would neccesitate the use of a computer. The presence of similarly loaded nearby piles leads to an increase in the settlement of a pile for a given load, and such an effect is quantified by the use of interaction factors (Poulos. 1968, 1977). Charts are prepared which give the stiffness of a pile group as a function of the total stiffness of the component group, for common group arrangements, and may be expressed in terms of either the settlement ratio, R_s (Poulos and Davis, 1980) or as an efficiency, η (Butterifeld and Douglas, 1981). Randolph (1985) presents a simplified approach to estimating the efficiency, hence settlement of large groups, without the need to conduct computer analysis.

Piles in a group have been established to settle more than a corresponding isolated pile for a given load, due to interaction effects. This leads to the concept of settlement ratio R_s, which can be defined as the ratio of the flexibility of a pile in a group to that of an isolated pile. The potentially more useful concept of efficiency, η, is defined as the ratio of the stiffness of the piles in a group to that of an isolated pile. Efficiency is thus equal to the inverse of the settlement ratio. The stiffness, k, of a single pile can be defined as the load, P, divided by settlement, w, i.e.: $k=P/w$. Therefore for a pile group with n identical piles, each with stiffness k, the overall group stiffness, K is then given by: $K=\eta.n.k$.

If the efficiency is plotted against the number of piles in the group, essentially, straight lines on a logarithmic scale axes are obtained (Butterfield and Douglas, 1981). The exact layout of the piles in the group appears to have no significant influence on the calculated efficiency. There is no real difference in efficiency between a rectangular pile group and a square pile group with the same number of piles and same pile spacing. Figures 2.43 and 2.44 show the typical graphs for square groups of n piles, $S/d=3$, $l/d(=L/D_0)=25$, $\lambda=1000$, degree of homogeneity of soil, $\rho=G_{1/2}/G_1=0.75$ and $v=0.3$. $G_{1/2}$, G_1 are the values of shear modulus at pile mid-depth and pile base respectively.

The effect of varying S/d is shown in Figure 2.43 while that of varying the pile stiffness, λ, is shown in Figure 2.44 above. These graphs were obtained by computer analysis of up to 169-pile group (13x13 square group). Results for up to n=1000 were extrapolated from the 13x13 square groups analyses. From the figures, it can be deduced that the efficiency of each pile falls for large pile groups, with piles' stiffnesses falling to as low as 5% as stiff as it would be as an isolated pile.

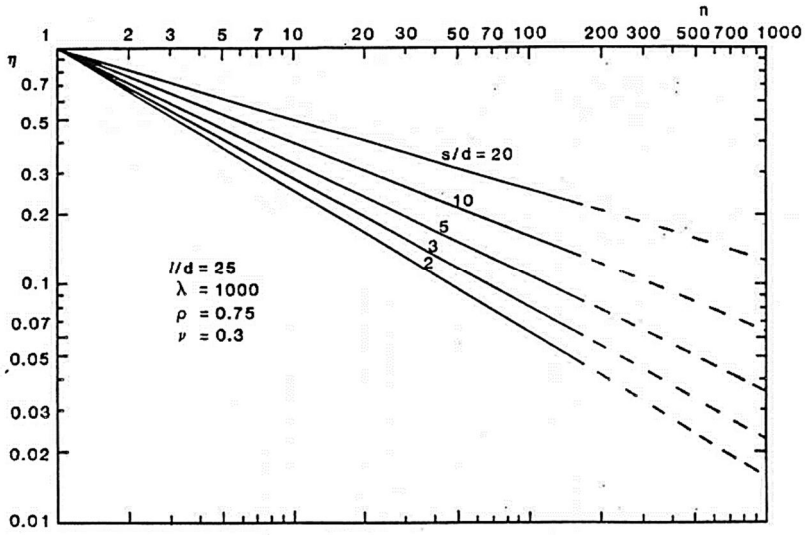


Figure 2.43: Efficiency of square pile groups at different spacing (after Randolph, 1985)

From Figure 2.43, it can also be inferred that widely spaced piles may be nearly as stiff as many but more closely spaced piles. From the figure, for n=256 and pile spacing *S/d*=3, the efficiency, η≈0.05. This gives an overall stiffness equivalent to 256x0.05≈13 isolated piles.

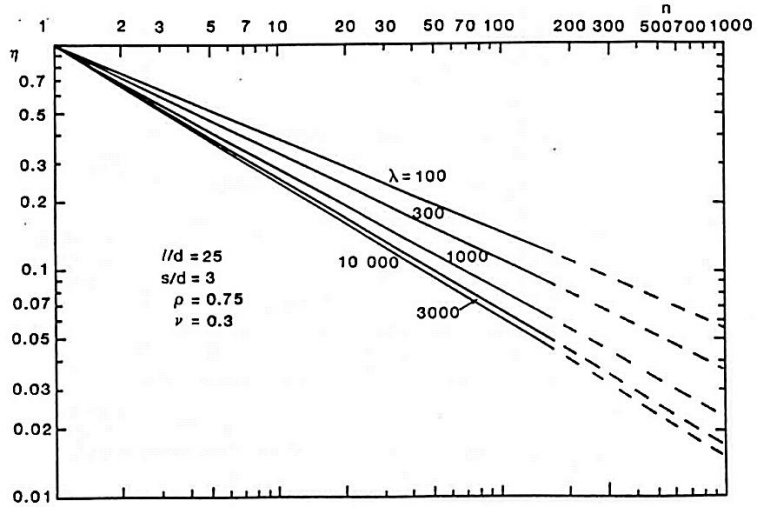


Figure 2.44: Efficiency of square pile groups for piles of different stiffness ratios (after Randolph, 1985)

A group of 25 piles spaced at *S/d*=11 (this covers almost the same ground area) has an efficiency of approximately 0.19, or an overall stiffness equivalent to 25x0.19≈5 isolated piles. Therefore, reducing the number of piles by an order of magnitude (256/10≈25 – order of magnitude) gives a group stiffness reduced by about 60%.

The curves of efficiency against number of piles are nearly straight on logarithmic axes as seen in Figure 2.43. Therefore the efficiency, η, of a pile group of n piles, can be written as: $\eta = n^{-e} = \frac{1}{n^e} = 1/R_s, \Rightarrow \mathrm{R_s} = \mathrm{n^e}$ Therefore $\rho_G = R_s S_1 = n^e S_1$

Where ρ_G is the pile group settlement, S_1 is the settlement of a single pile under same average load and the exponent value is in the range: $0.4 \leq e \leq 0.6$ for most pile groups. The actual value of e depends on:

- Pile length, *l/d*
- Pile stiffness, λ (=K)=(E_p/E_s).R_A
- Pile spacing, S/d
- Degree of homogeneity of the soil, ρ=$G_{L/2}/G_L$
- Poisson's ratio, *v*.

Curves are available for the estimation of the value of e for a given combination of factors.

2.8.9.1 Settlement of long piles

Long, slender piles are most likely to mobilise their full skin friction over the upper part of each pile at working load. The settlement prediction of such a group must allow for slip between the pile and the soil by applying settlement ratios (which are the inverse of efficiency) to the elastic component of the single pile settlement because the local plastic movement will not result in interactive effects between piles.

2.8.10 Equivalent raft method

There are many variants of this method including the one suggested by Tomlinson (1986). This approach is the common method of choice for estimating pile group settlements due to its convenience and fairly straightforward application. The method entails the replacement of a pile group with a raft foundation of some equivalent dimensions, with the full design load assumed to act at some representative depth below the underside of the pile cap. Tomlinson's representative depth varies between 2*L*/3 and L depending on the assessed founding conditions and thus type of pile foundation. A representative depth of 2*L*/3 applies to friction pile groups while that of L is for end bearing pile groups. (Tomlinson and Boorman, 2001). The load is assumed to be distributed in the ratio which of 2:1 (vertical:horizontal), commonly referred to as the "2:1 stress distribution", for floating pile groups and zero load/stress variation for end bearing piles. Figure 2.45 illustrates the 2:1 vertical stress distribution and the 'actual' versus the 'approximate' stress distribution.

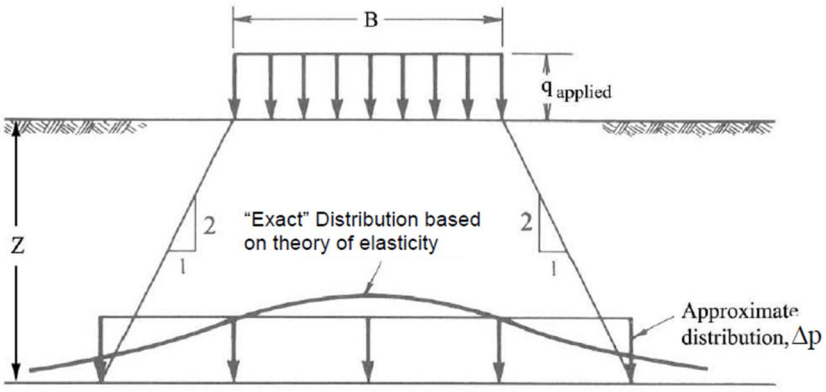


Figure 2.45: Distribution of vertical stress by the 2:1 method (Perloff and Baron, 1976)

The immediate settlement S_i, at the pile tip carrying a uniform pressure q on the surface of an elastic half-space, with a linear stress-strain relationship, can be expressed as:

$$S_i = \frac{qB}{E_s}(1 - v^2)I_S \qquad (2.92)$$

Where:

E_s is the soil's Young Modulus, *v* is the Poisson's ratio of the soil, *B* is the length of each side, for square piles and the diameter, for circular pile, I_S is an influence factor which depends on

the shape of the loaded area. Values of I_S are worked out from the values in Table 2.2. In this case, I_S=0.79 because pile cap is rigid and supporting circular piles. The soil is soft to intermediate clay. Figure 2.46 shows the schematic diagram of the piles and the equivalent raft to where reference is made for the definition of some dimensional symbols used in this section..

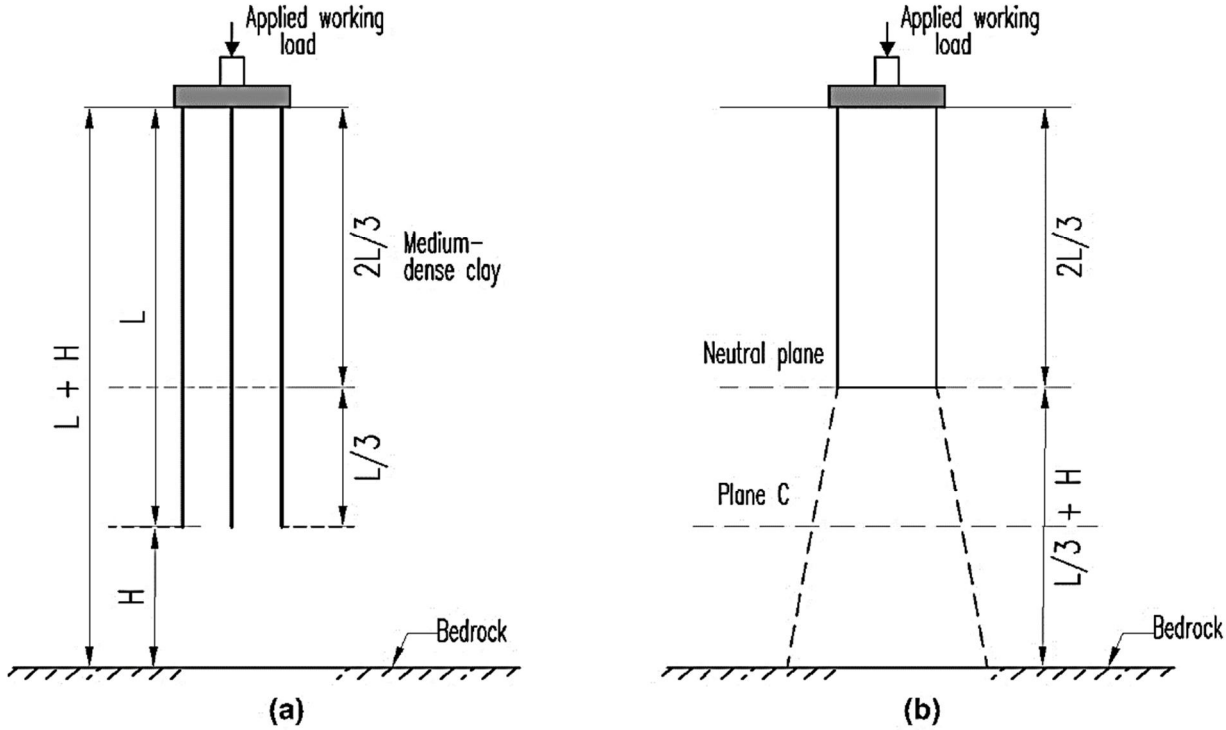


Figure 2.46: Schematic diagram of (a) a 3x3 pile group and (b) the equivalent raft method for a floating pile group (after Tomlinson, 1986)

The following steps are steps are taken to calculate pile group settlement:

1) Determination of the immediate settlement using Equation 2.92 where $q=nP_{safe}/A_G$, A_G being the plan area of the pile group. The pile spacing, $S=3D_0$ and square groups are under consideration for which the side lengths are: $4D_0$ for 2x2 pile group, $7D_0$ for 3x3 pile group and $10D_0$ for 4x4 pile group.
2) Calculations for immediate pile group settlement are automated to a spreadsheet and are tabulated in section 4.4.2.4 worked example.
3) Determination of the initial effective stress, σ_0' at the midpoint of the compressive layer. The depth of the bedrock h, below ground surface is normally determined from site investigations for finite layers as is the case in the example in section 4.4.2.4. The pile group is converted to an equivalent raft as described above and the thickness of the compressive layer, $T_{CL}=h-2L/3$ where L is the pile length. Therefore the depth to the midpoint for calculation of σ_0' is calculated from: $h-0.5(2L/3)$. The unit weight of the soil γ (kN/m^3) and the depth of the water table are also determined from laboratory tests on site samples and physical site investigations respectively.
4) Determination of the new effective stress σ_1', which is the stress after the pile group has been loaded. $\sigma_1'=\sigma_0'$+stress increase due to pile group load at the midpoint of the compressive layer. The area at the midpoint is determined by assuming a 2 vertical to

1 horizontal stress distribution to determine the width and length of the equivalent footing at the midpoint.

Consolidation settlement S_C, is then calculated using Janbu's equation:

$$S_C = T_{CL}.(1/m).\ln(\sigma_1'/\sigma_0') \quad (2.93)$$

Where; m is the dimensionless modulus number which is determined from Table 2.3 and T_{CL} is compressible layer thickness

Janbu (1963) method can be used to estimate the long term settlement for pile groups in both sand and clay soils, by assuming that the settlement is related to two parameters which are: :

- Stress exponent, j, which is dimensionless
- Modular number, m, also dimensionless.

Both the stress exponent and the modular number are unique to individual soils.

2.8.10.1 Janbu's equation for pile group settlement in clay soils

$$\text{Consolidation settlement, } S_c = T_{CL}.\frac{1}{m}\ln\left(\frac{\sigma_1'}{\sigma_r'}\right) \quad (2.94)$$

All the terms have already been defined in the above paragraphs and Equations.

The stress exponent, j=0 for pure clay soils and thus does not appear in Equation 2.94. The modulus number is obtained from Table 2.3 and as shown therein, $j \neq 0$ for silty clays and clayey silts.

Table 2.3: Soil settlement parameters (Janbu, 1963) (Rajapakse, 2008, p.210)

Soil Type	Modulus Number (m)	Stress Exponent (j)
Till (very dense to dense)	1,000-300	1.0
Gravel	400-40	0.5
Sand (dense)	400-250	0.5
Sand(medium dense)	250-150	0.5
Sand (loose)	150-100	0.5
Silt (dense)	200-80	0.5
Silt (medium dense)	80-60	0.5
Silt (loose)	60-40	0.5
Silty Clay (or Clayey Silt)		
Stiff silty clay	60-20	0.5
Medium silty clay	20-10	0.5
Soft silty clay	10-5	0.5
Soft marine clay	20-5	0
Soft organic clay	20-5	0
Peat	5-1	0

The equivalent footing located representing the pile group is located at a neutral plane, the plane being located at $\frac{2}{3}L$ from the pile cap soffit.

2.8.10.2 Janbu equation for pile group settlement in sandy soils

Sandy soils attain their maximum settlement within a short period of time. Janbu proposes the

following empirical relationship for pile settlement in sandy soils:

$$S_{sandy} = T_{CL}.(2/m).\left[\left(\sqrt{\sigma_1'/\sigma_r}\right) - \left(\sqrt{\sigma_0'/\sigma_r}\right)\right] \quad (2.95)$$

For sandy soils, the stress exponent, *j=0.5*, and is already integrated into Equation 2.95. Equation 2.95 is unit-sensitive, thus: T_{CL} = thickness of compressible sand layer in metres, *m* = modulus number which has no dimensions, σ_1' = new effective stress after load application in kN/m^2, σ_0' is the effective stress before pile loading in kN/m^2 and σ_r is a reference stress taken as equal to 100kPa (atmospheric pressure) for metric units

The following is a summary of the steps followed:

- The neutral axis is assumed at 2L/3.
- The pile group is simplified to a solid footing which ends at a depth of 2L/3.
- Computation of the original stress, which is stress due to overburden prior to construction of piles.
- Computation of stress increase due to pile group loading.
- Application of Janbu equation to determine consolidation settlement.

2.8.11 Poulos (1989) method

Continuum mechanics deal with the mechanical behavior of materials modelled as a continuous mass rather than as discrete particles. All soil is discontinuous to some extent, but this becomes irrelevant at some scale of aggregation when a continuum view becomes necessary and valid.

The continuum theory of soil mechanics includes mathematical theories of elasticity, plasticity and viscosity and the basic equations of equilibrium, conditions of compatibility of strains and displacements and stress-strain constitutive relationships of soil. The continuum-based analysis can be extended to the analysis of axially loaded pile groups. The elastic solution of Mindlin (1936) may be used in evaluating the displacement influence factors in order to determine the displacement of an element of a pile due to all elements of that pile and other piles in the group. El-Sharnouby and Novak (1985, as cited in Poulos, 1989) developed a convenient approximate method of evaluation which avoids the double integration of the Mindlin equations, thus reducing the computation time which the Mindlin solution requires.

Several methods of implementing the above analysis have been developed, among them the solutions for a two-pile group, obtained from a continuum analysis, which can be used to get interaction factors. An interaction factor expresses the increase in head settlement of a pile due to the presence of another similarly loaded nearby pile (Poulos, 1968; Randolph and Wroth, 1979). The interaction factor, α is defined by the following relationship:

$$\alpha = \Delta S/S_1 \quad (2.96)$$

Where ΔS is the increase in settlement of a pile due to the presence of another equally loaded pile and S_I is the settlement of a single pile under its own load. For a group of piles, the interaction factor may be superposed to develop a set of equations relating the settlement of each pile to the single pile settlement, the load in each pile head and the interaction factors.

Terzaghi (1939), in his James Forrest Lecture, intimated that there was no rational relationship between the behavior of single piles and pile groups. Such thinking rightly encouraged caution

when dealing with groups which contain very large number of piles, which are often better when dealt with as a large block foundation. For groups which contain relatively few piles, the settlement of single piles and pile groups can be theoretically linked at normal working loads. It is convenient to characterize the influence of interaction between piles with regards to settlement in terms of two dimensionless quantities which are:

- For two-pile group, the interaction factor α, defined by Equation 2.96 and denotes the relative increase in settlement due to the presence of another pile.
- For general pile group, the group settlement ratio R_s. R_s has an alternative quantity R_G, the group reduction factor, also termed the efficiency factor (Butterfield and Douglas, 1981; Fleming et al, 1985). Both Rs and R_G have already been defined in section 2.8.4 of this report. For a group of n piles, the relationship between R_s and R_G has been defined in Equation 2.72.

Poulos (1989) notes that pile group interaction depends, mainly, on two sets of dimensionless parameters under working load conditions. These are:

a) Those related to the pile and soil characteristics and
b) Those related to the geometry of the piles and pile groups.

The pile stiffness factor K, the ratio E_b/E_s, and the variation of the soil's Young's modulus E_s, with depth, are the important pile and soil characteristics. Poulos (1989) plotted the variation of the interaction factor α with the above parameters for a two-pile group and drew the following conclusions:

a) α decreases as K decreases
b) α decrease as E_b/E_s increases and
c) α decreases as E_s becomes less uniform with depth. Es is constant with depth for homogeneous soil and increases linearly with depth in a Gibson soil.
d) It was also be observed that there was a good agreement between the variation of α in a Gibson soil and the measured/actual values as presented by Cooke et al, (1980, as cited in Poulos, 1989).

Group interaction factors are influenced by the length to diameter ratio L/d, the relative spacing between the piles S/d, and the number of piles in the group. These are called the primary geometric factors.

Figure 2.47 shows the variation of settlement ratio Rs, with L/d and n, for the case of $v=0.3$, $S/d=4$ and $K=1000$, for square pile groups in a Gibson soil of finite thickness $h=2L$, h being the depth of the finite layer. It can be seen that Rs increases with increasing L/d and n, with the influence of L/d being fairly small for $L/d>25$. Fleming et al (1985, as cited in Poulos, 1989) suggest that R_s is approximately related to n by:

$$R_s \approx n^{\omega} \qquad (2.97)$$

Where n is the number of piles in the group, ω is an exponent and $0.4 \leq \omega \leq 0.6$ for most pile groups. For a group connected by a rigid pile cap, a given number of piles n, at a specified spacing, R_s does not depend on the geometric configuration of the piles because R_s for a *6x6* configuration is very similar to that of a *2x18, 3x12 or 4x9*.

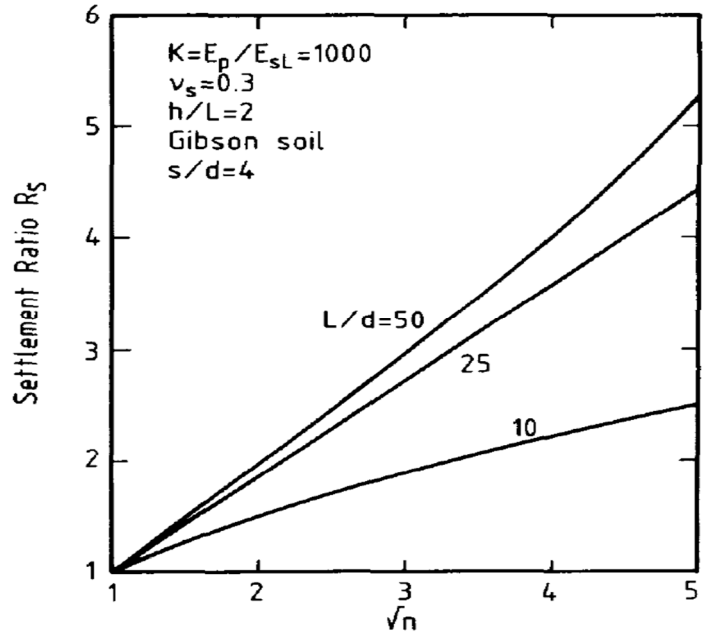


Figure 2.47: Influence of geometric parameters on group settlement ratio (after Poulos, 1989)

The group reduction factor R_G, mainly relies on group breadth for a given set of pile characteristics. Figure 2.48 shows the plots of R_G against normalized group breadth, together with plots for data used by Skempton (1953) to derive the empirical equation covered in section 2.8.1 of this report, for pile group settlement in sands. The trend and magnitude of the theoretical curves are in close agreement with the data used by Skempton.

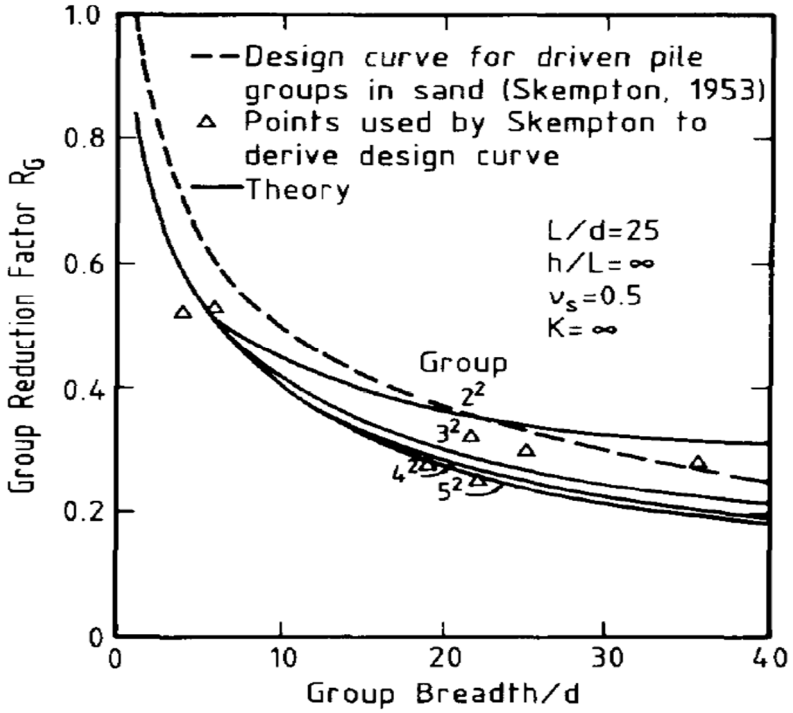


Figure 2.48: Variation of group reduction factor with group breadth (after Poulos, 1989)

The load distribution in a group with a rigid pile cap is generally not uniform. Piles at the

corners will bear the greater load portion while those at or near the centre carry the least. This theoretical conclusion was confirmed by field and model test results (Chow, 1986, as cited in Poulos, 1989). The interaction of piles in a group may also be influenced by the stiffness of the soil between the piles. Contrary to the commonly held assumption that a soil is horizontally homogeneous, the soil between piles in a group undergoes small strains deformation which in turn leads to high small strains Young's modulus E_0, and hence, high stiffness. Therefore the soil between piles, in reality, is likely to be stiffer than that near the pile-soil interface, thus reducing the interaction between piles. Poulos (1988a), carried out a simplified analysis to prove this. Consequently, for pile groups, the stiffer soil between piles leads to limited interaction between piles, hence smaller settlement.

Poulos (1989) concluded that as the size of the pile group increases, the relative proportion of the immediate settlement S_i, to the total final settlement S_{TF}, decreases and that K has an insignificant influence on S_i/S_{TF} value. However, immediate settlement still constituted the major portion of the total final settlement for a pile group, just like for a single pile, unless compressible layers exist under the pile groups. Pile group interaction and hence, settlement, is also significantly influenced by the stiffness of the underlying soil layers. When $Eb/Es<1$, it implies the presence of a softer layer below the pile base in the group and that such a scenario leads to a substantial increase in the group settlement compared to the case of a homogeneous soil mass when $Eb/Es=1$ (and means that Es is constant with depth).

Poulos also concluded that for most practical purposes, the effect on group settlement of a pile cap being in contact with the soil is relatively small and thus ignored, at working loads.

2.8.11.1 Pile group settlement from charts

Poulos developed charts enable rapid estimates of pile group settlements for both driven and bored piles in different soil types. One such convenient form of representation is in terms of group settlement ratio R_s, and the exponent of the settlement ratio ω, as given by Equation 2.97. Solutions have been generated by means of a computer program called DEFPIG and allowance for higher stiffness of soil between piles in a group than at the pile-soil interface made (Poulos, 1988a)

Figures 2.49 and 2.50 show the plots of settlement ratio exponent ω, against four different soil types and for driven and bored friction piles for $10 \leq L_P \leq 30m$, and $S/d=3$. The average value of ω for square pile groups ranging from $4 \leq n \leq 25$ piles in size, of diameters of 0.3m and 0.6m, is plotted for each pile length. The following deductions are made from the figures:

- For piles in clay, ω is approximately independent of pile length while for silica sand, ω decreases as the pile length increases.
- ω values range is narrow for short piles but increases as the pile length increases.
- ω varies between 0.41 and 0.52 for L=10m and $0.22 \leq \omega \leq 0.47$ for L=30m, which implies that the use of these design charts is likely to be less accurate for long piles than for short piles.

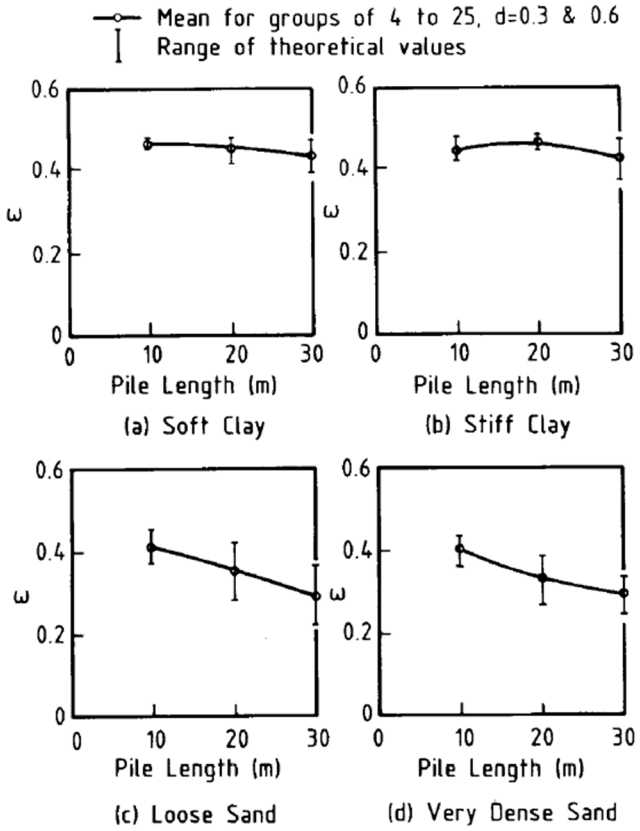


Figure 2.49: Settlement ratio exponent for driven piles, *S=3D*, (after Poulos, 1989)

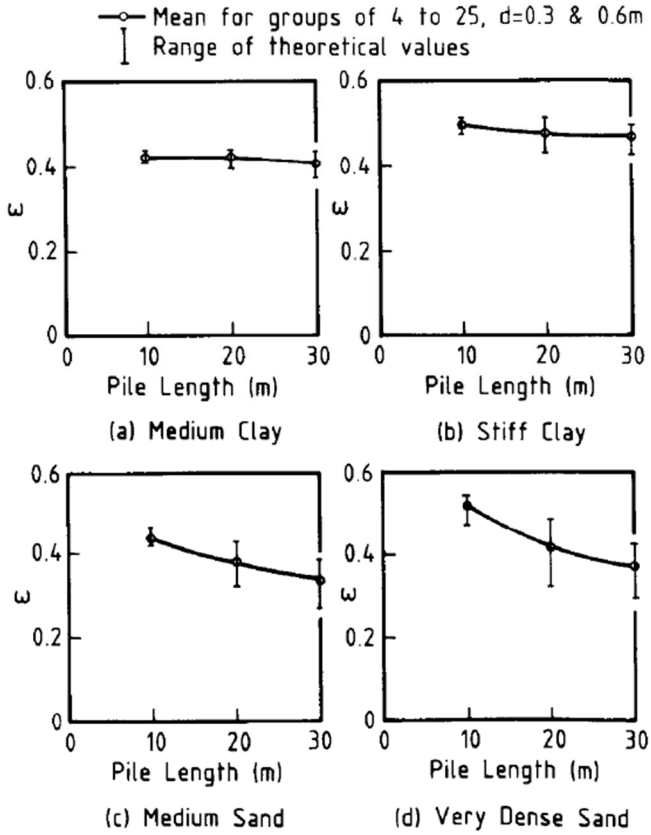


Figure 2.50: Settlement ratio exponent for bored piles, *S=3D*, (after Poulos, 1989)

2.8.12 Mylonakis and Gazetas (1998) method

From discussions in earlier sections, it is now accepted that when piles are installed at relatively close spacing in groups, the settlement of any of the piles in the group will cause settlement in the surrounding soil. The settlement of a given pile *i*, in the group is equal to the settlement under its own load plus a small additional amount of settlement induced by each of the other pile in the group, provided the pile behavior is still within the elastic limit, i.e.: the load is still below ultimate. The amount of additional settlement in the pile of interest *i*, induced by a nearby pile *j*, will reduce with increasing distance from the pile of interest. For a group of *n* piles which are identical, the settlement of pile *i* is given by:

$$S_i = \left(\frac{1}{K_p}\right)\left[P_i + \sum_{j=1}^{n} \alpha_j P_j\right] \qquad (2.98)$$

Where K_p is the overall pile head stiffness of pile *i*, P_i is the load applied to pile *i*, P_j is the load applied to pile *j* and α_j is the interaction factor describing the influence of pile *j* on the settlement of pile *i*. Poulos and Davis (1980) proposed the original interaction factor approach and presented simplified design charts for α_j which are dependent on the Young's modulus of the pile material E_p, the shear (or Young's) modulus of the soil G_s, the pile length L_p, pile diameter D_0 and pile spacing, *S*.

Mylonakis and Gazetas (1998) present amended interaction factors which embody the reinforcing effects of adjacent piles. These revised interaction factors are therefore presumably more accurate for use in design. The factors are derived from:

$$\alpha_{j=} \frac{ln(r_m/S)}{ln(2r_m/D_0)} F_\alpha \qquad (2.99)$$

Where r_m is the radius beyond which soil settlement is vanishingly small (Randolph and Wroth, 1978) and can be approximated from $r_m = L_p$, F_α is called the diffraction factor/coefficient whose value is determined from Equation 2.100 below.

$$F_\alpha = \frac{2\mu L_p + \mathrm{Sinh}(2\mu L_p) + \Omega^2[\mathrm{Sinh}(2\mu L_p) - 2\mu L_p] + 2\Omega[\mathrm{Cosh}(2\mu L_p) - 1]}{[2+2\Omega^2]\mathrm{Sinh}(2\mu L_p) + 4\Omega\mathrm{Cosh}(2\mu L_p)} \qquad (2.100)$$

Where:

$$\mu = \sqrt{\frac{2\pi G}{\ln(2r_m/D_0)E_p A_p}} \qquad (2.101)$$

and

$$\Omega = \frac{K_{bi}}{E_p A_p \mu} \qquad (2.102)$$

F_α can also be determined graphically from Figure 2.51 which is a plot of Equation 2.100 for a wide range of possible combinations of pile properties using the parameters μ and Ω which are defined in Equations 2.101 and 2.102 above.

The procedure to calculate the settlements and load distribution within a pile group is as summarised below:

1) The interaction factor αj, for each pile are determined for all the surrounding piles. This is best done in tabular form. The symmetry of the pile layout is utilised wherever there is symmetry.

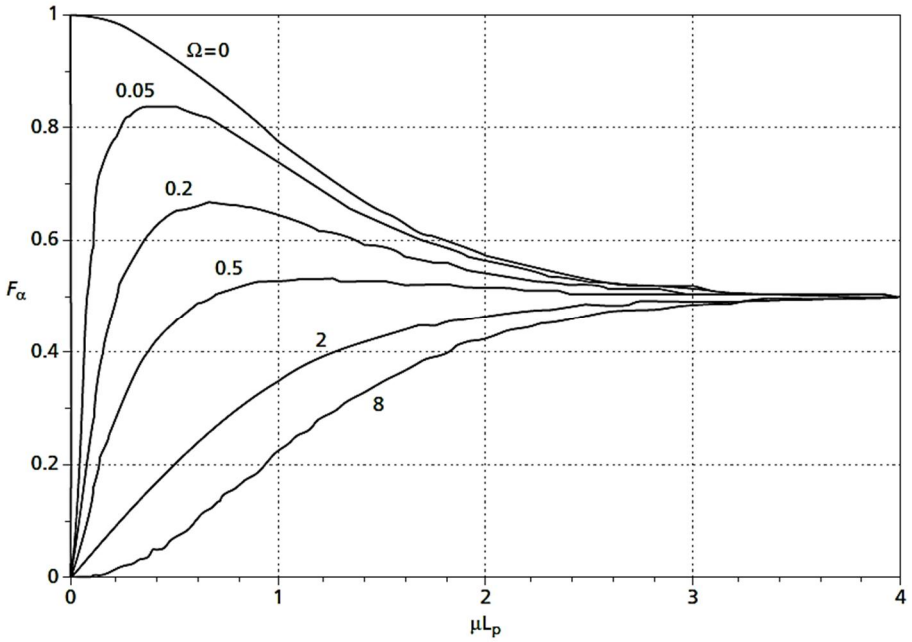


Figure 2.51: Diffraction coefficient (after Mylonakis and Gazetas, 1998)

.

2) Equation 2.98 is used to determine the settlement of each pile in terms of the unknown pile loads.
3) The total pile group load P_G, is equally distributed among the piles in a group where the pile cap is perfectly flexible. Thus load in each pile = P_G/n. These known pile loads are substituted into equations from step 2) above to determine the maximum possible settlement of each pile.
4) For a perfectly rigid pile cap, the settlement of each pile will be identical. This condition is used with equations from step 2) above to determine the load distribution among the piles in the group.

Steps 3) and 4) above represent limiting cases of pile cap flexibility and/or rigidity, thus the settlements of the piles and the loads carried by each pile will, in reality, be in-between the values calculated in these steps. This approach therefore helps to provide the bounds on which pile responses can be based for use in designs.
(Knappett and Craig, 2012)

2.9 Numerical Methods

When load is applied to the top of a pile, it is distributed to the surrounding soil or rock, either in skin friction or end bearing. It is now established, from the interpretation of results obtained from instrumented test piles, that initial deformations induced by the loads are usually absorbed in skin friction. Therefore, as the total load on the pile increases, more of the load is taken by end bearing. Numerous computer-based methods of pile settlement prediction exist such as the finite element and finite difference methods. These are some of the numerical approaches in common application. Solutions for both methods are based on solving partial differential equations PDEs (which are mathematical equations involving two or more independent variables), numerically (i.e. by using approximations that make the problem easier to solve) and the discretization (a process of converting continuous data attribute values into a finite set of points). The finite difference method FDM, uses topographically rectangular or square network of lines to construct the discretization of the PDEs, which is a limitation of the FDM

because it cannot handle complex geometries in multiple dimensions. This motivated the use an integral form of the PDEs and the subsequent development of the finite element method used in finite element analysis FEA.

The finite element method elegantly combines the best features of many approximate methods and has been used increasingly in recent years for the analysis of elements in structural and geotechnical engineering. Besides developments related to the method itself such as new constitutive models for soil and rock, new numerical procedures and calculation methods, role of FEM has evolved from a research tool into a daily engineering tool. This has been made possible by the increase of computer power and ready availability of such powerful computers to most engineers at home and workplaces worldwide.

The basic concept of the FEM is that a structural element, a pile in this case, is divided into smaller elements of finite dimensions called 'finite elements'. The original pile is then considered as an assemblage of these elements connected at a finite number of joints called 'nodes' or 'nodal points'. The properties of the element are formulated and combined to obtain the solution for the entire pile. Despite the development of the easy-to-use finite element programmes, it is difficult, particularly in geotechnical engineering applications, to create a good model that enables a realistic analysis of the physical processes involved in a real project because the highly non-linear and heterogeneous character of the soil material is difficult to capture in a numerical model. The complexity of soil behavior is caused by various phenomena on the soil particles and lead to microscopic observations such as stress, stress path, strain dependency of stiffness, critical state behavior and failure, etc.

When using FEM, soil is modelled by means of a constitutive model (stress-strain relationship) which is formulated in a continuum framework. The choice of the constitutive model and the corresponding set of model parameters are some of the most important issues to consider when creating a finite element model for a geotechnical project. It forms the main limitation in the numerical modelling process since the model, no matter how complex, will always be a simplification of the real soil behavior. Figure 2.52 shows a typical soil-pile mesh created using ABAQUS, a commercial programme used in FEA. Materials behavior of the concrete and the reinforcement steel were assumed to be linearly elastic while the behavior of the soil material surrounding the pile was assumed to be elasto-plastic based on the Mohr-Coulomb model.

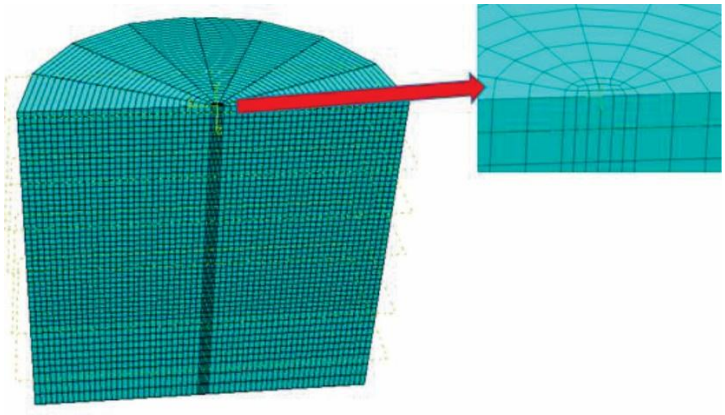


Figure 2.52: Depiction of a soil-pile mesh for particular FEA solution. Adapted from **Analysis of Cast-In Place Piles Using Finite Element Analysis, International Journal of Applied Engineering Research, 12(16), (**p. 6031), R. R.Salim and O. A. Abdulrazzaq, 2017, Research India Publications**.**

(Salim and Abdulrazzaq, 2017)

At workplaces, it is usually the young generation of engineers who are adept with geotechnical finite element software, performing numerical modelling and producing colourful results. Sometimes they do so without fully understanding the background and limitations of the constitutive models and numerical methods used in the software. The old generation of engineers may find it difficult to accept such results, especially if they do not tally with what they would expect from their experience. Such situations underscore the need for validation of geotechnical models.

PLEXIS, GEO5 FEM and ANSYS are some of the many FEA packages in commercial use and cost a significant amount of money to purchase and could not be procured for numerical modelling in this research project. Consequently, 'Pile', which is an ordinary computer programme of Prokon for the analysis and design of single piles was used in order to be able to compare settlement analysis results obtained by the computer method to those obtained by discussed empirical and theoretical methods. The programme had to be validated first in order for the results to be acceptable. Pile supports metric units of measurements only

2.9.1 Calculation of ultimate bearing capacity

The programme computes the pile bearing capacity from theory and empirical published data from the following:

$$Q_t = Q_s + Q_b = f.A_s + q.A_p \quad (2.103)$$

Where:

Q_t is the ultimate pile bearing capacity, Q_b is the total end bearing, Q_s is the skin friction resistance, A_p is the gross end area, A_s is the pile shaft side surface area, f is unit skin friction capacity and q is end bearing capacity.

The friction resistance and end bearing capacity depend on the soil properties and pile type.

2.9.1.1 Cohesive soils (Φ=0)

(a) Shaft friction

The shaft friction at any point along the pile founded in cohesive soils may be calculated from the following (Randolph and Murphy, 1985) for total stress analysis:

$$f = 0.5\sqrt{c.p_0} \quad (2.104)$$

Where c is the undrained shear strength of the soil at the point under consideration and p_0' is the effective overburden pressure at the point under consideration.

(b) End bearing

The unit end bearing is calculated from the following relationship:

$$q = 9c \quad (2.105)$$

$$\text{and } Q_b = q_b A_b \quad (2.106)$$

Where c=0.5UCS, UCS being the ultimate compression strength of the soil, Q_b is the pile base capacity and A_b is the pile base area.

The value of the undrained shear strength c, of the soil may be determined from tri-axial tests, shear box tests, visual soil descriptors and/or from the results of Standard Penetration Tests,

SPT values. Table 2.4 shows typical SPT and UCS values for saturated clay soils of varying consistencies.

Table 2.4: Typical SPT and UCS values for saturated clays

Consistency	SPT N-Value	UCS (kPa)
Very Soft	<2	<35
Soft	2-8	35-70
Firm	8-15	75-150
Stiff	15-40	150-300
Very Stiff	>40	>300

2.9.1.2 Cohesionless soils (c=0)

(a) Shaft friction

The shaft friction is calculated from the following equation:

$$f = K.p_0' tan\delta \quad (2.107)$$

$$Q_s = fA_s \quad (2.107a)$$

Where:

A_s = pile shaft surface area = $\pi D_s L$, K is the lateral earth pressure coefficient of the soil around the pile. $K=(K_0+K_a+K_p)/3$ where; K_0 is the lateral earth pressure coefficient at rest, K_a is the active earth pressure coefficient. K_a is always less than K_0. K_p is the passive earth pressure coefficient. K_p is always greater than K_0 and K_a. K, being for soils around the pile, which would be compressed for driven piles, and thus exerting more horizontal pressure than in-situ with K_p being maximum and K_0 minimum. δ is the friction angle between the soil and the pile shaft, which should be deduced from the soil's internal friction angle Φ, reduced in order to recognize the lower friction between the soil and the pile than within the soil itself. Table 3.5 contains typical values of δ and limiting values of *f*.

Design guidelines published by the American Petroleum Institute (API), (1984, 1991) fix the values of K as follows: K=0.8 for a partial displacement pile and K=1.0 for a full displacement pile, irrespective of the direction of loading (compressive or tensile). API also imposes limiting values of shaft friction ranging from 40kPa for loose sand to 120kPa for very dense sand.

(b) End bearing

The unit end bearing can be calculated from:

$$q = p_0'.N_q (= Q_b/A_b) \quad (2.108)$$

Where:

p_0' is the effective overburden pressure at the pile base and N_q is a dimensionless bearing capacity pressure. The values of q should also be limited as detailed in Table 2.5.

Table 2.5: Limiting values of *f* and *q*

Soil density	Soil type	Soil-pile friction angle(δ°)	Limiting s haft friction *f* (kPa)	Bearing capacity factor N_q	Limiting end bearing *q* (MPa)
Very loose Loose Medium	Sand Sand-Silt Silt	15	47.8	8	1.9
Loose	Sand				

Medium Dense	Sand-Silt Silt	20	67.0	12	2.9
Medium Dense	Sand Sand-Silt	25	81.3	20	4.8
Dense Very dense	Sand Sand-Silt	30	95.7	40	9.6
Dense Very dense	Gravel Sand	35	114.8	50	12.0

When only SPT results are available, Table 2.6 gives the descriptors and typical dry densities which may be assigned to saturated sands of varying dry density.

Table 2.6 Typical SPT results, descriptors and dry densities

Relative density	**SPT N-Value**	**DPC blow count (per 300mm)**	**Typical dry Density (kg/m^3)**
Very loose	0-4	0-7	<1450
Loose	4-10	7-18	1450-1600
Medium dense	10-30	18-54	1600-1750
Dense	30-50	54-90	1750-1925
Very dense	>50	>90	>1925

2.9.2 Deformation of single pile foundation

There are various methods available for the prediction of load-deformation curves among which one of the simplest and probably most cogent method is that proposed by Everett (1991) – 'load transfer functions and pile performance modelling'. A load transfer function is a mathematical relationship which exists between the load transferred from the structural element to a soil and the deflection of the element relative to the soil. Everett shows that for a pile, the side shear force which is transferred between the pile shaft and the soil is related to the deflection of the pile shaft relative to the soil, and that there is a similar relationship between the end bearing load transfer at the pile tip and the deflection of the pile toe.

Gezdi (1957, as cited in Everett, 1991) first proposed the empirical transfer function for the development of shear transfer between a structural element and a soil. Seed and Reese (1957), Coyle and Reese (1966) and Coyle and Sulaiman (1967) are some of the investigators who have contributed to the literature on empirical transfer functions. However, their published functions appear to have been developed for a specific pile type founded in a specific soil profile, which is at odds with field conditions where there are many soil types, which can have variations within the soil profile of a particular site. There are also many different types of piles with completely different installation methods which can affect soil properties. The ideal

modelling method would therefore be one that can accommodate all the different variations. Such a model would, no doubt, need a family of transfer functions in order to cope with all the variables. Everett (1991), proposes a single side shear function and a single end bearing function that can be modified to cope with most of the variations and fairly accurate results have been obtained from analyses using these functions. The application is fairly straightforward.

2.9.2.1 The side shear transfer function

Everett observes the variation in the shape of the side shear transfer function from the results of field tests and notes that cohesive soils tend to reach maximum shear transfer at a differential movement of less than 2mm and then usually experience a slight decrease in transfer due to the remoulding of the clay. On the other hand, sands tend to increase transfer with increasing differential movement. Similarly, a typical *c-Φ* soil increases side shear transfer with increasing slip although there is a marked change in the rate at which the increase occurs at a differential movement of about 2mm. (*c* and *Φ* are independent parameters of soil strength with no direct relationship between each other. The *c* value, which is the cohesion, comes from the binding between soil grains while the *Φ* value comes from the friction between the grains as they roll. A *c-Φ* soil has both cohesion and internal friction angle).

The concept of side shear transfer function having two components, was developed from the above observations. The two components are: (i) the adhesion component which is related to the cohesion of the soil and (ii) the intergranular component which is related to the angle of shear between the soil and the pile shaft. Everett's development of the side shear transfer function is mainly derived from Kedzi's (1957, as cited in Everett, 1991) conclusion that the side shear transfer function in sands is similar to the results obtained in the field for the same type of soil. Kedzi's function was modified by Everett through the introduction of two separate C and F component functions for the adhesion and intergranular component functions respectively, thus making it possible for the side shear transfer for all types of soil to be generated.

Everett proposed a shear transfer function which is mathematically represented by:

$$f = C_{ult}\left[1 - e^{(-K_1 d_{ps})}\right] + F_{ult}\left[1 - e^{(-K_2 d_{ps})}\right] \qquad (2.109)$$

f = unit side shear transfer (kPa); C_{ult} = ultimate adhesion transfer (kPa); F_{ult} = ultimate intergranular transfer; d_{ps} = pile shaft movement (mm); K_1, K_2 are constants.

The ultimate adhesion transfer is taken as the ultimate shaft friction, adjusted for the percentage fines, i.e.:

$$C_{ult} = C_f . PF \qquad (2.110)$$

Where:
C_f is the ultimate skin friction and PF is the percentage fines (%).

From Equation 2.110, it can be noted that the transfer is related to the total deflection of the pile shaft and not the differential deflection between the pile shaft and the soil immediately adjacent to the shaft as indicated in an earlier definition. This is so because Everett proved that provided the transfer function is developed from full-scale load tests, then the above simplification does not affect the accuracy of modelling short-term load/deflection results to a noticeable extent.

The values of the constants K_1 and K_2 have been determined from the back-analysis of several pile load tests in which the end bearing has been eliminated. K_1 varies from about 1.5 for a soft clay to 2.4 for a stiff clay, being about 2.0 for auger piles. K_2 is fairly constant at about 0.2. In order to illustrate how this Everett function compares with some published data, the function is plotted in comparison with the curve for sand (Tavenas, 1971, as cited in Everett, 1991) as shown in Figure 2.53. The function also checks out against the curves proposed by Vijayvergiya (1977, as cited in Everett, 1991) and Kraft et al (1981, as cited in Everett, 1991) for a stiff clay and as shown in Figure 2.54.

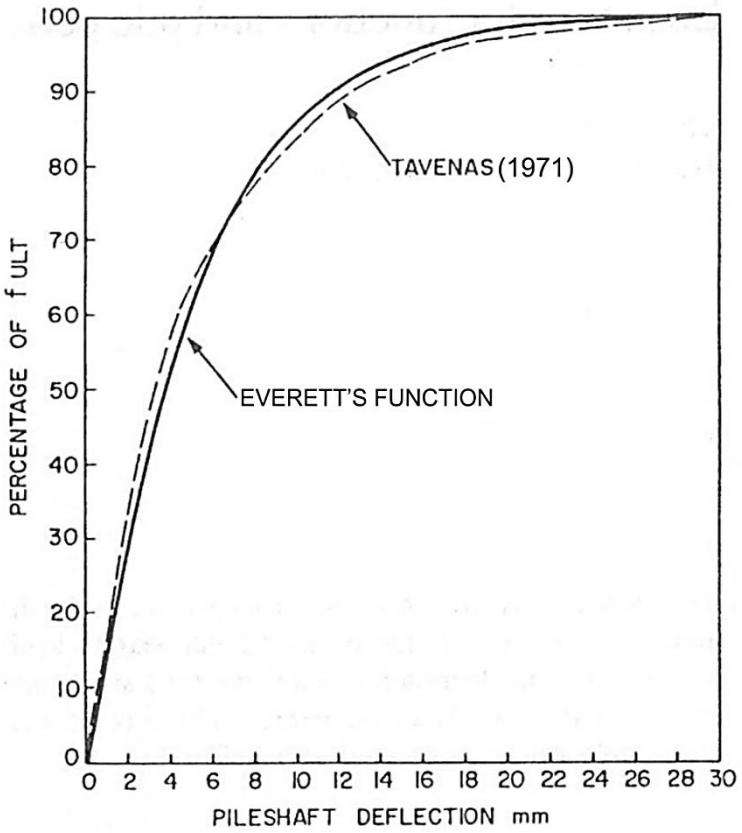


Figure 2.53: Everett's side shear transfer function compared with Tavenas' (1971) result.

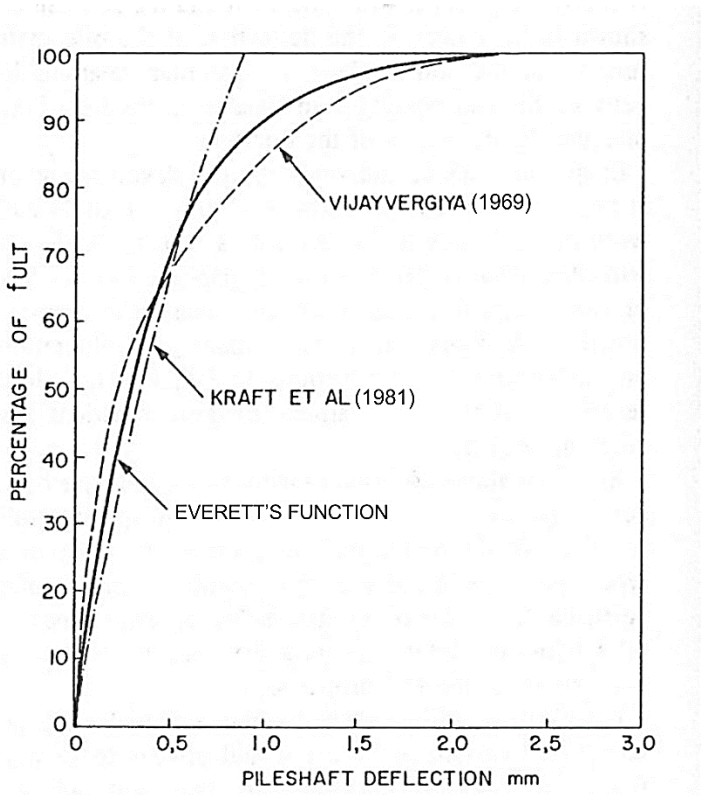


Figure 2.54: Everett's (1991) side shear transfer function compared with Vijayvergiya (1969) and Kraft and et al (1981) functions

When using the transfer function in Equation 2.110, the values of C_{ult} and F_{ult} have to be assessed by evaluating the ultimate side shear transfer and then splitting it between the C and F components on a simple percentage basis using the grading of the soil or its description.

2.9.2.2 The end bearing transfer function

Several researchers have added to the literature on load bearing load transfer functions, among them Vijayvergiya's (1969, 1977) empirical method and Kraft et al (1981) with their theoretical approach. The shape of the end bearing transfer function is not very different from that for the side shear transfer. There is a marked movement as the end bearing gradually builds up in sands while in clays, the end bearing tends to build up much faster, reach a maximum , then either hold at that level or decrease slightly.

Everett observed that there appears to be some excellent consistency between the end bearing performance of similar pile types in the same soil type with regard to end bearing transfer function. The other important observation made was that in the majority of cases, the ultimate end bearing of the pile appeared to be reached at a base deflection of approximately 10% of the base diameter. This observation was also noted by earlier investigators as Vesic (1977). Everett also notes that there is a remarkable consistency when the end bearing stress of piles of the same type but with varying base diameter are plotted against the ratio of deflection/0.1 (10%) times the pile diameter.

The above observations led to the development of the end bearing transfer function which is as follows:

$$q = q_{ult}\left[X^{(1-X)}\right]^{K_3} \qquad (2.111)$$

Where; q = end bearing stress at toe deflection, d_{toe} (kPa); q_{ult} = ultimate end bearing stress (kPa); X = ratio of the pile toe deflection d_{toe} to a percentage (S/EB) of the pile base diameter. The percentage is typically taken as 10% except for CFA piles when it is taken as 5%, and K_3 is a pile bearing constant which is constant, depending on the soil and pile type, but found to vary as shown in Table 2.7.

Table 2.7: Common values of K_3 (after Everett, 1991)

Soil and Pile Type Description	K_3 Value
Franki pile with enlarged base in sand	0.5
Franki pile with enlarged base in clay	0.2
Bored piles in soft rock	0.6
Bored piles in sand below water table	1.5
Precast and tube piles in sand	0.6
Precast piles in extremely dense sand	0.5

The function in Equation 2.111 is compared with actual base performance reported in the following:

a) In Figure 2.55 below where a value of K_3=0.2 models the end bearing curve of a Franki pile founded in clay.
b) Using a value of K_3=0.6, good agreement when compared to a bored pile founded on cretaceous mudstone as shown in Figure 2.56.

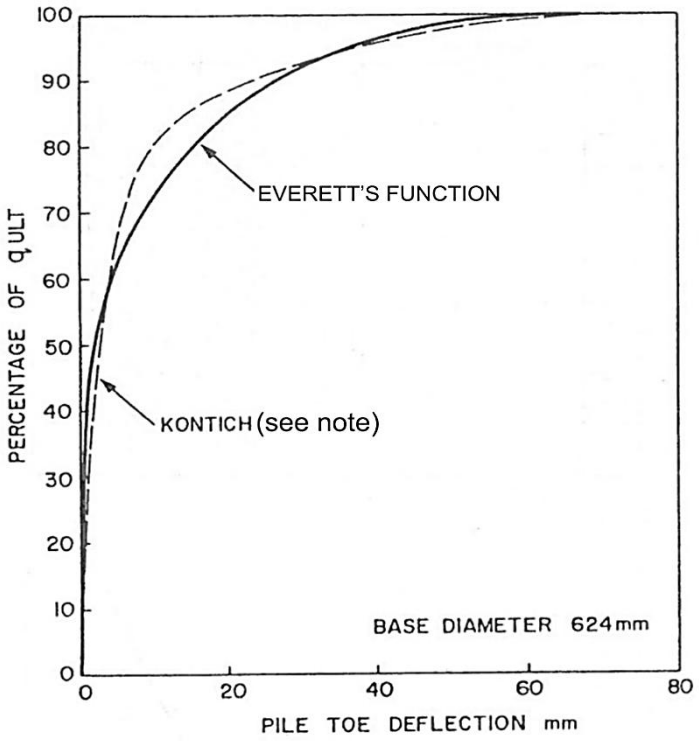


Figure 2.55: Everett's (1991) end bearing transfer function for a Franki pile in clay compared with the Kontich* result.

***Kontich** refers to results of a research performed at Kontich by Pieux Franki with the scientific cooperation of the Belgian Geotechnical Institute, the Civil Engineering Department of the Universite' Catholique De Louvain and the Laboratory for Soil Mechanics of the State University of Ghent. Publication No. 39 March 1977.

As with the side shear transfer, the ultimate values have to be assessed. It is important to consider the strength of the soil both above and below the tip of the pile when determining the ultimate end bearing. For soils which improve with depth, the average over $4D_0$ above the tip and D_0 below the tip should be used. Where the strength of the soil decreases below the base of the pile, a similar method of assessing a reduced ultimate end bearing stress should be applied.

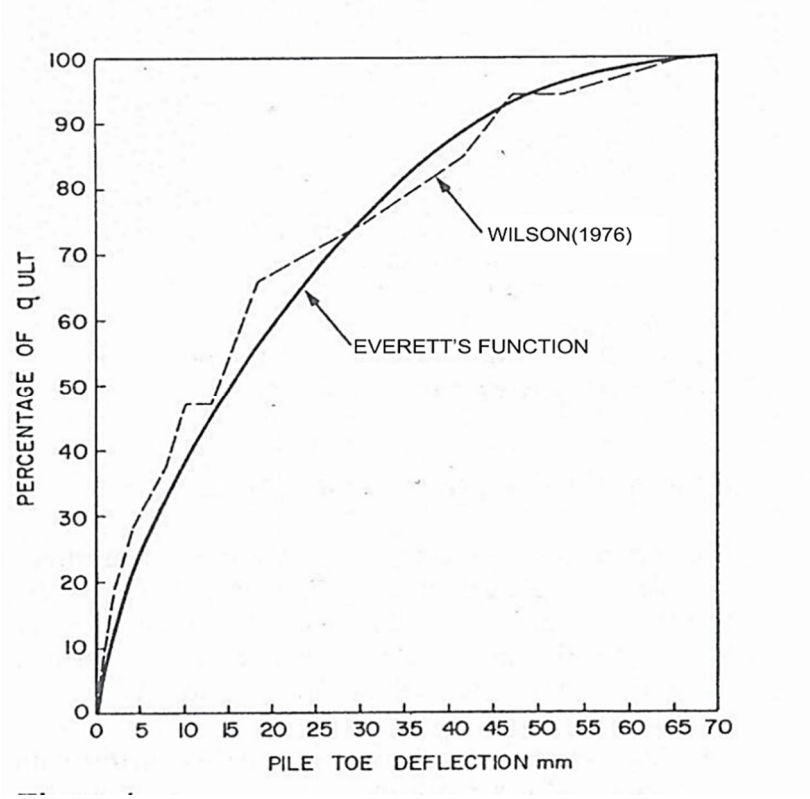


Figure 2.56: Proposed end bearing function for a bored pile base in soft rock compared to Wilson (1976) (after Everett, 1991)

The shape of the transfer function for sands is different from that for clays with variations for *c-Φ* soils in between.
(Everett, 1991, p. 229-234)

2.9.2.3 Pile performance modelling

The 'Pile' design suite of Prokon, a computer programme using the above transfer functions, provides a simple and effective method of modelling the settlement performance of a single pile under axial compression load. The difference in performance of different pile types in a particular soil profile can also be readily analysed. In Chapter 3 of this report, this computer programme method is validated first before it is applied to the calculation of a single pile settlement under the same conditions as done in Chapter 4 using the empirical and theoretical methods. The results are then compared. 'Pile' programme has a serious limitation in that it does not have specifically have a suite for pile group analysis. However, if a single pile can be modelled, this can be extended to any pile group size.

CHAPTER THREE

3 METHODOLOGY

In this chapter a description of the procedure followed is given with an explanation on the data collection methods adopted, the engineering analysis and a review of the methodological choices. The chosen area of study is Harare the capital city of Zimbabwe from where single and pile group settlements from case histories were to be compared with the values obtained using empirical, theoretical and/or analytical methods and to those obtained using 'pile' computer programme method. However, efforts to get some records from Harare in Zimbabwe have proved futile because no such case studies could be obtained from the Department of Roads or Ministry of Public Construction, the most likely sources of such records. However, a study of the geology of Harare and its surrounding areas was done. In summary, the most important and some of the oldest rocks in the Harare region form the greenstone belt sequence which in turn is divided into several lithostratigraphic formations. The iron mask is one such formation, being the oldest within the greenstone belt and consists mainly of felsic metavolcanic rocks, with associated minor metasediments. It forms the basal sequence of the Harare Greenstone Belt invaded by intrusive, foliated granodiorite and overlain by metabasalts. The geotechnical parameters of the soils in Harare can thus be obtained from literature since the Geological Map of Harare and its surrounding areas has fairly adequate geological detail. The map is included in Appendix A of this report.

3.1 Data used

Data values and magnitude were proposed as follows:

3.1.1 Applied load, Q_u

The maximum applied axial compressive load was limited to 1500kN (=1.5MN). However, each pile's load-carrying capacity was calculated first and then the actual maximum applied load decided from load capacity results. This was done to avoid situations were analysis using empirical methods is done using applied loads greater than the pile's load-carrying capacity.

3.1.2 Pile length, L (=L_P)

Pile lengths of 10, 20, 30, 40 and 50m were selected for investigation. The lowest pile length was motivated by the adopted pile lengths on two projects worked on in Harare where the depth to competent bearing stratum was of the order of 10m.The upper value of L=50m was adopted due to a desire to have a reasonable range from which clear variations may be achieved and solid conclusions drawn.

3.1.3 Pile cross-section dimensions

Circular piles were selected over other types because these are almost exclusively the type used in Zimbabwe at present. The D_0=0.5 and 1.0m piles are in most common use with formwork for D_0=0.3m, 0.4m and 0.7m also available at locally-based piling companies. A pile diameter range of $0.5 \leq D_0 \leq 2.5$m for single pile settlement and $0.3 \leq D_0 \leq 0.7$m for pile groups was selected to achieve a good range and thus be able to draw reasonable conclusions.

3.2 Soil properties

Two sites were arbitrarily chosen, one with predominantly clay soils with an underlying bedrock at significant depth while the other was dominated by sands. Geotechnical parameters needed in the settlement calculations were adapted from literature of given textbook examples.

The water table was assumed to be well below the bedrock for the clay soil site and well below the longest pile for the sandy site. This was done to limit the number of variables and achieve better clarity. A third case of layered soil was also formulated and investigated and the layer thickness= L/2 for each case, where Lis the pile length. The soil was restricted to 2 layers which were:

- Layer 1, Lyd1 where the top layer is clay, E_{s1}=30MPa and bottom layer being sand, E_{s2}=50MPa. Therefore E_{s1}/E_{s2}=0.6.
- Layer 2, Lyd2 where the top layer is sand, E_{s1}=50MPa and bottom layer being clay, E_{s2}=30MPa. Therefore E_{s1}/E_{s2}=1.7. This is the case of a weaker and compressible underlying strata

For example, Lyd1-PCPM refers to settlement determined by the Pile Computer Programme Method for layered soil type 1 where the top layer is clay soil and bottom layer is sand.

3.2.1 Clayey soil site

The undrained shear strength $c(=c_u)$ is assumed to be equal around the pile shaft and below the pile tip and that the unit weight of the soil γ, is uniform throughout. Clay often exhibits its lowest strength when saturated and subjected to undrained rapid loading. In undrained analysis, Φ_u=0 and the shear strength of the soil is due to the undrained shear strength c_u, only.

a) Pile capacity in cohesive soil

A DCIS (driven cast in-situ) pile, 20m long is founded is soft clay with the following properties: Unit weight of soil = 20kN/m^3, undrained shear strength = 25kPa. Pile design load, Qu=1500kN. The objective is to determine the load-carrying capacity of the pile and then plot the load distribution along the pile shaft for: (a) a conversional 1.0m diameter pile and (b) a pile with a shaft diameter of 1.0m and a base diameter of 1.5m.
The results were then compared to the computer output using 'Pile' programme.

b) General case of a pile founded in cohesive soil

A DCIS (driven cast in-situ) pile is founded is soft to medium clay underlain by a bedrock at 60m below the ground, with the following properties: Unit weight of soil=20kN/m^3, undrained shear strength=25kPa. The maximum pile load, Q_{max}=1500kN. The objective is to determine the settlement variation of a straight-shafted pile with D_0=0.5, 1.0, 1.5, 2.0 and 2.5m and for pile length, L_p=10, 20, 30, 40 and 50m using the various empirical and analytical/theoretical methods and comparing the results the computer output using 'Pile' programme. Shaft soil shear modulus, G_{si}=10MPa, E_{pi}=30GPa, Soil Poisson's ratio, v=0.5. Specifically, settlement calculations are carried out for an axial applied load, Q_u=250, 760, 1380, 1500 and 1500kN for L=10, 20, 30, 40 and 50m and D_0=0.5, 1.0, 1.5, 2.0 and 2.5 respectively, the magnitude of Q_u being dictated by pile load capacity.

3.2.2 Sandy soil site

a) Pile capacity in cohesionless soil

A concrete pile of 1.0m shaft diameter and 1.5m pile base diameter was driven into sand of loose to medium density to a depth of 20m. The ultimate applied load, Qu=1500kN. The following properties are known: Average unit weight of soil along the length of the pile, γ=17kN/m^3, angle of internal friction of the soil, Φ=36˚, dimensionless bearing capacity factor, N_q=20 and average coefficient of lateral earth pressure, K=1.0. The objective is to determine

the load-carrying capacity of: (a) a conversional 1.0m diameter pile and (b) a pile with a shaft diameter of 1.0m and a base diameter of 1.5m. The results are then compared to the computer output using 'Pile' programme.

b) General case of a pile founded in non-cohesive soil

A concrete pile was driven into sand of loose to medium loose density with pile diameter, D_0=0.5, 1.0, 1.5, 2.0 and 2.5m to different depths of L_p=10, 20, 30, 40 and 50m. The applied load, Qu=560kN for L=10m and 1500kN for all other pile lengths – see Table 4.5. The following properties are known - Average unit weight of soil along the length of the pile, γ=17kN/m^3, angle of internal friction of the soil, Φ=36°, dimensionless bearing capacity factor, N_q=*20* and average coefficient of lateral earth pressure, *K=1.0*. The Young's Modulus for loose-medium dense sand is 50MPa and the Poisson's ratio, ν=0.35. The objective is to determine the settlement variation of a straight-shafted pile using the various empirical and analytical/theoretical methods and comparing the results the computer output using 'Pile' programme.

3.2.3 General case of a pile founded in layered soil

The top half layer is clay soil with the same properties as those given for clay soil described in 3.4.1, E_{s1}=30MPa and the bottom half is sand with the same properties as described for the sand in 3.4.2 above, E_{s2}=50MPa. The arrangement of the layers is then reversed such that the compressive clay layer is below the medium dense sand. The objective is to determine the settlement variation of a straight-shafted pile using the selected empirical and analytical/theoretical methods and comparing the results the computer output using 'Pile' programme. Maximum applied load, Q_u=1500kN.

3.3 Methods of analysis

Settlement computations were carried out for both single piles and pile groups using some of the empirical, semi-empirical, analytical and Prokon's 'Pile' computer programme methods. The pile's load-carrying capacity is determined from the computer programme method after validation of this proposed computer programme method. The results obtained were then compared with those obtained from some selected empirical and/or semi-empirical and theoretical methods and some case histories from other parts of the world.

This paper is concerned with settlement analysis of pile foundations but it is also critical to ensure that the applied load does not exceed the pile's load-carrying capacity because if this happens, then there would be no reason to assess settlement because in practical terms, the pile may continue to sink into the ground (bearing capacity failure), fail by buckling or by compression if its load-carrying capacity is exceeded and a compressive axial load is applied.

3.3.1 Validation of Prokon's 'Pile' programme for 'numerical' method

The validation of a numerical model is a critical step which should be done before a numerical model can be adopted. If a model has not been validated, the results obtained from the numerical model cannot be accepted, as there would be no basis for accepting such results. However, in this report, numerical modelling could not be done due to the unavailability of the appropriate computer package and a computer programme method, 'pile suite' was adopted for comparison with the empirical and theoretical methods discussed in Chapter 3 of this report. The validation process consist of five steps which are:

- Analysis of the task on hand which is verification of the 'pile' computer method

- Selection of tests
- Administration of the tests
- Relating the tests to the criteria and
- Cross-validation and revalidation.

Consequently, the Pile package contained in Prokon programme was validated by comparison of manual calculations of pile capacity with that obtained from the 'Pile' computer programme, for both cohesive and cohesionless soils. Agreement of values obtained implied that the 'pile' computer programme method was validated. Settlement calculations obtained by this 'Pile' computer method are then compared with settlement calculations obtained by other method and from case histories from other parts of the world. No data could be obtained from Harare as was envisaged at the outset of this research. The records are simply not available.
As stated above, the validation of the 'Pile' computer method was done by manually calculating the pile load-carrying capacity of a driven cast in-situ, DCIS pile founded in clay soils and in sand, by calculating the skin and end bearing capacities. The load distribution along the length of the pile was also plotted and then compared with the values and graphs obtained by using the 'Pile' computer programme. A close agreement was obtained thereby validating the progrmme and results obtained from its use would be acceptable.

3.3.1.1 Solution for pile capacity in cohesive soil

(a) Straight-shafted (conventional) pile

$Q_b = f_b A_b = c_{u(base)} \times N_c \times A_b$ where N_c is a bearing capacity factor for cohesive soil, N_c=9.
$Q_b = 25 \times 9 \times \pi \times 1.0^2/4 = 176.71\text{kN}$

(b) Pile with enlarged base

$Q_b = f_b A_b = c_{u(base)} \times N_c \times A_b$ where N_c is a bearing capacity factor for cohesive soil, N_c=9.
$Q_b = 25 \times 9 \times \pi \times 1.5^2/4 = 397.61\text{kN}$

Pile shaft capacity (for both (a) and (b) above)

$Q_S = f_s A_s$ where A_s is the surface area of the pile shaft, $f_s = 0.5(c_u \times \sigma_0')^{1/2}$, where σ_0' is the effective overburden pressure at the point of interest. $\sigma_0' = \gamma.L/2 = 20 \times 20/2 = 200\text{kPa}$

$\Rightarrow Q_S = 0.5(25 \times 200')^{1/2} \times A_s = 35.36\text{kN/m}^2 \times \pi \times 1.0 \times 20\text{m}^2 = 2221.44\text{kN}$

Total capacity for conventional pile

Total pile capacity, Q_t (ULS) = 176.71+2221.44 = **2398.15kN**

Total capacity for pile with enlarged base

Total pile capacity, Q_t (ULS) = 397.61+2221.44 = **2619.05kN**

The 'Pile' programme output for the analysis of the above pile are included in Figure 4.1 below. It can be seen that the ultimate pile base and pile shaft capacity are exactly the same as those obtained by manual calculation. The programme then applies FoS=1.5 for shaft capacity, which results in an allowable pile shaft capacity of: 2221.44/1.5 = 1480.96kN and an end bearing FoS=2 for DCIS piles which yields an allowable end bearing capacity of 88.36kN for a conventional pile, FoS=3 to give an end bearing capacity of 397.61/3=132.54kN for a pile with an enlarged base.

Hence allowable pile capacity (SLS):
= 1480.96+88.36 = 1569.32kN for a conventional pile, and
= 1480.96+132.54 = 1613.5kN for a pile with enlarged base

Table 3.1(a): Allowable pile capacity for a pile in cohesive soil with L=20m, D_s=1.0m; D_b=1.0m (conventional pile)

Summary of Output		
Design Load	kN	1500.00
Calculated Capacity (SLS)	kN	1569.32
Shaft Stress	kPa	1909.86
Everett Settlement (SLS)	mm	3.53
Everett Settlement (ULS)	mm	14.53

Soil	Ultimate Pile Capacity (kN)			Allow able Pile Capacity (kN)		
Layer	Friction	Bearing	Total	Friction	Bearing	Total
1	2221.44	176.71	2398.16	1480.96	88.36	1569.32

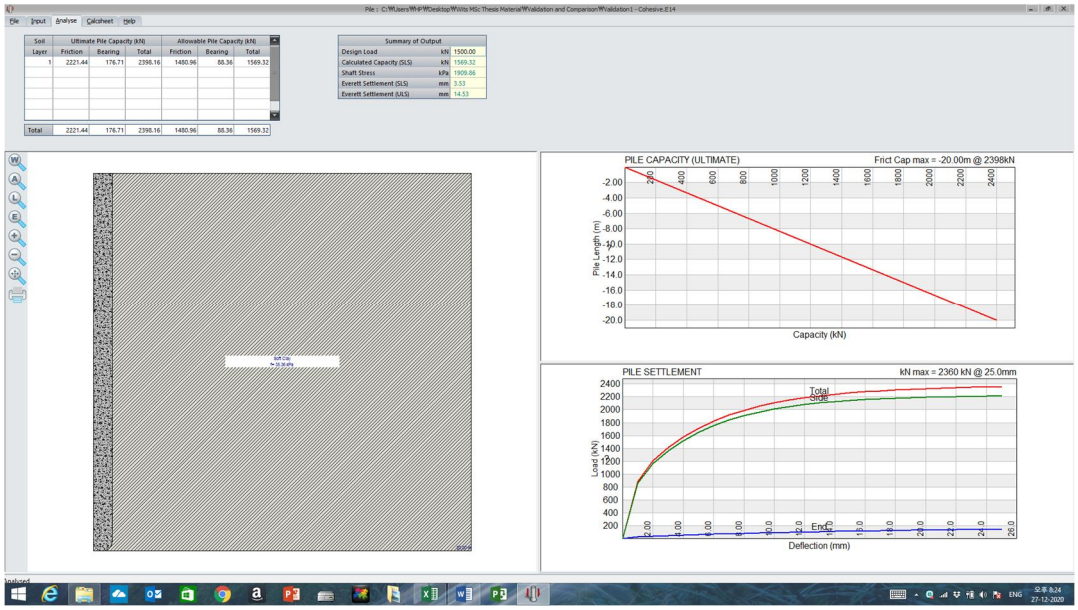


Figure 3.1(a): 'Pile' Output summary and graphs showing variation settlement with load and load with pile length for a pile founded in cohesive soil, D_s=D_b=1.0m.

Table 3.1(b): Allowable pile capacity for a pile in cohesive soil with L=20m, D_s=1.0m; D_b=1.5m (enlarged base pile)

Summary of Output		
Design Load	kN	1500.00
Calculated Capacity (SLS)	kN	1613.50
Shaft Stress	kPa	848.83
Everett Settlement (SLS)	mm	3.16
Everett Settlement (ULS)	mm	10.61

Soil	Ultimate Pile Capacity (kN)			Allowable Pile Capacity (kN)		
Layer	Friction	Bearing	Total	Friction	Bearing	Total
1	2221.44	397.61	2619.05	1480.96	132.54	1613.50

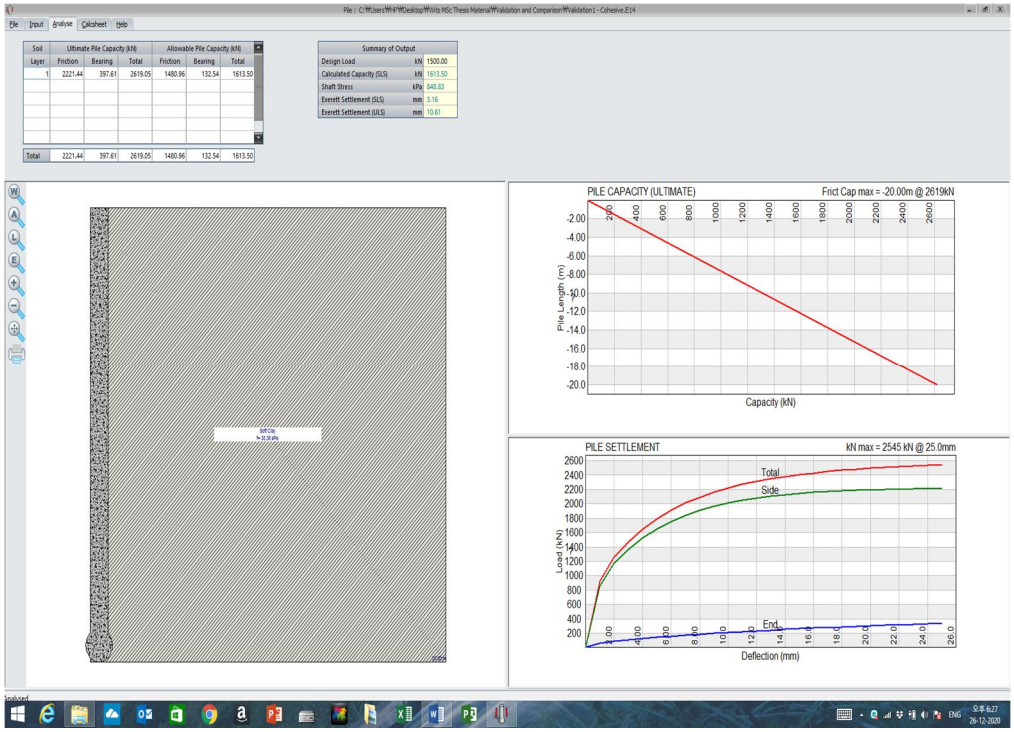


Figure 3.1(b): 'Pile' Output summary and graphs showing variation settlement with load and load with pile length for a pile founded in cohesive soil, D_s=1.0m and D_b=1.5m.

The load variation plot along the pile shaft, based on the above manual calculations, is contained in Figure 3.2 (a) and (b). It can be seen from the graph that the load is maximum at the pile head and decreases almost linearly until Q_b=88.36kN for conventional pile and Q_b=132.54kN for the pile with an enlarged base. The settlement values obtained by computer analysis are 3.53mm and 3.16mm while those obtained by the T-z method are 4.15mm and 4.12mm, respectively, for SLS, which is critical in settlement analysis. Tables 3.2 (a) and (b) give a summary of the T-z settlement calculation and the parameters used. The settlement values are fairly close to those obtained by the computer progamme method values. Therefore the Pile programme was validated with respect to cohesive soils. Thus settlement results

obtained through the 'Pile' computer method can be accepted.

Table 3.2(a): Comparison of load-carrying capacity and settlement for L=20m, D_s=D_b=1.0m–refer to section 2.7.3 for the T-z method

Node No	Nodal Depth (m)	Pile Dia (m)	Segment length, L_{si} (m)	Pile Area (m^2)	Ksi (kN/m)	Pile Load F(kN)	Settlement Δ (mm)
1	0.0	1.0	1.0	0.785	17033	1501	0.00415
2	1.0	1.0	1.0	0.785	17033	1431	0.00415
3	2.0	1.0	1.0	0.785	17033	1361	0.00415
4	3.0	1.0	1.0	0.785	17033	1290	0.00415
5	4.0	1.0	1.0	0.785	17033	1219	0.00415
6	5.0	1.0	1.0	0.785	17033	1149	0.00415
7	6.0	1.0	1.0	0.785	17033	1078	0.00415
8	7.0	1.0	1.0	0.785	17033	1007	0.00415
9	8.0	1.0	1.0	0.785	17033	937	0.00415
10	9.0	1.0	1.0	0.785	17033	866	0.00415
11	10.0	1.0	1.0	0.785	17033	795	0.00415
12	11.0	1.0	1.0	0.785	17033	725	0.00415
13	12.0	1.0	1.0	0.785	17033	654	0.00415
14	13.0	1.0	1.0	0.785	17033	583	0.00415
15	14.0	1.0	1.0	0.785	17033	513	0.00415
16	15.0	1.0	1.0	0.785	17033	442	0.00415
17	16.0	1.0	1.0	0.785	17033	371	0.00415
18	17.0	1.0	1.0	0.785	17033	300	0.00415
19	18.0	1.0	1.0	0.785	17033	230	0.00415
20	19.0	1.0	1.0	0.785	17033	159	0.00415
21	20.0	1.0	1.0	0.785	17033	88	0.00415

Shaft soil shear modulus, G_{si}=10MPa, E_{pi}=30GPa, Soil Poisson's ratio, v=0.5, r_m=L=20m

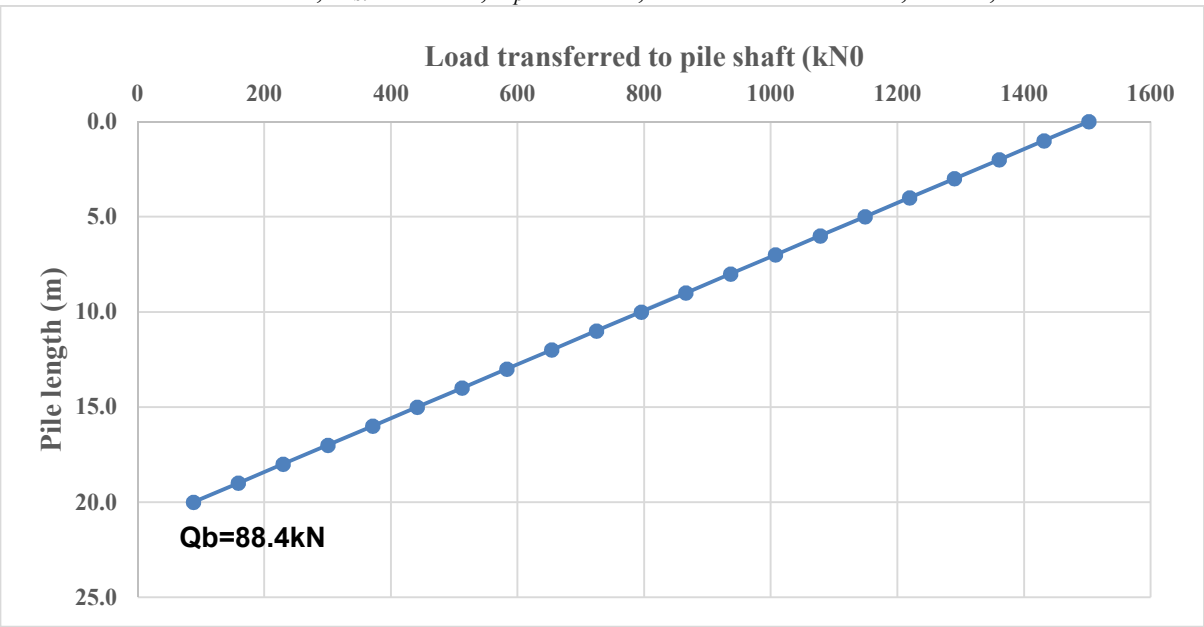


Figure 3.2(a): Load distribution along pile length, D_s=D_b=1.0m

Table 3.2(b): Comparison of load-carrying capacity and settlement for L=20, D_s=1.0m, D_b=1.5m – refer to section 2.7.3 for the T-z method

Node No	Nodal Depth (m)	Pile Dia (m)	Segment length, L_{si} (m)	Pile Area (m^2)	Ksi (kN/m)	Pile Load F(kN)	Settlement Δ (mm)
1	0.0	1.0	1.0	0.785	17033	1501	0.00412
2	1.0	1.0	1.0	0.785	17033	1431	0.00412
3	2.0	1.0	1.0	0.785	17033	1361	0.00412
4	3.0	1.0	1.0	0.785	17033	1290	0.00412
5	4.0	1.0	1.0	0.785	17033	1220	0.00412
6	5.0	1.0	1.0	0.785	17033	1150	0.00412
7	6.0	1.0	1.0	0.785	17033	1080	0.00412
8	7.0	1.0	1.0	0.785	17033	1010	0.00412
9	8.0	1.0	1.0	0.785	17033	940	0.00412
10	9.0	1.0	1.0	0.785	17033	869	0.00412
11	10.0	1.0	1.0	0.785	17033	799	0.00412
12	11.0	1.0	1.0	0.785	17033	729	0.00412
13	12.0	1.0	1.0	0.785	17033	659	0.00412
14	13.0	1.0	1.0	0.785	17033	589	0.00412
15	14.0	1.0	1.0	0.785	17033	519	0.00412
16	15.0	1.0	1.0	0.785	17033	448	0.00412
17	16.0	1.0	1.0	0.785	17033	378	0.00412
18	17.0	1.0	1.0	0.785	17033	308	0.00412
19	18.5	1.0	1.5	0.785	17033	238	0.00412
20	20.0	1.5	1.5	1.767	17033	133	0.00412

Shaft soil shear modulus, G_{si}=10MPa, E_{pi}=30GPa, Soil Poisson's ratio, v=0.5, r_m=L=20m

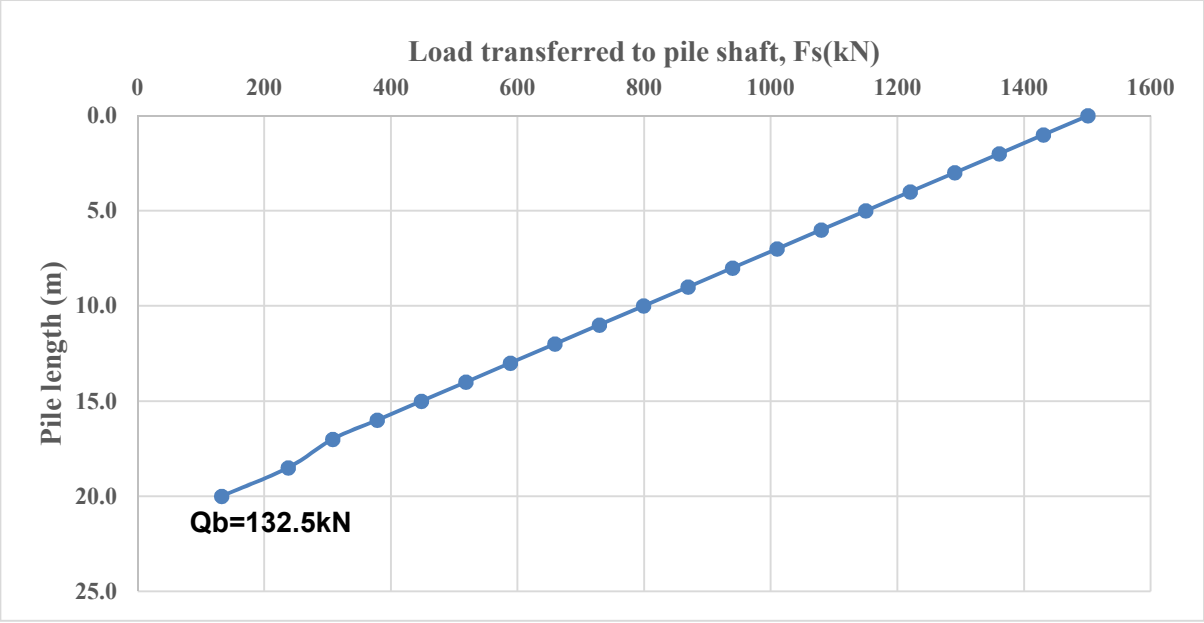


Figure 3.2(b): Load distribution along pile length, D_s=1.0m and D_b=1.5m

3.3.1.2 Solution for pile capacity in cohesionless soil

(a) Conventional pile

$Q_b = \sigma_{vb(av)} x N_q x A_b = 0.5(17x20)x20x\pi x(1.0)^2/4 = 2670.35kN$

(b) Pile with enlarged base

Similarly, $Q_b = \sigma_{vb(av)} x N_q x A_b = 0.5(17x20)x20x\pi x(1.5)^2/4 = 6008.30kN$

Pile shaft capacity (for both)

From Equations 3.102 and 3.102a,

$Q_s = f_s A_s$, where A_s = pile shaft surface area = $\pi D_s L = \pi x1.0x20 = 62.83185m^2$; $f_s = K\sigma_{vb(av)}\tan\delta$, where; $\sigma vb(av) = p_0'$, $\delta = 2\Phi/3 = 2x36/3 = 24^\circ$; $K = (K_0+K_a+K_p)/3$; $K_0 = 1-\sin\Phi = 1-\sin36^\circ = 0.412$; $K_a = \tan^2(45-\Phi/2)^\circ = \tan^2(45-36/2)^\circ = 0.260$; $K_p = \tan^2(45+\Phi/2)^\circ = \tan^2(45+36/2)^\circ = 3.852$; $\therefore$ K = (0.412+0.260+3.852)/3 = 4.524/3 ≈ **1.5** > 1.0, which complies with API (1984, 1991) which require $0.8 \leq K \leq 1.0$ and $40 \leq f(=f_s) \leq 120$kPa. $\Rightarrow f_s$ = 1.0x(17x20/2)tan24°=75.69kPa<~80kPa. $\therefore$ Pile shaft capacity $Q_s = f_s A_s$ = 75.69x62.832 = 4755.67kN

Total capacity for conventional pile

Pile capacity, Q_t (ULS) = 2670.35+4755.67 = 7426.02kN

Total capacity for pile with enlarged base

Therefore pile capacity, Q_t (ULS) = 6008.30+4755.67= 10763.97kN

The 'Pile' programme output summary for the analysis of the above are contained in Tables 4.2 (a) and (b). It can be seen that the ultimate pile base and pile shaft capacity are exactly the same as those manually determined above for both the conventional pile and that with an enlarged pile base. The programme then applies the appropriate FoS=1.5 for shaft capacity, which results in an allowable pile shaft capacity of 4755.67/1.5=3170.45kN for both pile types and pile base FoS=2 which yields allowable end bearing capacity of: 2670.35/2=1335.18kN and 6008.30/3=2002.77kN for a conventional and enlarged base pile respectively. It was observed that the FoS applied at base by the computer for conventional piles is different from that for piles with an enlarged base. The pile shaft FoS is the same for both types.

Table 3.3(a): Allowable pile capacity for a pile in non-cohesive soil for a conventional pile with L=20m and $D_s=D_b=1.0m$.

Summary of Output		
Design Load	kN	1500.00
Calculated Capacity (SLS)	kN	4505.63
Shaft Stress	kPa	1909.86
Everett Settlement (SLS)	mm	0.81
Everett Settlement (ULS)	mm	1.60

Soil	Ultimate Pile Capacity (kN)			Allow able Pile Capacity (kN)		
Layer	Friction	Bearing	Total	Friction	Bearing	Total
1	4755.67	2670.35	7426.03	3170.45	1335.18	4505.63

Hence allowable pile capacity (SLS):
= 3170.45+1335.18 = 4505.63kN for a conventional pile, and
= 3170.45+2002.77 = 5173.225kN for a pile with enlarged base.

The pile capacity for both the conventional pile and the one with an enlarged base have been determined manually and by 'Pile' computer method and found to be identical. Therefore the Pile programme has been validated with respect to cohesionless soils. Thus settlement results obtained through the Pile method can be acceptable.

Table 3.3(b): Allowable pile capacity for a pile founded in non-cohesive soil for pile with enlarged base with L=20m, D_s=1.0m and D_b=1.5m

Summary of Output		
Design Load	kN	1500.00
Calculated Capacity (SLS)	kN	5173.21
Shaft Stress	kPa	848.83
Everett Settlement (SLS)	mm	0.81
Everett Settlement (ULS)	mm	1.56

Soil	Ultimate Pile Capacity (kN)			Allow able Pile Capacity (kN)		
Layer	Friction	Bearing	Total	Friction	Bearing	Total
1	4755.67	6008.30	10763.97	3170.45	2002.77	5173.21

A comparison of the settlement and the load-carrying capacities of a single pile of L=10, 20, 30, 40, 50m in cohesionless and cohesive soils of properties as described in the validation examples above was carried out using 'Pile' analysis and the results are summarized in the Table 3.3(c) for a conventional and an enlarged base pile. The applied pile compressive axial load, *Qu*=600kN is applied in all cases, which is the least sustainable load.

Table 3.3(c): Comparison of load-carrying capacity and settlement for P=600kN and founded in different soil types

Soil Type	Shaft Dia (m)	Base Dia (m)	Base Capacity Q_b(kN)	Shaft Capacity Q_s(kN)	Total Pile Capacity Q_T(kN)	Applied Load (kN)	Settlement (mm)
L=10m							
Cohesive	1.0	0.5	88	524	612	600	4.12
Cohesive	1.0	1.5	133	524	657	600	3.15
Non-cohesive	1.0	0.5	668	793	1461	600	1.78
Non-cohesive	1.0	1.5	1001	793	1794	600	1.71
L=20m							
Cohesive	1.0	0.5	88	1481	1569	600	0.68
Cohesive	1.0	1.5	133	1481	1614	600	0.65
Non-cohesive	1.0	0.5	1335	3170	4505	600	0.33
Non-cohesive	1.0	1.5	2003	3170	5173	600	0.32
L=30m							

Cohesive	1.0	0.5	88	2721	2809	600	0.37
Cohesive	1.0	1.5	133	2721	2854	600	0.37
Non-cohesive	1.0	0.5	1885	5108	6993	600	0.20
Non-cohesive	1.0	1.5	2827	5108	7935	600	0.20
L=40m							
Cohesive	1.0	0.5	88	4189	4222	600	0.24
Cohesive	1.0	1.5	133	4189	4322	600	0.24
Non-cohesive	1.0	0.5	1885	6811	8696	600	0.15
Non-cohesive	1.0	1.5	2827	6811	9638	600	0.15
L=50m							
Cohesive	1.0	0.5	88	5854	5942	600	0.18
Cohesive	1.0	1.5	133	5554	5687	600	0.17
Non-cohesive	1.0	0.5	1885	8514	10399	600	0.12
Non-cohesive	1.0	1.5	2827	8514	11341	600	0.12

The following deductions can be made from Table 3.3(c):

a) The base resistance Q_b, and shaft resistance Q_s hence, the pile's load-carrying capacity Q_T, are significantly more in cohesionless soils than in cohesive soils, with the shaft capacity of a pile in non-cohesive soil being double that of a similar pile founded in cohesive soil for L=20,30, 40 and 50m.

b) The pile settles more in cohesive soil than in non-cohesive soils for the same applied load, settlement in cohesionless soil being of the order of 50% of that in cohesive soils.

c) The settlement for a straight-shafted pile is not different from that of a pile with an enlarged base when pile is founded in same soil type for L>10m. However, for L=10m, there is a noticeable difference in settlement. Further settlement computations done for L=8m produced values of 4.24mm and 2.98mm and 2.51mm and 2.30mm for D_s=1.0m and D_b=1.5m for piles in cohesive and cohesionless soils respectively even with P=450kN (<600kN). Therefore pile base enlargement has the effect of reducing the pile settlement L≤10m. The applied load was reduced to 450kN because the capacity of the conventional pile for L=8m was reduced to 463kN.

d) The amount of settlement generally decreases with increasing pile shaft or pile base diameter and as would be expected, the pile capacity also increases with increasing pile shaft and pile base diameters.

However, it is should be noted that in practice, piles with enlarged bases founded in non-cohesive soil are normally employed when there is need to resist uplift forces.

3.4 Comparison between calculated and measured settlement of test piles (case histories)

The application of elastic analysis theory to real soil requires that the 'elastic' soil parameters are determined over a stress range representative of that in the field. However, an assessment of the accuracy of elastic theory-based settlement predictions must await comparison with the results of carefully controlled model and field tests. In this section, the objective is to compare measured settlement results to those obtained by use of 'Pile' program computer method of analysis.

3.4.1 Wembley, England

Fleming (1992), used information found in Whitaker and Cooke (1966), to validate his method of single pile settlement prediction from the load-settlement curves. Whitaker and Cooke (1966) dealt with instrumented piles tests that were carried out at Wembley, England for both straight-

shafted and under-reamed piles.

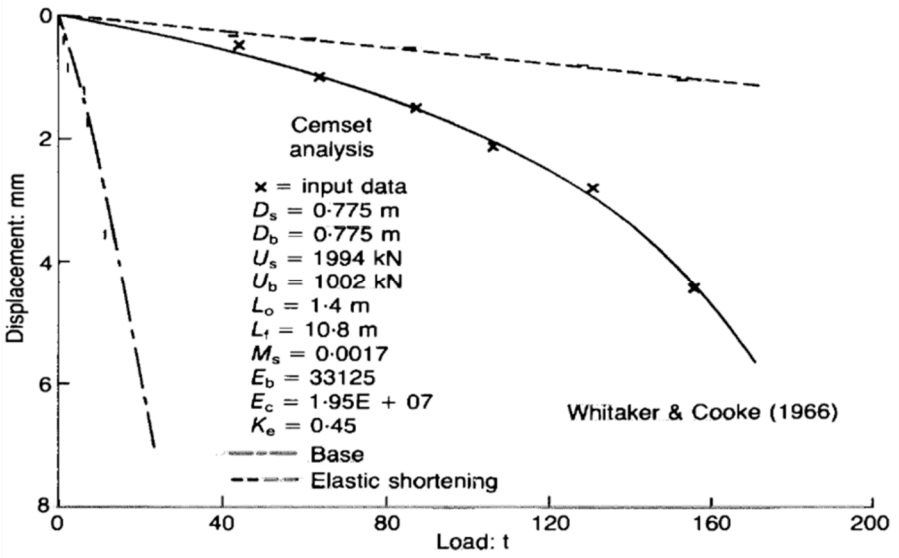


Figure 3.3: Comparison of results from Fleming (1992) study with those of Whitaker and Cooke (1966): pile H at Wembley

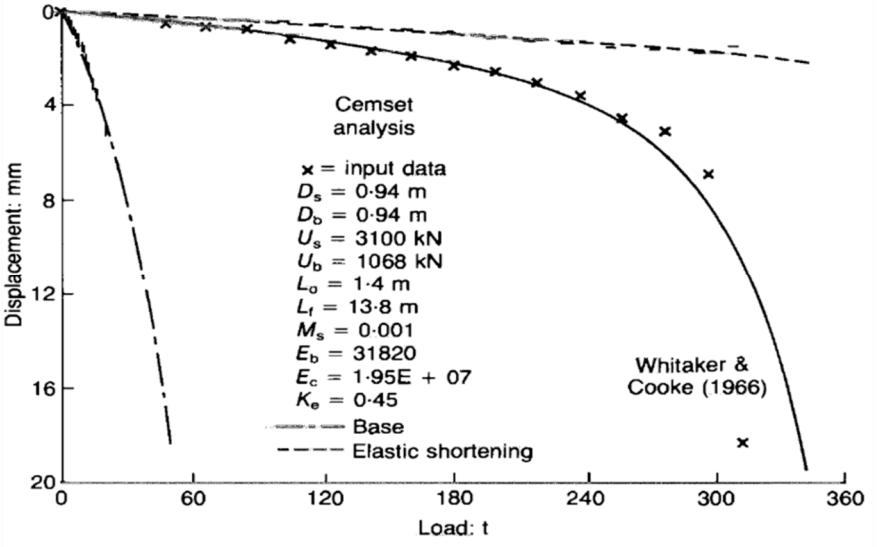


Figure 3.4: Comparison of results from Fleming (1992) study with those of Whitaker and Cooke (1966): pile N at Wembley.

Figures 3.3 and 3.4 show the solutions obtained by Fleming (1992) method, while Table 3.4(a) and Table 3.4(b) below show a summary of 'Pile' computer method results for two selected piles H and N (Whitaker and Cooke, 1966).

Table 3.4(a): 'Pile' computer output summary for pile H at Wembley, England after Whitaker and Cooke (1966)

Summary of Output		
Design Load	kN	1800.00
Calculated Capacity (SLS)	kN	2947.21
Shaft Stress	kPa	3815.74
Everett Settlement (SLS)	mm	1.92
Everett Settlement (ULS)	mm	5.20

Table 3.4(b): 'Pile' computer output sammary for pile N at Wembley, England after Whitaker and Cooke (1966)

Summary of Output		
Design Load	kN	3600.00
Calculated Capacity (SLS)	kN	4625.48
Shaft Stress	kPa	5187.49
Everett Settlement (SLS)	mm	3.38
Everett Settlement (ULS)	mm	10.61

Table 3.4(c) shows a summary of results obtained by Whitaker and Cooke (1966) from test pile measurements, Fleming (1992) in validation of his hyperbolic method and 'Pile' computer program in the present study**.**

Table 3.4(c): Wembley, England - Summary of actual and calculated results

Method	**Settlement (mm)**		**Shaft load (kN)**		**Base load (kN)**	
	Pile H	Pile N	Pile H	Pile N	Pile H	Pile N
Whitaker & Cooke (1966)	2.43	4.00	1960	3070	770	870
Fleming (1992)	2.53	3.93	1994	3100	1002	1068
This study - 'Pile' computer analysis	**1.92**	**3.38**	**2310**	**3689**	**637**	**938**

Whitaker and Cooke settlement values were measured from the load-settlement curves in Figures 3.3 and 3.4 while the Fleming method settlement values were read off from the load-settlement spreadsheet from the input values shown in Figures 3.3 and 3.4, at the working load. A factor of safety of 1.5 was used. The results were tabulated in Table 3.4(c). The measured settlement is reasonably close to that calculated by 'Pile' computer program and that determined by the Fleming method. It is also evident that the difference between measured values of shaft load and those calculated using 'Pile' were 17.86% and 20.16% for pile H and N respectively, the computer method-determined values being more than those measured by Whitaker and Cooke (1966). The maximum difference between measured base load and the computer method-calculated values is also about 20%. It is therefore, evident that there is good concordance between the measured results and the Fleming-determined settlement and those obtained by the 'Pile' computer program.

3.4.2 Iskenderun, Turkey

Mert and Ozkan – see Table 3.5, carried out settlement analysis of axially loaded bored piles by Finite Element Method, FEM (Plaxis 3-D) and compared the results obtained with those determined using other analytical and/or theoretical methods and measurements from test piles at a project site in Iskenderun, Turkey. The Iskenderun Power Plant Project (IPPP) is located in the east coast of Iskenderun Bay and boreholes drilled on the project site revealed that the site has mainly young alluvial deposits to more than 41.5m. These relatively new alluvial deposits are underlain by older alluvial deposits. The lowermost layer consist of very stiff clay whose thickness continues to significantly greater depth and not included in Table 4.8. Test piles of 800mm diameter were installed to depths of 30, 35, 40 and 45m and numbered TP1, TP2, TP3 and TP4 respectively. The soil's elastic properties together with other parameters were evaluated from both the SPT values and laboratory tests such as Unconsolidated Undrained (UU) triaxial tests and oedometer tests. Table 3.5 shows the idealized soil profile and the relevant parameters determined as above. The parameters for TP3 were noted to be similar to those for TP4.

Table 3.5: Idealised soil profile and parameters at IPPP site

Soil Description	Layer Thickness (m)	C_u (kN/m^2)	Shear strength angle Φ (°)	E_s (MPa)	Poisson's ratio ν_s
TP1					
Medium dense sand	6.0	0	32	25	0.30
Firm gravelly sandy clay	21.5	60	0	20	0.35
Very stiff clay*	-	150	0	80	0.30
TP2					
Medium gravelly clay	24.5	40	0	15	0.40
Medium dense sandy gravel	3.0	0	34	35	0.35
Very stiff clay*	-	150	0	80	0.30
TP3					
Medium gravelly clay	3.0	50	0	15	0.40
Medium dense sand	3.0	0	32	20	0.30
Very stiff sandy clay	10.5	100	0	30	0.30
Medium dense sandy gravel	4.5	0	34	35	0.35
Medium sandy clay	9.0	50	0	20	0.40
Very stiff clay*	-	150	0	80	0.30

Note. Adapted from "Settlement Analysis of Axially Loaded Bored Piles: A Case History", by M. Mert and M.T. Ozkan, 2019, *World Academy of Science, Engineering and Technology, International Journal of Geotechnical and Geological Engineering*, 13(6), p.395.

* Thickness of very stiff clay layer modelled as 2x21.5=43.0m for all the IPPP site trial pits.

The instrumented piles were subjected to different compression axial loads and settlements measured and recorded. Mert and Ozkan (2019) also determined the settlement for each load case using different analytical methods as detailed in Table 3.6. In this study, the soil was modelled as shown in Table 3.5 and the thickness of the very stiff clay was modelled as 43.0m for the 'pile' computer method input. The settlement values obtained are included in Table 3.6 for comparison.

Table 3.6: Pile settlement values obtained by different methods compared with pile tests results (Mert and Ozkan, 2019) and 'Pile' computer method results at IPPP site

Test Pile No and	TP1				TP2		
Applied Load (MN) / **Pile Length(m)** / **D(m)** / **Method**	**3.0** / **30** / **0.8**	**6.0** / **35** / **0.8**	**9.0** / **40** / **0.8**	**10.5** / **45** / **0.8**	**3.0** / **30** / **0.8**	**6.0** / **35** / **0.8**	**8.25** / **40** / **0.8**
Fleming (1992) (mm)	4.92	11.72	25.85	48.39	5.69	14.99	36.97
FEM (Plaxis 3D) (mm)	5.05	12.21	25.30	32.95	5.18	11.21	16.44
Bohn et al (2016) (mm)	3.52	10.56	36.51	75+	3.90	13.32	50+
Zhang et al (2016) (mm)	6.03	16.50	44.52	75+	5.32	15.63	43.05
Boonyatee & Lai (2017) (mm)	5.98	13.49	25.70	39.12	5.74	12.86	21.62
Actual/Measured (mm)	**2.76**	**8.82**	**21.49**	**41.48**	**3.03**	**10.66**	**35.65**
This study ('Pile' computer program method) (mm)*	**3.06**	**8.70**	**19.96**	**12.60**	**3.56**	**10.57**	**14.07**
Test Pile No	TP4				TP3		
Applied Load (MN) / **Pile Length(m)** / **D(m)** / **Method**	**3.0** / **30** / **0.8**	**6.0** / **35** / **0.8**	**9.0** / **40** / **0.8**	**10.5** / **45** / **0.8**	**3.0** / **30** / **0.8**	**6.0** / **35** / **0.8**	**9.0** / **40** / **0.8**
Fleming (1992) (mm)	5.45	11.99	22.65	36.02	5.45	11.99	22.65
FEM (Plaxis 3D) (mm)	4.60	10.13	17.69	21.00	4.60	10.13	17.69
Bohn et al (2016) (mm)	2.88	7.88	18.84	31.69	2.88	7.88	18.84
Zhang et al (2016) (mm)	3.97	9.72	20.46	33.21	3.97	9.72	20.46
Boonyatee & Lai (2017) (mm)	5.42	11.49	18.79	23.32	5.42	11.49	18.79
Actual/Measured (mm)	**3.34**	**9.01**	**17.71**	**56.99**	**3.34**	**9.01**	**17.71**
This study ('Pile' computer program method) (mm*)	**3.07**	**8.95**	**22.74**	**13.62**	**3.07**	**8.95**	**22.74**

Note. Adapted from "Settlement Analysis of Axially Loaded Bored Piles: A Case History", by M. Mert and M.T. Ozkan, 2019, *World Academy of Science, Engineering and Technology, International Journal of Geotechnical and Geological Engineering*, 13(6), p.399.

* This result was obtained from this study, all other results are from Mert and Ozkan (2019) study.

For TP1, TP2, TP3 and TP4, load case, Ld_c=3000, 6000 and 9000kN, there is very close agreement in settlement values between the measured and those determined using 'Pile' computer program method, with a maximum difference of 5.03mm for Ld_c=9.0MN at TP3/TP4, which is very satisfactory. The settlement value for Ld_c=8.25MN is very low for the computer method than all the other methods but increases compared to that for Ld_c=6000kN. However, for Ld_c=10.5MN, the trend changed with pile settlement by computer method decreasing from 19.96mm to 12.60mm and from 22.74mm to 13.62mm for an increase in applied load from Ld_c=9000kN to Ld_c=10500kN. Practically, this means that a slightly longer pile (pile length increased by 5m from L=40 to L=45m) has led to ≈67% reduction in settlement. Therefore when settlement is sensitive, it would be more economical to select the slightly longer pile.

For Ld_c>9000kN, measured and computer method-calculated settlement results are not comparable. The computer method results are far much smaller than the measured results and those obtained by other methods detailed in Table 3.6.

3.4.3 Baku, Azerbaijan

Mert and Ozkan (2019) also carried out settlement analysis of axially loaded bored piles by Finite Element Method, FEM (Plaxis 3-D) and compared the results obtained with those determined using other analytical and/or theoretical methods and measurements from test piles at a project site in Baku, Azerbaijan. The Baku Hotel Project (BHP) site is underlain by soils whose idealized profile is shown in Table 3.7. Test piles of 2000mm diameter were installed to depths of 59, 67, and 76m and numbered BTP1, BTP2 and BTP3 respectively. The soil's elastic properties and other parameters were similarly evaluated from both the SPT values and laboratory tests such as Unconsolidated Undrained (UU) triaxial tests and oedometer tests.

Table 3.7: Idealised soil profile and parameters at Baku Hotel site

Soil Description	Layer Thick (m)	C_u (kN/m^2)	Shear st rength an gle Φ (°)	E_s (MPa)	Poisson' s ratio v_s
Fill	4.0	0	32	10	0.35
Clayey sand	8.0	60	0	60	0.37
Stiff clay	10.0	170	0	75	0.30
Interbedded sand/clay	20.0	130	0	75	0.35
Plastic hard clay*	-	210	0	90	0.35

Note. Adapted from "Settlement Analysis of Axially Loaded Bored Piles: A Case History", by M. Mert and M.T. Ozkan, 2019, *World Academy of Science, Engineering and Technology, International Journal of Geotechnical and Geological Engineering*, 13(6), p.395.
* Thickness of plastic hard clay layer modelled as 2x20=40.0m for all the Baku site trial pits.

The instrumented piles were also subjected to varying loads and the soil modelled in accordance with Table 3.7 in order to comply with 'Pile' input format. The settlement values obtained are included with those determined by Mert and Ozkan (2019) in Table 3.8.

Table 3.8: Pile settlement values obtained by different methods compared with pile tests results and 'Pile' computer results at Baku Hotel site

Test Pile No and	BTP1		BTP2		BTP3	
Applied Load (kN) / Pile Length(m) / D(m) / Method	15.0 / 59 / 2.0	22.0 / 59 / 2.0	15.0 / 67 / 2.0	22.0 / 67 / 2.0	15.0 / 76 / 2.0	22.0 / 76 / 2.0
Fleming (1992) (mm)	6.84	12.60	8.75	17.34	11.56	19.52
FEM (Plaxis 3D) (mm)	6.43	10.15	6.95	10.35	10.41	18.11
Bohn et al (2016) (mm)	5.13	10.68	5.05	10.53	4.81	11.17
Zhang et al (2016) (mm)	5.84	9.75	6.40	10.74	8.22	14.18
Boonyatee & Lai (2017) (mm)	6.97	10.63	7.89	12.07	10.96	17.07
Actual/Measured (mm)	4.66	9.66	4.13	7.17	5.96	11.02
This study ('Pile' computer program method) (mm)*	**1.51**	**3.77**	**0.95**	**2.16**	**0.77**	**1.37**

Note. Adapted from "Settlement Analysis of Axially Loaded Bored Piles: A Case History", by M. Mert and M.T. Ozkan, 2019, *World Academy of Science, Engineering and Technology, International Journal of Geotechnical and Geological Engineering*, 13(6), p.399.
* This result was obtained from this study, all other results are from Mert and Ozkan (2019) study.

The settlements determined using 'Pile" program are more conservative than the actual settlement values for all the test piles and for all load cases. The difference may have resulted from errors in modelling soil parameters to suit 'Pile' input format.

3.5 Basis of selection of empirical methods to apply

In the following sections, single and pile group settlements are calculated using some selected methods discussed. The basis of selection was based on the following:

i) Applicability of a particular method to the type of soil in which the pile is founded.

ii) Whether or not direct use of parameters is possible which would reduce errors from estimating same.

iii) In the process of trying to find any case histories for Harare, it was mentioned to the researcher by an retired Bridge Engineer who was trying to assist in finding the case histories that the methods regularly used in practice (at Ministry of Transport – Bridges section in the 80's and 90's) to predict settlement of single piles and pile groups were the T-z method, Fleming (1992) and Randolph and Wroth (1978). Whenever possible, these three methods have been used in settlement calculation in Chapter 4.

iv) A Poulos-related method has also been included in almost all cases because of the extensive research on pile foundation, particularly their settlement analysis, carried by this investigator.

CHAPTER FOUR

4 SETTLEMENT CALCULATIONS AND COMPARISON OF RESULTS

In this chapter, settlement calculations were carried out using the various empirical, analytical and/or theoretical methods and computer method covered in Chapter 2.

4.1 Single Pile Settlement Calculations by empirical, analytical and/or theoretical methods

Single pile settlement calculations are carried out for piles founded in cohesive soil, cohesionless soil and layered soil.

4.1.1 Pile founded in cohesive soil

Refer to section 3.4.1 (b) for details.

4.1.1.1 T-z Method/Coyle and Reese method

From section 2.7.3, the settlement values obtained are contained in Table B8 from which the variations in Figure 4.1 have been plotted.

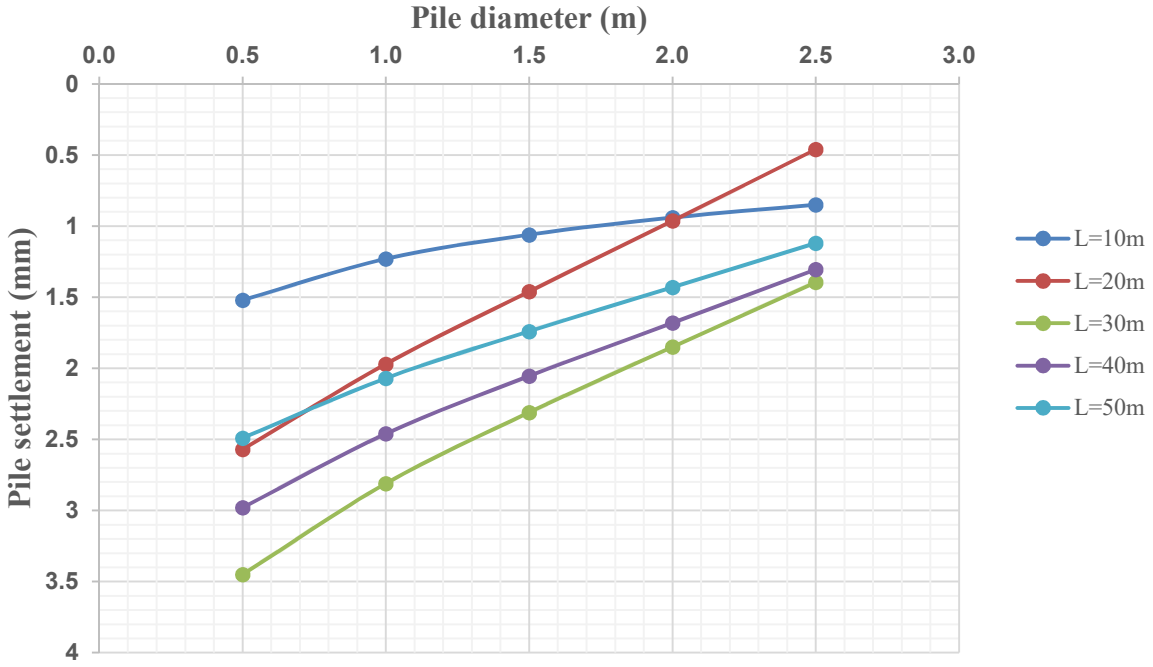


Figure 4.1: Variation of pile settlement with pile diameter and length using the T-z method

The following observations are made from both the graphs and the tabulated settlement vales:

a) For a particular value of pile length L, settlement decreases with increasing pile diameter for piles founded in uniform clay soil for all the pile length considered.
b) For a particular pile diameter, the settlement increases with increasing pile length up to a maximum at L=30m but this trend is reversed from L=30m when settlement decreases with increasing pile length for a specific pile diameter. The load-settlement variation also follows this similar trend.
c) For any specific pile length, the end-bearing capacity of the pile increases with increasing pile diameter. However, pile shaft resistance increases with increasing pile length and thus long piles tend to support load predominantly by frictional resistance.
d) End-bearing resistance of piles in clay soil is independent of pile length.

e) Both pile shaft capacity and end bearing capacity are independent of applied load but rely on pile length and diameter. The effect of type of founding soil is covered in section 3.5.1 of this report.

The load-transfer method of pile settlement estimation has the following limitations.

i) The use of load-transfer curves assumes that the pile movement at any time is related only to the shear stress at that point, being independent of stresses elsewhere on the pile. This inherent assumption takes no reasonable account of the continuity of soil mass. Because of this disregard of the soil continuity, the load-transfer method is rendered unsuitable for the analysis of load-settlement behaviour of pile groups.
ii) For a particular site, in order to be able to produce load-transfer curves, a significant amount of instrumentation is required. The costs of such instrumentation may exceed that for a normal load-test. Further, extrapolation of data between sites does not always apply and/or succeed.

4.1.1.2 Focth (1967) method

Refer to section 2.7.4. Soil's Young's modulus E_s=2G$_s$(1+v)=2x10x1.5=30MPa, E_p=30G. Pile stiffness factor, $K=E_P/E_S$=1000. Values of pile movement ratio, M_R are determined from Figure 2.10 for K=1000 and the appropriate value of L/D_0. A simple spreadsheet is developed to calculate the settlement.

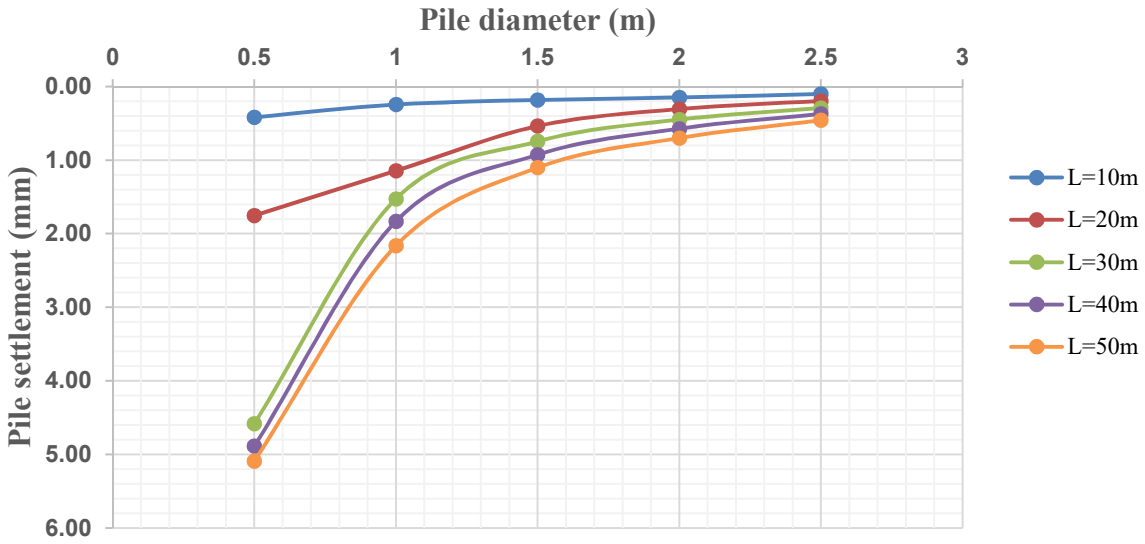


Figure 4.2: Variation of pile settlement with pile diameter and length after Focht (1967)

The settlement values are included in Table B8 and used to produce Figure 4.2 which shows the variation of settlement with pile diameter and pile length.

The following deductions are made from Figure 4.2, read concurrently with the appropriate column in Table B8. The deductions are applicable to piles supporting their loads by end-bearing, mainly.

a) For a specific pile diameter, the pile head settlement increases with increasing pile length.
b) For a given pile length, the pile head settlement initially decreases substantially with increasing pile diameter.
c) Settlement decrease is fairly rapid for $D_0 \leq 1.5$, becoming gradual for larger pile diameters, being asymptotic to the pile diameter axis.

4.1.1.3 Poulos and Davis (1968) method

I_ρ, the displacement factor for a finite soil layer, is determined from Figure 2.13 for $v=0.5$, $h=2L_i$ and h is the depth of the finite layer. E_s=2G(1+v)=30MPa.

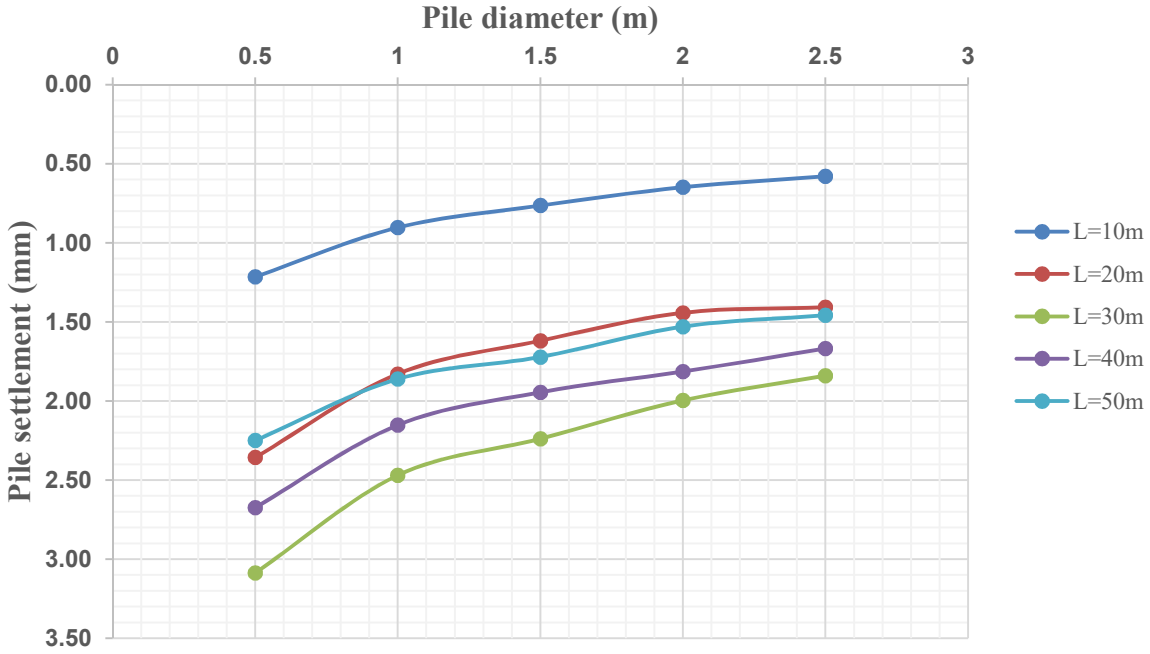


Figure 4.3: Variation of pile settlement with pile diameter and length after Poulos and Davis (1968)

Settlements are computed for the specified values of pile diameter and length for $I\rho$ values. The results are automated to a spreadsheet and the settlement values are summarised in Table B9 from which the variation of settlement with pile diameter and length are presented in Figure 4.3 whose form shows a fair measure of agreement with Figure 4.1 obtained by the T-z method. The following observations are made from both Figure 4.3 and the appropriate column of Table B9:

- The pile settlement decreases with increasing pile diameter for all the values of pile lengths considered in this study.
- For a fixed pile diameter, the pile settlement decreases with increasing pile length for 10≤L≤30m while for L>30m, the settlement decreases with increasing pile length, the same variation pattern exhibited by the T-z method in Figure 4.1.
- The pile settlement increases with increasing loading up to L=30m, decreasing with increased load values for L=40 and 50m.
- The lack of total smoothness to the graphs most likely resulted from estimation of I_ρ values from Figure 2.13.

Poulos and Davis (1968) presented results which apply to the case of a single pile in soft clay where the pile is practically incompressible relative to the surrounding soil. The compressibility of the pile itself in stiff clays may have a significant influence over pile settlement prediction and may lead to an underestimation of the settlement at the top of a compressible pile.

Elastic theory-based methods of pile settlement prediction rely heavily on the displacement theory of a homogeneous isotropic elastic soil mass and use constant soil parameters of E and

v. However, real soil does not behave as an ideal elastic solid. The stiffness of real soil increases as the average effective compressive stress increases, but may decrease as shear stresses increase, as failure is approached. Further, the interaction factors application is based on the assumption that the soil is a homogeneous elastic medium of constant modulus with depth. This assumption is an oversimplification of reality.
The assumption that the pile is perfectly rough and the soil assumed to be an ideal elastic material capable of resisting any shear stresses which may be developed between the pile and the soil, is not entirely practical because real soils have a finite shear strength. The interface between the soil and the pile also has a finite adhesive strength. When shear stress reaches the adhesive strength, slip between the pile and the soil will take place.

4.1.1.4 Mattes and Poulos (1969) method

Refer to section 2.7.6 of this report. Values of the settlement influence factor, I_ρ are obtained from Figure 2.16. Settlements are calculated for corresponding values of $I\rho$, pile diameter and pile length and the calculations were automated to a simple spreadsheet. Graphs were also plotted to show the variation of pile settlement with pile diameter for values of pile length as contained in Figure 4.4 and Table B8 from where the following observations are apparent:

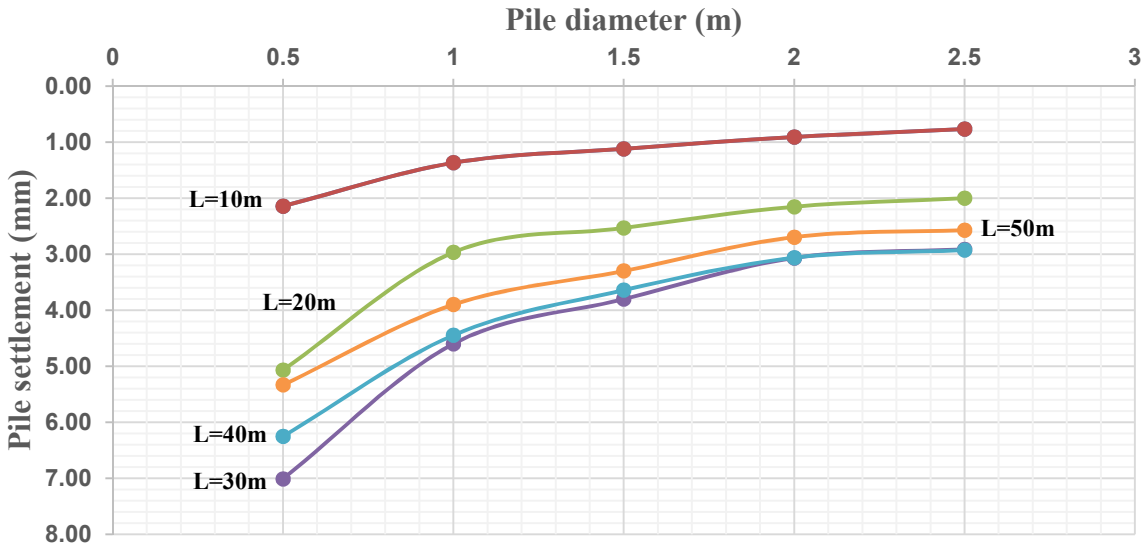


Figure 4.4: Variation of pile settlement with D_0 and length after Mattes and Poulos (1969)

- For all the pile length considered in this paper, the pile settlement decreases with increasing pile diameter. The pattern of the variations are in fair agreement with those in Figures 4.1, 4.2 and 4.3.
- Similarly, for a fixed pile diameter, the pile settlement decreases with increasing pile length for $10 \leq L \leq 30$m while for L>30m, the settlement decreases with increasing pile length.
- As would be expected and clearly depicted in the relevant column of Table B8, the pile settlement also increases with increasing applied load value. This trend is clearly depicted in Table 4.4(b).

Pile settlements were also separately calculated for E_s=3x10^{5}kN/m^2, up from 3x10^{4}kN/m^2 and down to 3x10^{3}kN/m^2. It was apparent that an increase in the value of E_s leads to a significant decrease in pile settlement and a decrease in E_s also leads to a marked increase in settlement for compressible piles.

The application of elastic theory analyses to real soil requires that the 'elastic' soil parameters be determined over a stress range representative of that in the field. However, an assessment of the accuracy of elastic theory-based settlement predictions must await comparison with the results of carefully controlled model and field tests.

4.1.1.5 Butterfield and Banerjee (1971) method

The values of f are determined from Figure 2.17(b) for the appropriate values of L/D. $\lambda=E_P/G=3000$, therefore take $\lambda=6000$ in Figure 2.17(b). From the appropriate column of Table B8 values of f and the corresponding settlement for each value of D $(=D_0)$ and pile length, L are tabulated from which graphs in Figure 4.5 are plotted which show the variation of the pile settlement against pile diameter for different values of pile length.

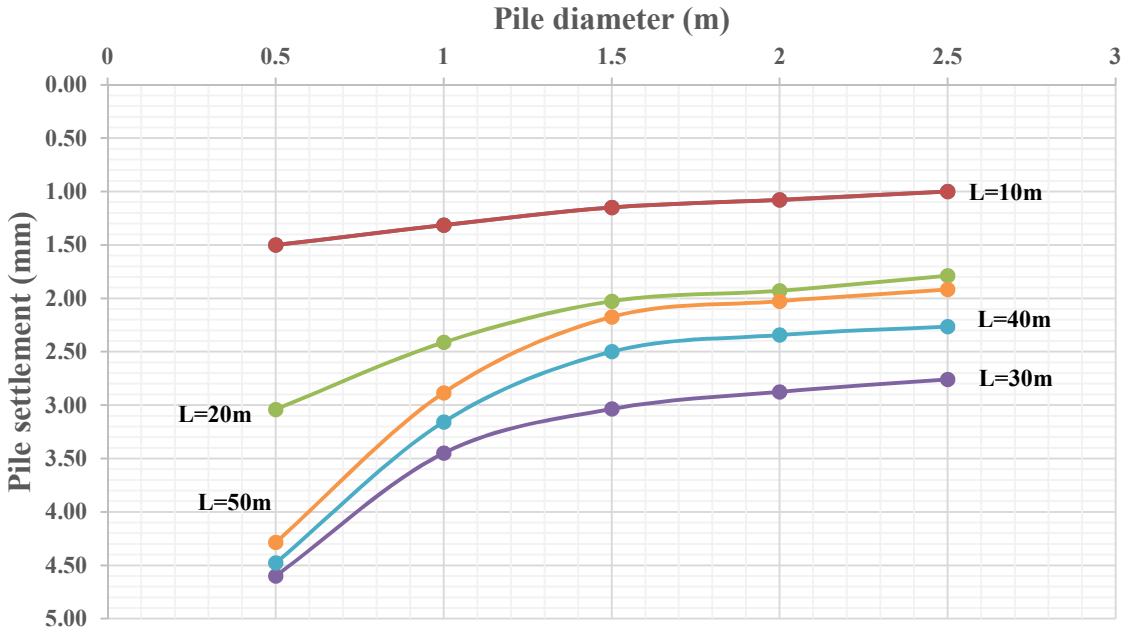


Figure 4.5: Variation of pile settlement with pile diameter and length after Butterfield and Banerjee (1971)

The following observations are made from both Table B8 and Figure 4.5:

1) For any particular value of pile length L, settlement decreases with increasing pile diameter and the pattern of the variations is in comparative agreement with other methods already considered.
2) Similarly, for a fixed pile diameter, the pile settlement decreases with increasing pile length for $10 \leq L \leq 30$m while for $L > 30$m, the settlement decreases with increasing pile length.
3) As clearly depicted in the relevant column of Table B8, the pile settlement also increases with increasing applied load value.
4) The lack of smoothness to the graphs most likely resulted from estimation of f values from Figure 2.17(b).

4.1.1.6 Randolph and Wroth (1978) method

Refer to section 2.7.9 and $r_m=L$. From the appropriate column of Table B8, values of the settlement computed and automated to a spreadsheet are given from which the variations of pile settlement with pile diameter and pile length are plotted as shown in Figure 4.6.

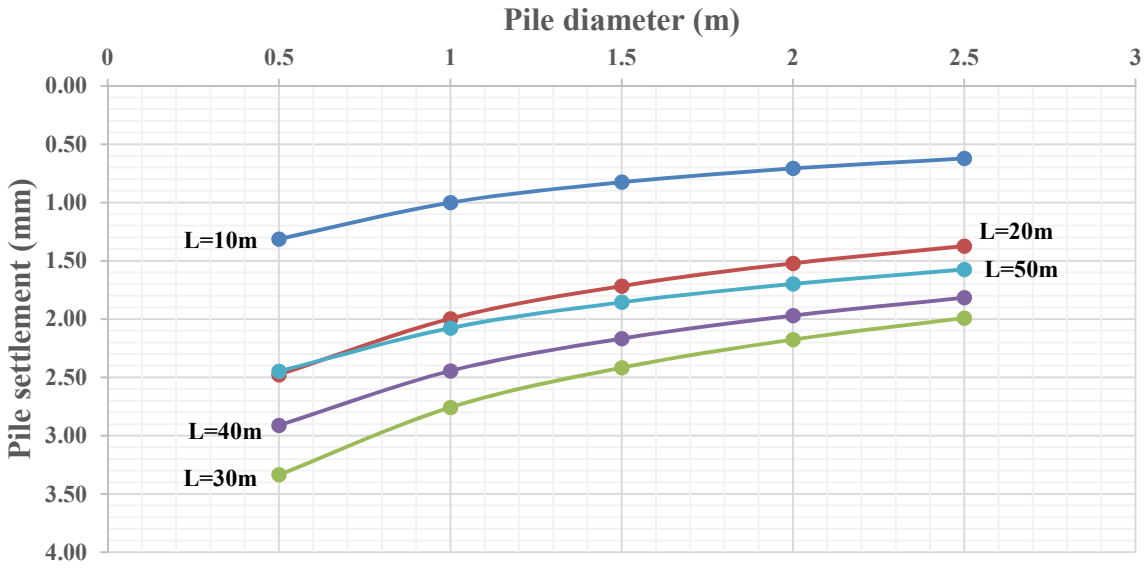


Figure 4.8: Variation of pile settlement with pile diameter and length after Randolph and Wroth (1978)

The following observations are made from both Table B8 and Figure 4.6:

a) For a particular value of pile length *L*, settlement decreases with increasing pile diameter for the range of pile lengths considered.
b) Settlement also initially increases with increasing pile length and applied loading for a specific pile diameter up to around L=30m, then decreases for L=40 and 50m, despite the applied load being higher than that for L≤30m.
c) There is a fair measure of similarity in the variations of Figure 4.6 with those of Figures 4.1 to Figure 4.5. Even the settlement values are of more or less the same order.

4.1.1.7 Poulos and Davis (1980) method

Factors I_0, R_k, R_h and R_v are determined from Figures 2.23, 2.24, 2.25 and 2.26. The settlement is calculated for different pile diameters and lengths and a summary of settlement values obtained is tabulated in Table B8. The settlement is then plotted against the pile diameter and lengths to produce graphs shown in Figure 4.7 from where the following observations are made:

- For a particular value of pile length *L*, settlement decreases with increasing pile diameter for the range of pile lengths considered.
- For D_0<1.0m, the pile settlement increases with increasing pile lengths but the pattern is not clearly defined for larger values of D_0.
- From D_0>1.0m, settlement also initially increases with increasing pile length and applied loading for a specific pile diameter up to around L=30m, then decreases for L=40 and 50m, despite the applied load being higher than that for L≤30m.
- The lack of curve smoothness exhibited by the settlement variation with diameter for some graphs above most likely resulted from errors in the estimation of the factors which make up settlement factor, *I*.

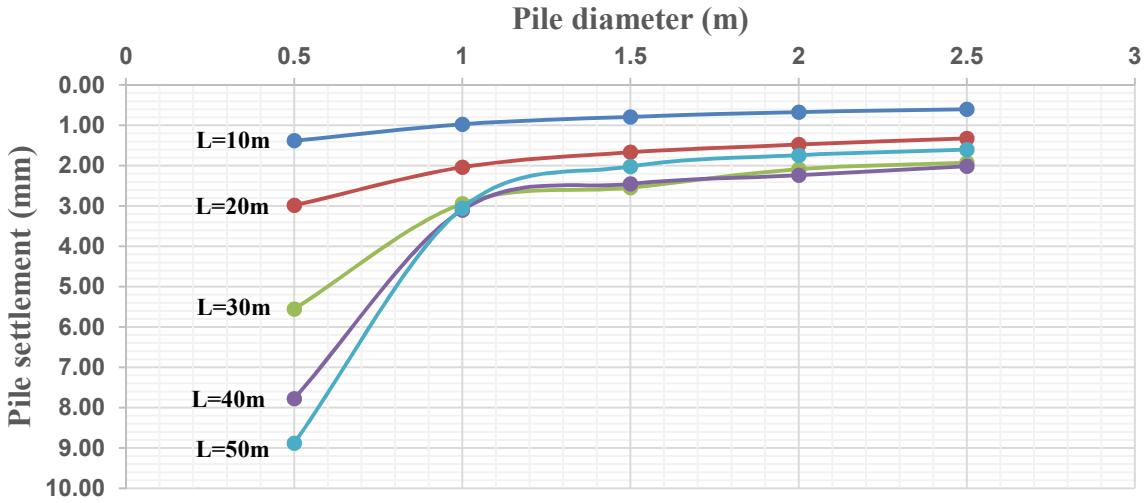


Figure 4.7: Variation of pile settlement with pile diameter and length after Poulos and Davis (1980)

4.1.1.8 Poulos (1989) method

Refer to section 2.7.11 from where the values of I_ρ are worked out from Figure 2.28. The determined values of I_ρ are tabulated together with the computed values of S_e and S_p and automated to a spreadsheet and values of the total settlement are summarized in Table B8.

The total settlement, S_{et}, is plotted against pile diameter and length to produce curves shown in Figure 4.8. The following deductions are made from both Figure 4.8 and the relevant columns of Table B8:

a) The pile settlement, in all cases, decreases with increasing pile diameter, the rate of decrease being particularly steep for L>30m.

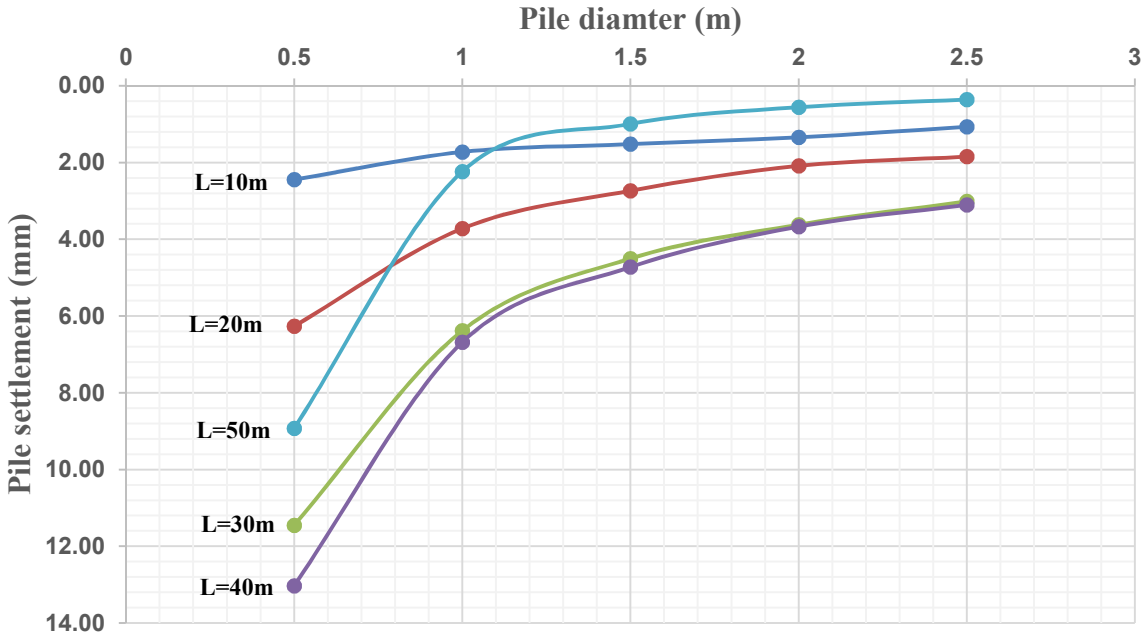


Figure 4.8: Variation of pile settlement with pile diameter and length after Poulos (1989)

b) The settlement increases with increasing pile length for 10≤L≤40m, but reduces for L=50m although the applied load is equal to that for L=40m and greater for lower values of L. The variation is very similar to that for Poulos and Davis (1980) exhibited in Figure 4.7..
c) From the raw data, it was observed that for any fixed pile length, both elastic settlement and elastic shortening decrease with increasing pile diameter.

The continuum analysis employed by Poulos (1989) is premised on the assumption that if incremental tensile stresses are developed in the soil mass from the loading of the pile, the soil continues to respond elastically, which is a reasonable assumption if the overall stress conditions remain compressive due to the compressive overburden stresses. However, if the overall stresses become tensile, the elastic continuum analysis becomes questionable. This caused doubts and criticism of the elastic continuum theory, (Leonards and Darrag, 1989) and preference for the load-transfer approach which does not consider stress in the soil apart from that at the pile-soil interface. However, the main limitation of the load-transfer method is that it can only be properly applied to a single pile but cannot be used directly to analyse a pile group.

4.1.1.9 Fleming (1992) method

Refer to section 2.7.12 and see Table B9 for settlement values generated form the calculations. Figure 4.9 shows the variation of pile head settlement with pile diameter and length. These graphs are plotted using the settlement calculations automated to spreadsheets, for L=10, 20, 30, 40 and 50m and D_0=0.5, 1.0, 1.5, 2.0 and 2.5m. The individual calculations have not been included in this report but a summary of the settlement values is contained in Table B9.

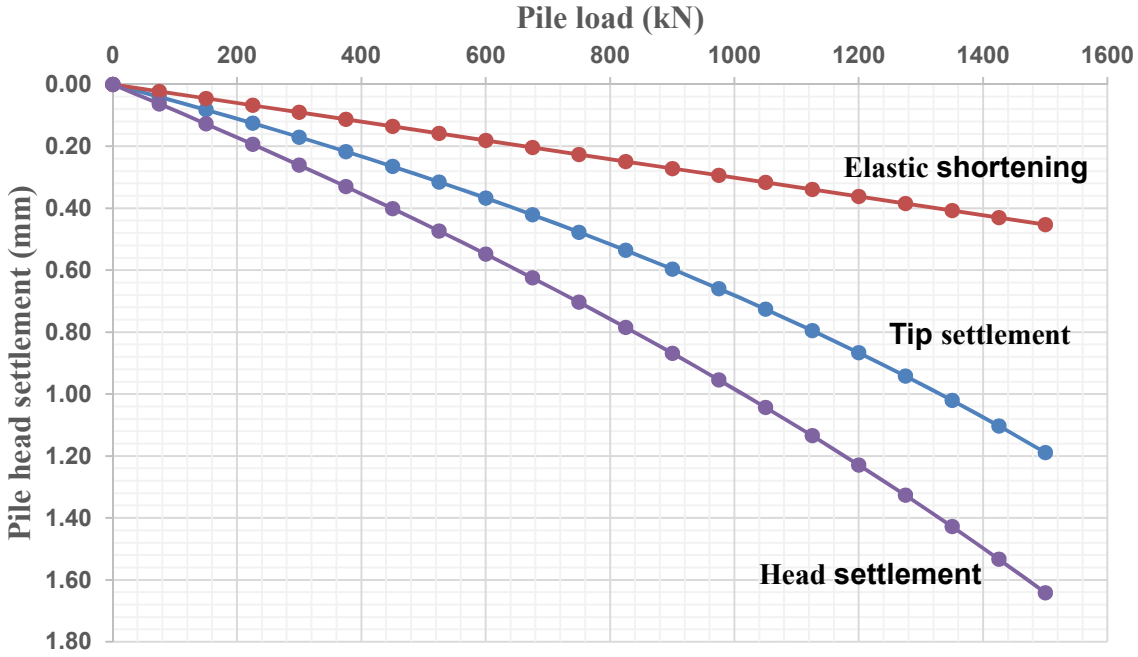


Figure 4.9: Load-settlement curves (typical form) for D_0=1.5m and pile length, L=30 after Fleming (1992)

The following observations are made from an analysis of both the relevant column of Table B9, Figure 4.9 and 4.10:

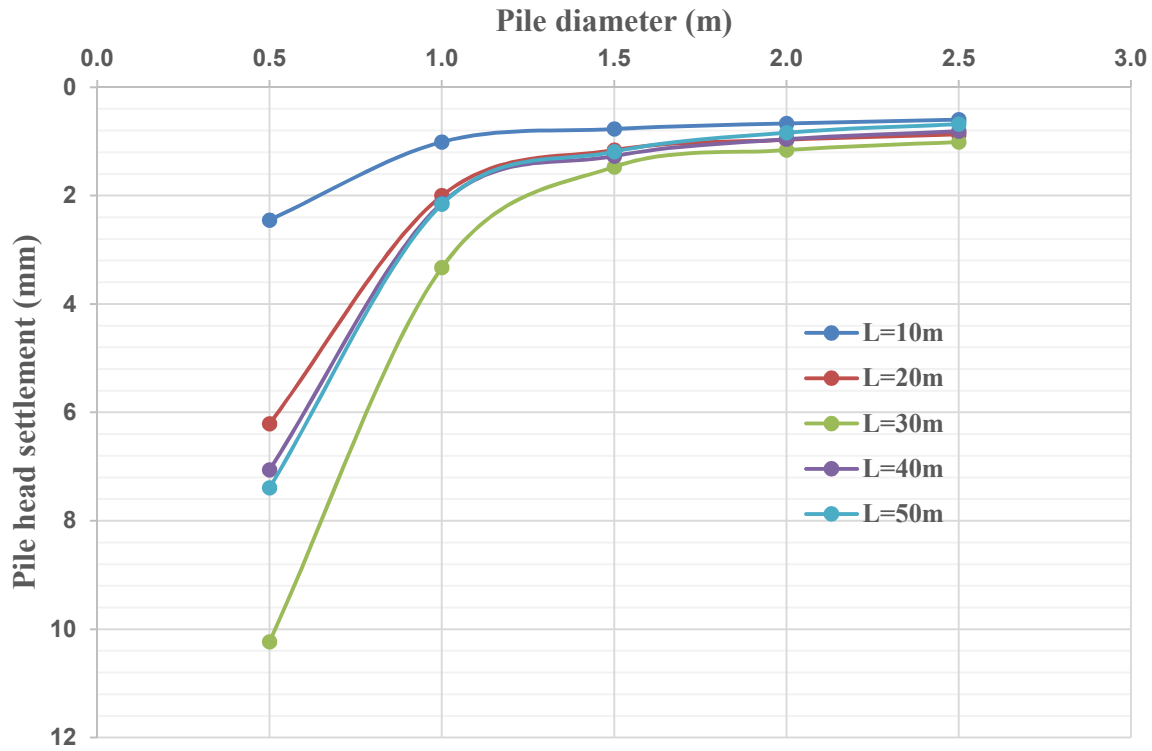


Figure 4.10: Variation of pile settlement with pile diameter and length after Fleming (1992)

1) Pile head settlement increases with increasing pile load for 10≤L≤30m but decreases for L=40 and 50m even though the applied load is higher, pile head settlement being the sum of pile tip settlement and elastic shortening as depicted in Figure 4.
2) For the cases considered pile head settlement decreases with increasing pile diameter which is the same trend exhibited by both elastic shortening and pile tip settlement.

The sensitivity of the pile settlement to each of Fleming's hyperbolic parameters is reviewed by varying one parameter while others are fixed and observing the effect on the settlement prediction. The developed spreadsheet progrmme is used for the parameters sensitivity analysis. The results of this analysis are summarized in the comments below. The actual analysis results have not been included in this report.

i) **Influence of pile diameter, D_0**

a) An increase in diameter leads to a substantial decrease in predicted pile settlement, decreasing asymptotically to the pile diameter axis.
b) Pile diameter change thus has a significant impact on the magnitude of the pile settlement.

ii) **Effect of pile length, L or L_P**

a) For a fixed pile diameter, settlement increases markedly with increasing pile length.
b) It is evident that settlement is very sensitive to change in pile length, all other factors remaining fixed in this analysis. There is a significant increase in settlement when L is increased from 10m to 20m and 20m to 30m. However, as pile length increases beyond L=30m, the rate of increase in settlement tends to decrease, which agrees

with Hull (1987) who found that embedding a pile beyond a certain critical length does not lead to any significant reduction in pile settlement.

iii) **Influence of effective column factor, K_E**

a) For a fixed value of pile diameter, settlement increases gradually with increasing value of column length factor, K_E.
b) For a particular value of K_E, settlement decreases asymptotically with increasing pile diameter.
c) Pile settlement is moderately sensitive to changes in effective column length factor. For a 60% increase in K_E, from 0.5 to 0.8, the settlement increases by about 50%.

iv) **Influence of shaft flexibility factor, M_S**

From the analyses done, it is evident that settlement is not very sensitive to a change in the value of M_S. For example, the settlement increases by 5% for a 66% increase in pile shaft flexibility factor, M_S. Pile settlement thus slightly increases for a substantial upward variation of shaft flexibility factor.

v) **Modulus of soil below pile base, E_B or E_b**

Analyses were done with varying moduli of soil below base and the following observations were made:

a) For pile base soil with $E_B \geq 3x10^3 kN/m^2$, a change in soil modulus for soil below the pile base does not lead to any significant change in settlement. Settlement generally decreases with increasing E_B.
b) For relatively small values of E_B, say $E_B=3x10^2 kPa$, settlement markedly increases mainly due to pile tip settlement.
c) Pile settlement is therefore generally insignificantly changed for stiffer soils but is very sensitive and hence increases noticeably for less stiff soil.
d) For a fixed pile base diameter, pile settlement generally increases with decreasing E_B.

vi) **Effect of concrete modulus, E_C**

The pile material can be in any of the material covered in section 2.1 of this report. However, in this report, only cylindrical concrete piles are considered. Settlement values were calculated for different concrete modulus values, E_C, L=30m, E_B=300kPa, M_S=0.0015 and the following observations were made:

a) For smaller diameter piles, the pile settlement increases fairly markedly with decreasing pile concrete modulus, rate of increase decreasing with increasing pile diameter.
b) The settlement tends to a limiting value irrespective of the pile diameter.
c) Changes in E_C have a very noticeable effect on the settlement of small diameter piles but becomes insignificant as the pile diameter gets bigger.

vii) **Effect of ultimate shaft load, U_S and ultimate base load, U_B**

The effect of U_B and U_S on pile settlement was also investigated by varying these parameters while keeping the other constant. The following deductions are made:

a) Pile settlement increases with increasing U_B and decreasing U_S, for any particular pile diameter.
b) The settlement is not very sensitive to changes in both U_B and U_S, increasing by less than 10% when U_B is quadrupled.

c) Pile settlement, however, appears to increase to significant levels as witnessed when U_B was increased 4 fold.

Sensitivity thus generally depends on the magnitude of the parameters in different soil conditions.

4.1.2 Pile founded in non-cohesive soils

Refer to section 3.4.2 (b) for details. The piles are founded in medium dense sand. The settlement for a single pile is calculated using the following selected empirical and theoretical methods:

4.1.2.1 Meyerhof (1959) method

Pile settlement in sands is given by: $\rho_p = D_0/30 \text{xFoS}$. As is to be expected from this empirical relationship, and displayed in Table 4.1, it is evident that in accordance with Mayerhof:

Table 4.1: Settlement calculation results (after Meyerhof, 1959)

Applicable Soil Type	Shaft Dia (mm)	Base Dia (mm)	Settlement(mm)		
			FoS=2.0	FoS=2.5	FoS=3.0
Sand	0.5	0.5	8.33	6.67	5.56
Sand	1.0	1.0	16.67	13.33	11.11
Sand	1.5	1.5	25.00	20.00	16.67
Sand	2.0	2.0	33.33	26.67	22.22
Sand	2.5	2.5	41.67	33.33	27.78

- Settlement decreases as the factor of safety increases.
- Pile settlement increases with increasing pile diameter.

Meyerhof's empirical method implies that the pile settlement in sands is dictated mainly by the pile diameter and the factor of safety and that it is independent of the applied load and the pile length.

4.1.2.2 T-z method

Settlement calculations but soil parameter for sand used. The settlement values obtained are contained in Table B10 from which the variations in Figure 4.11 have been plotted.

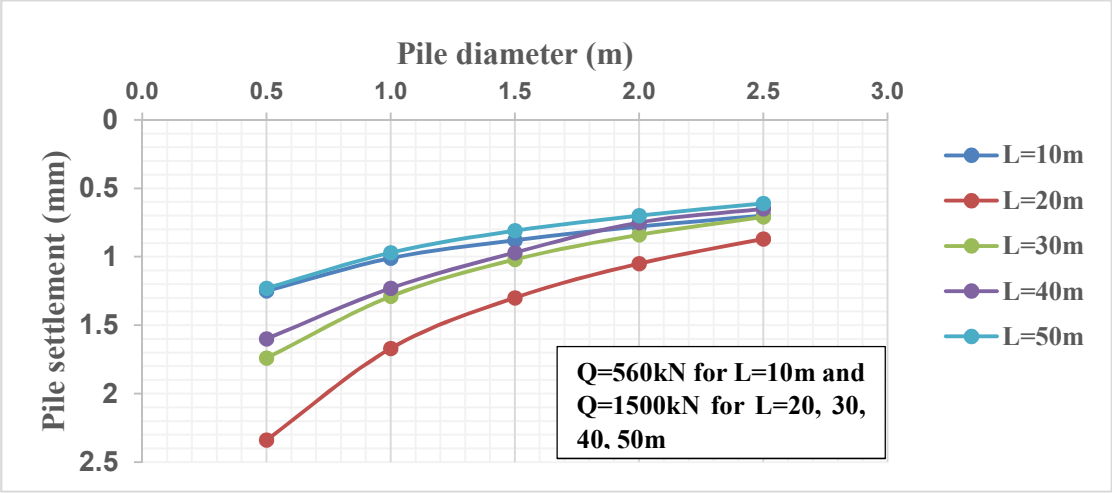


Figure 4.11: Variation of pile settlement with pile diameter and length, founded in sand using the T-z method

The following observations are made from both Figure 4.11 and Table B10:

a) For a particular value of pile length *L*, settlement decreases with increasing pile diameter for piles founded in uniform sand soil for for all values of L considered in this report.
b) Pile settlement increases with pile length up to around L=20m and thereafter, the trend reverses as pile settlement decreases with increasing pile length for L=30, 40 and 50m.
c) For any specific pile length, the end-bearing capacity of the pile increases with increasing pile diameter. However, pile shaft resistance increases with increasing pile diameter and pile length as well. Unlike piles founded in cohesive soil where long piles tend to support load predominantly by frictional resistance, piles founded in sand support load by both shaft resistance and end bearing resistance in fairly close proportions..
d) End-bearing resistance of piles in sand soil is independent of pile length, being the same for *L*=30, 40 and 50m in this case for corresponding pile diameters.
e) Both pile shaft capacity and end bearing capacity are independent of applied load but rely on pile length, diameter and types of soil through which the pile shaft traverses.
f) Piles founded in sand develop far much higher shaft and end bearing capacity than developed by piles founded in sand.

4.1.2.3 Randolph and Wroth (1978) method

Refer to section 2.7.9 for the details about this method detail. Settlement was calculated with soil parameters for sand replacing clay. $r_m=L_i$.

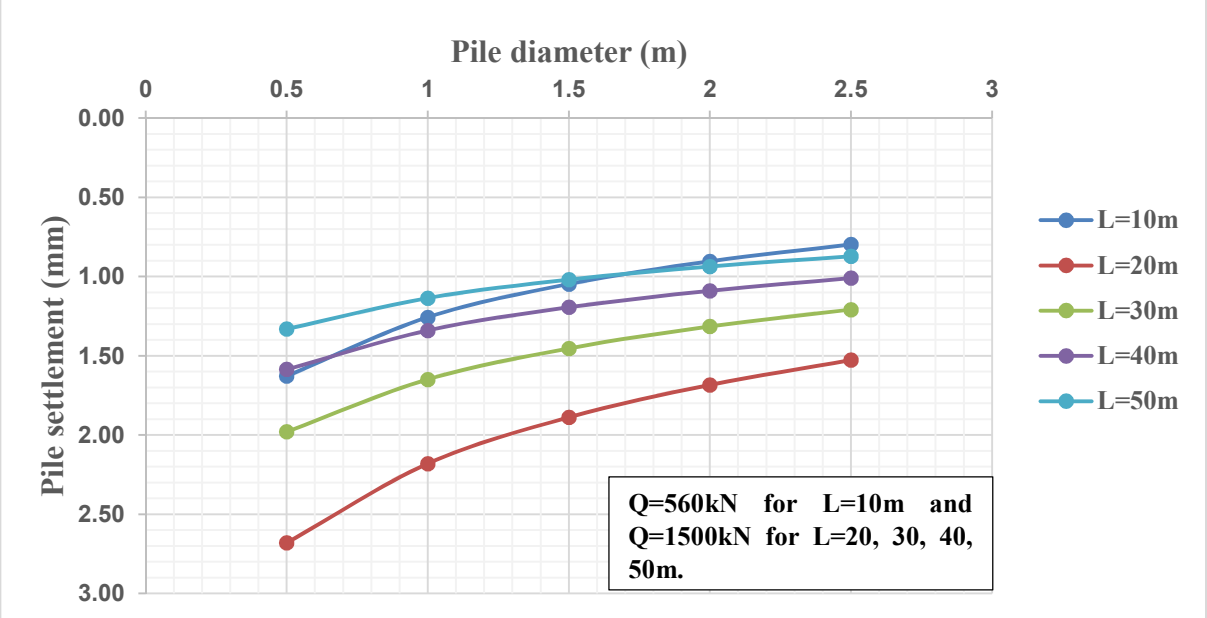


Figure 4.12: Variation of pile settlement with pile diameter and length after Randolph and Wroth (1978)

From the appropriate column of Table B10 a summary of the settlement calculations done and automated to a spreadsheet is given from which the variation of pile head settlement with pile diameter and pile length are plotted as depicted by the graphs in Figure 4.12 above. The following observations are made from both Table B10 and Figure 4.12:

a) The pile settlement decreases with increasing pile diameter for all the values of pile length considered.

b) For L=10 and 20m, the pile settlement increases with increasing pile length for a specific diameter but decreases with increasing pile length for L=30, 40 and 50m..
c) Pile settlement also increases with increasing applied load for L=10 and 20m, but decreases for L=30, 40 and 50m though the applied load remains constant at 1.5MN.

4.1.2.4 Poulos (1989) method

The values of I_ρ are worked out from Figure 2.28 for appropriate values of L/d. The determined values of I_ρ are tabulated together with the computed values of elastic settlement, S_e and pile elastic shortening, S_p and automated to a spreadsheet and values of the total settlement S_{et}, are summarized in Table B10. The total settlement is plotted against pile diameter and length to produce curves shown in Figure 4.13. The following deductions are made from both Figure 4.13 and the relevant column of B10.

a) Pile settlement decreases with increasing pile diameter for the different pile lengths considered in this report.

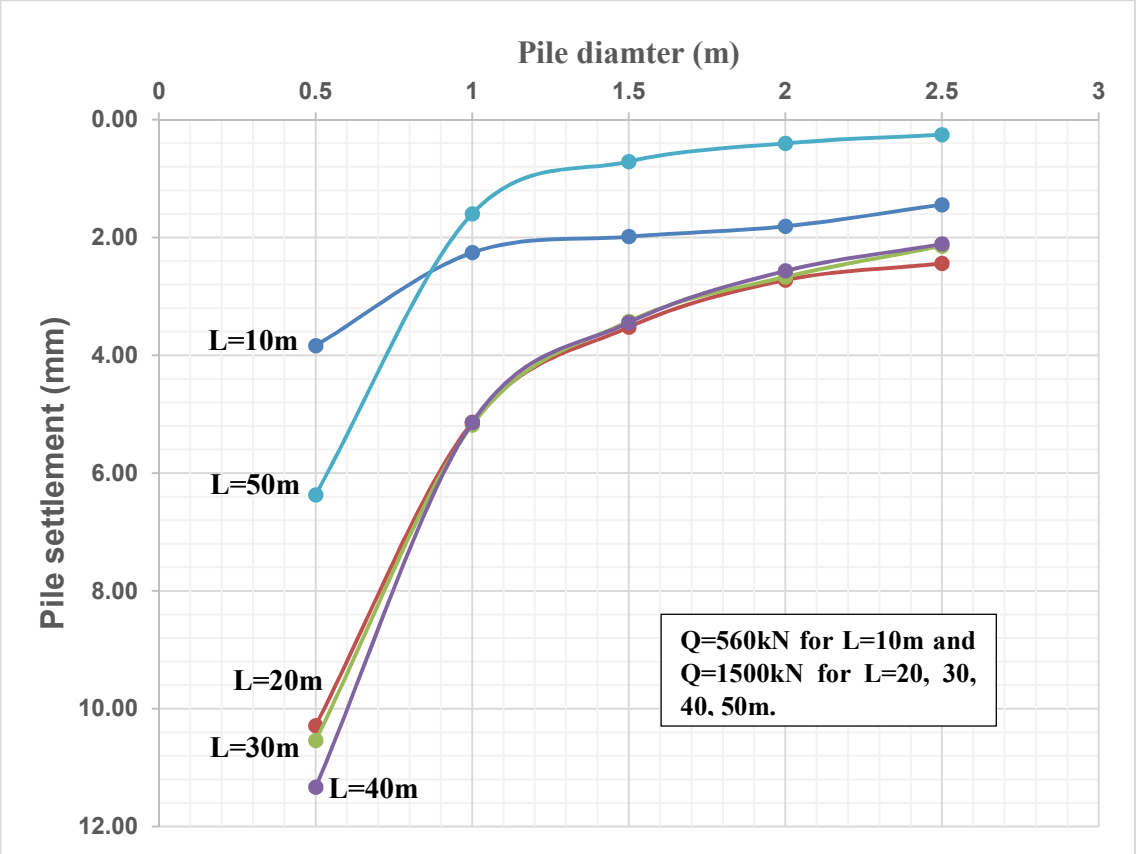


Figure 4.13: Variation of pile settlement with pile diameter and length founded in sandy soil after Poulos (1989)

b) The pile settlement variation with pile diameter for L=20, 30 and 40m is almost the same as the graphs nearly coincide.
c) Pile settlement increases with increasing pile length for 10≤L≤40m but decreases for L=50m despite the applied load remaining at 1.5MN.

4.1.2.5 Fleming (1992) method

Cohesive soil properties are replaced with those of cohesionless soil. Figure 4.17 shows the variation of pile head settlement with pile diameter and length. These graphs are plotted using

the calculations of settlement automated to spreadsheets. The raw calculations have not been included in this report but a summary of the settlement values is contained in Table B10.
The following observations are made from an analysis of both the relevant column of Table B10, Figure 4.14 and 4.15:

1) Pile head settlement generally increases with increasing pile load, as depicted in Figure 4.14.
2) Pile settlement decreases with increasing pile diameter for all values of pile length considered.
3) For a specific diameter, the settlement variation with pile length does not produce a clear pattern as observed with earlier methods reviewed. For D_0=0.5m for example, the pile settlement decreases for L=10m to L=20m, increases significantly for L=30m before reducing noticeably for L=40 and 50m. However, the general trend is comparable to others.

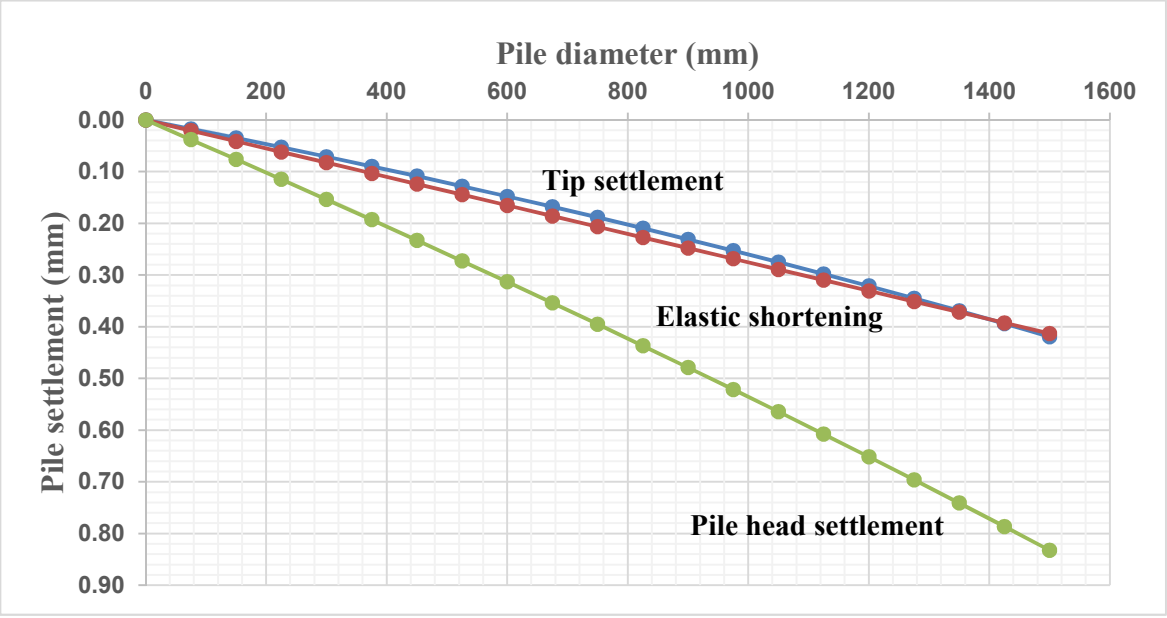


Figure 4.14: Load-settlement curves (typical form) for D_0=1.5m and pile length, L=30 after Fleming (1992)

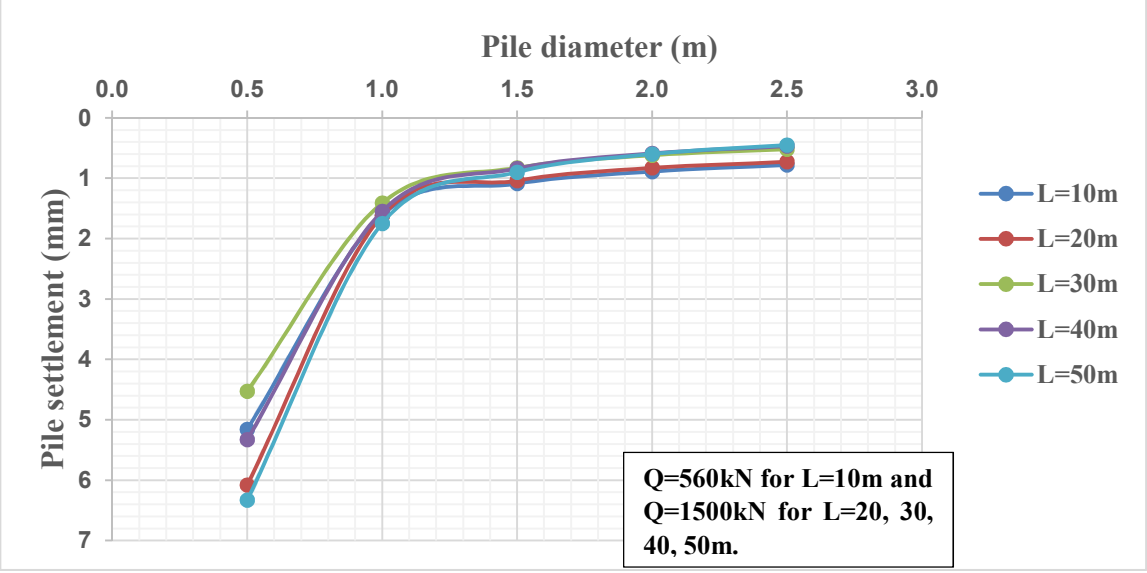


Figure 4.15: Variation of pile settlement with pile diameter and length founded in non-cohesive soil after Fleming (1992)

4.1.3 Pile founded in layered soil

Refer to section 3.4.3 for the definition of terms and other details. The settlement for a single pile in layered soil is calculated using the following selected theoretical and analytical methods:

4.1.3.1 T-z method

Refer to section 3.4.3 for the definition of terms and other details. Settlement calculations were done and the values obtained are contained in Table B11 from which the variations in Figure 4.16 have been plotted.

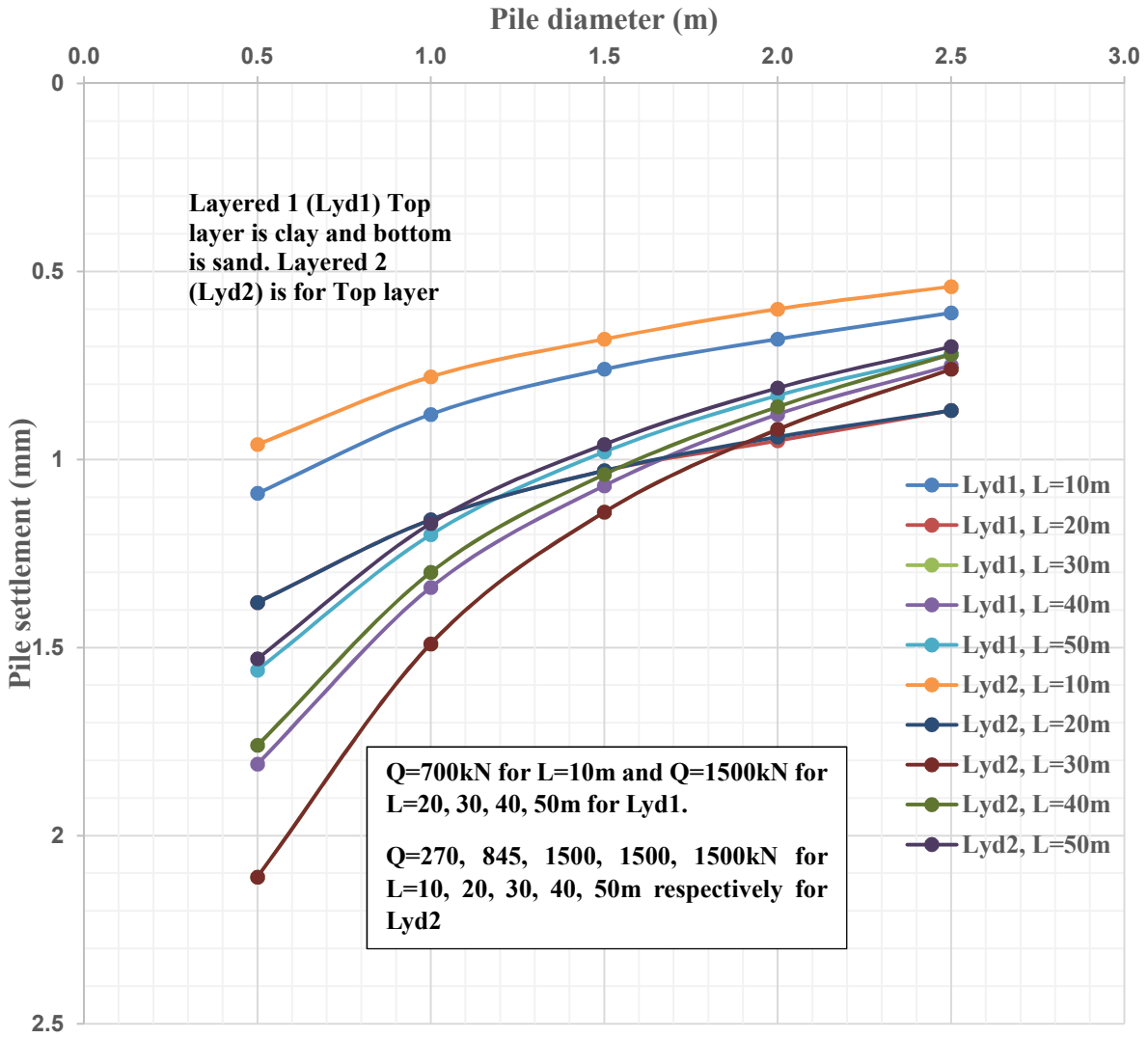


Figure 4.16: Variation of pile settlement with pile diameter and length, founded in layered soil using the T-z method – Layered (Lyd1), top layer is clay and bottom layer is sand and Layered (Lyd2), top layer is sand and bottom is clay.

The following observations are made from both the graphs and the tabulated data.

a) Pile settlement for layered soil 1 and layered soil 2 decreases with increasing pile diameter for all values of L.
b) The pile settlement for layered soil 1 is more than that for layered soil 2 for L=10m but the same for L=20 and 30m and slightly different for L=40 and 50m.

c) Settlement increases with increasing pile length for L=10 and 20m then reduces with increasing pile length but not in a clearly defined pattern because the settlement for L=50m is lower than that for L=30m but higher for L=40m.
d) The settlement values are not markedly different for the two layers but the difference affirms that the soil type through which piles traverse does affect settlement.

4.1.3.2 Randolph and Wroth (1978) method

Refer to section 2.7.9 for details. The weighted harmonic mean of both the Young's modulus, E_s (and hence shear modulus, G_s) and Poisson's ratio ν, for the two layers of soil were used and since the layer thicknesses are the same, the harmonic and arithmetic means are identical. $r_m=L_i$. The analysis is then carried out treating the 2-layered soil as a single layered soil having a uniform shear modulus. The results of the analysis are summarized in Table B11 and Figure 4.17 from where the following deductions are made:

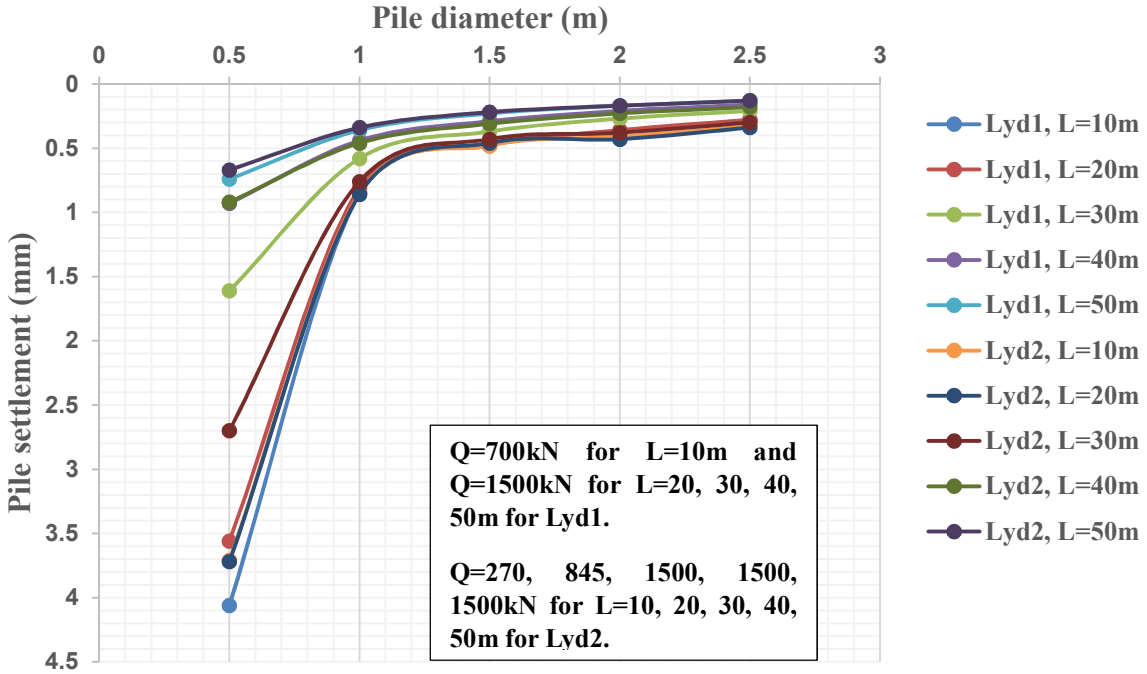


Figure 4.17: Variation of pile settlement with pile diameter and length for layered soil after Randolph and Wroth (1978)

a) The pile settlement decreases with increasing pile diameter, exhibiting the same general trend as for uniform soils by various methods.
b) Settlement increases with increasing pile length and applied load for L=10 and 20m, but decreases with increasing pile length and applied load for L=30, 40 and 50m.
c) If settlement considerations are the most critical, the 50m long pile would be ideal though uneconomic, but the 30m long pile would be more economic with fairly acceptable settlement levels.

4.1.3.3 Poulos (1989) method

The values of I_ρ are worked out from Figure 2.28. The determined values of I_ρ are tabulated together with the computed values of elastic settlement, S_e and pile elastic shortening, S_p and automated to a spreadsheet and values of the total settlement S_{et}, are summarized in Table B11.

The total settlement is plotted against pile diameter and length to produce curves shown in Figure 4.18. The following deductions are made from both Figure 4.18 and the relevant column of Table B11:

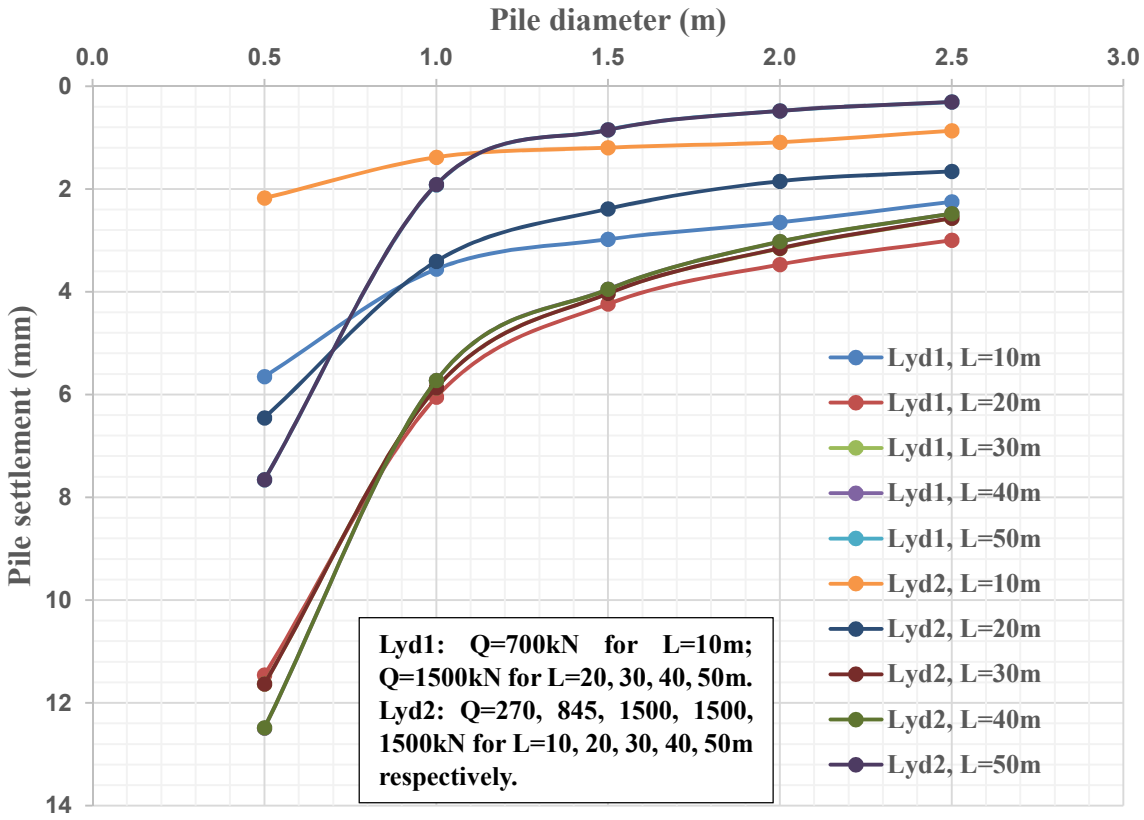


Figure 4.18: Variation of pile settlement with pile diameter and length for layered soil after Poulos (1989)

i) The pile head settlement decreases with increasing pile diameter for all values of pile length examined in this paper.

ii) The settlement decreases with increasing pile length for L=10 and 20m. The variation for L=30, 40 and 50m does not follow a defined pattern, being lowest for L=50m and highest for L=40m though the load applied increases with increasing pile length but is constant for each pile length for over the different diameters.

iii) Layered soil type 1 settles more than layered soil type 2 for L=10 and 20m but settlement values for Lyd1 and Lyd2 become similar for L=30, 40 and 50m.

iv) Variations obtained through Poulos (1989) method follow the general forms of those obtained through Randolph and Wroth (1978) and the T-z method.

4.2 Pile settlement computation using 'Pile' computer package

Pile software package is used to calculate settlement for piles with different pile length and diameter and founded in either uniform soils or layered soils. The results so obtained are then compared with those obtained using the various empirical, semi-empirical and theoretical methods under the same soil conditions. The computer outputs are summarized in Table B8 and B9 for cohesive soil and Table B for non-cohesive soils.

4.2.1 Pile settlement calculation using computer method for cohesive soil

The settlement variation with pile diameter and pile length for cohesive soils are shown graphically in Figures 4.19. The following deductions are made from the relevant column of Table B8, B9 and Figures 4.19.

- The computer calculated pile settlement follows similar variations to those exhibited using the empirical and analytical methods in earlier sections of this report.

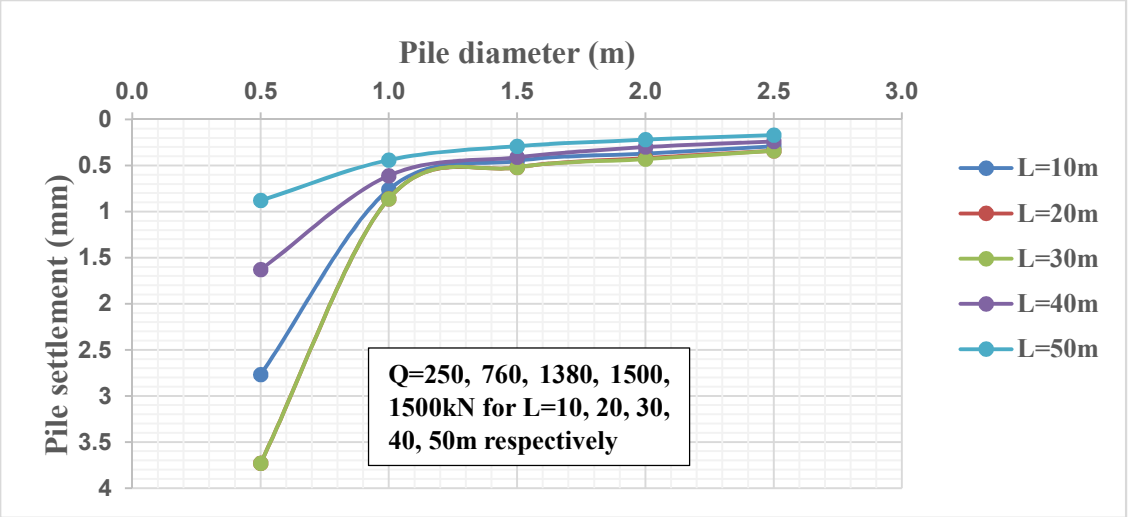


Figure 4.19: Variation of pile settlement with pile diameter and length calculated using 'Pile' computer method for cohesive soil

- The single pile settlement decreases with increasing pile diameter for the range of pile lengths considered.
- For a specific pile diameter, the settlement increases with increasing pile length for L=10 and 20m, that for L=20m is the same as that for L=30m. The settlement then decreases with increasing pile length for L=40 and 50m though the applied load remains constant at 1.5MN.

4.2.2 Pile settlement calculation using computer method for non-cohesive soil

The settlement variation with pile diameter and pile length for cohesionless soils are also shown graphically in Figures 4.20. The following deductions are made from the relevant column of Table B10 and Figures 4.20:

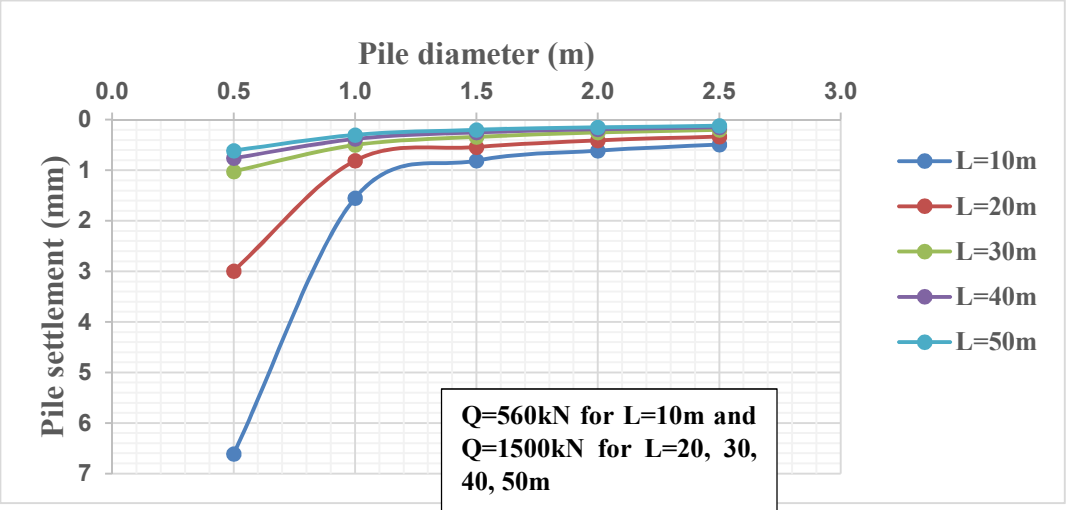


Figure 4.20: Variation of pile settlement with pile diameter and length calculated using 'Pile' computer method for noncohesive soil

i) Pile settlement significantly decreases with increasing pile length despite the applied load increasing with increasing pile length.
ii) The settlement also decreases with increasing pile diameter. The general appearance of the graphical variations is similar to those by other methods.

4.2.3 Pile settlement calculation using computer method for layered soil

The pile settlement was also determined for piles founded in layered soil and two scenarios were considered as follows:

- Scenario 1 – layered (lyd1) soil when clay soil is in the top layer and sand is in the lower layer.
- Scenario 2 – layered (lyd2) soil when sand soil is the top layer and clay in the lower layer.

The settlement values obtained are summarized in Table B8 and B9, presented graphically in Figure 4.21. The following observations are made from the relevant columns of Tables B8, B9 and Figure 4.21:

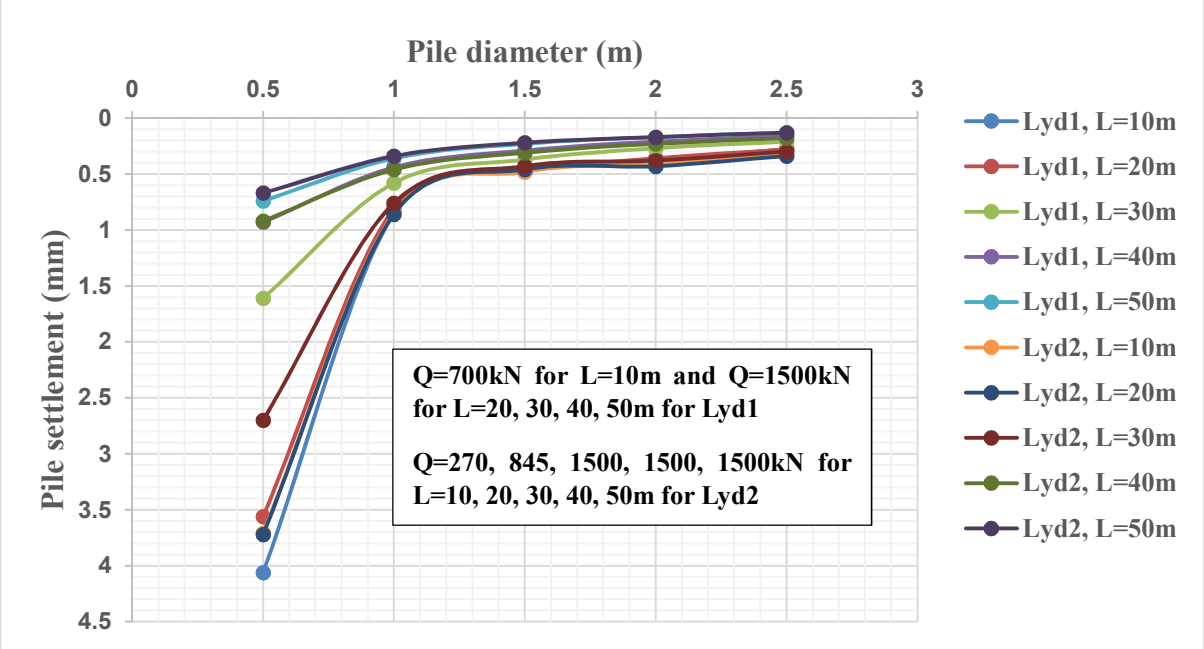


Figure 4.21: Variation of pile settlement with pile diameter and length calculated using 'Pile' computer method for layered soil

a) Like with all the other methods considered, the pile settlement decreases with increasing pile diameter in layered soil.
b) The maximum settlement occurs in layered type Lyd1 soil with L=10m while the least settlement is in Lyd1, L=50m. .
c) The computer method settlement variations in Figure 4.21 show a fair measure of agreement with that those obtained by theoretical methods for layered soils.

4.3 Single pile settlement comparison

Tables B8, B9, B10, B11 and B12 below summarise the single pile settlements determined by the various methods as follows:

- **Table B8, B9** – Pile capacity and pile settlement of a single pile founded in cohesive soil
- **Table 10** – Pile capacity and pile settlement of a single pile in non-cohesive soils

- **Table B11, B12** – Pile capacity and pile settlement of a single pile founded in layered soil.

The method abbreviations adopted in Figures 4.22 to 4.6 are as follows:

Full name of method	Abbreviation used	Full name of method	Abbreviation used
T-z method	**TZM**	Mattes and Poulos (1969)	**M&P69**
Butterfield and Banerjee (1971)	**B&B**	'Pile' Computer Programme Method	**PCPM**
Randolph and Wroth (1978)	**R&W**	Focht (1957)	**FOC**
Poulos and Davis (1980)	**P&D80**	Poulos and Davis (1968)	**P&D68**
Poulos (1989)	**PO89**	Fleming (1992)	**FL92**

4.3.1 Comparison for piles founded in uniform cohesive soil

The charts in Figure 4.22 were derived from settlement values in Tables B8 andB9.

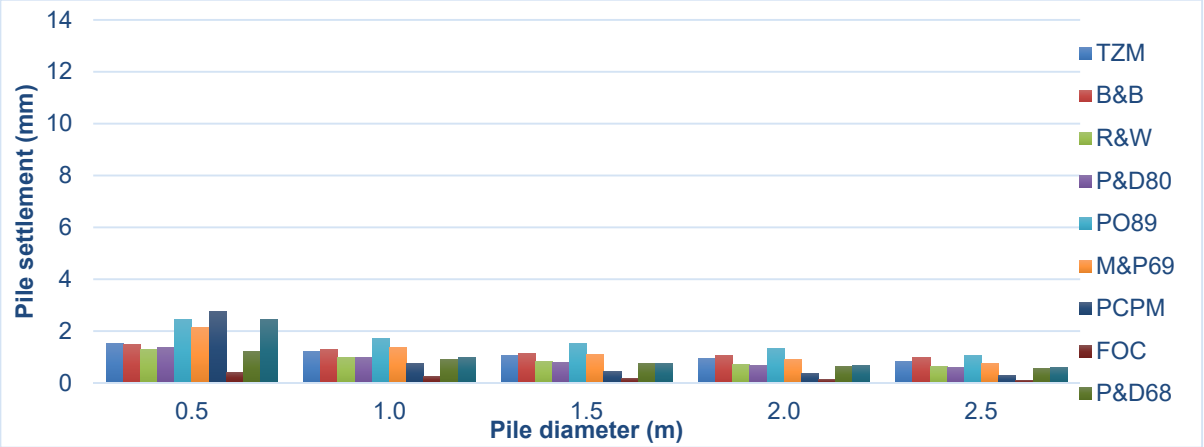


Figure 4.22(a): Comparison of settlement computed by different methods for a single pile founded in uniform cohesive soil for L=10m

Figure 4.22 (a) reveals a fair measure of agreement of settlement values computed by other methods except that by Focht (1957) method which is markedly low for all values of D_0. Pile settlement is more pronounced for the 0.5m diameter piles.

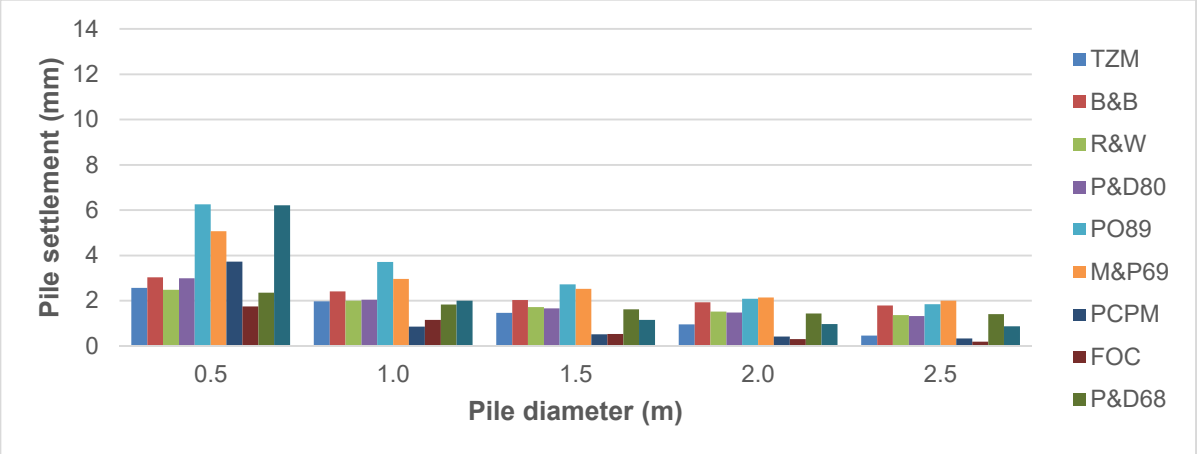


Figure 4.22(b): Comparison of settlement computed by different methods for a single pile founded in uniform cohesive soil for L=20m

From Figure 4.22(b), it is evident that settlement values calculated by Focht and 'Pile' computer program are lowest for all values of D_0, fairly high settlements being observed for D_0=0.5m, otherwise the settlement values are of comparable magnitude for each pile diameter. From Figure 4.22(c), it is observed that the settlement by Poulos (1989) and Fleming (1992) is markedly high for D_0=0.5m while that by Poulos (1989) and Mattes and Poulos (1969) for other values of D_0 dominate for a particular diameter, otherwise the settlement values are fairly comparable in general terms. Settlements determined by Focht (1957) method and pile computer programme method are very low, particularly for $D_0 \geq 1.5$m.

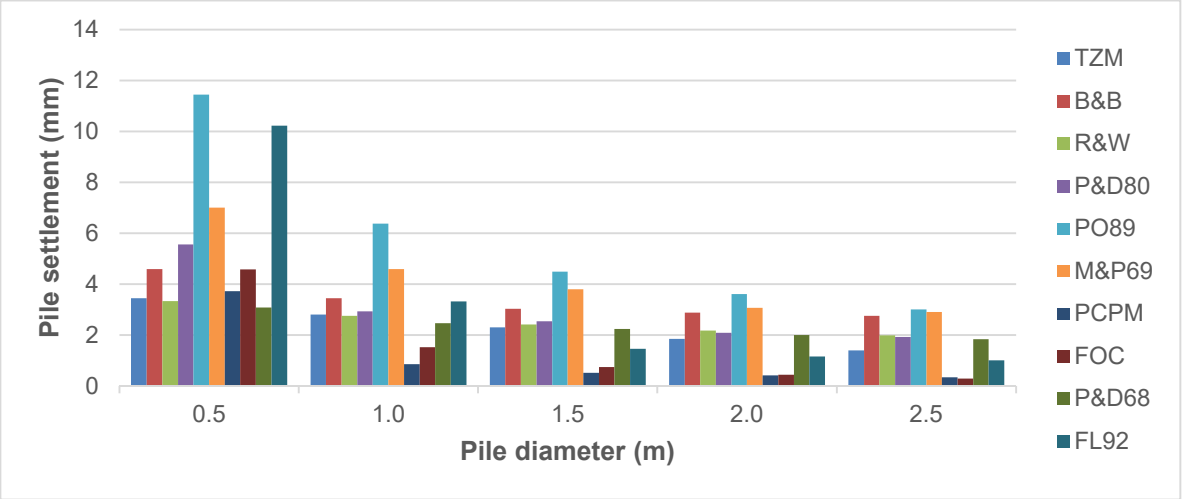


Figure 4.22(c): Comparison of settlement computed by different methods for a single pile founded in uniform cohesive soil for L=30m

From Figure 4.22(d) below, it is apparent that the settlement determined by Poulos (1989) is outstandingly high relative to that by other methods for D_0=0.5m and is the highest for all the other diameters though not markedly high. Settlement determined using Focht (1957) method and by computer method is still fairly low especially for $D_0 \geq 1.5$m. A fairly acceptable level of agreement is observed for each pile diameter save for the outstanding values noted.

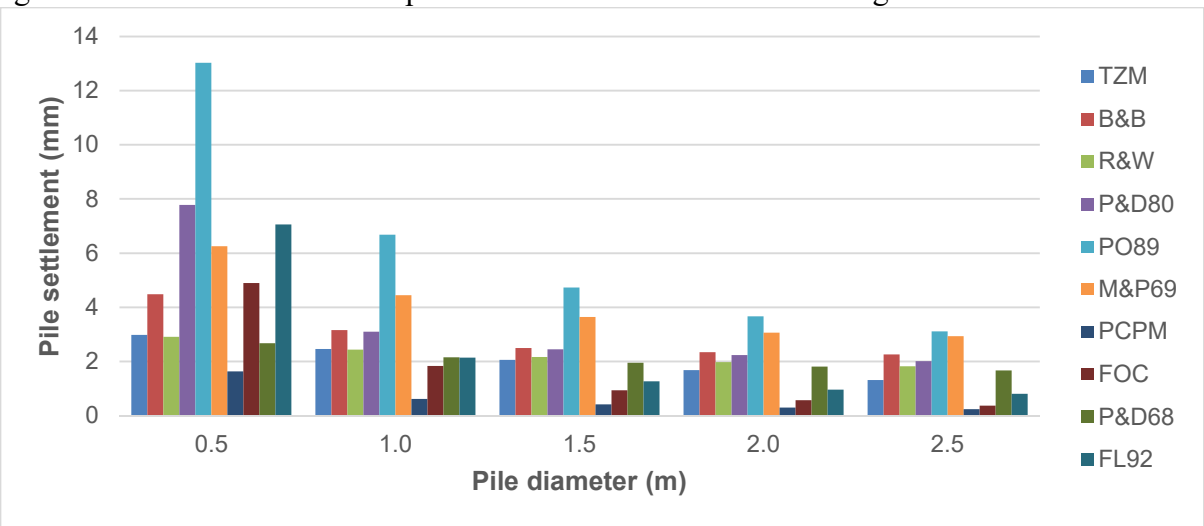


Figure 4.22(d): Comparison of settlement computed by different methods for a single pile founded in uniform cohesive soil for L=40m

In Figure 4.22(e), it is noted that the settlements determined by Poulos and Davis (1980), Poulos (1989) and Fleming (1992) are high compared to that obtained by other methods for

D_0=0.5m but settlement by all the other methods being in close comparison for D_0=0.5 and all the other diameters considered. Settlement by Mattes and Poulos is also slightly higher than that by other methods for D_0>0.5m. From all the figures, it is clear that settlement decreases with increasing pile diameter for all the pile lengths considered.

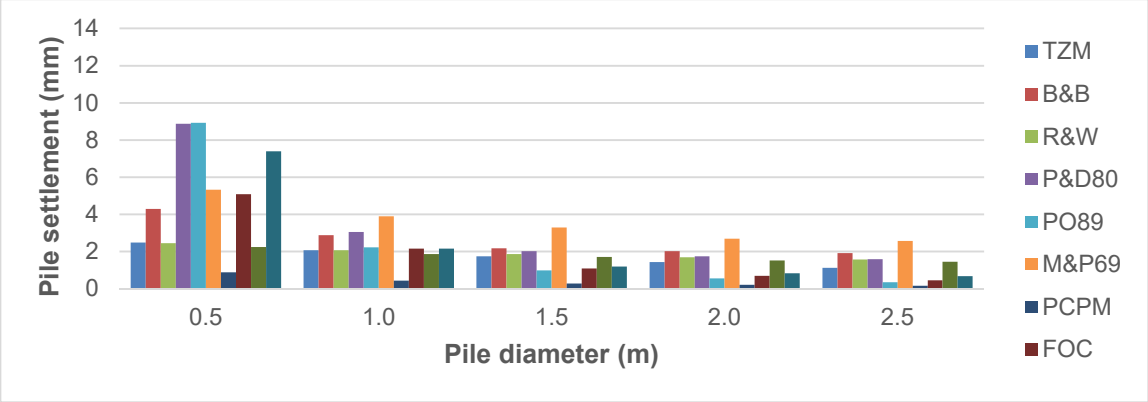


Figure 4.22(e): Comparison of settlement computed by different methods for a single pile founded in uniform cohesive soil for L=50m

Settlement values obtained using Focth (1957) method are lower than that determined using the other methods because the method only calculates settlement due to elastic shortening of the pile which in turn is determined from column theory. The method does not take into account pile settlement due to skin friction for floating piles. The method also fails to take into account the settlement of the soil material because the soil mass under a pile is subjected to compression from end bearing.

All the other methods take into account take into account pile settlement due to skin friction for floating piles and that due to settlement of soil mass due to compression caused by end bearing because the methods incorporate the elastic properties of soil which are the Young's modulus E_s, and the Poison's ratio v_s. In these methods, E_s may be used directly into the settlement prediction formula or indirectly through the use of the settlement influence factor I_ρ, which itself is a function of the stiffness coefficient K (=E_p/E_s) or the soil's shear modulus $G\ (=2E_s(1+v))$ where E_p is the Young's modulus of the pile material.

4.3.2 Settlement comparison for same load on varying pile length and vice versa

An analysis was also made of the variation and settlement when the same load is applied to varying pile length and when the pile length was fixed and the loading varied for the same diameter and for changing pile diameters. Table 4.2(a) and (b) give a summary of the variations obtained using some selected theoretical methods as indicated. The following deductions are made from Table 4.2(a):

- For the same magnitude of applied load to varying pile lengths, pile settlement decreases with increasing pile length. As an example and read from Table 4.2(a), for an applied axial load, P=250kN for D_0=0.5m, the pile head settlement decreases from: 1.50mm to 0.71mm using Butterfield and Banerjee (1971), 7.78mm to 0.89mm using Mattes and Poulos (1969) and 2.45mm to 1.49mm using Poulos (1989) from L=10m to L=50m respectively.
- Pile settlement also decreases significantly with increasing pile diameter for the same magnitude of applied load.
- The anomalous pile settlement variation calculated using Focth (1967) for the same applied load to varying pile lengths is due to the method's emphasis of pile settlement to elastic shortening when settlement increases significantly with increasing pile slenderness ratio,

L/D_0. The pile settlement increases from 1.12mm to 2.55mm for L=10m to L=50m respectively, which is atypical.

Table 4.2(a): Comparison of single pile settlement computed by various methods for same loading with varying D_0, and L founded in cohesive uniform soil, P=250kN

Pile Dia (mm)	Pile settlement (mm)				
	Focht (1967)	Poulos &Davis (1980)	Butterfield & Banerjee (1971)	Mattes & Poulos (1969)	Poulos (1989)
L=10m					
0.5	1.12	1.38	1.50	7.78	2.45
1.0	0.31	0.97	1.32	6.91	1.72
1.5	0.14	0.79	1.15	5.99	1.52
2.0	0.08	0.67	1.08	0.91	1.34
2.5	0.05	0.60	1.00	0.77	1.07
L=20m					
0.5	1.73	0.98	1.00	7.32	2.06
1.0	0.57	0.67	0.79	0.98	1.22
1.5	0.27	0.55	0.67	0.83	0.90
2.0	0.15	0.49	0.63	0.71	0.69
2.5	0.10	0.44	0.59	0.66	0.61
L=30m					
0.5	2.29	1.01	0.83	1.27	2.07
1.0	0.76	0.53	0.63	0.83	1.16
1.5	0.37	0.46	0.55	0.69	0.82
2.0	0.22	0.38	0.52	0.56	0.66
2.5	0.15	0.35	0.50	0.53	0.55
L=40m					
0.5	2.44	1.30	0.75	1.04	2.17
1.0	0.92	0.52	0.53	0.74	1.11
1.5	0.46	0.41	0.42	0.61	0.79
2.0	0.29	0.37	0.39	0.51	0.61
2.5	0.19	0.34	0.38	0.49	0.52
L=50m					
0.5	2.55	1.48	0.71	0.89	1.49
1.0	1.08	0.51	0.48	0.65	0.37
1.5	0.55	0.34	0.36	0.55	0.17
2.0	0.35	0.29	0.34	0.45	0.09
2.5	0.23	0.27	0.32	0.43	0.06

The following deductions are made from Table 4.2(b):

- For varying loading applied to a fixed pile length, pile settlement increases with increasing load intensity. From Table 4.2(b) and for applied load varying from P=250 to1250kN, L=30m and D_0=1.53, the settlement increases from 0.55mmto 2.75mm using Butterflied and Banerjee (1971) method and from 0.49mm to 4.75mm when using Poulos (1989) method.
- Pile settlement also increases noticeably with increasing pile diameter when the pile length is fixed but load intensity varies.

Table 4.2(b): Comparison of single pile settlement computed by various methods for same pile length L, with varying D_0 and P founded in cohesive uniform soil, L=30m

Pile Dia (mm)	Pile settlement (mm)				
	Fleming (1992)			Butterfield & Banerjee(1971)	Poulos (1989)
	Tip	Elastic	Pile head		
P=250kN					
0.5	0.17	0.68	0.85	0.83	3.04
1.0	0.15	0.17	0.32	0.63	0.96
1.5	0.14	0.08	0.22	0.55	0.49
2.0	0.14	0.04	0.18	0.52	0.30
2.5	0.13	0.03	0.16	0.50	0.04
P=500kN					
0.5	0.42	1.36	1.78	1.67	-
1.0	0.32	0.34	0.66	1.25	2.60
1.5	0.30	0.15	0.45	1.10	1.44
2.0	0.28	0.08	0.36	1.04	0.93
2.5	0.28	0.05	0.33	1.00	0.07
P=750kN					
0.5	0.86	2.04	2.90	2.50	-
1.0	0.54	0.51	1.05	1.88	4.42
1.5	0.48	0.23	0.71	1.65	2.45
2.0	0.45	0.13	0.58	1.56	1.64
2.5	0.43	0.08	0.51	1.50	0.11
P=1000kN					
0.5	1.77	2.72	4.49	3.33	-
1.0	0.82	0.68	1.50	2.50	6.09
1.5	0.68	0.30	0.98	2.20	3.60
2.0	0.62	0.17	0.79	2.08	2.37
2.5	0.59	0.11	0.70	2.00	0.14
P=1250kN					
0.5	4.07	3.40	7.47	4.17	-
1.0	1.17	0.85	2.02	3.13	8.41
1.5	0.92	0.38	1.30	2.75	4.75
2.0	0.82	0.21	1.03	2.60	3.22
2.5	0.77	0.14	0.91	2.50	0.20

4.3.3 Comparison for piles founded in uniform cohesionless soil

The comparative charts in Figure 4.23(a) were derived from settlement values contained in Table B10.

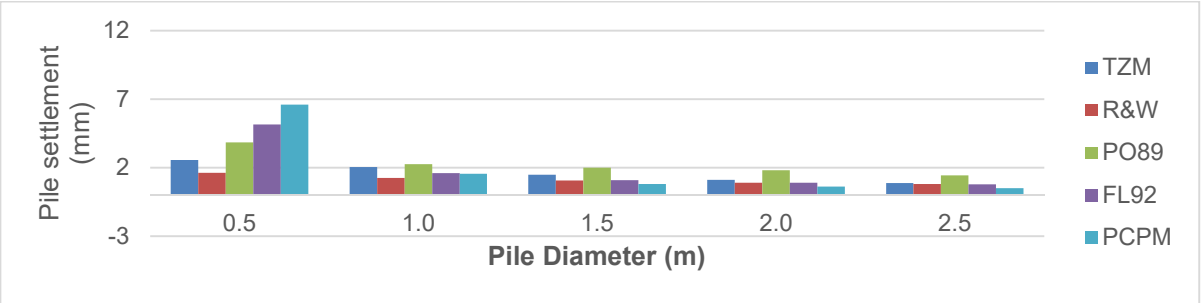


Figure 4.23(a): Comparison of settlement computed by different methods for a single pile founded in uniform non-cohesive soil for L=10m

From an analysis of Figure 4.23(a) and for L=10m in Table B10, it is observed that settlement determined by Poulos (1989), Fleming (1992) and the computer methods are higher compared to that by the other three methods for D_0=0.5m, otherwise the settlement values are very comparable by all methods for D_0>0.5m. It is all self-evident that the pile settlement decreases with diameter, the decrease being distinct from D_0=0.5m to D_0=1.0m.

The charts in Figure 4.23(b) were derived from settlement values contained in Table B10, for L=20m. It is noticeable that the pile settlements determined by Poulos (1989) and Fleming (1992 methods are higher than by other methods, the Poulos (1989) method being highest for all values of D_0 but being markedly so for D_0=0.5m. Settlement is fairly comparable for other diameters by all other methods

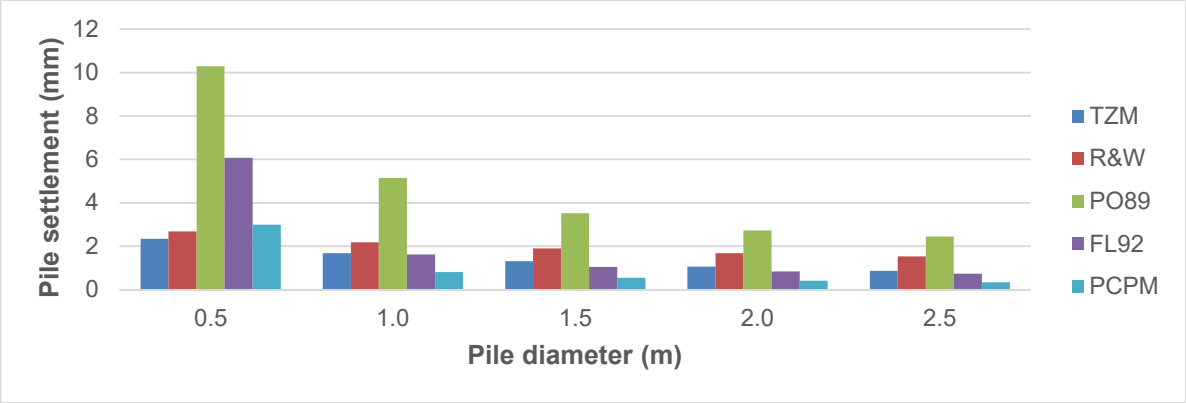


Figure 4.23(b): Comparison of settlement computed by different methods for a single pile founded in uniform non-cohesive soil for L=20m

Figure 4.23(c) below contains comparative charts derived from values in Table B10. It is clear that settlement derived using Poulos (1989) method is the highest for all pile diameters but is markedly so for D_0=0.5m. The computer-determined settlement is lowest in each diameter class. Generally, settlement is fairly close for all other methods except by Poulos as noted and by Fleming for D_0=0.5m.

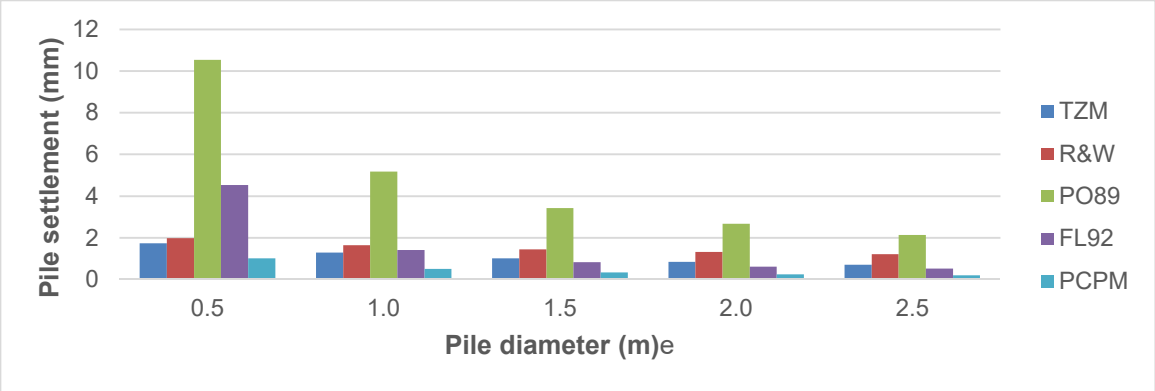


Figure 4.23(c): Comparison of settlement computed by different methods for a single pile founded in uniform non-cohesive soil for L=30m

Again, in Figure 4.23(d), the Poulos (1989)-determined settlement is the highest for all pile diameters but being particularly so for D_0=0.5m, followed by Fleming (1992) method for D_0=0.5m only. Except as noted, the settlement is generally in close agreement for all other

methods. A similar trend is also apparent in Figure 4.23(e) but the Fleming determined settlement is almost equal to Poulos (1989) method-determined one for the 0.5m diameter pile. The rest agree closely in each diameter class. Settlement values are very small for larger diameter piles.

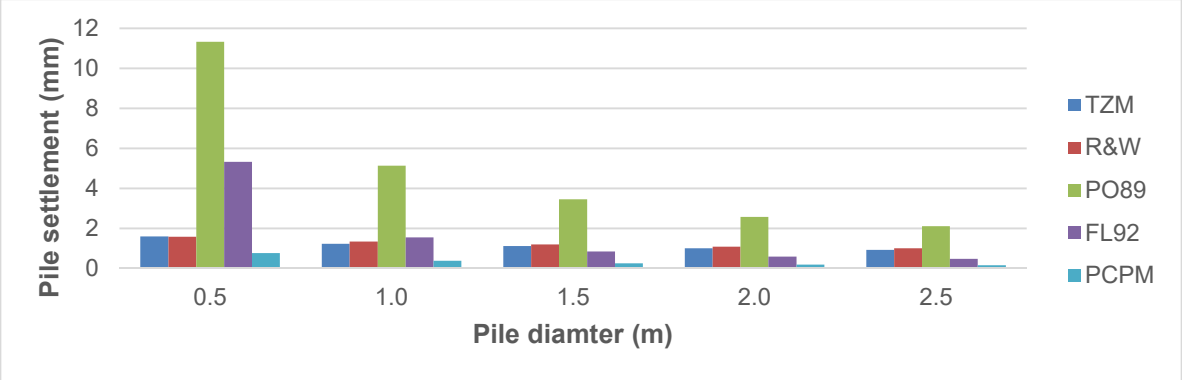


Figure 4.23(d): Comparison of settlement computed by different methods for a single pile founded in uniform non-cohesive soil for *L*=40m

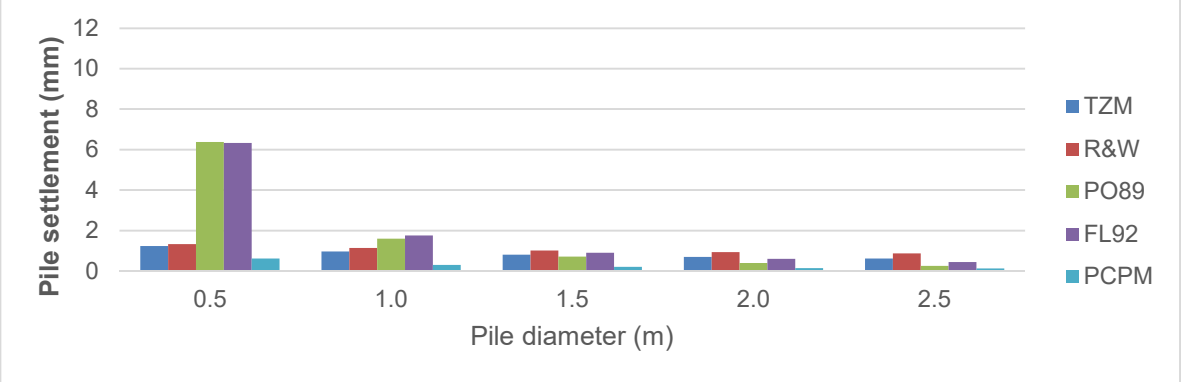


Figure 4.23(e): Comparison of settlement computed by different methods for a single pile founded in uniform non-cohesive soil for L=50m

The settlement for D_0=0.5m is markedly high for most methods because high slenderness which significantly increases elastic shortening.

4.3.4 Comparison for piles founded in layered soil

Refer to section 3.4.3 for details and only two layers were considered with thickness of each layer=0.5L. The comparative charts in Figures 4.24 (a) to (e) were derived from settlement values contained in Tables B8 and B9.

From Figures 4.24 (a) to (e), the following inferences are made:

a) For the same method of settlement calculation, the layered soil type 1 settlement value (when top layer is clay and bottom layer is sand), is very similar to that for layered soil type 2 (when layers are reversed).
b) In these calculations, the Young's modulus for the sand is 50MPa while that for clay is 30MPa. Therefore layered soil type 2 is the case for which there is an underlying softer compressible layer. This does not appear to significantly affect the pile settlement.

c) Settlement calculated by Poulos (1989) method is significantly higher than that by other methods for all values of pile diameter. Settlement clearly decreases with increasing diameter.

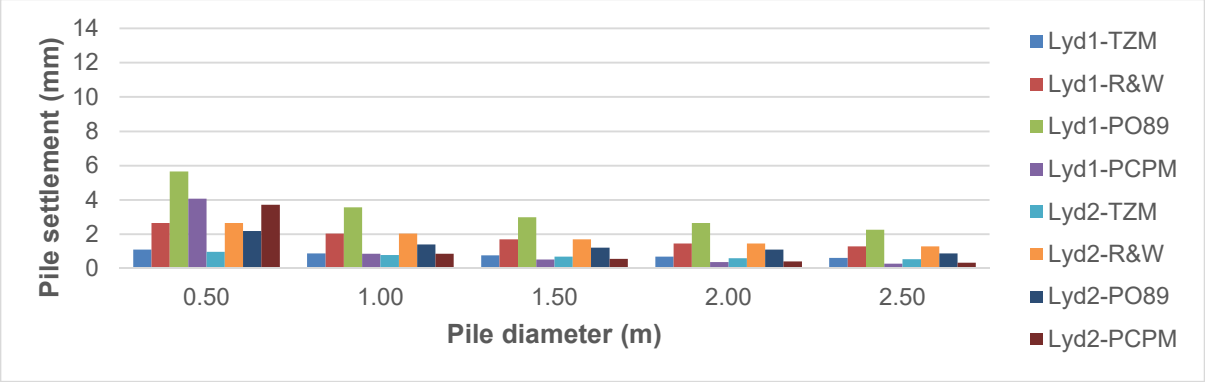


Figure 4.24(a): Comparison of settlement computed by different methods for a single pile founded in layered soil for L=10m

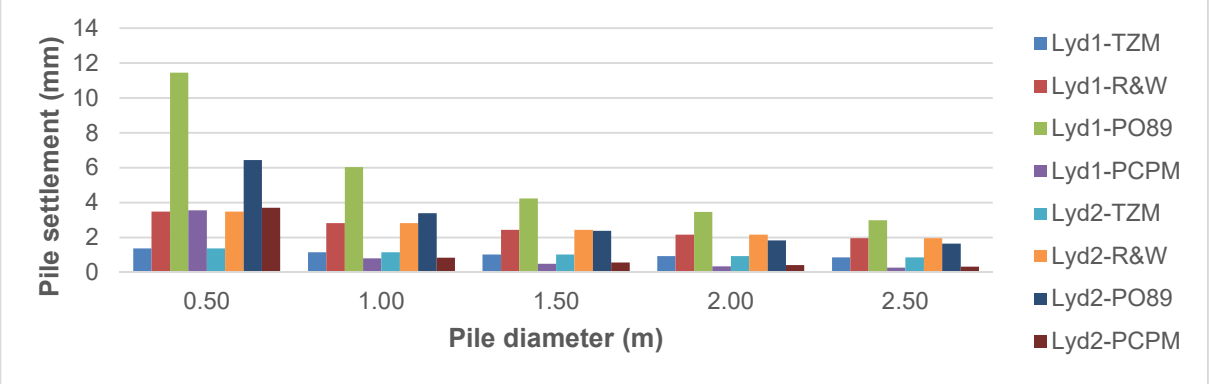


Figure 4.24(b): Comparison of settlement computed by different methods for a single pile founded in layered soil for L=20m

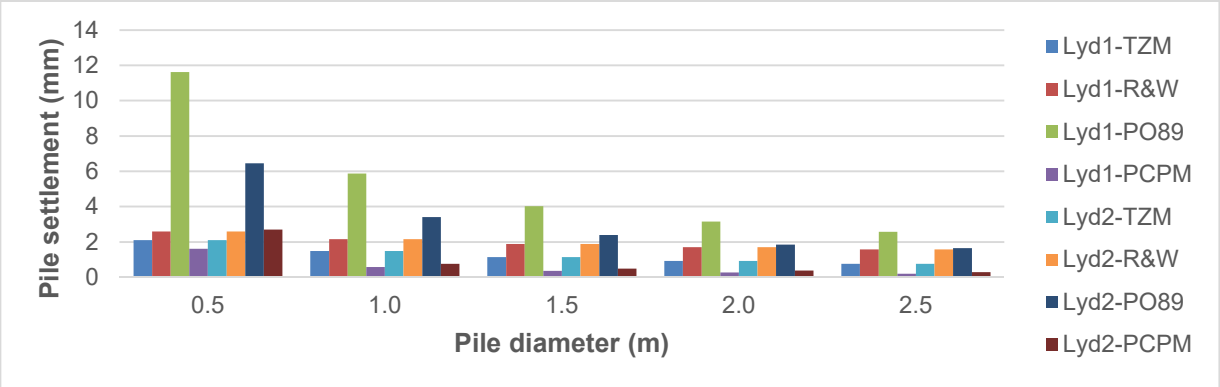


Figure 4.24(c): Comparison of settlement computed by different methods for a single pile founded in layered soil for L=30m

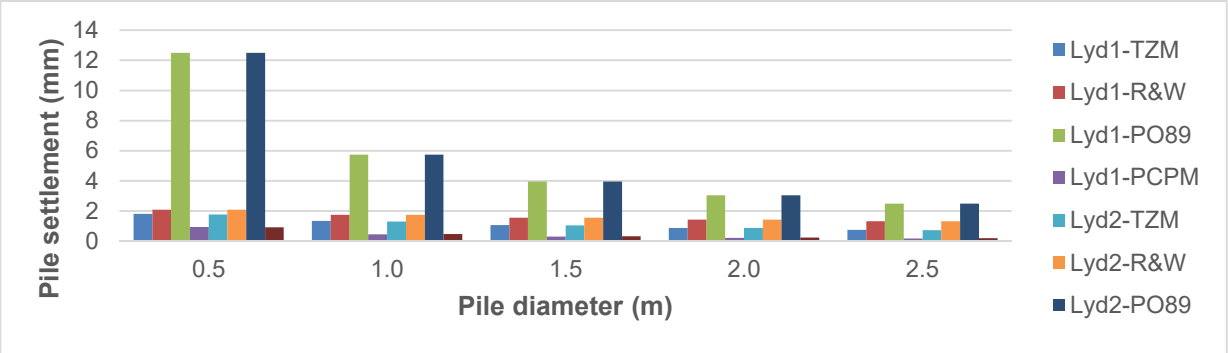


Figure 4.24(d): Comparison of settlement computed by different methods for a single pile founded in layered soil for L=40m

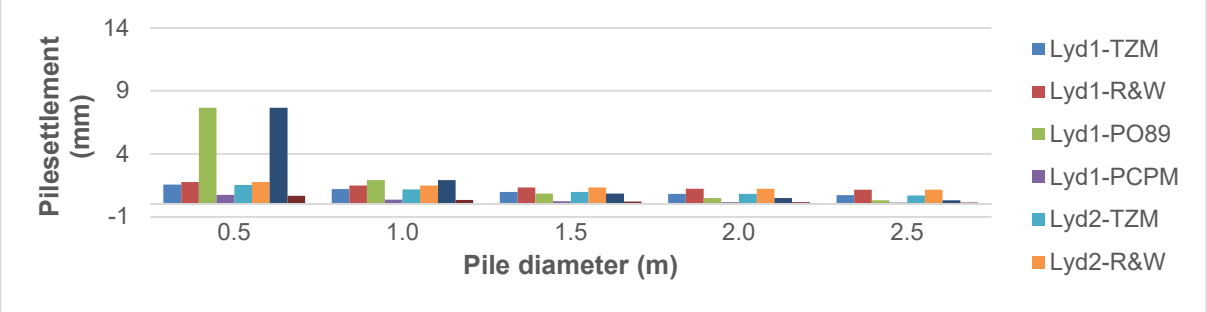


Figure 4.24(e): Comparison of settlement computed by different methods for a single pile founded in layered soil for L=50m

4.4 Pile Group Settlement Calculations

The pile group settlement using some selected empirical and theoretical methods will be analysed and compared. The pile spacing, $S=3D_0$ and $S=4D_0$ are adopted throughout and square pile groups will mainly be considered, restricted to 2x2, 3x3 and 4x4 square pile groups. The 2x1 pile group will also be reviewed because it is the simplest case of a pile group. The pile group settlement analysis will be for circular bored concrete piles of D_0=300, 400, 500, 600, 700mm. The maximum applied load for a single pile is 1.5MN and all the other parameters are as given in section 3.4.1(b) of this report. Care will be taken to ensure loading applied is below the single pile load carrying capacity and that the shaft stress is within limit. 'Pile' programme is used to calculate both pile capacity and shaft stress

4.4.1 Pile groups founded in cohesionless soil

The pile groups are founded in medium dense sand. The settlement for a pile group is predicted using the following selected but very empirical methods:

4.4.1.1 Skempton (1953) method

Skempton's empirical method for the estimation of pile group settlement S_G, for driven piles in non-cohesive soils, with same load per pile, is given by: $S_G/S_1=[(4B+2.7)/(B+3.6)]^2$ where B is the width of the pile group in metres. If the spacing between the piles in the group, $S=3D_0$, then the following are values of B in relation to the pile diameter:

- For a 2x2 pile group: $B=3D_0+D_0=4D_0$

  $\Rightarrow S_G/S_1=[4(4D_0)+2.7]/(4D_0+3.6)]2=[(16D_0+2.7)/(4D_0+3.6)]^2$

- For a 3x3 pile group: $B=6D_0+D_0=7D_0$

  $\Rightarrow S_G/S_1=[4(7D_0)+2.7]/(7D_0+3.6)]^2=[(28D_0+2.7)/(7D_0+3.6)]^2$

- For a 4x4 pile group: $B=9D_0+D_0=10D_0$

  $\Rightarrow S_G/S_1=[4(10D_0)+2.7]/(10D_0+3.6)]^2=[(40D_0+2.7)/(10D_0+3.6)]^2$

Where S_1 is single pile settlement. Table 4.3 is a summary of the ratio: pile group settlement to single pile settlement using Skemptom (1953) method.

Table 4.3: 2^2, 3^2 and 4^2 – Pile group settlement after Skempton (1953)

Pile Dia (m)	L/D_0 ratio	$16D_0$ +2.7	$4D_0$+ 3.6	$28D_0$+ 2.7	$7D_0$+ 3.6	$40D_0$+ 2.7	$10D_0$+ 3.6	Ratio: Pile Group Settlement/ Single pile settlement, S_1		
								2^2-pile group	3^2-pile group	4^2-pile Group
L=10m										
0.3	33	7.50	4.80	11.10	5.70	14.70	6.60	2.44	3.79	4.96
0.4	25	9.10	5.20	13.90	6.40	18.70	7.60	3.06	4.72	6.05
0.5	20	10.70	5.60	16.70	7.10	22.70	8.60	3.65	5.53	6.97
0.6	17	12.30	6.00	19.50	7.80	26.70	9.60	4.20	6.25	7.74
0.7	14	13.90	6.40	22.30	8.50	30.70	10.60	4.72	6.88	8.39
L=20m										
0.3	67	7.50	4.80	11.10	5.70	14.70	6.60	2.44	3.79	4.96
0.4	50	9.10	5.20	13.90	6.40	18.70	7.60	3.06	4.72	6.05
0.5	40	10.70	5.60	16.70	7.10	22.70	8.60	3.65	5.53	6.97
0.6	33	12.30	6.00	19.50	7.80	26.70	9.60	4.20	6.25	7.74
0.7	29	13.90	6.40	22.30	8.50	30.70	10.60	4.72	6.88	8.39

The following deductions can be made from Table 4.3:

a) The pile group settlement increases with increasing number of piles in the group but the increase is almost double for from a 4-pile group to a 16-pile group.
b) The pile group settlement is independent of pile length hence the settlement remains constant when the pile length increases.
c) Pile group settlement also increase with increasing pile diameter as the pile group width is related to the pile diameter through the pile spacing, S, which is usually expressed in terms of pile diameters. Pile settlement must decrease with increasing pile diameter as demonstrated by the analyses of several cases for a single pile.
d) Skempton's method implies that pile group settlement is dictated by pile group width, hence single pile diameter and that the pile group settlement is independent of the pile length and applied load.

4.4.1.2 Meyerhof (1959) method

For driven piles in sand, Meyerhof's empirical relationship for a square pile group is given by: $\rho_G/\rho_1=[S(5-S/3)]/[1+1/r]^2$, where S the ratio of pile spacing to pile diameter and r is the number of rows in the square group.

ρ_G and ρ_1 are the pile group and single pile settlement respectively.
In this example, the pile spacing=$3D_0$ where D_0 is the pile diameter. Therefore according to Meyerhof, $S=3D_0/D_0=3$
For a 2x2 pile group, $r=2$

$\Rightarrow \quad \rho_G/\rho_1=[3(5-3/3)]/[1+1/2]^2=5.33$

For a 3x3 pile group, $r=3$

$\Rightarrow \quad \rho_G/\rho_1=[3(5-3/3)]/[1+1/3]^2=6.75$

For a 4x4 pile group, $r=4$

$\Rightarrow \quad \rho_G/\rho_1=[3(5-3/3)]/[1+1/4]^2=7.68$

From the above calculations, the following can be inferred from the trend:

a) Pile group settlement increases as the number of rows, hence number of piles in the square group, increases. This contradicts what happens in reality.
b) The group settlement decreases with increasing pile spacing to diameter ratio, S. For S=6, $\rho_G/\rho_1=[3(5-6/3)]/[1+1/2]^2=4.00<5.33$ for a 2x2 pile group.
c) The method does not take the pile length into account thus implying that pile group settlement is independent of the length of the pile in sands.
d) The applied load does not appear in Meyerhof's equation, suggesting that settlement is not influenced by the applied load.

Meyerhof's method also has limitations of being applicable to non-cohesive soils only.

4.4.1.3 Vesic (1977) method

Vesic's empirical method to determine the settlement of a pile group in sandy soil is given by: $S_G/S_1=[B/D_0]^{1/2}$, where: S_G is the settlement of the pile group, S_1 is the settlement of a single pile at same average loading, B is the width of the pile group and D_0 is the diameter of the single pile.

For a 2x2 pile group: $B=3D_0+D_0=4D_0$

$\Rightarrow \quad S_G/S_1=[4D_0/D_0]^{1/2}=\sqrt{(4)}=2.00$

For a 3x3 pile group: $B=6D_0+D_0=7D_0$

$\Rightarrow \quad S_G/S_1=[7D_0/D_0]^{1/2}=\sqrt{(7)}=2.65$

For a 4x4 pile group: $B=9D_0+D_0=10D_0$

$\Rightarrow \quad S_G/S_1=[10D_0/D_0]^{1/2}=\sqrt{(10)}=3.16$

The following deductions can be made from the results of the above calculations:

- Pile group settlement increases with increasing pile group plan size, i.e.: with increasing number of piles in the square group while maintaining the spacing at the same value. But settlement of pile groups is known to decrease with increasing the number of piles in the group.
- Vesic's method also implies that the pile group settlement in sand is not influenced by pile length and pile diameter.
- Vesic's empirical method also implies that pile group settlement is independent of the applied load.

Not much literature exist on pile group settlement in sandy soils.

4.4.2 Pile groups founded in cohesive soil

The pile groups are founded in soft clay. The settlement for a pile group is calculated using the following selected theoretical methods:

4.4.2.1 Poulos (1968b) method

$S_G=R_S.S_1$ where R_S is the settlement ratio and S_1 is the settlement of a single pile carrying the same average load as a pile in the group. S_1 is determined in accordance with Poulos and Davis (1968). The following parameters are used in this example:

- Values of R_S determined by extrapolation from Table B1 which are for a friction pile group with a rigid pile cap in a deep, uniform soil mass.
- Average single pile maximum applied load, P=165, 452, 824, 1264 and 1500kN Pile group applied load, $P_G=nP$ where n is the number of piles in the group.
- $S/D=S/D_0=3$. Extrapolation had to be done because values of S/D in Table B1 are for S/D=2.5 and 10.
- $0.3\leq D0\leq 0.7$m and pile length L=10, 20, 30, 40 and 50m. Values of R_S are tabulated for $L/D_0=10$, 25, 50 and 100. Intermediate values were determined by extrapolation as well.

Table B13 is a summary of the data used to calculate the pile group settlement for the 4, 9 and 16-pile groups.

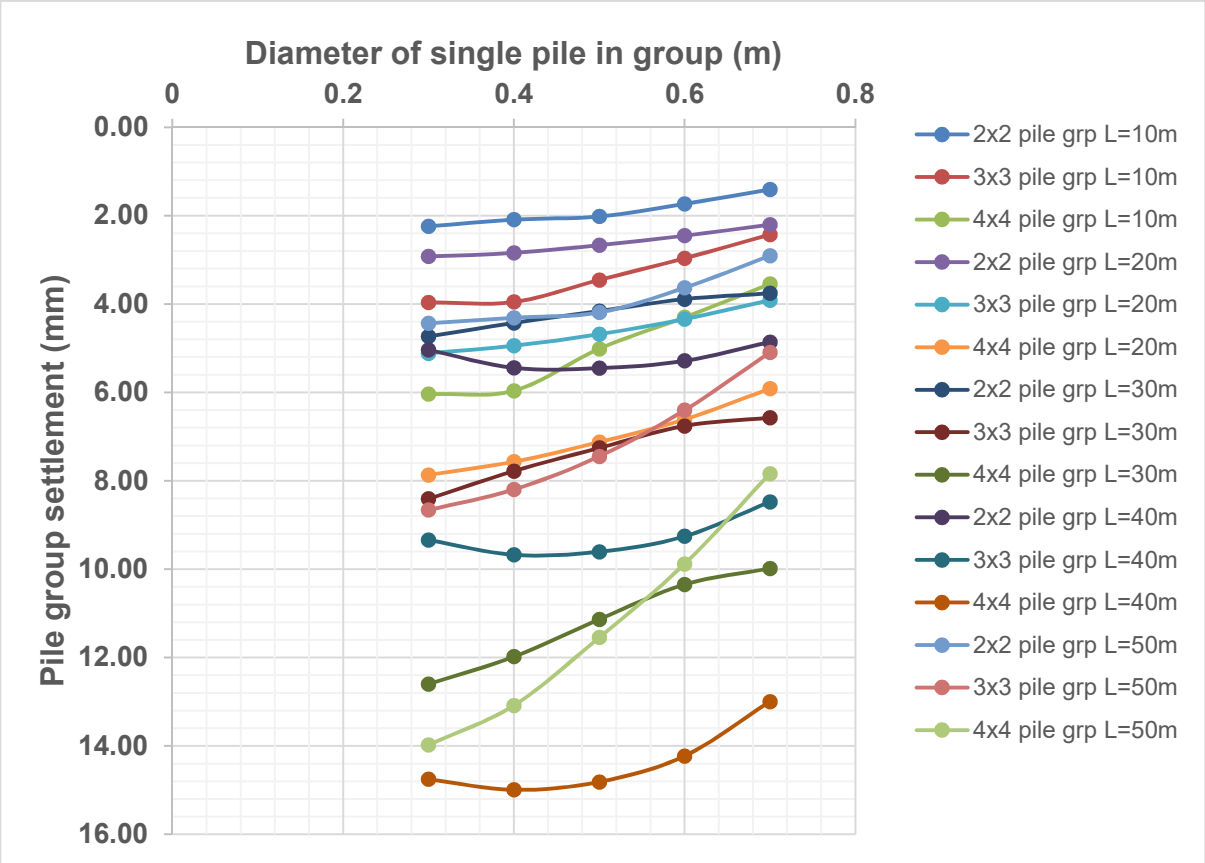


Figure 4.25: Pile group settlement variation with pile diameter, length and pile group size for $S/D_0=3$ and v=0.5 after Poulos (1968b)

From both Table B13 and Figure 4.25 which are graphs constructed from the tabulated data, the following inferences are made:

1) The pile group settlement decreases with increasing pile diameter, a similar pattern to that for single piles as observed from the previous sections of this report.
2) If the pile group applied load is taken as P_G=nP, then pile group settlement would increase with increasing number of piles in the group as was the case in Table B13. Separate calculations were done when the pile group applied load, P_G, was taken as P_G=P. The results indicated that when the same magnitude of load is applied to the various sized groups, the pile group settlement decreased with increasing size of the group.
3) It is apparent that the settlement of a pile group generally increases with increasing pile length until a maximum level is reached and thereafter settlement will decrease with increasing pile group load and length. As an example, in Figure 4.25 and for a 4x4 pile group, pile group settlement increases with increasing pile length from L=10 to L=40m, but decreases for L=50m although the applied load is increased from 1264kN to 1500kN.

4.4.2.2 Poulos and Mates (1971b) method

$S_G=m.R_G.S_I$ where m is the number of piles in the group, m=4, 9 and 16 for 2x2, 3x3 and 4x4 pile groups respectively. S_I is the settlement of a single pile carrying the same average load as a pile in the group and determined in accordance with Mattes and Poulos (1969). The following parameters are used in this example: Values of R_G determined by extrapolation from Table B6 which has values for a floating pile group with a rigid pile cap in a deep, uniform soil mass; Applied load per group is mP where m is the number of piles in the group and P is single pile applied load and recorded in Table B14; $S/D=S/D_0$=3; $0.3\leq D_0\leq 0.7$m and pile length L=10, 20, 30, 40 and 50m.

Table B14 is a summary of the data used to calculate the pile group settlement for the 4, 9 and 16-pile groups.

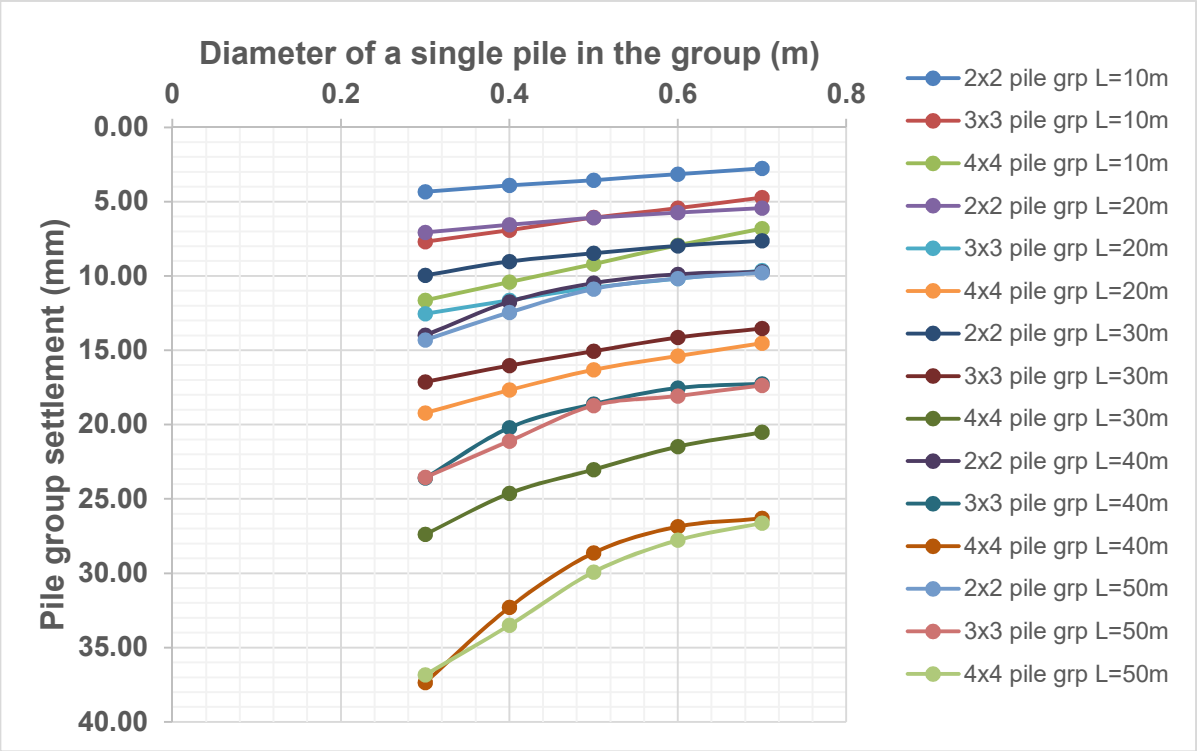


Figure 4.26: Pile group settlement variation with pile diameter, length and pile group size for S/D_0=3 and v=0.5 after Poulos and Mattes (1971b)

From both the Table B14 and Figure 4.26 which are graphs constructed from the tabulated data, the following deductions are made which are similar to the observations noted under Poulos (1968) above:

1) The pile group settlement decreases with increasing pile diameter, a similar pattern to that for single piles as observed from the previous sections of this report.
2) If the pile group applied load is taken as P_G=nP, then pile group settlement would increase with increasing number of piles in the group as was the case in Table B14. Separate calculations were done when the pile group applied load, P_G, was taken as P_G=P. The results indicated that when the same magnitude of load is applied to the various sized groups, the pile group settlement decreased with increasing size of the group.
3) Poulos & Mattes (1971b) method of group settlement prediction produced fairly high settlement values relative to those by Poulos (1968b), especially for shorter piles. This could be attributed to the applied load being close to the short pile capacity.

4.4.2.3 Poulos (1989) method

Poulos developed charts to enable pile group settlement for both driven and bored piles to be predicted in different soil types, as previously detailed in section 2.8.11 of this report. The pile group settlement, S_G is given by: $S_G=R_S S_1$, where S_1 is the settlement of a single pile under the same average load, R_S is the settlement ratio given by $R_S=n^{\omega}$ where ω is the exponent of the settlement ratio. Refer to section 3.4.1 for parameters and founding soil condition, with the pile spacing, for $S=3D_0$. The settlement of the single pile has been determined in section 4.2.1.9 of this paper and $300 \leq D_0 \leq 700$mm. Values of ω are determined from Figure 2.50(a), noting that

0.4≤ω≤0.6 for most pile groups. Table B15 is a summary of the computations leading to the determination of the pile group settlement.

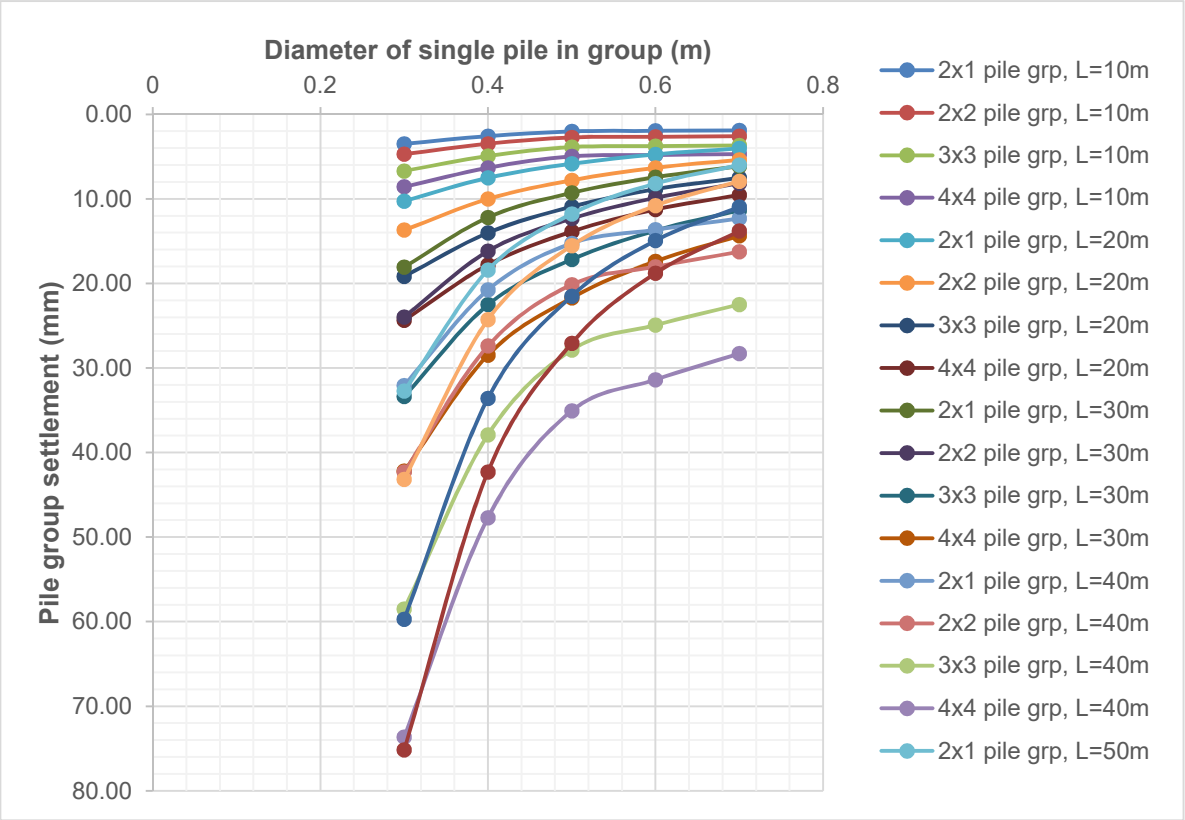


Figure 4.27: Pile group settlement variation with pile diameter, length and pile group size for E_p=30GPa and E_s=30MPa after Poulos (1989)

From the analysis of Table B15 and Figure 4.27 above, the following inferences are made:

- The pile group settlement decreases with increasing pile diameter, a similar pattern to that for single piles as observed from the previous sections of this report.
- If the pile group applied load is taken as P_G=nP, then pile group settlement would increase with increasing number of piles in the group as is the case in Table B15 below. Separate calculations were done when the pile group applied load, P_G, was taken as P_G=P. The results indicated that when the same magnitude of load is applied to the various sized groups, the pile group settlement decreased with increasing size of the group.
- Poulos and Mattes (1989) method of group settlement prediction produced even higher settlement values compared to those by Poulos & Mattes (1971b), especially that for shorter piles. This could be attributed to the applied load being close to the short pile capacity.
- From Table B15, settlement calculations for a 2x1 pile group exhibit the following:
  (i) For the same pile length, settlement decreases with increasing pile diameter.
  (ii) For any fixed pile diameter, settlement significantly increases with pile length, increasing from 3.50mm for L=10m to 32.72mm for L=50m all for

D_0=0.3m and from 1.93mm to 6.01mm for L=10 and 50m respectively both for D_0=0.7m.

(iii) As would be expected, for each pile length, the highest settlement is for D0=0.3m which is attributable to high slenderness, hence significant elastic shortening.

4.4.2.4 Equivalent raft method (ERM)

Refer to section 2.8.10, section 3.4.1(b) and Figure 2.46 where terms are defined. The following steps are steps are taken to calculate pile group settlement:

1) Determination of the immediate settlement using Equation 2.92 where $q=nP_{safe}/A_G$, A_G being the plan area of the pile group. The pile spacing, $S=3D_0$ and square groups are under consideration for which the side lengths are: $4D_0$ for 2x2 pile group, $7D_0$ for 3x3 pile group and $10D_0$ for 4x4 pile group.
2) Calculations for immediate pile group settlement are automated to a spreadsheet and are tabulated in section 4.4.2.4 worked example.
3) Determination of the initial effective stress, σ_0' at the midpoint of the compressive layer. The depth of the bedrock h, below ground surface is normally determined from site investigations for finite layers. The pile group is converted to an equivalent raft as described in section 2.8.10 and the thickness of the compressive layer, $T_{CL}=h-2L/3$ where L is the pile length and T_{CL} is compressible layer thickness. Therefore the depth to the midpoint for calculation of σ_0' is calculated from: $h-0.5(2L/3)$.
4) Determination of the new effective stress σ_1', which is the stress after the pile group has been loaded. $\sigma_1'=\sigma_0'$+stress increase due to pile group load at the midpoint of the compressive layer. The area at the midpoint is determined by assuming a 2 vertical to 1 horizontal stress distribution to determine the width and length of the equivalent footing at the midpoint.

Consolidation settlement S_C, is then calculated using Janbu's equation: $S_C=T_{CL}.(1/m).\ln(\sigma_1'/\sigma_0')$ where m is the dimensionless modulus number which is determined from Table 2.3. The value of m=15 has been used from the given range of $5\leq m\leq 20$ in the table. A summary of the consolidation settlement is included in Table B16. However, consolidation settlement is not considered further in this report. The calculations are also automated to a spreadsheet and Table B16 is summary of the results obtained. From both Table B16 and Figure 4.28 the following inferences are made:

- Consolidation settlement is fairly high compared to the immediate settlement. This is likely so because when the load approaches ultimate significant time-dependent settlements occur, which may be due to shear creep and/or pore pressure dissipation
- Immediate settlement decreases with increasing pile diameter but appear to mainly increase with increasing pile length before decreasing the trend is reversed around L=40m.

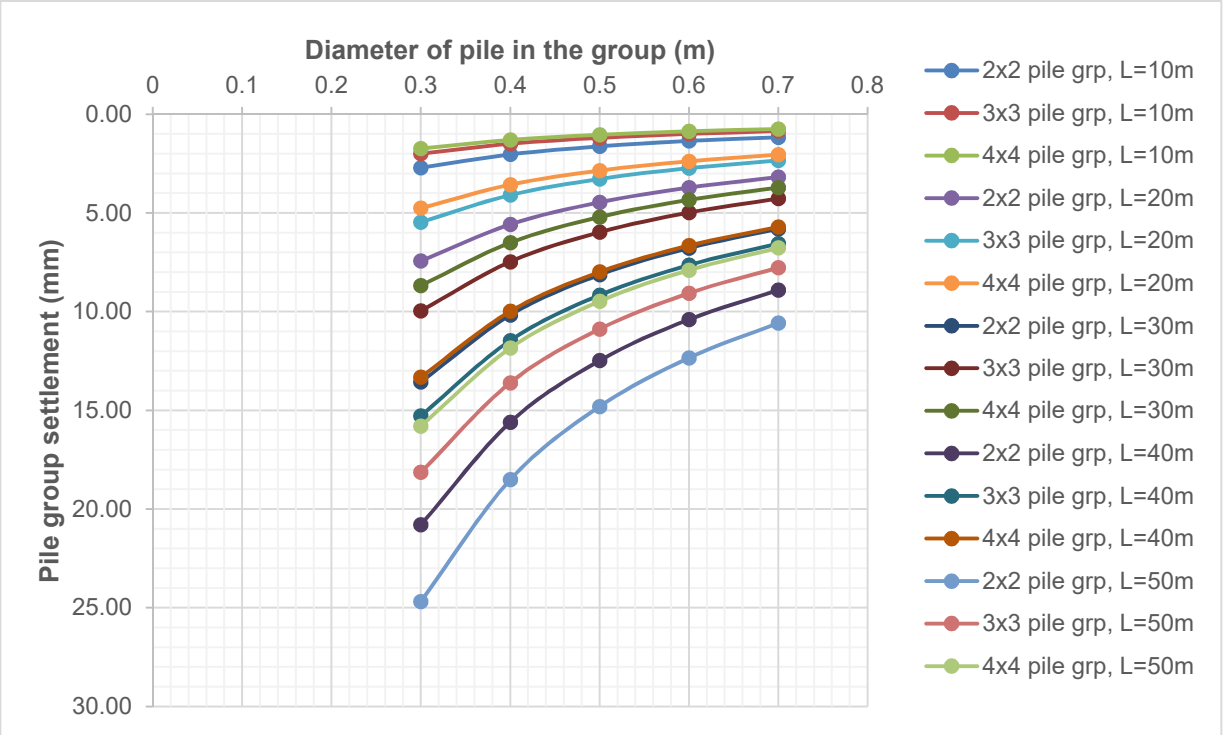


Figure 4.28: Pile group settlement variation with pile diameter, length and pile group size using the equivalent raft method after Tomlinson (1986)

- The magnitude of the applied pile group working load has a very sensitive effect on the pile group settlement, which increases with increasing group loading.

4.5 Comparison of pile group settlement

The settlement of pile groups in cohesionless soil is compared separate from that of pile groups in cohesive soil as detailed in the following sections.

4.5.1 Pile group settlement in non-cohesive soil

The ratio of the group settlement to single pile settlement S_G/S_1 was used to compare pile group settlement in sand and summarized in Table 4.4.

Table 4.4: 2^2, 3^2 and 4^2 – Pile group settlement in sand

Pile Dia (m)	S_G/S_1 after Skempton (1953)			S_G/S_1 after Meyerhof (1959)			S_G/S_1 after Vesic (1977)		
	2x2 pile grp	3x3 pile grp	4x4 pile grp	2x2 pile grp	3x3 pile grp	3x3 pile grp	2x2 pile grp	3x3 pile grp	4x4 pile grp
L=10m									
0.3	2.44	3.79	4.96	5.33	6.75	7.68	2.00	2.65	3.16
0.4	3.06	4.72	6.05	5.33	6.75	7.68	2.00	2.65	3.16
0.5	3.65	5.53	6.97	5.33	6.75	7.68	2.00	2.65	3.16
0.6	4.20	6.25	7.74	5.33	6.75	7.68	2.00	2.65	3.16
0.7	4.72	6.88	8.39	5.33	6.75	7.68	2.00	2.65	3.16

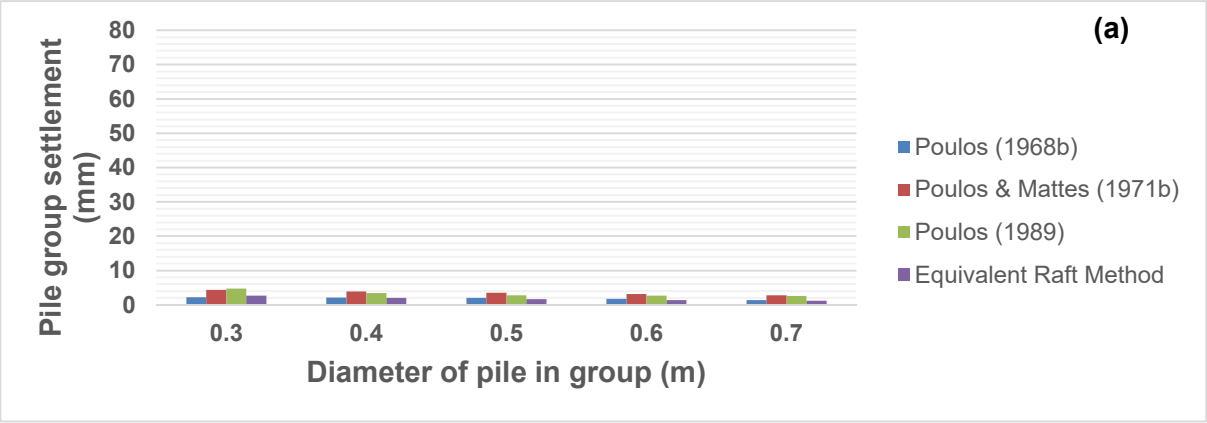
L=20m									
0.3	2.44	3.79	4.96	5.33	6.75	7.68	2.00	2.65	3.16
0.4	3.06	4.72	6.05	5.33	6.75	7.68	2.00	2.65	3.16
0.5	3.65	5.53	6.97	5.33	6.75	7.68	2.00	2.65	3.16
0.6	4.20	6.25	7.74	5.33	6.75	7.68	2.00	2.65	3.16
0.7	4.72	6.88	8.39	5.33	6.75	7.68	2.00	2.65	3.16

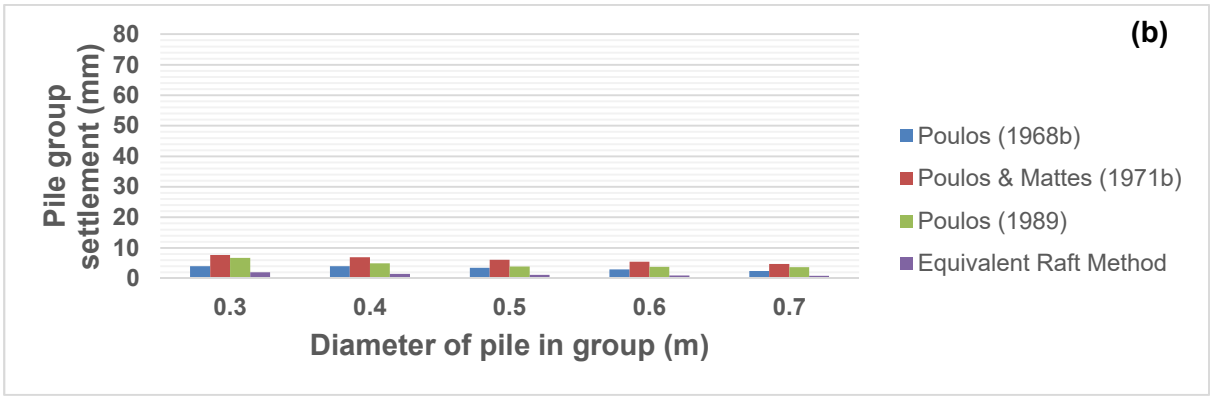
The following observations are made from the comparison Table 4.4 for pile groups in sand:

1) According to Skempton, pile group settlement varies with pile diameter and size of the group but is completely independent of pile length.
2) Meyerhof and Vesic agree that pile group settlement is dependent on the size of the pile group, being totally unrelated to the pile diameter and the pile length.
3) The ratio of pile group settlement to the single pile settlement S_G/S_1, for 300mm diameter piles for the Skempton method is in close agreement with that of Vesic although Vesi's is applicable to all diameters and lengths.
4) The S_G/S_1 ratio from Meyerhof's method is in closest agreement with that from the Skempton method for 600 and 700mm diameter piles but the Meyerhof one is the same for all pile diameters and pile length, being influenced by the group size only.
5) S_G/S_1 from Skempton's method are generally comparable with the Meyerhof ones. The Vesic figures are on the less conservative side in this particular case.

4.5.2 Pile group settlement in cohesive soil

Pile group settlement in clay soil was analysed using Poulos (1968b), Poulos and Mates (1971b), Poulos (1989) and the equivalent raft method. Table B18 gives a tabular comparison while Figures 4.29 to 4.33 bar charts comparison of the settlement of the different pile groups under review for L=10, 20, 30, 40 and 50m respectively.





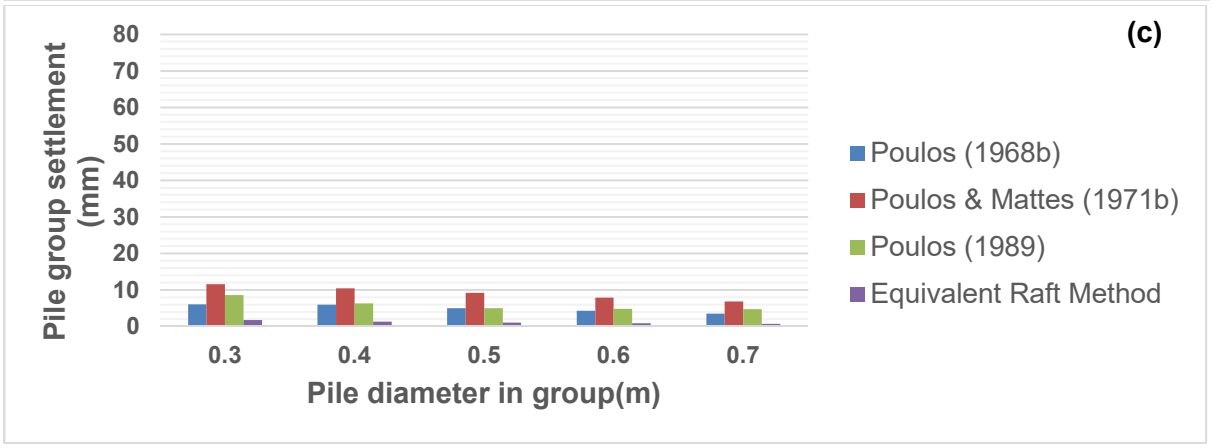
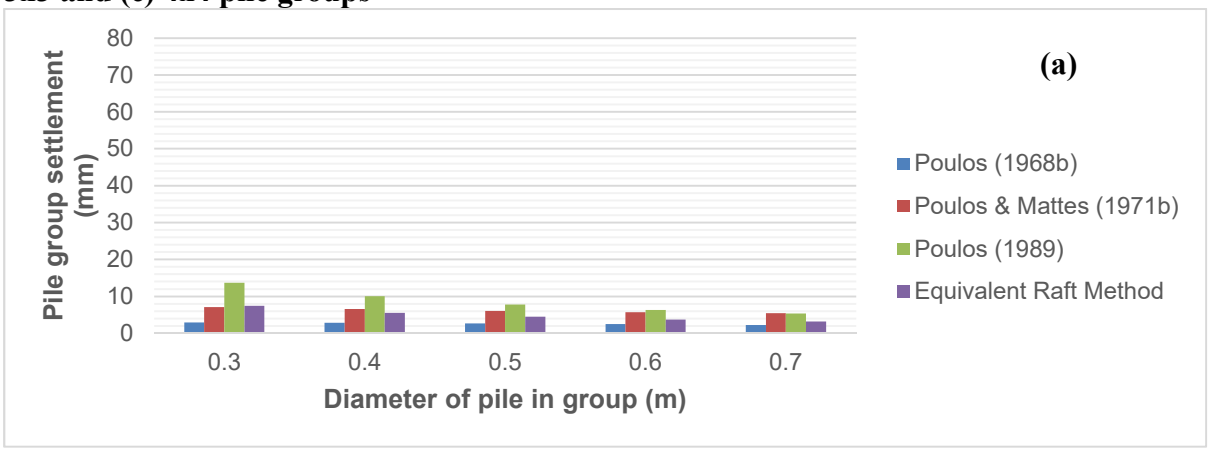
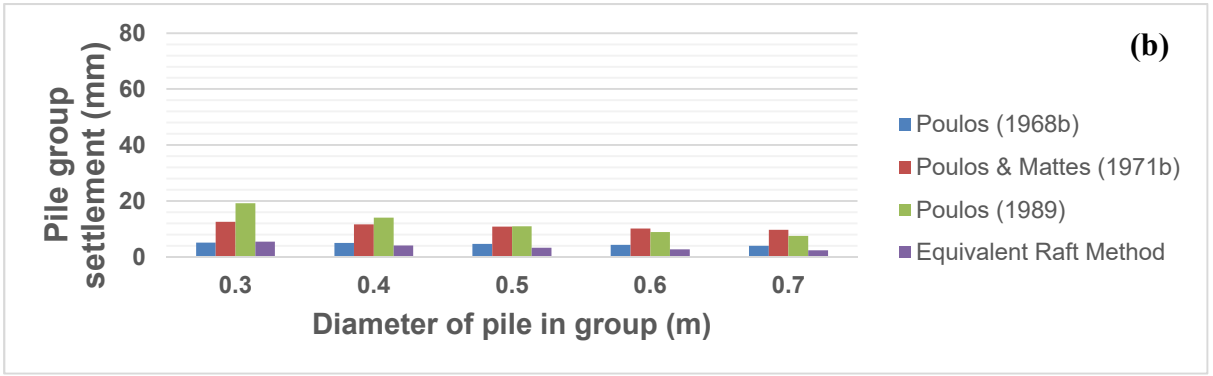


Figure 4.29: Variation pile group settlement with pile diameter for L=10m for (a) 2x2, (b) 3x3 and (c) 4x4 pile groups





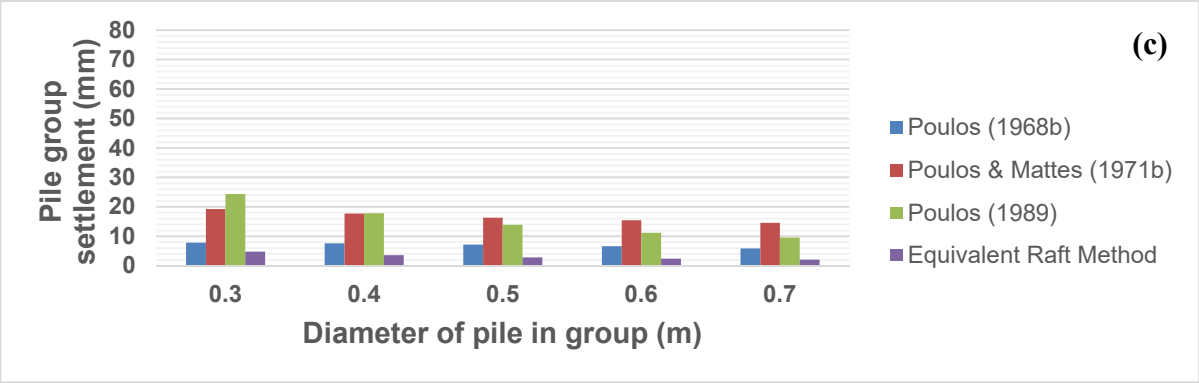


Figure 4.30: Variation pile group settlement with pile diameter for L=20m for (a) 2x2, (b) 3x3 and (c) 4x4 pile groups

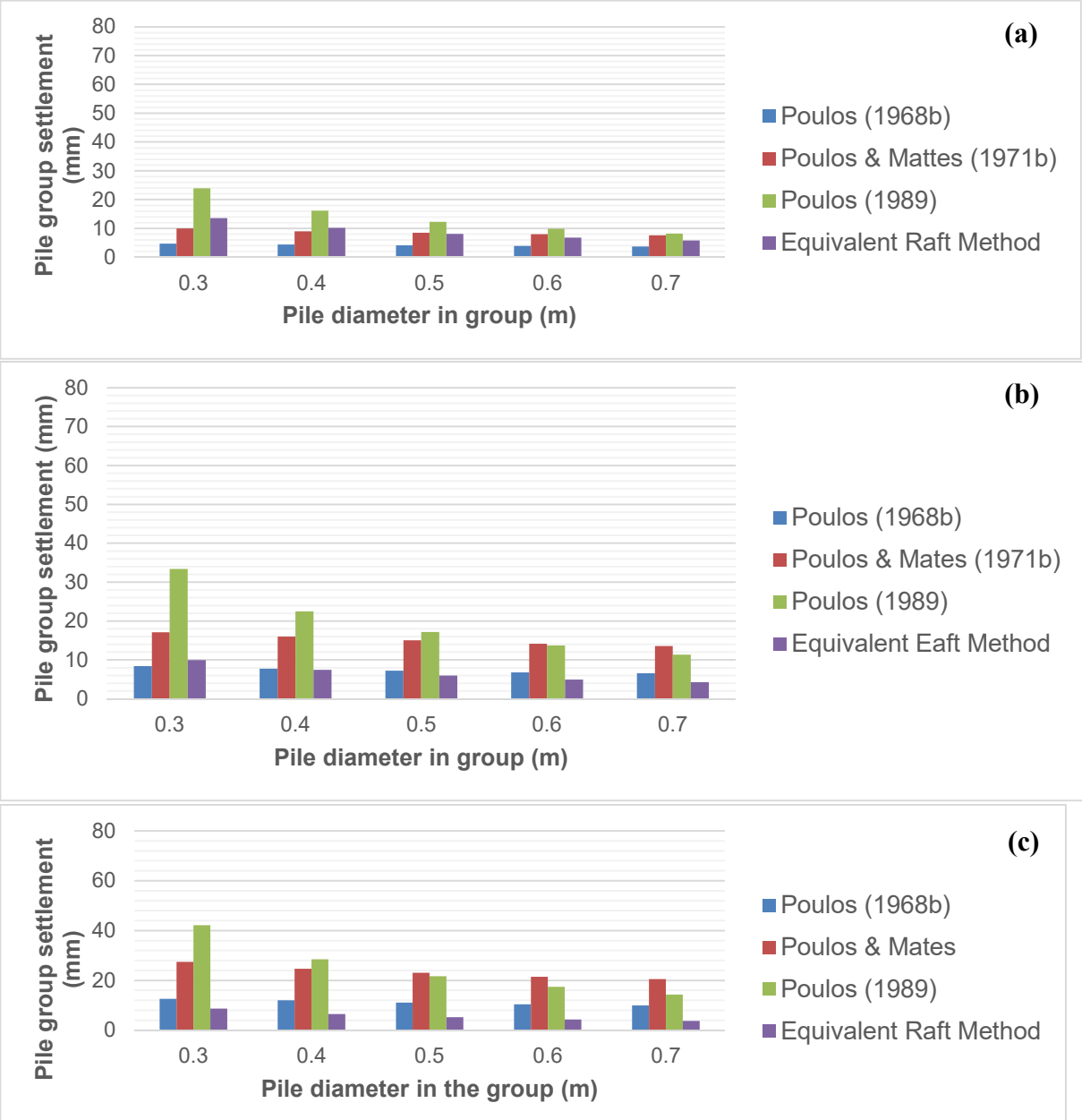


Figure 4.31: Variation pile group settlement with pile diameter for L=30m for (a) 2x2, (b) 3x3 and (c) 4x4 pile groups

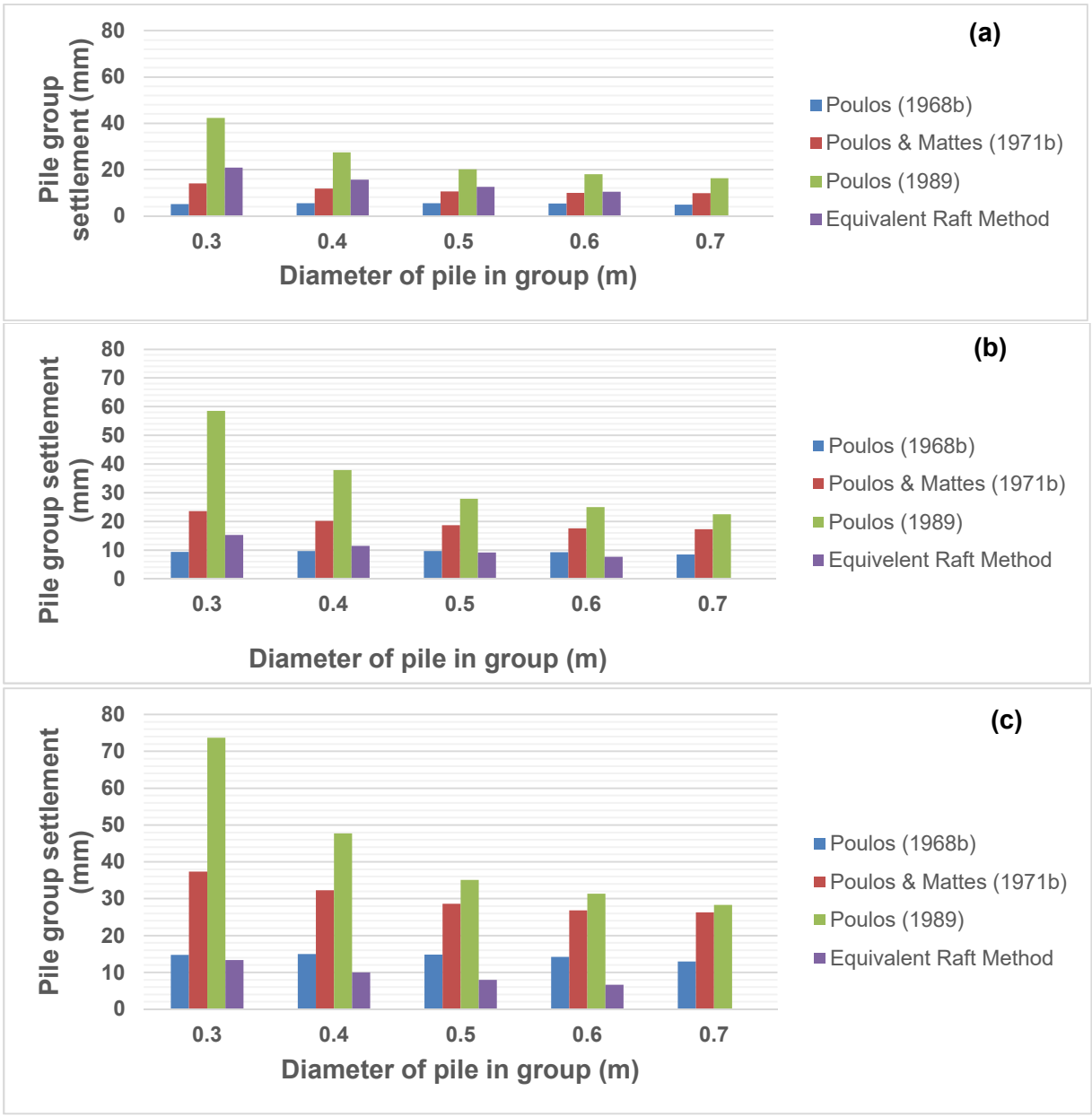
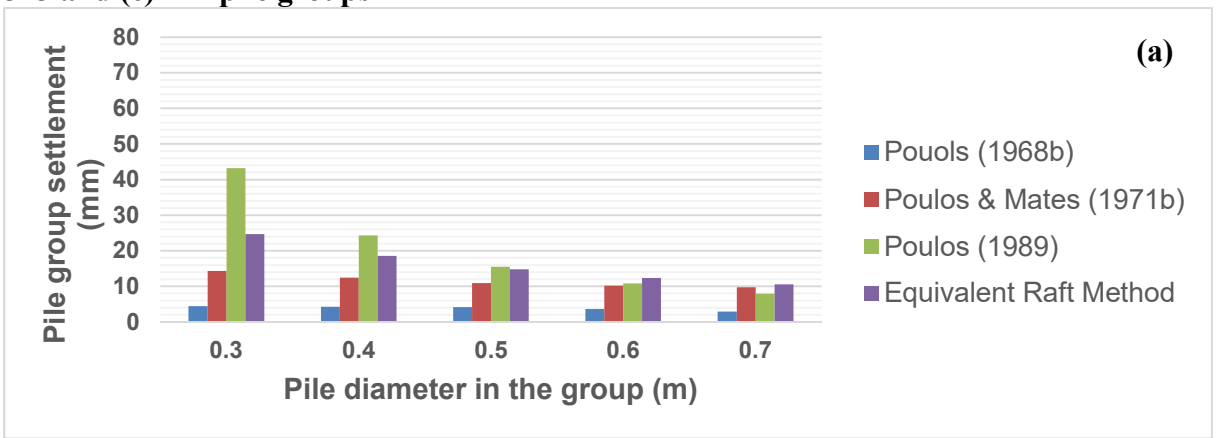


Figure 4.32: Variation pile group settlement with pile diameter for L=40m for (a) 2x2, (b) 3x3 and (c) 4x4 pile groups



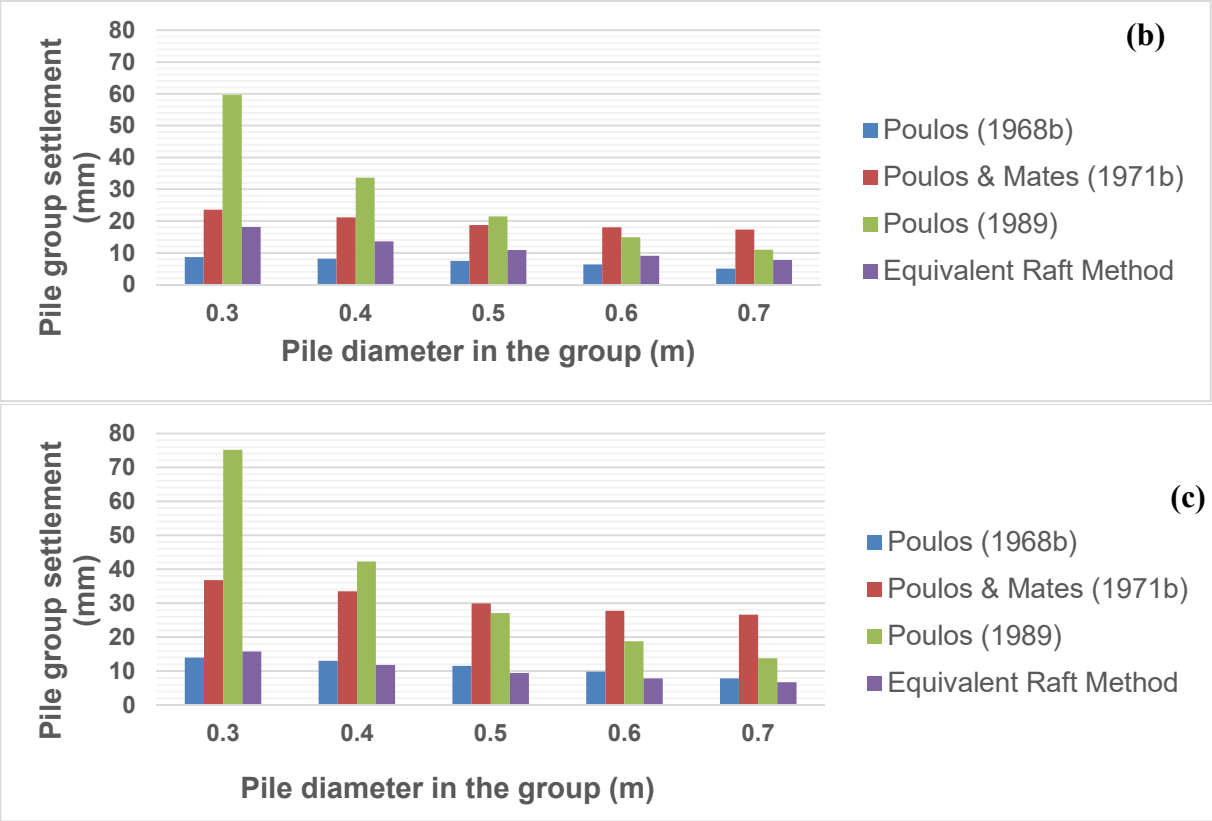


Figure 4.33: Variation pile group settlement with pile diameter for L=50m for (a) 2x2, (b) 3x3 and (c) 4x4 pile groups

The following deductions are made from both Table B17 and Figures 4.29 to 4.33:

a) For *L*=10 and 20m, pile group settlement values are in good agreement for each pile length and respective pile diameter class. For L=30m, group settlement by Poulos (1989) is higher than for other methods while for L=40 and 50m, group settlement predicted by Poulos and Mattes (1971b) and Poulos (1989) is very high relative to the other methods. The applied load is constant across all diameters but different for each pile length, hence the observation of settlement increasing with pile group size. Pile group loading, P_G=nP

b) For each method of group settlement evaluation, settlement clearly decreases with increasing diameter of piles in the group.

c) For each method of settlement prediction, the settlement was also observed to decrease with increasing number of piles in the group. This was observed only when only a constant load was applied to each pile group. This variation was not pursued much because practically, there is no situation where you use a 4x4 pile group for example, to support a load that can be adequately carried by a 2x2 pile.

d) Poulos and Mattes (1971b) method produced the highest and hence most conservative group settlement prediction while the equivalent raft method produced the lowest settlement values which may be the least conservative or an under-prediction.

e) For each pile group, settlement decreases with increasing pile length if the applied load is constant for all the different pile length sand groups which, again from a

practical point of view, is not feasible. Different pile group sizes and pile lengths are selected in design because of the varying nature of the loads to be resisted, among other considerations.

4.6 Computer method for pile group analysis

The ‘Pile’ computer programme that was used for single pile settlement analyses in this paper has limitations which include absence of a suite for pile group design. However, if a single pile behavior can be modelled, the pile group behavior can always be developed from the single pile behavior through the application of appropriate factors available in literature. Computer analysis of pile groups was thus not included in this study.

CHAPTER FIVE

5 DISCUSSION AND CONCLUSIONS

The discussions below highlight some limitations of some of the settlement prediction methods.

5.1 Discussion

The following comments with regard to the preceding analyses are noteworthy:

a) The empirical correlations by Meyerhof (1959) and Focht (1967) for single pile settlement prediction in sand and clay respectively, and those by Skempton (1953) and Meyerhof (1959) both in sand are too simplistic. Pile settlement is a complex phenomenon which cannot rely on pile diameter alone or pile group spacing only.
b) The assumption of an ideal elastic half space is also an oversimplification of reality because in practice, soil is layered and varies in composition and texture both horizontally and vertically.
c) Most of the theoretical method assume a stress-free pile after installation but piles must have significant residual stress resulting from their installation. The magnitude would depend on the installation technique used. Further, the stress state of the soil before pile installation is not known in most practical situations.
d) When using the elastic theory for the estimation of deep foundations settlements, the stiffness of the soil is a key geometrical parameter. Soil stiffness can be expressed by the soil's Young's modulus E_s, or its shear modulus, G_s E_s and G_s are never constant but vary depending on factors such as soil type, initial soil stress, stress history, foundation type, the applied loading system, the stress level relative to the ultimate load-carrying capacity, etc.

(Budhu, 2011; Knappett and Craig, 2012; Poulos and Davis, 1980)

5.2 Conclusions

Although case histories could not be found for Harare, a study of geological map for greater Harare has been undertaken and the following conclusions, drawn from the settlement analyses of both single piles and pile groups presented in this study are applicable to pile and pile group design in Harare.

- Deep foundations derive their load resistance from a combination of end-bearing at the pile base and shaft friction along the pile length. Piles generally develop higher shaft and end bearing resistance in non-cohesive soil than in cohesive one. Single piles settle more in cohesive soil than in cohesionless soil for the same load, pile diameter and pile length.
- Pile base enlargement has the effect of increasing the load supported by the pile base, reducing the pile settlement relative to a similar pile without an enlarged base. This effect was more pronounced for $L \leq 10$ than for L=20, 30, 40 and 50m.
- Pile settlement also depends on a pile or pile group's load-carrying capacity which in turn relies on pile diameter and pile length, and on the magnitude of the applied load together with the type of soil through which the pile traverses and on which it is founded. For a given load, the settlement of a pile decreases as the soil's stiffness (or Young's modulus) increases and vice versa.

- For the cases investigated, the capacity of a pile depends on the pile diameter and length and the type of soil surrounding the pile shaft and that at the pile base. It was also found that pile capacity is not dependant on the applied load but on pile diameter (and enlarged pile base), pile length, soil stiffness, etc.
- In both single piles and piles groups, immediate settlement is a major portion of the total settlement but is more dominant in single piles than in pile groups.
- The presence of an underlying compressible soil layer has very little influence on the immediate settlement of a single pile.
- Single settlement predicted by the 'Pile' computer program method was in most instances more conservative than that predicted by other theoretical and/or analytical methods.
- Elastic soil properties and other soil parameters can be estimated from published data if the full soil is available. This was the case when settlement determined by analytical methods was being compared with case histories which resulted in reasonably close settlement values.
- Some empirical methods as Meyerhof (1959) applicable to single piles and pile groups and Skempton (1953) and Vesic (1977) both for pile group settlement are too simplistic to be of significant practical application. Single pile settlement cannot rely on pile diameter alone, nor pile group settlement be dictated by pile spacing and pile group size only.
- The behaviour of a general pile group is derived from a 2-pile group which in turn is derived from a single pile settlement behaviour. Consequently, the effects of pile length, pile diameter and elastic properties of soil on the settlement of the pile group should be similar to those for a single pile.
- Pile group settlement is also dependent on pile length and pile diameter and the type of soil along the piles lengths and below the pile tip. For any given pile spacing, pile group settlement increases with increasing pile length and decreases with increasing pile diameter.
- In computer methods, the adopted geotechnical model for the pile foundation assessment should take into account the non-linear behaviour of soil. Complex computer analyses of deep foundations must always be checked with simple calculations to try and ensure that the complexities involved do not overwhelm the basics of the problem. Therefore ground investigation to enable establishment of a geotechnical model, checking calculations with a simple method of assessment to verify that the pile settlements are of the correct order and consistent, should be axiomatic steps in any proper deep foundation settlement evaluation. Thus the study and evaluation of case histories and comparison between predicted and measured settlements can be very valuable.

"Although numerous investigations, both theoretical and experimental, have been conducted in the past to predict the settlement behaviour and load-bearing capacity of piles, the mechanisms are not yet fully understood and may never be", Dr Braja M Bas.

REFERENCES

API (2011). Recommended Practice 2GEO Geotechnical and Foundation Design Considerations, 1st ed., American Petroleum Institute, Washington

Bolin, H.W., 1941. The pile efficiency formula of the Uniform Building Code. Building Standards Monthly 10, 4–5.

Bowles, J.E., 1982. Foundation analysis and design ″ McGraw-Hill Book Company. New York, 816p.

Budhu, M., 2011. Soil mechanics and foundations, 3rd ed. ed. Wiley, New York.

Butterfield, R., Banerjee, P.K., 1971. The Elastic Analysis of Compressible Piles and Pile Groups. Géotechnique 21, 43–60. https://doi.org/10.1680/geot.1971.21.1.43

Byrne, G., Everett, J.P., Schwartz, K., 1995. A guide to practical geotechnical engineering in southern Africa. Franki.

Chin, F.K., 1972. The inverse slope as a prediction of ultimate bearing capacity of piles, in: Proc. 3rd SE Asia Conf. on Soil Engrg., 1972. 2nd SE Asia Conf. on Soil Engrg, South East Asia, pp. 83–91.

Chin, F.K., 1970. Estimation of the ultimate load of piles from tests not carried to failure, in: Proc. 2nd Southeast Asian Conference on Soil Engineering, Singapore, 1970. 2nd Southeast Asian Conference, Singapore, pp. 85–104.

Everett, J.P., 1991. Load transfer functions and pile performance modelling, in: Geotechnics in the African Environment. Regional Conference for Africa on Soil Mechanics and Foundation Engineering. pp. 229–234.

Fellenius, B., 1980. The Analysis of Results from Routine Pile Load. General Engineering, London, 13(6), pp19-31.

Fleming, W.G.K., 1992. A New method for Single pile settlement prediction and analysis. Geotechnique 42, 411–425.

Hull, T.S., 1987. The static behaviour of laterally loaded piles.

Knappett, J., Craig, R.F., 2012. Craig's soil mechanics, 8th ed. ed. Spon Press, Abingdon, Oxon ; New York.

Mattes, N.S., Poulos, H.G., 1969. Settlement of Single Compressible Pile. J. Soil Mech. and Found. Div. 95, 189–207. https://doi.org/10.1061/JSFEAQ.0001217

Mert, M., Ozkan, M.T., 2019. Settlement Analysis of Axially Loaded Bored Piles: A Case History 13, 8.

Mylonakis, G., Gazetas, G., 1998. Settlement and additional internal forces of grouped piles in layered soil. Géotechnique 48, 55–72. https://doi.org/10.1680/geot.1998.48.1.55

Ng, C.W., Simons, N., Menzies, B., 2004. Soil-structure engineering. Thomas Telford, London.

Perloff, W.H., Baron, W., 1976. Soil mechanics. Principles and applications.

Poulos, H., 1977. Estimation of Pile Group Settlements.

Poulos, H.G., 1989. Pile behaviour—theory and application. Géotechnique 39, 365–415. https://doi.org/10.1680/geot.1989.39.3.365

Poulos, H.G., 1968. Analysis of the Settlement of Pile Groups. Géotechnique 18, 449–471. https://doi.org/10.1680/geot.1968.18.4.449

Poulos, H.G., Davis, E.H., 1980. Pile foundation analysis and design.

Poulos, H.G., Davis, E.H., 1968. The Settlement Behaviour of Single Axially Loaded Incompressible Piles and Piers. Géotechnique 18, 351–371. https://doi.org/10.1680/geot.1968.18.3.351

Poulos, H.G., Mattes, N.S., 1971. Settlement and load distribution of pile groups. Australian Geotechnical Journal.

Rajapakse, R., 2007. Pile Design for Structural and Geotechnical Engineers.

Randolph, M.F., 1985. Settlement of Pile Groups.

Randolph, M.F., Wroth, C.P., 1979. An analysis of the vertical deformation of pile groups. Geotechnique 29, 423–439.

Randolph, M.F., Wroth, C.P., 1978. Analysis of deformation of vertically loaded piles. Journal of the geotechnical engineering division 104, 1465–1488.

Salim, R.R., 2017. Analysis of Cast in Place Piles Using Finite Elements Method 12, 8.

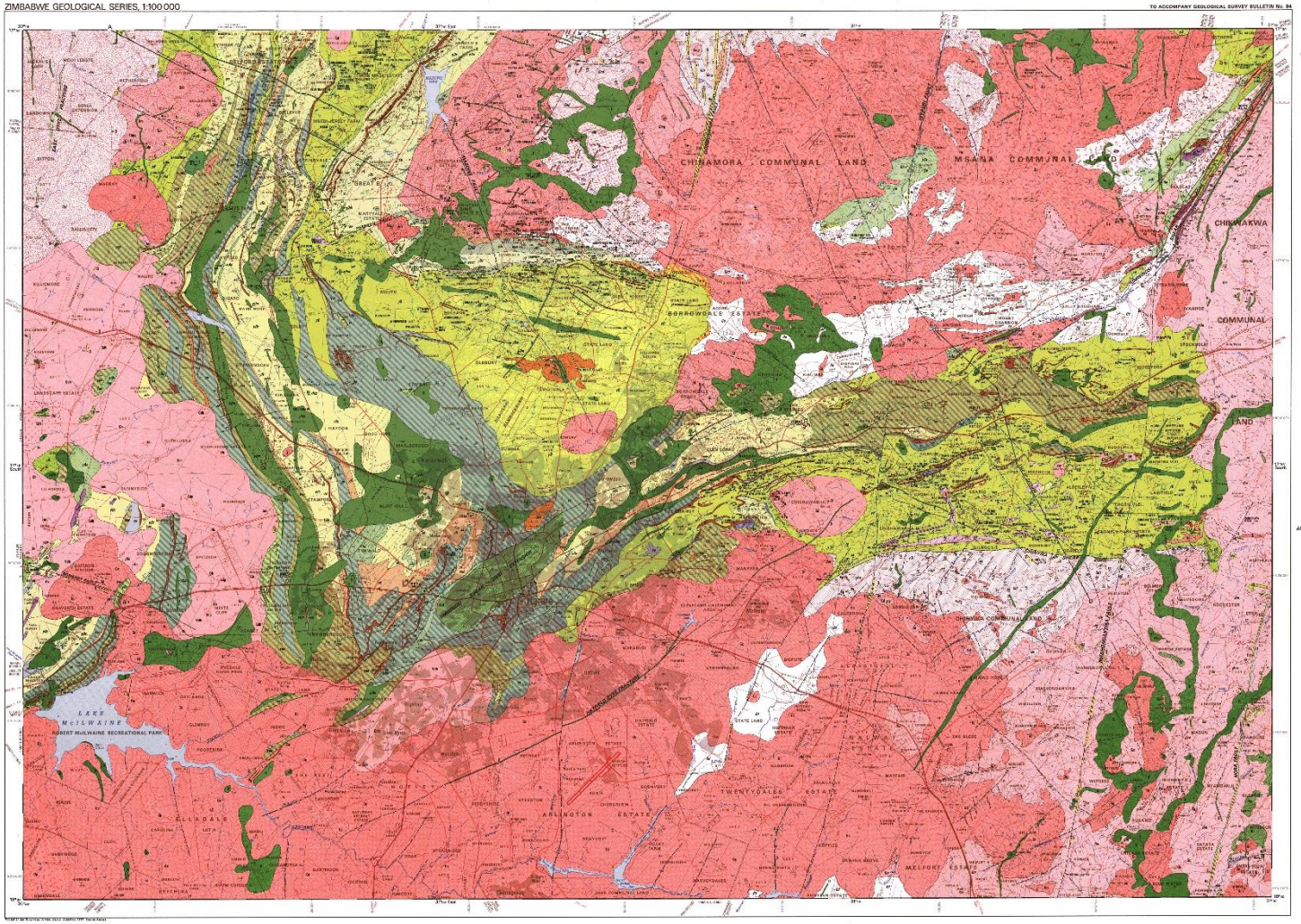
Tomlinson, M.J., Boorman, R., 2001. Foundation design and construction, 7. ed. ed. Prentice Hall, Harlow.

Vesić, A.S., 1977. Design of pile foundations, Synthesis of highway practice. Transportation Research Board, National Research Council, Washington.

APPENDIX A
GEOLOGICAL MAP OF HARARE AND ITS ENVIRONS

ZIMBABWE GEOLOGICAL SERIES, 1:100 000

TO ACCOMPANY GEOLOGICAL SURVEY BULLETIN No. 94



HARARE

Scale 1:100000

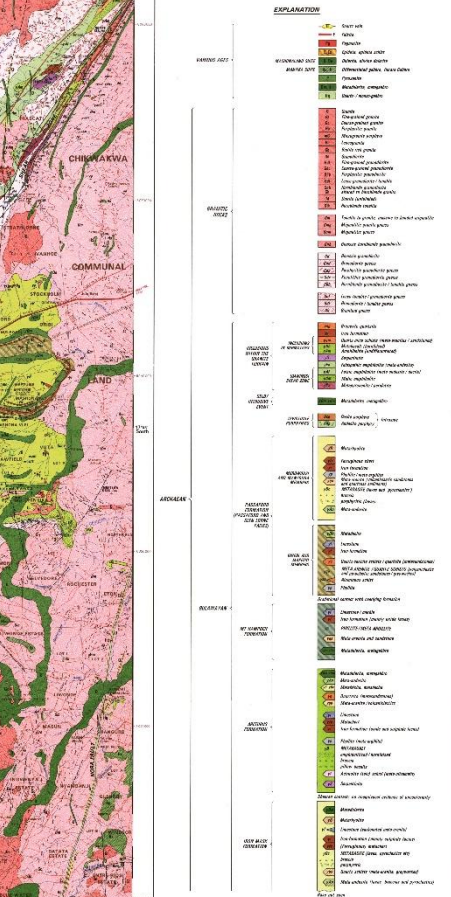
Geology by J.W.Boldock, 1962-66

Interpreting previous mapping by F.A.Bisschoff, V.R.Steedman, A.G.Cox and R.S.Hatherley, 1935-77

Compiled and drawn in the Geological Survey Office, Harare, Zimbabwe, 1980. Cartographer P.Turner

Topography controlled by photogrammetric methods from aerial photographs taken in 1971, 1977 and 1978 with ground control by the Department of Surveys

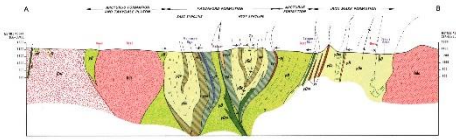
EXPLANATION



INTERPRETATIVE CROSS-SECTIONS

Horizontal Scale 1:100000 Vertical Scale 1:50000

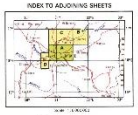
SECTION A–B



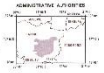
SECTION C–D



INDEX TO ADJOINING SHEETS



ADMINISTRATIVE AUTHORITIES



TOPOGRAPHICAL EXPLANATION



B 94

752

APPENDIX B - TABLES

Table B1: Theoretical values of settlement ratio, R_s for friction pile groups with rigid pile cap on deep soil mass

No of piles in group		4				9				16				25			
L/d	***s/d K***	**10**	**100**	**1000**	∞	**10**	**100**	**1000**	∞	**10**	**100**	**1000**	∞	**10**	**100**	**1000**	∞
10	2	1.83	2.25	2.54	2.62	2.78	3.80	4.42	4.48	3.76	5.49	6.40	6.53	4.75	7.20	8.48	8.68
	5	1.40	1.73	1.88	1.90	1.83	2.49	2.82	2.85	2.26	3.25	3.74	3.82	2.68	3.98	4.70	4.75
	10	1.21	1.39	1.48	1.50	1.42	1.76	1.97	1.99	1.63	2.14	2.46	2.46	1.85	2.53	2.95	2.95
25	2	1.99	2.14	2.65	2.87	3.01	3.64	4.84	5.29	4.22	5.38	7.44	8.10	5.40	7.25	9.28	11.25
	5	1.47	1.74	2.09	2.19	1.98	2.61	3.48	3.74	2.46	3.54	4.96	5.34	2.95	4.48	6.50	7.03
	10	1.25	1.46	1.74	1.78	1.49	1.95	2.57	2.73	1.74	2.46	3.42	3.63	1.98	2.98	4.28	4.50
50	2	2.43	2.31	2.56	3.01	3.91	3.79	4.52	5.66	5.58	5.65	7.05	8.94	7.26	7.65	9.91	12.66
	5	1.73	1.81	2.10	2.44	2.46	2.75	3.51	4.29	3.16	3.72	5.11	6.37	3.88	4.74	6.64	8.67
	10	1.38	1.50	1.78	2.04	1.74	2.04	2.72	3.29	2.08	2.59	3.73	4.65	2.49	3.16	4.76	6.04
100	2	2.56	2.31	2.26	3.16	4.43	4.05	4.11	6.15	6.42	6.14	6.50	9.92	8.48	8.40	10.25	14.35
	5	1.88	1.88	2.01	2.64	2.80	2.94	3.38	4.87	3.74	4.05	4.98	7.54	4.68	5.18	6.75	10.55
	10	1.47	1.56	1.76	2.28	1.95	2.17	2.73	3.93	2.45	2.80	3.81	5.82	2.95	3.48	5.00	7.88

Table B2: Theoretical values of settlement ratio, Rs for end-bearing pile groups with rigid pile cap bearing on rigid stratum

No of piles in group		4				9				16				25			
L/d	***s/d K***	**10**	**100**	**1000**	∞	**10**	**100**	**1000**	∞	**10**	**100**	**1000**	∞	**10**	**100**	**1000**	∞
10	2	1.52	1.14	1.00	1.00	2.02	1.31	1.00	1.00	2.38	1.49	1.00	1.00	2.70	1.63	1.00	1.00
	5	1.15	1.08	1.00	1.00	1.23	1.12	1.02	1.00	1.30	1.14	1.02	1.00	1.33	1.15	1.03	1.00
	10	1.02	1.01	1.00	1.00	1.04	1.02	1.00	1.00	1.04	1.02	1.00	1.00	1.03	1.02	1.00	1.00
25	2	1.88	1.62	1.05	1.00	2.84	2.57	1.16	1.00	3.70	3.28	1.33	1.00	4.48	4.13	1.50	1.00
	5	1.36	1.36	1.08	1.00	1.67	1.70	1.16	1.00	1.94	2.00	1.23	1.00	2.15	2.23	1.28	1.00
	10	1.14	1.15	1.04	1.00	1.23	1.25	1.06	1.00	1.30	1.33	1.07	1.00	1.33	1.38	1.08	1.00
50	2	2.49	2.24	1.59	1.00	4.06	3.59	1.96	1.00	5.83	5.27	2.63	1.00	7.62	7.06	3.41	1.00
	5	1.78	1.73	1.32	1.00	2.56	2.56	1.72	1.00	3.28	3.38	2.16	1.00	4.04	4.23	2.63	1.00
	10	1.39	1.43	1.21	1.00	1.78	1.87	1.45	1.00	2.20	2.29	1.71	1.00	2.62	2.71	1.97	1.00
100	2	2.54	2.26	1.81	1.00	4.40	3.95	3.04	1.00	6.24	5.89	4.61	1.00	8.18	7.93	6.40	1.00
	5	1.85	1.84	1.67	1.00	2.71	2.77	2.52	1.00	3.54	3.74	3.47	1.00	4.33	4.68	4.45	1.00
	10	1.44	1.44	1.46	1.00	1.84	1.99	1.98	1.00	2.21	2.48	2.53	1.00	2.53	2.98	3.10	1.00

Table B3: Settlement influence factor, I_1 for a single pile (after Poulos and Davis, 1968)

	v=0.5			v=0		
L/d / *h/L*	**10**	**25**	**100**	**10**	**25**	**100**
∞	1.41	1.86	2.54	1.16	1.47	1.95
5	1.31	1.76	2.44	1.07	1.37	1.86
2.5	1.20	1.64	2.31	0.96	1.27	1.75
1.5	0.98	1.42	2.11	0.80	1.11	1.58
1.2	0.72	1.18	1.89	0.62	0.94	1.44

Table B4: Values of R_G for pile groups with rigid pile cap for L/d=25 and v=0.5 (after Poulos, 1968b)

Group	**2^2**					**3^2**				
h/L / *s/d*	∞	**5**	**2.5**	**1.5**	**1.2**	∞	**5**	**2.5**	**1.5**	**1.2**
1.0	0.839	0.819	0.815	0.745	0.621	0.715	0.677	0.670	0.593	0.465
5.0	0.547	0.519	0.501	0.422	0.348	0.415	0.363	0.339	0.256	0.195
10	0.425	0.408	0.385	0.323	0.291	0.303	0.245	0.220	0.165	0.141
20	0.366	0.317	0.297	0.267	0.258	0.214	0.157	0.142	0.122	0.116
40	0.307	0.260	0.254	0.250	0.250	0.159	0.117	0.114	0.111	0.111
Group	**4^2**					**5^2**				
h/L / *s/d*	∞	**5**	**2.5**	**1.5**	**1.2**	∞	**5**	**2.5**	**1.5**	**1.2**
1	0.643	0.599	0.590	0.500	0.371	0.584	0.538	0.525	0.432	0.309
2.5	0.460	0.409	0.388	0.296	0.206	0.403	0.349	0.325	0.235	0.160
5	0.334	0.277	0.250	0.176	0.128	0.281	0.220	0.194	0.129	0.091
10	0.227	0.166	0.143	0.100	0.083	0.180	0.119	0.100	0.067	0.055
20	0.148	0.093	0.083	0.069	0.066	0.112	0.062	0.054	0.045	0.042
40	0.105	0.066	0.064	0.063	0.063	0.070	0.041	0.041	0.040	0.040

Table B5: Values of S_{max}/S_R for L/d=25 and v=0.5

Group	**3^2**			**4^2**			**5^2**		
h/L / *s/d*	∞	**1.5**	**1.2**	∞	**1.5**	**1.2**	∞	**1.5**	**1.2**
1 2.	1.13	1.15	1.15	1.13	1.17	1.18	1.18	1.25	1.26
5	1.13	1.17	1.16	1.14	1.20	1.17	1.19	1.30	1.24
5	1.13	1.18	1.13	1.15	1.20	1.15	1.21	1.30	1.23
10	1.14	1.15	1.10	1.16	1.16	1.11	1.24	1.20	1.11
20	1.14	1.05	1.01	1.13	1.05	1.01	1.18	1.04	1.02
40	1.08	1.00	1.00	1.06	1.00	1.00	1.17	1.00	1.00

Table B6: Group reduction factor, R_G for floating pile groups with rigid cap, v=0.5 (after Poulos and Mattes, 1971b)

Group	Size	2^2				3^2				4^2				5^2			
	K	**10**	**100**	**1000**	∞	**10**	**100**	**1000**	∞	**10**	**100**	**1000**	∞	**10**	**100**	**1000**	∞
L/d	***s/d***																
	2	0.457	0.562	0.636	0.654	0.309	0.422	0.491	0.498	0.235	0.343	0.400	0.408	0.190	0.288	0.339	0.347
	5	0.351	0.432	0.471	0.476	0.203	0.277	0.313	0.317	0.141	0.203	0.234	0.239	0.107	0.159	0.188	0.190
10	**10**	0.302	0.347	0.370	0.374	0.158	0.196	0.219	0.221	0.102	0.134	0.154	0.154	0.074	0.101	0.118	0.118
	20	0.276	0.295	0.310	0.310	0.135	0.152	0.166	0.166	0.083	0.097	0.109	0.109	0.056	0.069	0.079	0.079
	∞	0.250	0.250	0.250	0.250	0.111	0.111	0.111	0.111	0.062	0.062	0.062	0.062	0.040	0.040	0.040	0.040
	2	0.497	0.534	0.662	0.718	0.334	0.404	0.538	0.588	0.264	0.336	0.465	0.506	0.216	0.290	0.411	0.450
	5	0.367	0.436	0.532	0.547	0.220	0.290	0.387	0.415	0.154	0.221	0.310	0.334	0.118	0.179	0.260	0.281
25	**10**	0.313	0.365	0.435	0.445	0.166	0.217	0.286	0.303	0.109	0.154	0.214	0.227	0.079	0.119	0.171	0.180
	20	0.278	0.313	0.358	0.366	0.137	0.167	0.209	0.214	0.084	0.110	0.147	0.148	0.059	0.080	0.112	0.112
	∞	0.250	0.250	0.250	0.250	0.111	0.111	0.111	0.111	0.062	0.062	0.062	0.062	0.040	0.040	0.040	0.040
	2	0.640	0.578	0.565	0.789	0.492	0.450	0.457	0.683	0.401	0.384	0.406	0.620	0.339	0.336	0.370	0.574
	5	0.471	0.470	0.502	0.661	0.311	0.327	0.375	0.541	0.234	0.253	0.311	0.471	0.187	0.207	0.270	0.422
100	**10**	0.368	0.391	0.441	0.569	0.217	0.241	0.303	0.437	0.153	0.175	0.238	0.364	0.118	0.139	0.200	0.315
	20	0.310	0.327	0.380	0.481	0.165	0.183	0.239	0.338	0.109	0.125	0.179	0.270	0.080	0.094	0.144	0.228
	∞	0.250	0.250	0.250	0.250	0.111	0.111	0.111	0.111	0.062	0.062	0.062	0.062	0.040	0.040	0.040	0.040

Table B7: Group reduction factor, R_G for end-bearing pile groups with rigid cap, v=0.5 (after Poulos and Mattes, 1971b)

Group	Size	2^2				3^2				4^2				5^2			
L/d	**K**	10	100	1000	∞	10	100	1000	∞	10	100	1000	∞	10	100	1000	∞
	s/d																
	2	0.379	0.285	0.250	0.250	0.224	0.146	0.111	0.111	0.149	0.093	0.062	0.062	0.108	0.065	0.040	0.040
	5	0.287	0.270	0.252	0.250	0.137	0.124	0.113	0.111	0.081	0.071	0.063	0.062	0.053	0.046	0.041	0.040
10	**10**	0.256	0.252	0.250	0.250	0.115	0.133	0.111	0.111	0.065	0.063	0.062	0.062	0.041	0.041	0.040	0.040
	20	0.250	0.250	0.250	0.250	0.111	0.111	0.111	0.111	0.062	0.062	0.062	0.062	0.040	0.040	0.040	0.040
	∞	0.250	0.250	0.250	0.250	0.111	0.111	0.111	0.111	0.062	0.062	0.062	0.062	0.040	0.040	0.040	0.040
	2	0.471	0.405	0.263	0.250	0.316	0.286	0.129	0.111	0.231	0.205	0.083	0.062	0.179	0.165	0.060	0.040
	5	0.341	0.341	0.271	0.250	0.186	0.189	0.129	0.111	0.121	0.125	0.077	0.062	0.086	0.089	0.051	0.040
25	**10**	0.284	0.288	0.259	0.250	0.137	0.140	0.118	0.111	0.081	0.083	0.067	0.062	0.053	0.055	0.043	0.040
	20	0.259	0.259	0.251	0.250	0.116	0.117	0.112	0.111	0.066	0.066	0.063	0.062	0.042	0.042	0.040	0.040
	∞	0.250	0.250	0.250	0.250	0.111	0.111	0.111	0.111	0.062	0.062	0.062	0.062	0.040	0.040	0.040	0.040
	2	0.636	0.565	0.452	0.250	0.489	0.439	0.338	0.111	0.390	0.368	0.288	0.062	0.327	0.317	0.256	0.040
	5	0.463	0.459	0.418	0.250	0.301	0.308	0.280	0.111	0.221	0.234	0.216	0.062	0.173	0.187	0.178	0.040
100	**10**	0.359	0.373	0.365	0.250	0.204	0.221	0.220	0.111	0.138	0.155	0.158	0.062	0.101	0.119	0.124	0.040
	20	0.296	0.310	0.317	0.250	0.149	0.165	0.173	0.111	0.093	0.107	0.115	0.062	0.066	0.078	0.085	0.040
	∞	0.250	0.250	0.250	0.250	0.111	0.111	0.111	0.111	0.062	0.062	0.062	0.062	0.040	0.040	0.040	0.040

Table B8: Comparison of single pile settlement computed by various methods for varying D_0, and L founded in cohesive uniform soil

Pile Dia (m m)	Pile Settlement (mm)							Allowable pile capacity (kN) (Computer - Uniform)		
	T-z Method	Butterfield & Banerjee (1971)	Randolph & Wroth (1978)	Poulos& Davis (1980)	Poulos (1989)	Mattes & Poulos (1969)	Pile Computer Program	Shaft Friction Q_s (kN)	End Bearing Q_b (kN)	Applied Load Q_{ap}(kN)
L=10m										
0.5	1.52	1.50	1.31	1.38	2.45	2.14	2.77	262	22	250
1.0	1.23	1.32	1.00	0.97	1.72	1.37	0.76	524	88	250
1.5	1.06	1.15	0.83	0.79	1.52	1.12	0.45	785	199	250
2.0	0.94	1.08	0.71	0.67	1.34	0.91	0.37	1047	353	250
2.5	0.85	1.00	0.62	0.60	1.07	0.77	0.29	1309	552	250
L=20m										
0.5	2.57	3.04	2.48	2.99	6.26	5.07	3.73	741	22	760
1.0	1.97	2.41	2.00	2.04	3.72	2.97	0.86	1481	88	760
1.5	1.46	2.03	1.72	1.67	2.73	2.53	0.52	2221	199	760
2.0	0.96	1.93	1.52	1.48	2.09	2.15	0.42	2962	353	760
2.5	0.46	1.79	1.37	1.32	1.85	2.00	0.34	3703	552	760
L=30m										
0.5	3.45	4.60	3.34	5.56	11.45	7.01	3.73	1360	22	1380
1.0	2.81	3.45	2.76	2.94	6.38	4.60	0.86	2721	88	1380
1.5	2.31	3.04	2.42	2.54	4.50	3.80	0.52	4081	199	1380
2.0	1.85	2.88	2.18	2.09	3.62	3.07	0.42	5441	353	1380
2.5	1.40	2.76	1.99	1.93	3.01	2.91	0.34	6802	552	1380
L=40m										
0.5	2.98	4.48	2.91	7.78	13.03	6.25	1.63	2094	22	1500
1.0	2.46	3.16	2.44	3.10	6.68	4.45	0.61	4189	88	1500
1.5	2.06	2.50	2.17	2.45	4.73	3.64	0.41	6283	199	1500
2.0	1.68	2.34	1.97	2.24	3.67	3.06	0.30	8379	353	1500
2.5	1.31	2.26	1.82	2.01	3.11	2.93	0.24	10472	552	1500
L=50m										
0.5	2.49	4.29	2.45	8.88	8.93	5.33	0.88	2927	22	1500
1.0	2.07	2.88	2.08	3.05	2.23	3.90	0.44	5854	88	1500
1.5	1.74	2.17	1.86	2.02	0.99	3.30	0.29	8781	199	1500
2.0	1.43	2.03	1.70	1.74	0.56	2.70	0.22	11708	353	1500
2.5	1.12	1.92	1.58	1.60	0.36	2.57	0.17	14635	552	1500

Table B9: Comparison of single pile settlement computed by various methods for varying D_0, and L founded in cohesive uniform soil

Pile Dia (mm)	Pile Settlement (mm)					Comp Allowable pile capacity (kN)		
	Focht (1967)	Poulos &Davis (1968)	Fleming (1992)			Shaft Friction Q_s (kN)	End Bearing Q_b (kN)	Applied Load Q_a(kN)
			Tip	Elastic	Head			
L=10m								
0.5	0.42	1.22	2.19	0.25	2.45	262	22	250
1.0	0.24	0.90	0.95	0.06	1.01	524	88	250
1.5	0.18	0.76	0.74	0.03	0.77	785	199	250
2.0	0.15	0.65	0.65	0.02	0.67	1047	353	250
2.5	0.10	0.58	0.59	0.01	0.60	1309	552	250
L=20m								
0.5	1.75	2.36	4.80	1.02	6.21	741	22	760
1.0	1.15	1.83	1.65	0.35	2.00	1481	88	760
1.5	0.54	1.62	1.00	0.16	1.16	2221	199	760
2.0	0.31	1.44	0.88	0.09	0.97	2962	353	760
2.5	0.20	1.41	0.81	0.06	0.87	3703	552	760
L=30m								
0.5	4.58	3.09	6.49	3.75	10.23	1360	22	1380
1.0	1.53	2.47	1.39	0.94	3.33	2721	88	1380
1.5	0.75	2.24	1.05	0.42	1.47	4081	199	1380
2.0	0.45	2.00	0.93	0.23	1.16	5441	353	1380
2.5	0.29	1.84	0.86	0.15	1.01	6802	552	1380
L=40m								
0.5	4.89	2.67	1.72	5.35	7.06	2094	22	1500
1.0	1.83	2.15	0.80	1.34	2.14	4189	88	1500
1.5	0.93	1.95	0.67	0.59	1.27	6283	199	1500
2.0	0.57	1.81	0.62	0.33	0.96	8379	353	1500
2.5	0.37	1.67	0.59	0.21	0.81	10472	552	1500
L=50m								
0.5	5.09	2.25	0.77	6.62	7.39	2927	22	1500
1.0	2.16	1.86	0.51	1.66	2.16	5854	88	1500
1.5	1.10	1.72	0.45	0.74	1.19	8781	199	1500
2.0	0.70	1.53	0.43	0.41	0.84	11708	353	1500
2.5	0.46	1.46	0.41	0.26	0.68	14635	552	1500

Table B10: Comparison of pile settlement computed using various methods for varying pile diameter D_0, and pile length L for a single pile founded in non-cohesive uniform soil

Pile Dia (mm)	T-z Method	Randolph and Wroth (1978)	Poulos (1989)	Fleming (1992)	Pile Computer Program (Uniform)	Shaft Friction Q_s (kN)	End Bearing Q_b (kN)	Applied Load Q_{ap}(kN)
L=10m								
0.5	2.56	1.63	3.84	5.16	6.61	415	167	560
1.0	2.04	1.26	2.26	1.61	1.55	793	668	560
1.5	1.48	1.05	1.99	1.09	0.81	1189	1502	560
2.0	1.11	0.90	1.81	0.89	0.61	1585	2670	560
2.5	0.87	0.80	1.44	0.78	0.49	1982	4172	560
L=20m								
0.5	2.34	2.68	10.29	6.08	2.99	1585	334	1500
1.0	1.67	2.18	5.14	1.62	0.81	3170	1335	1500
1.5	1.30	1.89	3.52	1.04	0.54	4756	3004	1500
2.0	1.05	1.68	2.72	0.83	0.41	6341	5342	1500
2.5	0.87	1.53	2.44	0.73	0.33	7926	8345	1500
L=30m								
0.5	1.74	1.98	10.54	4.53	1.02	2554	471	1500
1.0	1.29	1.65	5.18	1.41	0.50	5108	1885	1500
1.5	1.02	1.45	3.42	0.83	0.34	7662	4241	1500
2.0	0.84	1.32	2.67	0.62	0.25	10216	7540	1500
2.5	0.71	1.21	2.14	0.52	0.20	12771	11781	1500
L=40m								
0.5	1.60	1.59	11.33	5.33	0.76	3406	471	1500
1.0	1.23	1.34	5.14	1.55	0.38	6811	1885	1500
1.5	1.11	1.19	3.45	0.84	0.25	10217	4241	1500
2.0	1.01	1.09	2.57	0.59	0.19	13622	7540	1500
2.5	0.93	1.01	2.11	0.47	0.15	17027	11781	1500
L=50m								
0.5	1.23	1.33	6.37	6.33	0.61	4257	471	1500
1.0	0.97	1.14	1.60	1.75	0.30	8514	1885	1500
1.5	0.81	1.02	0.71	0.90	0.20	12771	4241	1500
2.0	0.70	0.94	0.40	0.60	0.15	17027	7540	1500
2.5	0.61	0.87	0.26	0.45	0.12	21284	11781	1500

Table B11: Comparison of pile settlement computed using various methods for varying pile diameter D_0, and pile length L for a single pile founded in layered (Lyd1) soil – Top layer is clay, bottom layer is sand

Pile Dia (mm)	T-z Method	Randolph and Wroth (1978)	Poulos (1989)	Pile Computer Program	Shaft Friction Q_s (kN)	End Bearing Q_b (kN)	Applied Load Q_{ap}(kN)
L=10m							
0.5	1.09	2.65	5.65	4.06	425	280	700
1.0	0.88	2.04	3.56	0.85	850	1119	700
1.5	0.76	1.69	2.98	0.52	1274	2518	700
2.0	0.68	1.45	2.65	0.37	1699	4477	700
2.5	0.61	1.28	2.25	0.28	2124	6995	700
L=20m							
0.5	1.38	3.50	11.46	3.56	1113	471	1500
1.0	1.16	2.84	6.05	0.81	2226	1885	1500
1.5	1.03	2.45	4.24	0.51	3340	4241	1500
2.0	0.95	2.18	3.47	0.36	4452	7540	1500
2.5	0.87	1.97	3.00	0.28	5566	11781	1500
L=30m							
0.5	2.11	2.59	11.63	1.61	1758	471	1500
1.0	1.49	2.15	5.87	0.58	3516	1885	1500
1.5	1.14	1.89	4.03	0.37	5274	4241	1500
2.0	0.92	1.71	3.16	0.27	7032	7540	1500
2.5	0.76	1.57	2.57	0.21	8790	11781	1500
L=40m							
0.5	1.81	2.08	12.49	0.93	2443	471	1500
1.0	1.34	1.75	5.73	0.44	4886	1885	1500
1.5	1.07	1.56	3.95	0.29	7330	4241	1500
2.0	0.88	1.42	3.03	0.21	9773	7540	1500
2.5	0.75	1.31	2.48	0.16	12216	11781	1500
L=50m							
0.5	1.56	1.75	7.66	0.74	3163	471	1500
1.0	1.2	1.49	1.92	0.36	6327	1885	1500
1.5	0.98	1.33	0.85	0.23	9490	4241	1500
2.0	0.83	1.22	0.48	0.17	12653	7540	1500
2.5	0.72	1.14	0.31	0.13	15816	11781	1500

Table B12: Comparison of pile settlement computed using various methods for varying pile diameter D_0, and pile length L for a single pile founded in layered (Lyd2) soil – Top layer is sand, bottom layer is clay

Pile Dia (mm)	T-z Method	Randolph and Wroth (1978)	Poulos (1989)	Pile Computer Program	Shaft Friction Q_s (kN)	End Bearing Q_b (kN)	Applied Load Q_{ap}(kN)
L=10m							
0.5	0.96	2.65	2.18	3.71	251	22	270
1.0	0.78	2.04	1.39	0.85	502	88	270
1.5	0.68	1.69	1.20	0.56	751	199	270
2.0	0.6	1.45	1.09	0.41	1005	354	270
2.5	0.54	1.28	0.87	0.33	1256	552	270
L=20m							
0.5	1.38	3.50	6.45	3.72	826	22	845
1.0	1.16	2.84	3.41	0.86	1653	88	845
1.5	1.03	2.45	2.39	0.57	2479	199	845
2.0	0.94	2.18	1.85	0.43	3306	354	845
2.5	0.87	1.97	1.66	0.34	4132	552	845
L=30m							
0.5	2.11	2.59	6.45	2.70	1682	22	1500
1.0	1.49	2.15	3.41	0.76	3364	88	1500
1.5	1.14	1.89	2.39	0.50	5046	199	1500
2.0	0.92	1.71	1.85	0.38	6728	354	1500
2.5	0.76	1.57	1.66	0.30	8410	552	1500
L=40m							
0.5	1.76	2.08	12.49	0.92	2802	22	1500
1.0	1.3	1.75	5.73	0.46	5604	88	1500
1.5	1.04	1.56	3.95	0.31	8406	199	1500
2.0	0.86	1.42	3.03	0.23	11208	354	1500
2.5	0.72	1.31	2.48	0.18	14010	552	1500
L=50m							
0.5	1.53	1.75	7.66	0.67	3829	22	1500
1.0	1.17	1.49	1.92	0.34	7658	88	1500
1.5	0.96	1.33	0.85	0.22	11487	199	1500
2.0	0.81	1.22	0.48	0.17	15315	354	1500
2.5	0.70	1.14	0.31	0.13	19144	552	1500

Table B13: 2^2, 3^2 and 4^2 – Pile group settlement after Poulos (1968b)

Pile Dia (m)	L/D_0 ratio	Single pile settlement factor Iρ	Safe Load per Pile, P (kN)	Single pile settlement, S_1 (mm)	Settlement Ratio, R_S (refer to Table B1)			Pile Group Settlement(mm) due to pile group load, $P_G=nP$		
					2x2 Pile group	3x3 Pile group	4x4 Pile group	2^2-pile group	3^2-pile group	4^2-pile group
L=10m										
0.3	33	1.667	165	0.92	2.445	4.322	6.585	2.24	3.96	6.04
0.4	25	1.639	165	0.90	2.320	4.387	6.613	2.09	3.95	5.96
0.5	20	1.550	165	0.85	2.368	4.053	5.880	2.02	3.46	5.01
0.6	17	1.333	165	0.73	2.366	4.046	5.865	1.73	2.97	4.30
0.7	14	1.075	165	0.59	2.383	4.107	5.998	1.41	2.43	3.55
L=20m										
0.3	67	1.667	452	1.26	2.328	4.076	6.264	2.92	5.12	7.87
0.4	50	1.569	452	1.18	2.407	4.183	6.403	2.85	4.94	7.57
0.5	40	1.458	452	1.10	2.429	4.265	6.487	2.67	4.68	7.13
0.6	33	1.333	452	1.00	2.445	4.322	6.585	2.46	4.34	6.61
0.7	29	1.193	452	0.90	2.454	4.354	6.580	2.21	3.91	5.91
L=30m										
0.3	100	2.375	824	2.17	2.177	3.867	5.795	4.73	8.41	12.60
0.4	75	2.111	824	1.93	2.292	4.025	6.198	4.43	7.78	11.98
0.5	60	1.924	824	1.76	2.361	4.120	6.321	4.16	7.26	11.13
0.6	50	1.765	824	1.62	2.407	4.183	6.403	3.89	6.76	10.35
0.7	43	1.698	824	1.55	2.418	4.226	6.421	3.76	6.57	9.98
L=40m										
0.3	133	2.417	1264	2.55	1.979	3.669	5.795	5.04	9.34	14.75
0.4	100	2.375	1264	2.50	2.177	3.867	5.993	5.45	9.67	14.99
0.5	80	2.284	1264	2.41	2.267	3.993	6.157	5.45	9.61	14.81
0.6	67	2.156	1264	2.27	2.328	4.076	6.264	5.29	9.26	14.23
0.7	57	1.944	1264	2.05	2.374	4.139	6.346	4.86	8.48	12.99
L=50m										
0.3	167	2.500	1500	2.50	1.775	3.465	5.591	4.44	8.66	13.98
0.4	125	2.298	1500	2.30	1.877	3.567	5.693	4.31	8.20	13.08
0.5	100	1.926	1500	1.93	2.177	3.867	5.993	4.19	7.45	11.54
0.6	83	1.611	1500	1.61	2.255	3.974	6.133	3.63	6.40	9.88
0.7	71	1.258	1500	1.26	2.310	4.050	6.231	2.91	5.09	7.84

Table B14: 2^2, 3^2 and 4^2 – Floating Pile group settlement after Poulos and Mates (1971b) with rigid cap

Pile Dia (m)	L/D	Single pile settle'factor Iρ	Safe Load P(kN)	Single pile settle S_1 (mm)	Group settlement reduction factor, R_G, (refer to Table B6)			Pile Group Settlement (mm)		
					2x2 pile group	3x3 pile group	4x4 pile group	2^2-pile group	3^2-pile group	4^2-pile group
L=10m										
0.3	33	3.000	165	1.78	0.611	0.481	0.409	4.34	7.70	11.63
0.4	25	2.86pur7	165	1.58	0.619	0.488	0.413	3.90	6.93	10.42
0.5	20	2.667	165	1.47	0.606	0.460	0.392	3.56	6.07	9.20
0.6	17	2.400	165	1.32	0.598	0.458	0.376	3.16	5.44	7.94
0.7	14	2.134	165	1.17	0.591	0.447	0.363	2.77	4.72	6.82
L=20m										
0.3	67	4.067	452	3.06	0.577	0.455	0.392	7.07	12.55	19.22
0.4	50	3.667	452	2.76	0.594	0.468	0.400	6.56	11.64	17.68
0.5	40	3.440	452	2.52	0.604	0.476	0.405	6.08	10.79	16.31
0.6	33	3.000	452	2.35	0.611	0.481	0.409	5.75	10.18	15.39
0.7	29	2.933	452	2.21	0.615	0.485	0.411	5.44	9.64	14.53
L=30m										
0.3	100	5.000	824	4.58	0.544	0.416	0.374	9.96	17.14	27.39
0.4	75	4.333	824	3.97	0.569	0.449	0.388	9.03	16.03	24.63
0.5	60	4.000	824	3.66	0.579	0.457	0.393	8.48	15.06	23.03
0.6	50	3.667	824	3.36	0.594	0.468	0.400	7.98	14.14	21.49
0.7	43	3.467	824	3.17	0.601	0.474	0.404	7.63	13.54	20.52
L=40m										
0.3	133	6.500	1264	6.85	0.511	0.383	0.341	13.99	23.60	37.36
0.4	100	5.000	1264	5.40	0.544	0.416	0.374	11.75	20.21	32.30
0.5	80	4.413	1264	4.65	0.564	0.445	0.385	10.49	18.62	28.63
0.6	67	4.067	1264	4.28	0.577	0.455	0.392	9.89	17.54	26.87
0.7	57	3.933	1264	4.14	0.587	0.463	0.397	9.73	17.26	26.31
L=50m										
0.3	167	7.500	1500	7.50	0.477	0.349	0.307	14.31	23.56	36.84
0.4	125	6.000	1500	6.00	0.519	0.391	0.349	12.46	21.11	33.50
0.5	100	5.000	1500	5.00	0.544	0.416	0.374	10.88	18.72	29.92
0.6	83	4.533	1500	4.53	0.561	0.443	0.383	10.17	18.07	27.78
0.7	71	4.268	1500	4.27	0.573	0.452	0.390	9.78	17.36	26.63

Table B15: 2x1, 2^2, 3^2 and 4^2 – Pile group settlement after Poulos (1989)

Pile Dia (mm)	Single Pile settlement, S_1 (mm)	Settlement ratio exponent, ω	Settlement Ratio, $R_S=n^{\omega}$				Pile Group Settlement (mm)			
			n=2	n=4	n=9	n=16	2-pile group	2^2-pile group	3^2-pile group	4^2-pile group
L=10m										
300	2.60	0.431	1.348	1.818	2.578	3.3035	3.50	4.72	6.70	8.58
400	1.92	0.431	1.348	1.818	2.578	3.3035	2.58	3.48	4.94	6.33
500	1.51	0.431	1.348	1.818	2.578	3.3035	2.03	2.74	3.88	4.97
600	1.46	0.431	1.348	1.818	2.578	3.3035	1.96	2.65	3.75	4.81
700	1.43	0.431	1.348	1.818	2.578	3.3035	1.93	2.60	3.68	4.72
L=20m										
300	7.70	0.415	1.333	1.778	2.489	3.160	10.27	13.70	19.18	24.35
400	5.63	0.415	1.333	1.778	2.489	3.160	7.51	10.01	14.02	17.80
500	4.39	0.415	1.333	1.778	2.489	3.160	5.85	7.80	10.92	13.87
600	3.56	0.415	1.333	1.778	2.489	3.160	4.74	6.33	8.86	11.25
700	3.02	0.415	1.333	1.778	2.489	3.160	4.03	5.37	7.52	9.55
L=30m										
300	13.62	0.408	1.327	1.761	2.451	3.099	18.07	23.97	33.37	42.20
400	9.19	0.408	1.327	1.761	2.451	3.099	12.19	16.18	22.52	28.48
500	7.00	0.408	1.327	1.761	2.451	3.099	9.29	12.33	17.16	21.70
600	5.61	0.408	1.327	1.761	2.451	3.099	7.44	9.88	13.75	17.39
700	4.64	0.408	1.327	1.761	2.451	3.099	6.15	8.16	11.37	14.37
L=40m										
300	24.30	0.400	1.320	1.74	2.41	3.03	32.07	42.31	58.52	73.67
400	15.74	0.400	1.320	1.74	2.41	3.03	20.77	27.40	37.90	47.71
500	11.57	0.400	1.320	1.74	2.41	3.03	15.27	20.14	27.86	35.07
600	10.35	0.400	1.320	1.74	2.41	3.03	13.66	18.02	24.93	31.38
700	9.34	0.400	1.320	1.74	2.41	3.03	12.32	16.26	22.49	28.31
L=50m										
300	24.80	0.400	1.320	1.74	2.41	3.03	32.72	43.17	59.71	75.17
400	13.95	0.400	1.320	1.74	2.41	3.03	18.41	24.29	33.59	42.29
500	8.93	0.400	1.320	1.74	2.41	3.03	11.78	15.54	21.50	27.07
600	6.20	0.400	1.320	1.74	2.41	3.03	8.18	10.80	14.93	18.80
700	4.56	0.400	1.320	1.74	2.41	3.03	6.01	7.93	10.97	13.81

Table B16: 2^2, 3^2 and 4^2 – Pile group immediate settlement from equivalent raft method

Pile Dia (m)	Safe Load P (kN)	q=nP/A_G (kN/m^2), n=no of piles in group			Immediate pile group settlement, S_i (mm)			Consolidation pile group settlement, S_c (mm)		
		2x2 pile grp	3x3 pile grp	4x4 pile grp	2x2 pile group	3x3 pile group	4x4 pile group	2^2-pile group	3^2-pile group	4^2-pile group
L=10m										
0.3	165	458	337	293	2.72	2.00	1.74	3.50	7.41	12.41
0.4	165	258	189	165	2.04	1.50	1.30	3.41	7.08	11.66
0.5	165	165	121	106	1.63	1.20	1.04	3.32	6.77	10.97
0.6	165	115	84	73	1.36	1.00	0.87	3.23	6.48	10.34
0.7	165	84	62	54	1.16	0.86	0.74	3.15	6.21	9.77
L=20m										
0.3	452	1256	922	804	7.44	5.47	4.76	8.85	18.66	31.12
0.4	452	706	519	452	5.58	4.10	3.57	8.61	17.79	29.14
0.5	452	452	332	289	4.46	3.28	2.86	8.37	16.98	27.33
0.6	452	314	231	201	3.72	2.73	2.38	8.14	16.22	25.69
0.7	452	231	169	148	3.19	2.34	2.04	7.92	15.51	24.20
L=30m										
0.3	824	2289	1682	1465	13.56	9.96	8.68	15.20	31.85	52.82
0.4	824	1288	946	824	10.17	7.47	6.51	14.74	30.28	49.28
0.5	824	824	605	527	8.14	5.98	5.21	14.31	28.82	46.08
0.6	824	572	420	366	6.78	4.98	4.34	13.90	27.46	43.18
0.7	824	420	309	269	5.81	4.27	3.72	13.50	26.20	40.54
L=40m										
0.3	1264	3511	2580	2247	20.80	15.28	13.31	22.29	46.43	76.50
0.4	1264	1975	1451	1264	15.60	11.46	9.99	21.59	44.00	71.09
0.5	1264	1264	929	809	12.48	9.17	7.99	20.91	41.76	66.23
0.6	1264	878	645	562	10.40	7.64	6.66	20.27	39.68	61.85
0.7	1264	645	474	413	8.92	6.55	5.71	19.66	37.75	57.89
L=50m										
0.3	1500	4167	3061	2667	24.69	18.14	15.80	25.68	53.14	87.02
0.4	1500	2344	1722	1500	18.52	13.60	11.85	24.81	50.18	80.50
0.5	1500	1500	1102	960	14.81	10.88	9.48	23.98	47.46	74.67
0.6	1500	1042	765	667	12.34	9.07	7.90	23.19	44.95	69.46
0.7	1500	765	562	490	10.58	7.77	6.77	22.45	42.64	64.77

Table B17: Comparison of pile group settlement computed using various methods for varying pile diameter D_0, and pile length L

Pile Dia (mm)	Pile group settlement (mm) Pouolos (1968b)			Pile group settlement (mm) Pouolos & Mates (1971b)			Pile group settlement (mm) Pouolos (1989)			Pile group settlement (mm) ERM		
	2x2 pile group	3x3 Pile group	4x4 Pile group	2x2 Pile group	3x3 Pile group	4x4 Pile group	2x2 Pile group	3x3 Pile group	4x4 Pile group	2x2 Pile group	3x3 Pile group	4x4 Pile group
L=10m												
0.3	2.24	3.96	6.04	4.34	7.70	11.63	4.72	6.70	8.58	2.72	2.00	1.74
0.4	2.09	3.95	5.96	3.90	6.93	10.42	3.48	4.94	6.33	2.04	1.50	1.30
0.5	2.02	3.46	5.01	3.56	6.07	9.20	2.74	3.88	4.97	1.63	1.20	1.04
0.6	1.73	2.97	4.30	3.16	5.44	7.94	2.65	3.75	4.81	1.36	1.00	0.87
0.7	1.41	2.43	3.55	2.77	4.72	6.82	2.60	3.68	4.72	1.16	0.86	0.74
L=20m												
0.3	2.92	5.12	7.87	7.07	12.55	19.22	13.70	19.18	24.35	7.44	5.47	4.76
0.4	2.85	4.94	7.57	6.56	11.64	17.68	10.01	14.02	17.80	5.58	4.10	3.57
0.5	2.67	4.68	7.13	6.08	10.79	16.31	7.80	10.92	13.87	4.46	3.28	2.86
0.6	2.46	4.34	6.61	5.75	10.18	15.39	6.33	8.86	11.25	3.72	2.73	2.38
0.7	2.21	3.91	5.91	5.44	9.64	14.53	5.37	7.52	9.55	3.19	2.34	2.04
L=30m												
0.3	4.73	8.41	12.60	9.96	17.14	27.39	23.97	33.37	42.20	13.56	9.96	8.68
0.4	4.43	7.78	11.98	9.03	16.03	24.63	16.18	22.52	28.48	10.17	7.47	6.51
0.5	4.16	7.26	11.13	8.48	15.06	23.03	12.33	17.16	21.70	8.14	5.98	5.21
0.6	3.89	6.76	10.35	7.98	14.14	21.49	9.88	13.75	17.39	6.78	4.98	4.34
0.7	3.76	6.57	9.98	7.63	13.54	20.52	8.16	11.37	14.37	5.81	4.27	3.72
L=40m												
0.3	5.04	9.34	14.75	13.99	23.60	37.36	42.31	58.52	73.67	20.80	15.28	13.31
0.4	5.45	9.67	14.99	11.75	20.21	32.30	27.40	37.90	47.71	15.60	11.46	9.99
0.5	5.45	9.61	14.81	10.49	18.62	28.63	20.14	27.86	35.07	12.48	9.17	7.99
0.6	5.29	9.26	14.23	9.89	17.54	26.87	18.02	24.93	31.38	10.40	7.64	6.66
0.7	4.86	8.48	12.99	9.73	17.26	26.31	16.26	22.49	28.31	8.92	6.55	5.71
L=50m												
0.3	4.44	8.66	13.98	14.31	23.56	36.84	43.17	59.71	75.17	24.69	18.14	15.80
0.4	4.31	8.20	13.08	12.46	21.11	33.50	24.29	33.59	42.29	18.52	13.60	11.85
0.5	4.19	7.45	11.54	10.88	18.72	29.92	15.54	21.50	27.07	14.81	10.88	9.48
0.6	3.63	6.40	9.88	10.17	18.07	27.78	10.80	14.93	18.80	12.34	9.07	7.90
0.7	4.44	8.66	13.98	9.78	17.36	26.63	7.93	10.97	13.81	10.58	7.77	6.77